



# 2022


## 中華民國核醫學學會 年會暨國際學術研討會

### 2022 Annual Conference of Society of Nuclear Medicine, Taiwan

- ❖ 時間 ❖ 111年11月12日（星期六）
- ❖ 地點 ❖ 福華國際文教會館
- ❖ 地址 ❖ 台北市大安區新生南路三段30號

主辦單位  中華民國核醫學學會

協辦單位  國立台灣大學醫學院附設醫院

 行政院原子能委員會核能研究所

 經濟部技術處

# INER MIBG $^{123}\text{I}$ Injection 「核研心交碘-123注射劑」

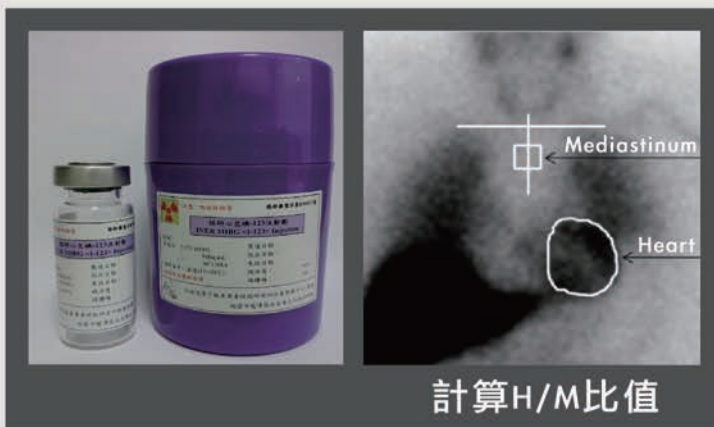
(衛部藥製字第R00037號)

交感神經功能診斷利器

有效期延長至10小時, 品質與國際接軌

2022年正式供應學術臨床試驗

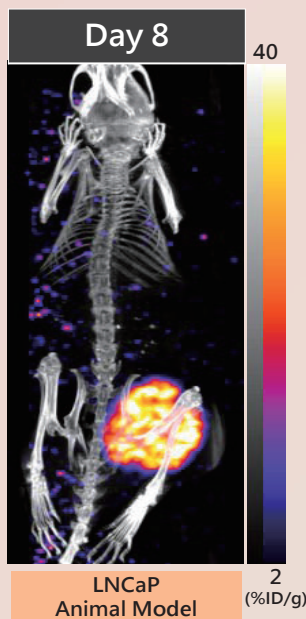
建置符合PIC/S GMP規範的無菌製備生產線  
預計2024年可產製上市藥品



聯絡人: 彭正良博士 [clpeng@iner.gov.tw](mailto:clpeng@iner.gov.tw) (03)4711400#7298

# 癌末攝護腺癌治療新希望

## 長效型低劑量攝護腺癌治療藥物 $^{177}\text{Lu}$ -PSMA-INER-56

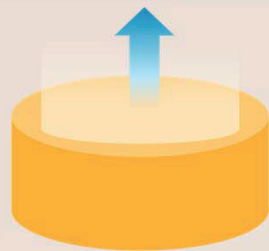


> 8天  
骨轉移腫瘤蓄積

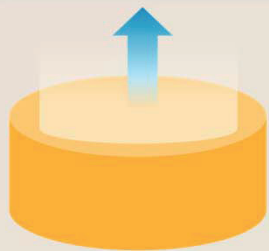
臨床前治療效果優於標竿藥物

- 僅需單次給予單一劑量
- 延長治療效果
- 降低60%治療成本

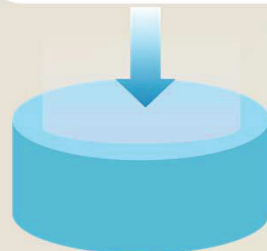
Increase tumor retention



Maximize tumor uptake



Reduce dosage of isotope



腫瘤生長抑制率<sub>D58</sub>

98%

存活率<sub>D90</sub>

90%

IC<sub>50</sub>

3.35 nM

藥物放化純度\*

96%

\*mCi級自動化生產系統

藥物產率\*

89%

\*mCi級自動化生產系統

藥物腫瘤蓄積量比較 (vs. 標竿藥物)

2.5x

(Maximum)

藥物長期安定性

>95%

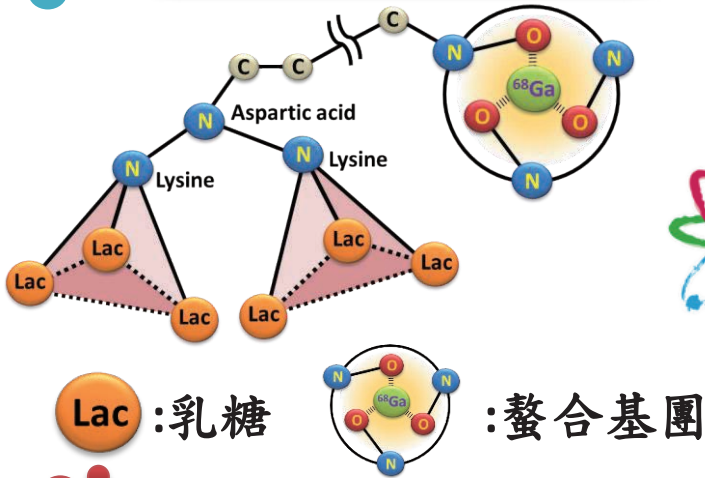
(96HR)

體內吸收劑量評估

推估成人各器官/組織所受的輻射劑量  
皆低於其放射線耐受劑量

# 核研-多蕾克鎳肝功能造影劑

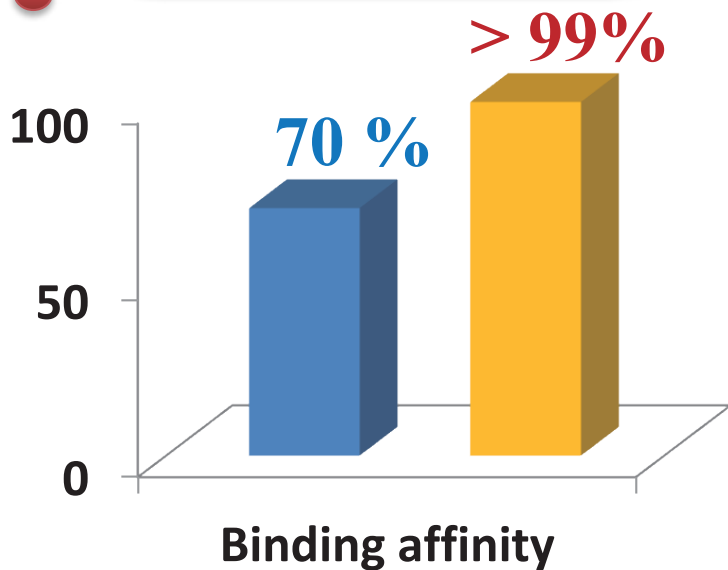
## 創新藥物設計



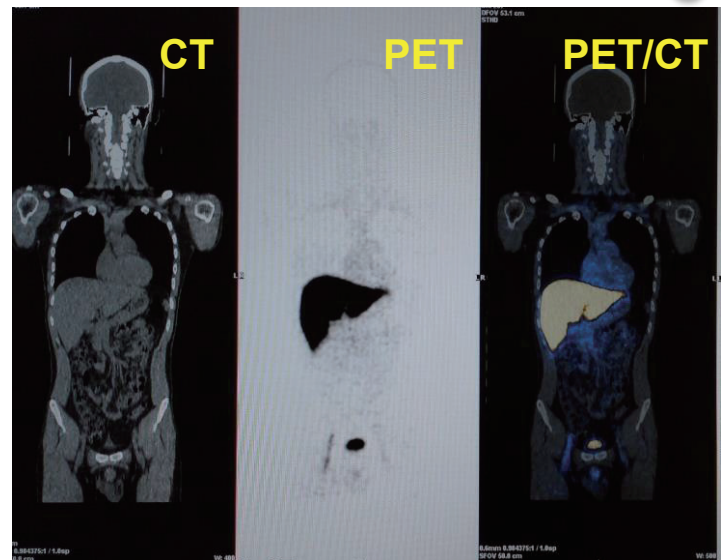
## 凍晶製劑產業化



## 肝受體造影靈敏度



## 第一期臨床試驗



試驗單位：台大醫學院

■ 傳統檢測    ■ 本產品

## 歷年得獎成就

- ✓ 全球專利超過20件
- ✓ 102年國家新創獎
- ✓ 103年紐倫堡發明獎
- ✓ 108年新創精進獎
- ✓ 109年國家發明創作獎銀牌
- ✓ 110年台灣創新技術博覽會鉑金獎
- ✓ 111年國家藥物科技研究發展獎

## 肝功能診斷優勢

TOP 高靈敏度肝受體造影

TOP 獨特Ga-68凍晶製劑

TOP 可用以評估肝病嚴重程度

行政院原子能委員會核能研究所王美惠博士實驗室  
 聯絡方式：(03)471-1400 #7162; mhwang@iner.gov.tw  
 地址：325207 桃園市龍潭區佳安里文化路1000號

泛視神經脊髓炎  
重症肌無力  
自體免疫腦炎  
腫瘤伴生神經症候群  
多發性神經病變  
皮膚炎  
乳糜瀉  
阿茲海默症相關蛋白  
發炎因子  
特殊蛋白或抗體 專案檢測



### | 檢測服務 |

神經疾病檢測的好選擇  
與時俱進\_輔助判斷無距離

### 分子影像用藥

FBB (Florbetaben F-18)  
FDG (Fludeoxyglucose F-18)  
NaF (Sodium Fluoride F-18)

### | 正子藥物 |

核醫醫師可靠的好夥伴  
完整佈局\_串聯全台無距離



士宣生技 x 吉晟藥品

# 讓距離不再是距離

### | 冷鏈技術 |

三種溫層 穩定控溫  
規格多樣\_冷鏈運輸無距離

重複使用  
Credo Cube 系列  
Credo ProMed 系列  
Credo Xtreme 系列  
(可提供租賃服務)

單次使用  
CoolGuard Advance 系列  
CoolGuard PCM 系列  
NanoCool 系列

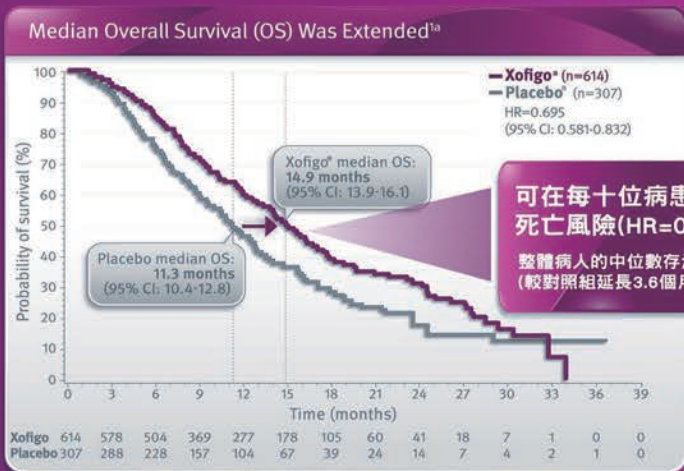


Xofigo® 鐳治骨 用於治療去勢抗性攝護腺癌病患，其合併有症狀的骨轉移且尚未有臟器轉移者



# Xofigo® 鐳治骨 健保給付生效！

## EXTEND SURVIVAL WITH XOFIGO®



健保給付規定：Radium-223 [如Xofigo] 限用於治療去勢抗性攝護腺癌[castration-resistant prostate cancer]病患，其合併有症狀的骨轉移且尚未有臟器轉移者等，且病患需符合下列三項條件：

1. 患者須合併有症狀之骨轉移且骨轉移≥2處
2. 每位患者最高使用六個療程
3. 須經事前審核核准後使用，申請時需檢附：
  - (1) 用藥紀錄(證明為有症狀的骨轉移、需常規使用止痛藥物)
  - (2) 三個月內影像報告證明骨轉移≥2處
  - (3) 三個月內影像報告證明無臟器轉移
4. 不得合併使用abiraterone、enzalutamide及其他治療因惡性腫瘤伴隨骨骼事件之藥品，如denosumab、bisphosphonates等。

<sup>a</sup>Plus best standard of care.<sup>1</sup>

### 3

3個月內  
影像報告

### 2

2處以上  
骨轉移

### 1

1種常規  
使用止痛藥物

### 0

0處  
器官轉移

鐳治骨®注射劑 Xofigo® solution for injection  
衛部醫字第R00981號 本藥限由醫師使用

Xofigo® 適應用於治療去勢抗性攝護腺癌(castration-resistant prostate cancer)病人，其合併有症狀的骨轉移且尚未有臟器轉移者。劑量與給藥方式 Xofigo®的劑量應為每公升轉量給予55 kBq的放射活性，每隔4週給予一次(隔週注射)。劑量對注射Xofigo®的安全性與療效進行研究，Xofigo®以靜脈注射使用。必須以緩慢注射(通常為1分鐘)的方式給藥。 Xofigo®應於合格醫師為病人評估後，由處理放射性藥物之合格人員在指定的臨床場所進行給藥。 禁忌症 Xofigo®的使用上目前已知的主要禁忌症，包括對藥劑與使用注意事項 併用Abiraterone和Prednisone/Prophylaxis增加骨折及死亡。 於臨床試驗中，Xofigo®不建議與abiraterone, acalabrutinib上precoicocic(或prednisolone)之藥劑合併使用。 骨髓抑制 接受Xofigo®治療的病人中曾有骨髓抑制的通報，特別是血小板減少症、中性白血球減少症、白血球減少症及全血球減少症。 骨髓性惡性腫瘤 尚未在受試者中與濃度性結腸炎病人中對Xofigo®的安全性與療效進行研究。 在急性發炎性腸道疾病病人中，只有在仔細評估後才應給予Xofigo®治療。 腎臟功能 在治療前應先評估腎臟功能。 腎臟功能 在接受雙標藥物與Xofigo®治療的病人中，無法排除有喉嚨痛(ONJ)惡化增加的情況。 繼發性惡性腫瘤 Xofigo®會增加病人長期累積的整體放射劑量。 於臨床試驗中，長達3年的追蹤期間並無Xofigo®惡化惡化的案例通報。 畸形胎 依據給藥量，本藥品每次劑量可能含有高達2.36 mrad (54 mg)的鈉。 對控制劑量敏感的病人應考慮到這點。 注意事項 鐳治骨尚未對生殖力和胎毒性進行試驗，根據動物試驗，Xofigo®產生的放射劑量可能有造成生殖力不良反應的潛在風險。 男性病人在治療前應尋求關於精子保存的醫學建議。 由於有放射線對精子生成的潛在影響，應告知男性病人於Xofigo®治療期間以及治療後6個月內使用有效的避孕方式。 Xofigo®不適用於女性病人。 副作用 在接受放射線治療的病人中非常常見(>1/10)的副作用為腹瀉、噁心、嘔吐、血小板減少症。 常見(>1/100至<1/10)的副作用為中性白血球減少症、白血球減少症、全血球減少症、注射部位反應，例如：皮膚發紅、疼痛和腫脹。 嚴重與其他處理的特別注意事項 Xofigo®的使用方式應同時符合放射安全及藥物品質規定。應採取適當的無菌預防措施。 應由合格人員於專門指定的臨床場所收取、使用及給予放射性藥物。其收取、儲存、使用、轉移及棄置均應遵照政府主管機關的規定和取得適當許可。 放射性藥物製劑說明 每個瓶底僅供單次使用。 使用本藥品前應目視檢查。 Xofigo®為室溫無色溶液，若變色、出現顆粒物質或包裝損壞即不應使用。 Xofigo®為即用型溶液，不應稀釋或與任何溶液混合。

詳細產品資訊請參考衛生福利部核准之產品說明書，版本: Xofigo / CCDS + US PI / TW04 / Jun 2019  
MA-XOF-TW 0022-1/07-2019





**PHILIPS**

Advanced molecular imaging

# Proven accuracy inspires confidence

Philips Vereos Digital PET/CT

# VERITON-CT<sup>®</sup> D-SPECT<sup>®</sup> CARDIO

CHANGING THE SHAPE OF NUCLEAR MEDICINE  
CZT BASED SOLID STATE SPECT IMAGING

## D-SPECT Series CARDIOLOGY DIGITAL SPECT IMAGING



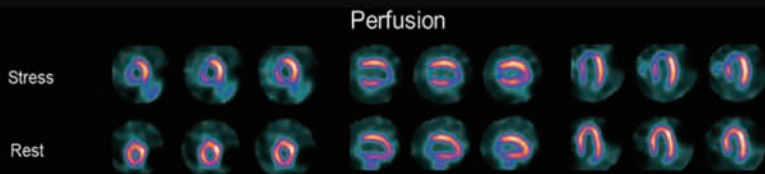
**D-SPECT CARDIO**

## VERITON Series 360° TOTAL BODY DIGITAL SPECT/CT IMAGING



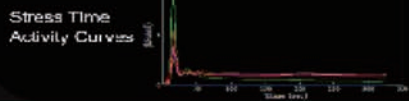
**VERITON-CT**  
SPECT/CT 64

Digital SPECT Technology for Throughput  
and Diagnostic Efficiency

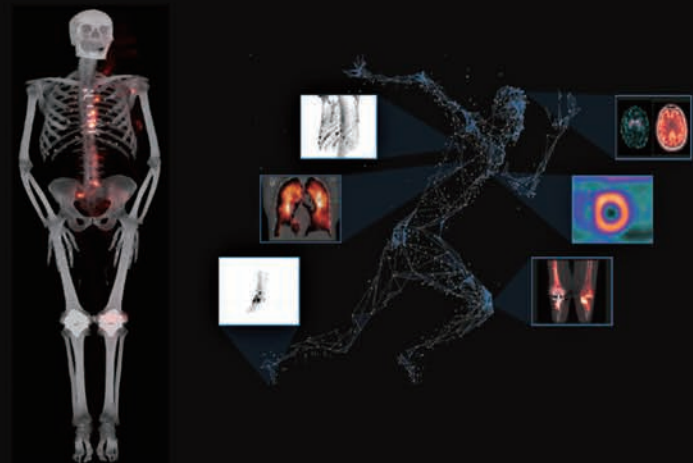


### Dynamic Coronary Flow

Region	Str	Rest	Reserve
LAD	2.40	2.13	1.12
LCX	3.05	2.16	1.41
RCA	1.87	1.20	1.55
TOI	2.41	1.86	1.30



Benefits of 360 CZT Digital SPECT/CT Imaging



**SPECTRUM**  
DYNAMICS MEDICAL

[www.spectrum-dynamics.com](http://www.spectrum-dynamics.com)

總代理

常捷生醫科技股份有限公司 (02)2808-5960

[www.grever.com.tw](http://www.grever.com.tw)



# 德國ABX

獨家代理超過

20年

## Chemicals for Nuclear Medicine & Radiopharmaceuticals

01

**PET and SPECT  
precursors and  
reference standards**

02

**Reagents and  
Cassettes for various  
synthesizers**

FDG, FDOPA, FES, FET, FLT, F-Acetate,  
F-Choline, F-MISO, PSMA-1007, etc.

03

**Chelators for  
Radionuclides**

CuMIBI, EC/ECD, Hynic,  
MAF3, Mebrofenin, etc.

04

**Peptides**

DOTA-NOC, DOTA-TATE,  
DOTA-TOC, PSMA-11, etc.

05

**Custom Synthesis**

## 專業代理行銷

同位素 Isotopes  
手套箱 Glove Boxes  
隔離箱 Isolators

電磁量測儀器：電流和磁場傳感器  
EM Instrumentation: Current & Magnetic Field Sensors

雷射、高壓脈衝產生器和探針  
Lasers, High Voltage Pulse Generators and Probes

歡迎洽詢



龍靈科技企業有限公司  
Upton Technical & Trading Ltd.

📍 新竹市光復路二段295號12樓之4

☎ 03-572-2373, 0933-949-665

✉ [uptontwn@ms24.hinet.net](mailto:uptontwn@ms24.hinet.net)

# NOW AVAILABLE

▶ RAPID ▶ PRONOUNCED ▶ DURABLE

對於放射性碘 (RAI) 治療無效之分化型甲狀腺癌 (DTC) 患者，  
顯著延長無惡化存活期 (PFS) 中位數超過 **18個月**



健保給付規定 (給付生效日 2018 年 7 月 1 日)

用於放射性碘治療無效之局部晚期或轉移性的進行性 (progressive) 分化型甲狀腺癌 (RAI-R DTC) :

1. 需經事前審查核准後使用，每次申請之療程以 3 個月為限，送審時需檢送影像資料，每 3 個月評估一次。
2. Lenvatinib 與 sorafenib 不得合併使用。

#### 適應症

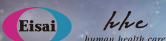
放射性碘治療無效之進行性，且為局部晚期或轉移性之分化型甲狀腺癌之成人患者。

#### 劑型劑量

LENVIMA® 有 4 mg 和 10 mg 兩種劑量之膠囊劑型。

#### 用法用量

- 建議起始劑量為 24 mg 每日一次 (兩顆 10 mg + 一顆 4 mg 膠囊)
- 重度腎功能不全 (CLcr < 30 mL/min) 及重度肝功能不全 (Child-Pugh C) 患者，建議起始劑量為 14 mg 每日一次 (一顆 10 mg + 一顆 4 mg 膠囊)



TW-LV-MH-18G-01 衛部藥輸字第 026933、026934 號 北市衛藥廣字第 111010063 號

衛采製藥股份有限公司 [www.eisai.com.tw](http://www.eisai.com.tw) 電話：02-2531-4175

Ref:Schlumberger M, et al. Lenvatinib versus placebo in radioiodine-refractory thyroid cancer. N Engl J Med. 2015 Feb 12;372(7):621-30

# 目次

👉 大會致詞 ·····	2
👉 會場平面圖 ·····	4
👉 大會議程表 ·····	6
👉 講師及演講摘要 ·····	7
👉 口頭論文發表摘要 - 基礎組 ·····	26
👉 口頭論文發表摘要 - 臨床組 ·····	32
👉 壁報論文發表摘要 - 基礎組 ·····	48
👉 壁報論文發表摘要 - 臨床組 ·····	83
👉 大會組織 ·····	242
👉 贊助廠商 ·····	243



陳長盈 核研所所長

首先感謝核醫學會顏若芳會長的誠摯邀請，核能研究所非常榮幸能參加一年一度的核醫學盛會。在後 COVID19 疫情之際，台灣邁向全面解封之時，將於 11 月 12 日假福華國際文教會館實體舉辦「2022 年會暨國際學術研討會」。長期以來，憑藉國內外核醫學專家、學者和臨床醫生的遠見卓識，為國家核子醫學發展研發方向提供許多關鍵且精闢的經驗。然因應中美貿易戰和新冠肺炎疫情所導致全球經濟和供應鏈的快速變化與不確定性，蔡英文總統於就職演說提出順應國際情勢與科研方向變動而強調六大產業，其中，台灣精準健康也就是生技醫藥領域為當今國家發展的重點之一。

核研所的重要宗旨以增進全民健康與福祉為使命與目標。除積極穩定核醫藥物之生產供應外，另肩負著創新發展核醫藥物的責任。具體成果包括：(一)、穩定核醫藥物生產供應：由於全球新冠肺炎疫情造成的藥物進口短缺，核研所亦緊急投入專業人力以確保國內核醫藥物之穩定供應，妥善維持迴旋加速器與 PIC/S GMP 核醫藥廠之穩定運作，並加速推動新一代 70 MeV 迴旋加速器之規劃建置。今年核研所的核研氯化亞鉈 [鉈 -201] 注射劑供應市占率將達 45%。(二)、核醫藥物創新研究包括：(1) 核研心交碘 -123 注射劑 (I-123-MIBG injection) 已正式於台大、中山、北榮、亞東醫院等進行心臟神經學術研究用臨床試驗。(2) 核研多蕾克鎳肝功能造影劑已於林口長庚醫院執行第二期臨床試驗。(3) 開發中藥物：包括進行攝護腺癌放射治療藥物、腫瘤缺氧及動脈粥狀硬化診療造影劑等臨床前試驗進程。此外，本所已於 110 年 10 月獲行政院核定，並將自明 (112) 年起至 115 年共四年，以「國家中子與質子科學應用研究：70 MeV 中型迴旋加速器建置計畫」擴展迴旋加速器應用範疇，預定開發斬新治療 (如鈾 -225、銅 -67) 與診斷 (鋇 -82) 放射性同位素，提供臨床放射診治療藥物新選擇。

核研所秉持與各先進攜手邁向核子醫學發展新藍海，將持續與國內外產、學、醫研界合作，共同開發具潛力與價值之核醫藥物，促進核醫藥物市場之蓬勃發展。並持續提供國人所需之臨床核醫用藥，藉以落實原子能科技應用於民生用途，促進國人福祉達成照護國民健康之目的。最後，感謝各位先進人士對核研所的支持和幫助。預祝大會圓滿成功。各位先進身體健康，平安喜樂！

核能研究所所長 陳長盈



顏若芳 理事長

在後 COVID19 疫情之際，台灣也正邁向全面解封之時，中華民國核醫學學會 (The Society of Nuclear Medicine ROC) 將於 11 月 12 日假福華國際文教會館實體舉辦 2022 年會暨國際學術研討會。同時今年也由台灣舉辦第十屆亞洲核子醫學技術學會 (ASNMT) 會議，黃副理事長奕璋擔任會長，外賓以視訊參加。

我於 2018 年底承蒙大家不嫌棄委託為學會服務，也即將在這次年會後卸任。這四年當中，學會的各項業務因為全體會員共同努力，第九屆理監事們定期開會做決策與監督，各委員會主委和委員們承擔各項任務，秘書處協助業務的執行，不負所托順利完成，在此非常感謝大家的幫忙與協助。

最近四年的年會分別為：2019 年在台南奇美醫院及 2020 在台北榮總實體舉辦；2021 年因疫情升溫由台中榮總主辦以全視訊會議型態舉行。承蒙奇美、北榮及中榮院方、核醫主任及同仁們全力支持而順利完成。2022 年回到台北由台大醫院主辦，這也是台大醫院首次承辦學會的這項年度盛會。感謝台大鄭媚方主任、路景竹醫師及和信醫院黃玉儀主任共同籌畫，更要感謝台大核醫同仁的支援。

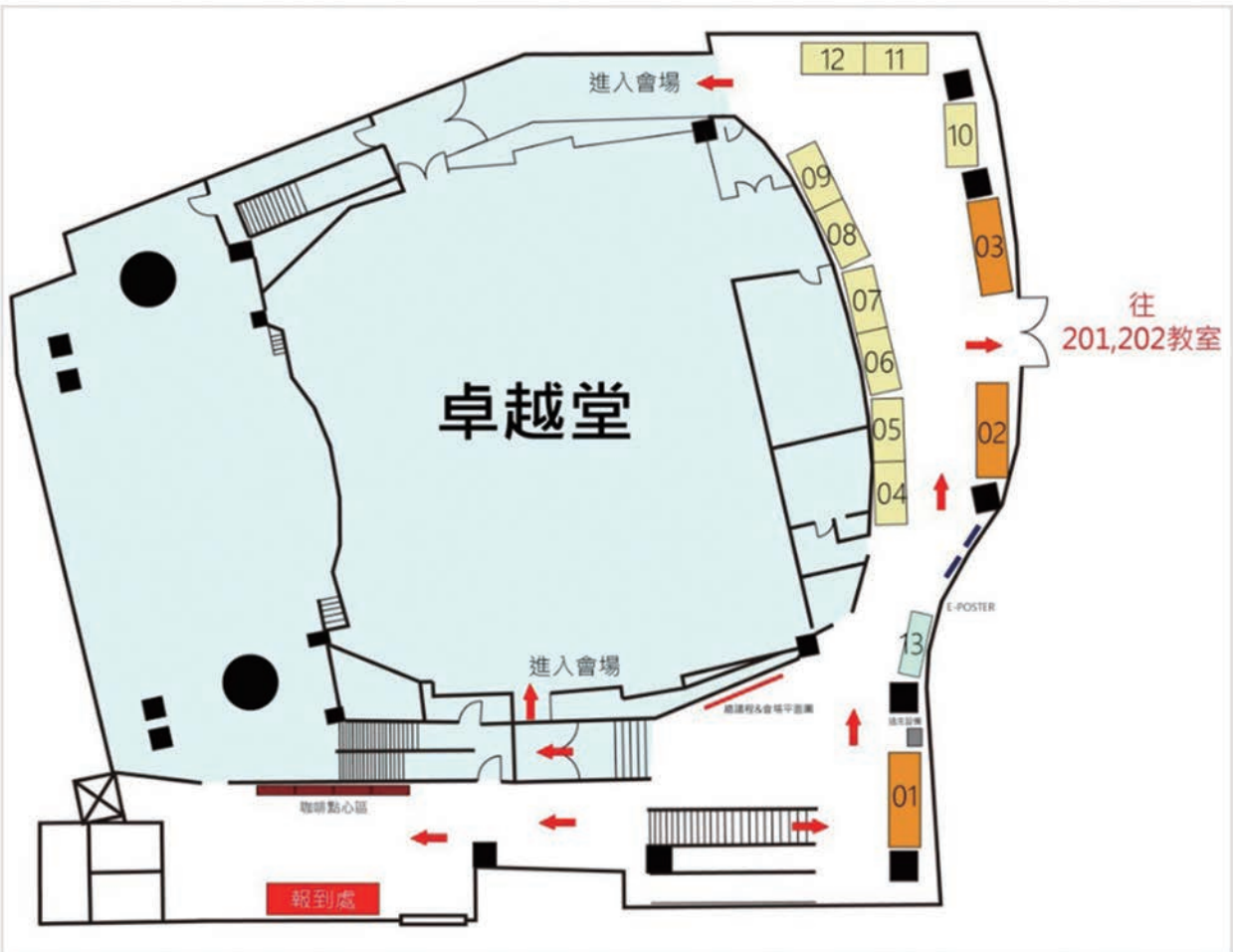
這四年中，儘管有 COVID19 疫情，核醫的分子標靶診療 (Theranostics)、新分子藥物的發展，還有人工智慧協助影像的收集、處理、分析和報告都有愈來愈重要的角色，希望這些今年年會的主軸經由國內外講師們的分享，可以讓國內核醫更迅速進展和國際接軌。

最後，謹代表中華民國核醫學學會誠摯的邀請各位共襄盛舉，也預祝大會成功圓滿。

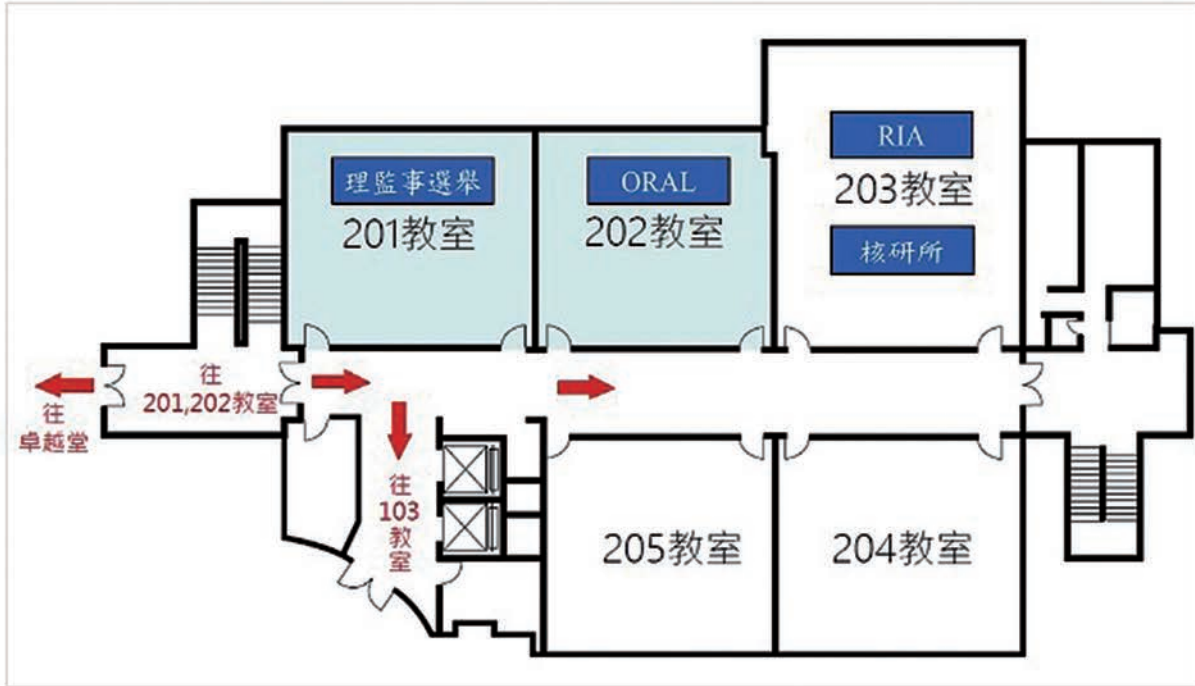
中華民國核醫學學會 理事長 顏若芳

會場平面圖

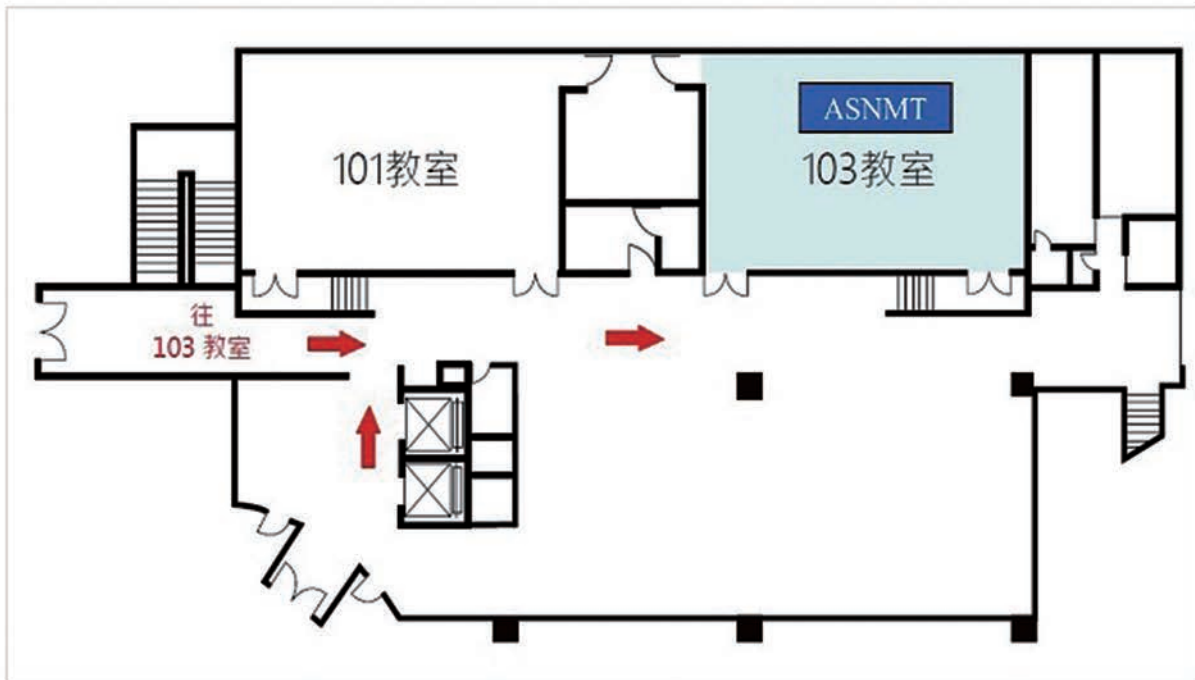
福華國際文教會館2F



福華國際文教會館2F



福華國際文教會館1F



	卓越堂會場	203(RIA、核研所)	202(ORAL)
08:30-08:50	會員報到		
08:50-09:00	大會開幕		
09:00-09:30	<b>Immunotherapy</b> 癌症免疫治療 講者：楊志新 院長 國立臺灣大學醫學院附設醫院癌醫中心分院	座長： 顏若芳理事 長、 彭南靖主任、 蔡世傳主任	
09:30-10:00	Use of PET imaging, other than FDG, in immunotherapy 講者：Prof. Orhan Öz University of Texas Southwestern Medical Center, USA		9:30-10:20 如何使用品管 4+3 政策建立實驗室內部品管? 講者：Randex 莊智淵 業務代表 座長：王安美 主任
10:00-10:30	FDG PET for the evaluation of Immunotherapy 講者：黃玉儀 主任 和信治癌中心醫院		09:30-10:20 口頭報告臨床 (1)
10:30-11:00	Break		
11:00-11:30	<b>AI in Nuclear Medicine</b> 講者：Prof. Piotr Slomka University of California, Los Angeles, USA	座長： 洪光威副院 長、 吳東信教授	11:00-11:50 放免疫分析試劑評估及注意事項 講者：馬偕醫院 王安美 主任 座長：陳宜伶 放射師
11:30-12:00	AI in Nuclear Medicine: Neurology 講者：程子翔 助理教授 國立臺灣大學		10:30-11:20 口頭報告臨床 (2)
12:00-12:30	Clinical Experience with Digital PET scanner 講者：Dr. Walter Noordzij University Medical Center Groningen, Netherlands		11:30-12:20 口頭報告臨床 (3)
12:30-14:00	會員大會/午餐		13:30-14:00 PET Imaging of Synaptic Density for Alzheimer's Disease and Other Neuropsychiatric Disorders 講者：耶魯大學 陳明楷副教授 座長：高梓木執秘、林昆儒主任
14:00-14:30	<b>Next theranostic tracers</b> Theranostics targeting FAP 講者：Prof. Tadashi Watabe University of Osaka, Japan	座長： 鄭媚方主任、 何恭之主任、 路景竹醫師	Exploring the neural basis in the disease model of neurodegeneration- the application of PET 講者：國防醫學院 馬國興教授 座長：林昆儒主任、高梓木執秘
14:30-15:00	CXCR4 theranostics 講者：Prof. Andreas Buck University Hospital Würzburg, Germany		14:00-15:00 住院醫師考試
15:00-15:20	Break		
15:20-15:50	<b>Precision Therapy</b> Target therapy for radioiodine refractory thyroid cancer 講者：施翔蓉 醫師 國立臺灣大學醫學院附設醫院	座長： 林立凡主任、 張晉銓主任	Preclinical Evaluation of a long-acting Theranostic Targeting Agents for prostate cancer 講者：核能研究所 樊修秀副組長 座長：馬國興教授、李振弘組長
15:50-16:30	Theranostics in NET and prostate cancer 講者：Prof. Ken Herrmann University Hospital Essen, Germany		The Current and Perspective status of Atherosclerotic Imaging 講者：核能研究所 夏建忠博士 座長：黃文盛教授、樊修秀副組長
16:30-17:00	Ra-223 for prostate cancer 講者：路景竹 醫師 國立臺灣大學醫學院附設醫院		A Dual-motif CAIX probe as a nuclear imaging agent for Hypoxic Colorectal Carcinoma Detection in Vivo 講者：核能研究所 官孝勳博士 座長：樊修秀副組長、黃文盛教授





Name: 楊志新

Title: 院長

Institute: 國立臺灣大學醫學院附設醫院癌醫中心分院

## 癌症免疫治療

癌症免疫治療已有 100 多年的歷史，但是真正的突破是使用免疫核對點抑制劑恢復殺手 T 細胞對特定癌細胞原有的殺傷功能。使用免疫核對點單株抗體對大多數癌症都有治療效果，但不同癌症有效的比例相差很大，此外絕大部分病人對單獨使用免疫核對點抗體仍效果不佳。但相信我們對癌細胞所處之免疫微環境更了解，將來之免疫治療應會更進步。



Name: **Orhan Öz**

Title: Professor

Institute: University of Texas Southwestern Medical Center, USA

---

## **Use of PET Imaging, Other than FDG, in Immunotherapy**



Name: 黃玉儀

Title: 主任

Institute: 和信治癌中心醫院

## FDG PET for the Evaluation of Immunotherapy

<sup>18</sup>F FDG PET/CT is by far the most widely available, and the most experienced functional molecular imaging modality. It has a role in response assessment of immunotherapy. In addition, it can help identify and monitor immune-related toxicities. There is also increasing evidence of the role of <sup>18</sup>F FDG PET/CT in predicting response before and during immunotherapy by means of semiquantitative measures, including of tumor burden (MTV, TLG). Various response criteria including the PERCIMT (PET Response Evaluation Criteria for Immunotherapy), PECRIT (PET/CT Criteria for Early Prediction of Response to Immune Checkpoint Inhibitor Therapy), iPERCIST, or other PERCIST (PET Response Criteria in Solid Tumors)-adapted criteria, imPERCIST5 were developed for response assessment. These immune PERCIST criteria were developed with pseudoprogression in mind, with the introduction of unconfirmed progressive metabolic disease requiring confirmation with further <sup>18</sup>F FDG PET/CT.



Name: **Piotr Slomka**

Title: Professor

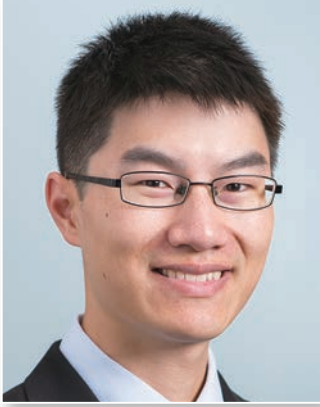
Institute: David Geffen School of Medicine, University of California Los Angeles/Cedars-Sinai Medical Center, USA

---

## AI in Nuclear Medicine

Recent breakthroughs in data science, machine learning, and artificial intelligence (AI) have been applied broadly to pre- and post-processing of imaging data. Nuclear medicine with its quantitative and digital data has been at the forefront of the new AI-applications.

Novel computing approaches hold the promise of improved image quality, automated detection and segmentation of abnormal regions, image registration, and modality-to-modality transformation. The wealth of imaging information, which can be automatically extracted from nuclear medicine images, offers new opportunities – but requires new methods for analysis and integrating the diverse data such as multimodal images and electronic health records. AI may allow meaningful improvements in image quality, clinical efficiency, reproducibility, diagnostic accuracy, and quantitative outcome prediction. Interpretable AI systems can explain to the physician and patient, the primary factors driving the diagnosis or prognosis, dispelling the “black-box” perception of AI. I will overview the latest AI developments in nuclear medicine with special focus on nuclear cardiology. I will cover issues related to data registries needed for the development of AI methods, methods for image quality improvement, image segmentation, diagnosis, and risk prediction. Both classical AI methods and deep learning methods will be discussed, demonstrating practical examples in nuclear medicine and PET/CT SPECT/CT. I will also discuss issues related to the validation and deployment of AI systems for nuclear medicine applications.



Name: 程子翔

Title: 助理教授

Institute: 國立臺灣大學醫學工程學系

---

## AI in Nuclear Medicine: Neurology

Machine learning techniques such as imaging segmentation, denoising, and synthesis can be applied to the technical aspects of PET, where other modalities such as MRI can be used to improve the PET image quality and quantification. Examples of this in neurology include attenuation correction (solved to an acceptable degree in the head), image denoising for low-dose imaging, and the correlation of biomarkers such as CBF derived from different modalities.



Name: **Walter Noordzij**  
Title: Nuclear Medicine Physician  
Institute: University Medical Center Groningen, Netherlands

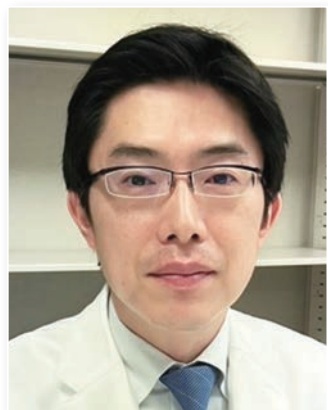
---

## Clinical Experience with Digital PET Scanner

In May 2018, the Biograph Vision PET/CT system was installed at the University Medical Center Groningen. We have evaluated the initial experiences with this new PET/CT system in terms of perceived image quality and semiquantitative analysis in comparison to the Biograph mCT as a reference. Ten patients were scanned on the Biograph mCT first, whereas the other 10 patients were scanned on the Biograph Vision first. The locally preferred clinically reconstructed images were blindly reviewed by 3 nuclear medicine physicians and scored (using a Likert scale of 1-5) on tumor lesion demarcation, overall image quality, and image noise. In addition, these clinically reconstructed images were used for semiquantitative analysis by measurement of SUVs in tumor lesions.

Afterwards, we evaluated the effects of reduced scan duration in oncologic  $^{18}\text{F}$ -FDG PET imaging on quantitative and subjective imaging parameters and its influence on clinical image interpretation. Acquired PET data were reconstructed using the vendor-recommended clinical reconstruction protocol, using the clinical protocol with additional 2-mm gaussian filtering, and in conformance with European Association of Nuclear Medicine Research Ltd. (EARL) specifications using different scan durations per bed position (180, 120, 60, 30, and 10 s). Reconstructed images were quantitatively assessed for comparison of SUVs and noise.

Biograph Vision showed improved image quality compared with the Biograph mCT in terms of lesion demarcation, overall image quality, and visually assessed signal-to-noise ratio. Furthermore, scan duration or activity administration could be reduced by a factor of 3 or more with the use of the clinical+G2 or the EARL-compliant reconstruction protocol.



Name: **Tadashi Watabe**

Title: Assistant Professor

Institute: Osaka University Graduate School of Medicine, Japan

---

## Theranostics Targeting FAP

The tumor microenvironment plays an important role in the invasion and metastasis of cancers. Cancer-associated fibroblasts (CAF) is the main component of the tumor stroma and have been shown to play a crucial role in cancer growth and progression. CAFs express a membrane protein, fibroblast activation protein (FAP), and the level of FAP expression has been reported to correlate with the prognosis of cancer patients. In addition, FAP has been confirmed to be expressed in a wide variety of cancers, including breast cancer, colorectal cancer, pancreatic cancer, ovarian cancer, and hepatocellular carcinoma, while its expression is not observed in normal organs. FAPI (FAP inhibitor), a ligand of FAP, has attracted attention as an excellent PET probe for the precise detection of many types of cancers compared to conventional FDG-PET. Globally,  $^{68}\text{Ga}$ -labelled FAPI ( $[^{68}\text{Ga}]\text{FAPI-04}$  and  $[^{68}\text{Ga}]\text{FAPI-46}$ ) are mainly used for the FAPI-PET. However,  $^{18}\text{F}$ -labelled FAPI ( $[^{18}\text{F}]\text{FAPI-74}$ ) has an advantage of mass-production and capability for the delivery to other sites. In this talk, I would like to introduce the utility and superiority of FAPI-PET compared to FDG-PET based on our experience using  $[^{18}\text{F}]\text{FAPI-74}$  PET. Furthermore, recent progress of therapeutic application targeting FAP are also introduced.



Name: **Andreas Buck**

Title: Professor

Institute: University Hospital Würzburg, Germany

---

## CXCR4 Theranostics





Name: 施翔蓉

Title: 副教授 / 主治醫師

Institute: 國立台灣大學醫學院 / 國立台灣大學醫學院附設醫院

## Target Therapy for Radioiodine Refractory Thyroid Cancer

Differentiated thyroid cancer (DTC) accounts for 90–95% of newly diagnosed thyroid cancers and includes papillary (80%) and follicular (10–15%) carcinomas, and the less frequent Hürthle cell and poorly differentiated histologies (5–10%). Treatment strategies for DTC include active surveillance, surgery, and RAI therapy. The prognosis for patients is relatively favorable, but up to 15% of patients develop radioiodine (RAI)-refractory metastatic disease and have a poor prognosis. Treatment options for these patients include the tyrosine kinase inhibitors (TKIs) sorafenib and lenvatinib.

Sorafenib and lenvatinib target the vascular endothelial growth factor receptor (VEGFR) and other kinase receptors involved in tumor proliferation, survival, and angiogenesis. Although the majority of patients with RAI-refractory DTC initially achieve disease control with sorafenib or lenvatinib, most will eventually develop treatment resistance and have disease progression. Cabozantinib is an inhibitor of several tyrosine kinases that mediate tumor growth and angiogenesis in DTC. It has clinical benefit in patients with RAI-refractory DTC previously treated with lenvatinib and/or sorafenib.

Lapatinib (HER2 inhibitor) and neratinib (pan-ErbB inhibitor) target on HER2/3 receptor to block MAPK and PI3K pathways. ALK translocation, especially STRN-ALK fusion, occurs in thyroid cancer. It will stimulate MEK and activate MAPK pathway. Crizotinib is an ALK inhibitor. Temozolomide and everolimus are mTOR inhibitors, which block PI3K pathway. BRAF inhibitors and MEK inhibitors block MAPK pathway, and can be used in combination to treat thyroid cancers with BRAFV600E mutation. For TRK-fusion positive thyroid cancers, two highly selective TRK inhibitors have been approved; larotrectinib and entrectinib. RET inhibitors, selpercatinib and pralsetinib, have been approved for RET-fusion positive thyroid cancers.

Down-regulation of sodium-iodide symporter (NIS) gene results in disability of iodine absorption in thyroid cancer and thus radioiodine refractories. Several medications, such as retinoids, rosiglitazone, selumetinib, and dabrafenib, were shown to be able to improve NIS gene expression and thus radioiodine sensitivity.



Name: **Ken Herrmann**

Title: Professor

Institute: Essen University Hospital, Germany

---

## Theranostics in NET and Prostate Cancer

The field of Theranostics is revolutionizing the daily clinical life in Nuclear Medicine and shifting the focus from diagnostic imaging more towards therapy. The recent FDA approvals of  $^{177}\text{Lu}$ -DOTATATE and  $^{177}\text{Lu}$ -PSMA 617 changed the perception of radionuclide therapies and have established Theranostics as a significant contributor in the care of NETs and prostate cancer patients.

The talk will give an introduction to the field of Theranostics, summarize the pivotal studies leading to the regulatory approval of  $^{177}\text{Lu}$ -DOTATATE and  $^{177}\text{Lu}$ -PSMA 617 and their implementation into clinical guidelines and then present an outlook to the next steps of establishing Theranostics in earlier lines, new tumor indications as well as discussing the option of combination therapies.



Name: 路景竹

Title: 主治醫師

Institute: 國立台灣大學醫學院附設醫院

---

## Ra-223 for Prostate Cancer

Radium-223 is effective in treating metastatic bone lesions in prostate cancer. It is approved by US FDA in 2013 and by TFDA in 2015. It is further reimbursed by NHI in 2019. Radium-223 had advantages in prolonging overall survival, reducing skeletal-related event and improving quality of life. In this section, review of real-world data and experience in NTUH are introduced.



Name: 莊智淵  
Title: Technical Sales Specialist  
Institute: Radox Laboratories Ltd

---

## 如何使用品管 4+3 政策建立實驗室內部品管？

透過 4 個步驟建立實驗室適當的內部品管目標，3 個檢查點監控品管政策有效性，以實務經驗分享導入符合 ISO15189 醫學實驗室的品質要求，以提升檢驗系統準確性和實驗室品質管理。



Name: 王安美

Title: 技術主任

Institute: 馬偕紀念醫院

## 放免疫分析試劑評估及注意事項

放免疫分析試劑若是新增檢驗品項或更換試劑廠牌，需有評估的機制，以確保新增檢驗品項或更換試劑廠牌之試劑能符合實驗室之需求及確效。ISO15189 之技術要求中 5.3.2.3 說明，每個變更試劑或程序的新配方試劑組應在檢驗使用前加以查證其性能，故變更試劑之評估是非常重要的，除了要確認性能與品質，更要符合實驗室流程之適切性。



Name: 陳明楷

Title: 助理教授

Institute: 耶魯大學

## PET Imaging of Synaptic Density for Alzheimer's Disease and Other Neuropsychiatric Disorders

Synaptic vesicle glycoprotein 2A (SV2A) is an integral glycoprotein in synaptic vesicle membranes and has been investigated as a potential positron emission tomography (PET) biomarker of synaptic density. Regional brain SV2A levels correlate with synaptophysin, a commonly used marker of synapse density, providing the basis for the broad utility of SV2A-PET imaging in neurological diseases. In this talk, we focus on the human SV2A-PET imaging results for multiple neurodegenerative diseases. Research in Alzheimer's disease (AD) and Parkinson's disease has progressed most rapidly across multiple centers, with largely consistent results for SV2A/synaptic loss patterns. In AD, synaptic loss patterns differ from amyloid, tau, and FDG, although intertracer and interregional correlations have been observed. Other diseases including dementia with Lewy bodies, frontotemporal dementia, Huntington's disease, progressive supranuclear palsy, and corticobasal degeneration have also been reported. In summary, initial SV2A-PET studies across indications suggest that the regional pattern of SV2A loss may be specific to disease-associated brain regions and is consistent with loss of synaptic density. Future studies in larger patient cohorts are needed to determine the clinical value of SV2A-PET.



Name: 馬國興

Title: 教授

Institute: 國防醫學院生物及解剖學研究所

## 探索神經退化性疾病模式的神經基礎 — 正子造影技術之應用 /

### Exploring the Neural Basis in the Disease Model of Neurodegeneration- the Application of PET

阿茲海默症 (Alzheimer's disease) 與巴金森氏症 (Parkinson's disease) 是老年最常見的兩種神經退化性疾病，目前並無有效的治療策略可阻止此兩種疾病的病程發展。本實驗室探索過氧化物酶體增植物激活受體 (peroxisome proliferator-activated receptor, PPARs) 全致效劑 -bezafibrate 應用於治療鍊左黴素 (Streptomycin, STZ) 誘導之阿茲海默症大鼠模式，並利用正子斷層造影搭配放射性示蹤劑：[18F]T807 (tau 蛋白的造影劑) 與 [18F]FDG (葡萄糖的類似物)，以評估治療效果。也研究異種移植 (xenotransplantation) 策略對於巴金森氏症大白鼠模式的治療效益，並利用正子斷層造影 (positron emission topography; PET) 搭配放射性示蹤劑：[18F]ADAM (血清素轉運體的造影劑)、[18F]DOPA (L-DOPA 的類似物)、[18F]FE-PE2I (多巴胺轉運體的造影劑)，評估植入細胞的存活狀態。



Name: 高潘福

Title: 教授 / 主治醫師

Institute: 中山醫學大學 / 中山醫學大學附設醫院

## 探索神經退化性疾病模式的神經基礎 — 正子造影技術之應用 /

### Simultaneous I-123-MIBG and Tc-99m-MIBI Dual-isotope Myocardial Imaging in Differentiate Innervation and Perfusion Comorbidity in Parkinsonism Patients

研究合併兩種放射製劑應用在 30 位疑似疑似巴金森症候群動作障礙病患，偵測 99mTc-MIBI 及 123I-MIBG 在心肌分佈的一致性。受檢者接受臨床評量動作障礙與失智嚴重度，並與各項臨床造影結果進行相關性比對。研究有利於提升 CZT 探頭 SPECT 造影診療技術，並減少動作障礙患者就診的不便。進行同時間 99mTc-MIBI 及 123I-MIBG 的雙核種心肌 SPECT 造影，能有助於分類巴金森症候群患，並診斷冠狀動脈心血管疾病與巴金森氏病共病的存在，有利於正確臨床用藥治療的決策。





Name: 樊修秀

Title: 研究員兼副組長

Institute: 核能研究所同位素應用組

## 長效型攝護腺癌診療藥物之臨床前試驗研究 / Preclinical Evaluation of a Long-acting Theranostic Targeting Agents for Prostate Cancer

攝護腺癌為全世界男性癌症發生率第 2 大以及本國第 5 大之癌症，好發於年長男性。核研所開發我國欠缺且具臨床需求 (unmet need) 之長效型攝護腺癌核醫標靶治療藥物 Lu-177-PSMA-INER-56，經 LNCaP 攝護腺癌小鼠實驗證明，單一次注射核醫標靶治療藥物，Lu-177-PSMA-INER-56 腫瘤抑制率 (第 58 天) 達 97.6%；90 天存活率達標準藥物 3 倍 (90% vs. 30%)；透過體內劑量評估及大鼠毒理試驗，Lu-177-PSMA-INER-56 具高度安全性；並已完成自動生產製程、臨床前生物試驗及 CMC 文件資料等。核研所目前盡速推動 Lu-177-PSMA-INER-56 臨床應用或技術移轉，朝向商品化發展，期許能嘉惠本國患者造福國人健康。



Name: 夏建忠  
Title: 簡任副研究員  
Institute: 核能研究所同位素應用組

## 動脈粥狀硬化造影診斷的國際現況與未來 / The Current and Perspective Status of Atherosclerotic Imaging

代謝症候群造成動脈的慢性發炎，導致動脈壁結締組織的增長、細胞內外膽固醇、脂肪酸以及碳酸鈣的沉積，動脈壁變硬變厚及失去彈性，產生動脈粥狀硬化病變。趨化因子 C-X-C 受體 4 型 (CXCR4) 在發炎與腫瘤生物上都扮演極為重要的角色，此研究透過電腦模擬的技術，以 CXCR4 小分子拮抗劑 TIQ-15 為基礎，設計出全新小分子 CXCR4 拮抗劑 APD，透過放射性同位素 Ga-68 的標誌，然後利用動脈粥狀硬化 ApoE<sup>-/-</sup> 小鼠模式進行有效性驗證，並與 18F-FDG 及 18F-NaF 進行比對，結果發現，68Ga-APD 可快速經由腎臟排出，在 ApoE<sup>-/-</sup> 小鼠的動脈粥狀硬化病變部位 / 背景比值 (TBR) > 10 (注射藥物後 1~2 小時)，且優於 68Ga-Pentixafor 的結果 5 倍以上，且 18F-FDG 及 18F-NaF 並無法在 ApoE<sup>-/-</sup> 小鼠的動脈粥狀硬化部位進行造影診斷，此研究結果顯示，透過電腦模擬技術，確實可快速且有效提升藥物的有效性，縮短新藥研發周期、降低研發成本和失敗風險。



Name: 官孝勳

Title: 副工程師

Institute: 核能研究所同位素應用組

## 雙靶向碳酸酐酶第九型放射性示蹤劑 在缺氧性結直腸癌檢測的研究 /

### A Dual-motif CAIX Probe as a Nuclear Imaging Agent for Hypoxic Colorectal Carcinoma Detection in Vivo

國內每年大腸直腸癌的發生人數持續攀升，至今已蟬聯 14 年十大癌症之首。這些患者腫瘤部位常伴隨缺氧的現象。研究指出，腫瘤缺氧會造成腫瘤治療抗性產生。因此，若能預先評估腫瘤缺氧程度即可提供醫師規劃最佳的治療程序。而利用分子影像診斷的方式，能有效提供腫瘤缺氧的程度及位置判斷，甚至是腫瘤轉移或療效評估。碳酸酐酶 9 蛋白在缺氧性大腸癌之腫瘤組織會大量表現，被認為是理想的腫瘤缺氧生物標記。因此，將介紹核能研究所依據 CA9 蛋白質為標的位置，如何設計可對應的雙靶向探針及前驅物製備流程，並接上放射性同位素 (銦 -111)，形成大腸癌腫瘤缺氧造影劑 (INER-In-111-CA9P)，用於體內大腸直腸癌腫瘤缺氧造影。最後從細胞及動物試驗，觀察此造影劑之穩定性、結合力、生物分布及影像呈現等數據，證明具有發展潛力。目前已取得專利並規畫執行 GLP 動物毒性試驗，朝向臨床試驗申請做準備。期盼 INER-In-111-CA9P 能在臨床上實際應用，達到精準醫學之目的。

OB-001

## Develop Novel Brain Neurodegenerative Tau Protein Contrast Agent and Validation of its Validity Using Deep Generative Neural Network

Liang Hsun Huang<sup>1</sup>, Ming-Hsin Li<sup>2</sup>, Yu-Yi Huang<sup>2</sup><sup>1</sup>*Insilico Medicine, Taiwan*<sup>2</sup>*Radiopharmaceutical Theranostic Center, Department of Nuclear Medicine Department, Koo Foundation Sun Yat-Sen Cancer Center, Taipei, Taiwan*

**Introduction:** The breakthrough commercial development of precision diagnosis and treatment drugs opens a new era of personal medical treatment of radionuclide medicines. The prostate diagnosis and treatment drug Pluvicto®/Locametz®, which will be simultaneously approved by the FDA in 2022, is the highlight and exemplary drug of theranostic. Therefore, the resources and goals required to accelerate drug innovation are already supported by a solid business model, and breakthrough R&D technologies are an important strategic core capability for reversing the development of nuclear medicine in the future. Traditionally drug design is time-consuming and costly, with an average probability of 1 in 100,000 of US\$1 billion over a decade. In this paper, we use deep learning to accelerate the development of new drugs, which can greatly increase the speed of research and development and reduce the cost of development.

**Methods:** We use the Variational Auto-Encoder (VAE) architecture to design a neural network for drug generation. The input of the model is a text-based Simplified Molecular-Input Line-Entry System (SMILES) notation, which is an ASCII string represents the molecular structure. However, in order to enrich the number of training samples, we try to enumerate each SMILES in the training data set to enforce the generation model to learn the same molecular structure. In addition, in order to reconstruct valid compound in SMILES string representation from sampling of latent space. We convert the SMILES into Self-Referencing Embedding Strings (SELFIES) and use this as the input representation. The generative neural network design can be divided into two parts: the encoder (Encoder) and the decoder (Decoder), because the input representation is a text-based input, we adopt the 1-D convolution layer (1-D Convolution Layer) to extract the features of the molecular structure represented by the string representation, in this paper, we set the kernel size of the 1-D convolutional layer in range of 3 to 5, and the output of the encoder forms a statistical distribution in the latent space, where we restrict it to be a normal distribution. We then reconstruct the molecule representation from sampled latent vector, which feeds to Long-Short Term Memory (LSTM) layer.

**Results:** We used ZINC20 250,000 druglike molecules as the training set, and obtained nearly 3 million SELFIES molecule representation strings through enumeration. After training, we used MK-6240 as the model input to generate compounds with similar molecular structures. The aforementioned compounds were verified by the AI logic of the brain neurodegeneration Tau protein receptor pattern docking test, and it was found that the target brain neurodegeneration Tau protein contrast agent was superior to the clinical

benchmark drug (state-of-the-art) MK-6240.

**Conclusions:** Designing nuclear medicine generation models through deep learning is promising, especially for small-molecule diagnostic drugs for neurodegenerative diseases with molecular weights below 1000 Da. The generated novel compound structures are novel and progressive. This AI model is highly competitive superior ability. In addition to the development of patentable novel and progressive drugs, this AI model can also be used to verify the validity, which can improve the research and development personnel to think differently in drug design, and greatly reduce the development cost.

OB-002

## Evaluation of $^{18}\text{F}$ -THK5351 Stability for Human Clinical Trial

Min-Tzu Ku<sup>1,2</sup>, Shih-Pei Chen<sup>1</sup>, Wen-Yi Chang<sup>1</sup>,  
Chun-Tse Hung<sup>1</sup>, Geng-Ying Li<sup>1</sup>, Nan-Jing Peng<sup>1</sup>

<sup>1</sup>National PET/Cyclotron Center and Department of Nuclear Medicine,  
Taipei Veterans General Hospital, Taipei, Taiwan

<sup>2</sup>Department of Biomedical Imaging and Radiological Science, National Yang-Ming University, Taipei, Taiwan

**Introduction:**  $^{18}\text{F}$ -THK5351 is a novel PET radiotracer in clinical research for Neurodegenerative disease, Alzheimer's disease, binding to tau protein. However, this new radiotracer is still not widely used in Taiwan, there must have many things to do for application in human clinical trial. To make sure the quality of  $^{18}\text{F}$ -THK5351 for each time use, we established a method to evaluate the stability and optimize the validity in the production.

**Methods:**  $^{18}\text{F}$ -THK5351 was generated from cyclotron and EZ synthesizer (F-18) system in National PET/Cyclotron Center and Department of Nuclear Medicine, Taipei Veterans General Hospital. First, we did quality control tests at 0 hour, each of the test had complied with the standard. At 2, 4, 6 hours, we kept observing its appearance, PH value, radiochemical purity, and K-222 residual. In addition, we would repeat this procedure three times, including production and quality control tests, to ensure the consistency of the evaluation. Quality control tests contain appearance, PH value, time of half life, radionucleotide purity, radiochemical purity, endotoxin, specific activity, K-222 residual, residual solvent, filter completeness, and sterility test.

**Results:** At 0 hour, quality control tests of  $^{18}\text{F}$ -THK5351 were all passed, which including appearance, PH value, time of half life, radionucleotide purity, radiochemical purity, endotoxin, specific activity, K-222 residual, residual solvent, filter completeness, sterility test. Then, at 2,4,6 hours, the appearance of  $^{18}\text{F}$ -THK5351 was still clear and colorless, and the PH value maintained at same value. Radiochemical purity detected by HPLC and radio-TLC also achieved the standard, and so did the K-222 residual. Besides, we repeated this procedure three times and got the same results.

**Conclusion:** The preliminary result show that  $^{18}\text{F}$ -THK5351 is stable for at least 6 hours, in this period, the quality is assured without spoiled. This work provides an optimal validity of product so that the much more safe injection could be promised in human clinical trial. Our result is not only essential to  $^{18}\text{F}$ -THK5351 while using in FDA compliant research use in humans, but also beneficial for developing other novel radiotracers which tend to utilize on clinical research in the future.

OB-003

## Synthesis and Preliminary Evaluation of $^{18}\text{F}$ -FEFAP Probe for PET Tumor Imaging

Pei-Wen Wu<sup>1</sup>, Shun-Fu Chang<sup>2</sup>, Yu-Yun Chen<sup>1</sup>, Chuan-Lin Chen<sup>1,\*</sup><sup>1</sup>Department of Biomedical Imaging and Radiological Sciences, National Yang Ming Chiao Tung University, Taiwan<sup>2</sup>Chiayi Chang Gung Memorial Hospital, Taiwan

**Introduction:** Cancer associated fibroblasts (CAF) are key components in tumor microenvironments (TME) playing a significant role in cancer cells' proliferation and migration. Fibroblast activation protein (FAP) is abundantly expressed on cancer associated fibroblast. As such, FAP is the potential target for diagnosis and therapy against cancer. In this study, we designed and synthesized novel radioactive fluorine-labeled probes  $^{18}\text{F}$ -FEFAP based on the structure of fibroblast associated protein inhibitor (FAP) and evaluated in in vitro and in vivo studies with genetically engineered FAP expression cell line.

**Methods:** The new type of radioactive fluorine-18 labeled tracers [ $^{18}\text{F}$ ]-FE-FAP was synthesized with suitable yield. In vitro experiments were performed with FAP-GFP<sup>+</sup>-HT-1080 cells and wild type-HT-1080 cells. In vivo studies containing  $\mu\text{PET}/\text{CT}$  scans and biodistribution were conducted with FAP-GFP<sup>+</sup>-HT-1080 and wild type-HT-1080 cells tumor xenograft-bearing BALB/c Nude mice.

**Results:** The novel fluorine-labeled FAP inhibitors [ $^{18}\text{F}$ ]-FE-FAP were prepared via direct F-18 fluoride substitution with the suitable radiochemical yield  $12 \pm 2\%$  ( $n = 5$ ) and radiochemical purity  $> 95\%$ . The high in vitro stability ( $> 90\%$ ) of these radiotracers be observed after 2 h incubation in the FBS medium. In vitro cellular uptake study, the steady accumulation in FAP expression FAP-HT-1080 cells were observed. There is a significant difference in the uptake of FAP-HT-1080 cells with FAP expression and wild type-HT-1080 cells, and the specificity can be identified by cold FE-FAP competition. In animal study, the dual FAP-HT-1080 and wild type-HT-1080 tumor bearing mice were used for biodistribution and PET imaging. The specific accumulation [ $^{18}\text{F}$ ]-FE-FAP also showed in FAP-HT-1080 tumor that consistent with cellular uptake result.

**Conclusions:** In this conclusion, the novel fluorine-18-labeled [ $^{18}\text{F}$ ]-FEFAP will be a potential candidate for FAP PET imaging.

**Key words:** cancer-associated fibroblasts (CAF); fibroblast-associated protein (FAP); PET

OB-004

## *In vivo* Preclinical Research of Novel Peptidic Molecules for Triple Negative Breast Cancer Treatment

Mao-Chi Weng<sup>1</sup>, Yu-Wei Liu<sup>2</sup>, Lun Kelvin Tsou<sup>2</sup>, Kai-Hung Cheng<sup>1</sup>,  
Ya-Jane Chang<sup>1</sup>, Chung-Li Ho<sup>1</sup>, Yu-Min Kuo<sup>1</sup>, Wei-Chuan Hsu<sup>1</sup>,  
Shih-Min Wang<sup>1</sup>, Shiou-Shiow Farn<sup>1</sup>

<sup>1</sup>*Institute of Nuclear Energy Research, Taoyuan, Taiwan*

<sup>2</sup>*Institute of Biotechnology and Pharmaceutical Research, National Health Research Institutes, Miaoli, Taiwan, ROC*

**Introduction:** In Taiwan, Institute of Biotechnology and Pharmaceutical Research (IBPR) has put lots of efforts on developing of effective treatment for triple negative breast cancer (TNBC) which is considered the most serious subtype of human breast cancer. However, effective tracers and drugs specific for TNBC are still under investigation. Receptors of luteinizing hormone-releasing hormone (LHRH-R) are regarded as potential targets for TNBC and widely investigated as yet. In this preclinical research, a novel peptidic molecule, BPRSY22, was successfully developed and provided by IBPR and investigated by Institute of Nuclear Energy Research (INER) after its radio-iodination.

**Materials and methods:** BPRSY22 was first synthesized and evaluated by a mass spectrometer and HPLC at IBPR. After radiolabeled with I-131, <sup>131</sup>I-BPRSY22 was purified by a C18 cartridge at INER. The radiochemical purity (R.C.P.) was analyzed by both radio-TLC and radio-HPLC systems. HCC 1806 cells as TNBC were subcutaneously inoculated on mice. After intravenous (i.v.) injection of <sup>131</sup>I-BPRSY22 in HCC 1806-bearing mice, the bio-distribution test was performed at 1, 4 and 24 h.

**Results:** The R.C.P. of <sup>131</sup>I-BPRSY22 was determined > 90% by both radio-TLC and radio-HPLC after purification. In results of bio-distribution, <sup>131</sup>I-BPRSY22 was mainly collected in liver, kidney, spleen and HCC 1806 tumors at 1, 4 and 24 h; in addition, there found many signals in urine and feces. The tumor-to-muscle count ratio (T/M) were then calculated as  $1.57 \pm 0.33$ ,  $2.50 \pm 0.72$  and  $4.38 \pm 0.33$  and the tumor-to-brain count ratio (T/B) were  $4.13 \pm 0.47$ ,  $10.39 \pm 1.53$  and  $21.41 \pm 1.24$  at 1, 4 and 24 h, respectively.

**Conclusions:** The preclinical research has demonstrated the characteristics of BPRSY22 for LHRH-R over-expressive tumors *in vivo*. It showed that activity selectively collected in tumors at 24 h which is increased by three times of that at 1 h; the T/M and T/B also performed an upward trend within 24 h. We suggested that BPRSY22 will be an appropriate candidate for IBPR's next research and it would also bring innovative information for development of TNBC patient's treatment strategies in the future in Taiwan.



OB-005

## $^{89}\text{Zr}$ -ImmunoPET Tracer for Imaging of PD-L1 Expression on Colorectal Cancer

Feng-Yun J. Huang<sup>1</sup>, Fang-Yu Ou-Yang<sup>2</sup>, Wei-Lin Lo<sup>2</sup>, Liang-Chen Chen<sup>2</sup>,  
Yong-Ching Kang<sup>1</sup>, Jui-Yin Kung<sup>3</sup>, Jenn-Tzong Chen<sup>2</sup>, Kuo-Ting Chen<sup>4</sup>,  
Shiou-Shiow Farn<sup>2</sup>, Shih-Chuan Tsai<sup>3</sup>

<sup>1</sup>*Department of Medical Imaging and Radiological Sciences, Central Taiwan University  
of Science and Technology, Taichung, Taiwan*

<sup>2</sup>*Institute of Nuclear Energy Research, Taoyuan, Taiwan*

<sup>3</sup>*Department of Nuclear Medicine, Taichung Veterans General Hospital, Taichung, Taiwan*

<sup>4</sup>*Department of Chemistry, National Dong Hwa University, Hualien, Taiwan*

**Introduction:** The recently emerged PD-L1/PD-1 immune checkpoint blockade therapies have revolutionized cancer treatment over the past few years. Development of ImmunoPET tracer for patient stratification before the therapy and follow-up after the treatment become urgent issue in the field of nuclear medicine.

**Methods:** The DFO-B7H1 conjugates were prepared through random conjugation method. Then, the prepared DFO-B7H1 conjugates were radiolabeled with  $^{89}\text{Zr}$  and then evaluated in PD-L1 expressed CT-26 mouse model of colorectal cancer. For in vivo study, PET imaging, pharmacokinetic, biodistribution, and ROI analysis of PET images experiments were conducted.

**Results:** The DFO-B7H1 conjugates with different chelator-to-antibody (CAR) ratio were prepared and presented from 0.4 to 2.0. The radiochemical yield of  $^{89}\text{Zr}$ -DFO-B7H1 could achieve from 74% to 92% for conjugates with CARs of 0.4 to 2.0. The radiochemical purity of the purified  $^{89}\text{Zr}$ -DFO-B7H1 was larger than 98%. PET scan of  $^{89}\text{Zr}$ -DFO-B7H1 showed that tracer accumulated in the tumor successfully and reached maximum uptake and tumor-to-muscle uptake ratio on 24 h and 48 h postinjection, respectively.

**Conclusions:** The preparation and characterization of  $^{89}\text{Zr}$ -DFO-B7H1 tracer was established successfully. The  $^{89}\text{Zr}$ -DFO-B7H1 tracer with CARs of 1 to 2 displays an excellent ability to image PD-L1 expressed colorectal tumors.

OC-001

## Changes of $^{99m}\text{Tc}$ - pyrophosphate Activity after Tafamidis Therapy in Patients with Transthyretin Amyloid Cardiomyopathy

Yi-Chieh Chen<sup>1</sup>, Chia-Ju Liu<sup>1</sup>, Chi-Lun Ko<sup>1</sup>, Yih-Hwen Huang<sup>1</sup>, Ting-Yen Lee<sup>1</sup>, An-Li Yu<sup>2</sup>, Cheng-Hsuan Tsai<sup>2</sup>, Yen-Hung Lin<sup>2,3</sup>, Chi-Chao Chao<sup>4</sup>, Mei-Fang Cheng<sup>1</sup>

<sup>1</sup>Department of Nuclear Medicine

<sup>2</sup>Department of Internal Medicine and Division of Cardiology

<sup>3</sup>Cardiovascular Center, National Taiwan University Hospital, Taipei, Taiwan

<sup>4</sup>Department of Neurology, National Taiwan University Hospital and National Taiwan University College of Medicine, Taipei, Taiwan

**Introduction:**  $^{99m}\text{Tc}$ -pyrophosphate (PYP) scintigraphy has been used as a noninvasive diagnostic tool for transthyretin amyloid cardiomyopathy (ATTR-CM). However, the role of PYP scan in follow-up of ATTR-CM after tafamidis remains unclear. We investigated the quantitative change of PYP uptake in myocardium of those diagnosed of A97S (Ala97Ser) hereditary ATTR-CM before and after tafamidis treatment to explore the potentials of PYP scan in monitoring therapeutic response.

**Methods:** Patients diagnosed with ATTR-CM by PYP scans during April 2019 and April 2022 in our institute were included retrospectively. All patients had planar and single-photon emission computed tomography/computed tomography (SPECT/CT) images of PYP scans at diagnosis and 1-2 years follow-up after receiving tafamidis treatment or without tafamidis treatment. The PYP images were analyzed using visual score (VS), planar heart to contralateral lung (H/CL) ratio, and volumetric heart to lung (H/L) ratio.

**Results:** Fifty PYP studies were collected from 25 patients, including 21 patients treated by tafamidis (61 mg/day) and four who did not. The median duration between the first and second scans was  $1.64 \pm 0.53$  years. McNemar's tests showed significantly lower VS after treatment (47.6% [10/21] improved, 52.4% [11/21] stationary, and none increased,  $p = 0.004$ ). Similarly, decreased H/CL ratios were observed in both planar (mean  $1.63 \pm 0.20$  to  $1.43 \pm 0.11$ ,  $p < 0.001$ ) and volumetric quantitative methods (mean  $3.80 \pm 0.88$  to  $2.98 \pm 0.47$ ,  $p < 0.001$ ) in those treated by tafamidis using the paired t-test. No significant change of PYP uptake at diagnosis and follow-up was noted in the untreated group.

**Conclusions:** In patients with hereditary ATTR-CM receiving tafamidis therapy, a decrease in myocardial  $^{99m}\text{Tc}$ -PYP uptake was observed. PYP scan can be used as a potential tool to monitor cardiac amyloid burden during tafamidis therapy.

OC-002

## 評估 $^{18}\text{F}$ -FBB PET/MRI 早期相臨床應用可行性之研究

楊邦宏<sup>1</sup> 李哲皓<sup>1</sup> 傅中玲<sup>2</sup> 吳承翰<sup>3</sup>

<sup>1</sup> 臺北榮民總醫院核醫部

<sup>2</sup> 臺北榮民總醫院神經醫學中心

<sup>3</sup> 衛生福利部雙和醫院影像醫學部

**背景介紹：**目前在核子醫學中常使用 F-18 標定的  $^{18}\text{F}$ -FBB (florbetaben) 藥物對阿茲海默症病人進行腦部造影，藉由觀察其腦內乙型類澱粉蛋白 (beta-amyloid protein deposition) 沉積的情況來輔助診斷阿茲海默症。此種核醫藥物須在注射後等待 90 分鐘，接著進行 20 分鐘的造影，等候時間較長，造成有些嚴重病患配合度較差，故本研究目的為比較注射後 60 分鐘造影的  $^{18}\text{F}$ -FBB 影像，與標準注射後 90 分鐘造影影像的差異性。

**方法：**我們回溯性收集 29 筆臺北榮民總醫院核醫部近幾年由 GE SIGNA PET/MRI 造影儀進行造影的 Bravo T1 MRI 以及 90-110 分鐘 (Standard protocol; SP) 和 60-80 分鐘 (early phase; EP) 的  $^{18}\text{F}$ -FBB PET 影像。將收集到之影像經過去辨識化處理後，再進行影像處理轉換至標準空間的正規化 PET 與 MRI 影像，隨後利用相同之 VOI 計算出 90-110 分鐘 SP  $^{18}\text{F}$ -FBB SUVR (standardized uptake value ratio) 以及 60-80 分鐘 EP  $^{18}\text{F}$ -FBB SUVR 數值。

**結果：**本研究發現 EP 與 SP 在影像定量的指標有良好的相關性，其 R-squared 值高達 0.98。在臨床醫師判讀方面使用 RCTU score (regional cortical tracer uptake score) 進行評分，EP 與 SP 的影像在 amyloid positive 與 negative 的 Cohen's kappa 等於 1，在 BAPL score (brain amyloid plaque load score) 則為 0.92。

**結論：**結果顯示 EP  $^{18}\text{F}$ -FBB 造影步驟與 SP 造影步驟，在影像定量的指標有很強的相關性，可用簡單的線性方程式進行轉換。並在影像判讀方面，醫師在 amyloid positive 與 negative 的判讀無明顯的差異，故 EP 方法在影像定量分析與醫師判讀方面有其一定的臨床可行性，因此能為病人減少等待時間，並增加造影人次的效率。

OC-003

## 利用 Q.LUNG 分析立體肺部灌注分率檢查之程序 以及與平面影像分析結果的比較

姜振豪 胡蓮欣 楊邦宏

臺北榮民總醫院核子醫學部

口頭論文發表摘要，  
臨床組

**目的：**本研究目的為介紹目前 GE Xeleris 已提供肺部影像處理程式 -Q.Lung 的使用時注意事項，且比較立體肺部灌注分率檢查 (SPECT/CT) 與平面檢查之結果是否存在有意義的落差。

**方法：**本研究造影儀器使用 GE NM870 CZT，將 21 位肺纖維化的病人 ( $73.5 \pm 9.7$  歲；17 位男性、4 位女性) -MAA ( $210.8 \pm 19.1$  MBq) 在同一天分別收平面 (800 kcounts) 與立體影像 (35 秒 / 張；共 60 張)，平面影像利用 Xeleris 內建肺部分析軟體，會直接將左、右肺由上往下切成各三等份；立體影像利用 Xeleris 的 Q.Lung 分析，首先要界定支氣管與左、右肺的輪廓，要注意在切 CT 時不能切太多肩膀以上的範圍，由於會按照 CT 值去做肺部的選定，當病人肺部纖維化嚴重時程式會誤認肩膀以上含有空氣的範圍為病人的肺部，另外由於肺部纖維化嚴重時肺的內部會有很多區域沒有被正常選取，由於在特定張數手畫的方式較花時間，可視肺部狀況利用 Manual、Expand、Shrink 鍵調整：1) Manual 會從滑鼠所指的位置根據相近的 CT 值自動擴散其圈選範圍，注意滑鼠左鍵不可以長壓太久，還是會圈到其他器官。2) Expand、Shrink 就會以最外圍輪廓去做擴大、縮小的動作，此過程中會把整個肺部自動填滿，很適用於像肺部纖維化病人一樣肺內很多細節未自動圈選到的病人。肺部 ROI 圈選完接下來要辨認各肺裂的位置，由於 CT 須配合 SPECT 不做呼吸調控，因此最後還是建議回到 Hybrid QC 端確認 SPECT 與 CT 是否在肺裂的部分是吻合的。

**結果：**本次比較只有右肺，平面造影條件為收滿 800 kcounts，因此為了與立體影像做比較，先將其上、中、下肺的計數值改為百分比再進行結果的比較，其結果分別為立體影像的右上肺： $47.02 \pm 12.37$ 、右中肺： $23.35 \pm 7.09$ 、右下肺： $29.63 \pm 10.58$  (單位：%)；平面影像的右上肺： $24.58 \pm 5.28$ 、右中肺： $48.27 \pm 4.83$ 、右下肺： $26.99 \pm 7.91$  (單位：%)，可見平面影像在右上肺有低估，右中肺有高估，右下肺有些微低估的狀況發生，造成此差異的原因可能是因為平面分析沒有電腦斷層影像的輔助，沒辦法表現出實際各肺葉對藥物的吸收，直接將右肺分三等份一定會造成右中肺體積過度圈選，並進一步影響到右上肺、右下肺的分析結果。

**結論：**雖然利用 SPECT/CT 造影以及 Q.Lung 分析肺部檢查需要花比較多的時間，但若能夠呈現出各個肺葉對於藥物吸收的狀況，進一步讓醫師能夠評估肺葉與肺節的功能，對病人來說絕對會是有意義的。

OC-004

## Before and After CCRT 18 F- FDG PET/CT Derived Parameters for Survival Prognosis of Patients with Esophageal Cancer

Meng-Ting Chiang<sup>1,2</sup>, Mei-Fang Cheng<sup>1</sup>, Pei-Ju Chuang<sup>3</sup>, Jei-Yie Huang<sup>1</sup>

<sup>1</sup>Department of Nuclear Medicine, National Taiwan University Hospital, Taipei, Taiwan

<sup>2</sup>Graduate Institute of Philosophy, National Tsing Hua University, Hsinchu City, Taiwan

<sup>3</sup>Department of Nuclear Medicine, National Taiwan University Hospital, Yun-Lin Branch, Yun-Lin County, Taiwan

**Introduction:** F-18 fluorodeoxyglucose positron emission tomography/computed tomography (FDG PET/CT) is a useful imaging modality in esophageal cancer, routinely used in staging and restaging. However, the prognostic value of FDG PET/CT is still under research. In this study, we aimed to investigate the prognostic value of FDG PET/CT both before and after concurrent chemoradiotherapy (CCRT).

**Methods:** In this single center retrospective study, 170 patients (mean age  $59 \pm 9$  years old, 11 women) who underwent two times of FDG PET/CT studies before and after CCRT since January 2013 to the end of 2016 were analyzed. The clinical data was reviewed till Sep. 2022. We measured metabolic parameters including maximum standardized uptake value (SUVmax), metabolic tumor volume (MTV), and total lesion glycolysis (TLG) of pre and post- CCRT FDG PET/CT. The prognostic value was evaluated by Kaplan-Meier (KM) analysis, univariable and multivariable Cox proportional hazards model.

**Results:** After a mean follow-up of  $4.3 \pm 3.3$  years, 92 patients died. The Youden index was used for choosing optimal cut-point of SUVmax, MTV and TLG. The KM analysis for overall survival (OS) showed significantly worse in higher pre-CCRT MTV (log rank  $p < 0.01$ ), pre-CCRT TLG ( $p = 0.02$ ), and post-CCRT SUVmax ( $p < 0.01$ ). Also, the faster SUVmax of main tumor reduced (SUVmax decrease rate) after CCRT the longer the survival (log rank  $p < 0.01$ ) was observed. In multivariable Cox proportional hazards model, the pre-CCRT MTV (hazard ratio (HR): 1.01,  $p = 0.02$ , 95% confident interval (CI) = 1.00 to 1.01), pre-CCRT TLG (HR: 1.00,  $p < 0.01$ , C I = 1.001 to 1.002), and post-CCRT SUVmax (HR: 1.07,  $p = 0.02$ , CI = 1.012 to 1.134) showed to be significant predictors for mortality. The SUVmax decrease rate of main tumor (HR: 0.89,  $p = 0.03$ , 95% CI = 0.80 to 0.98) also showed a protective effect for mortality.

**Conclusions:** The pre- and post- CCRT FDG PET/CT provided prognostic value in predicting overall survival of esophageal cancer. The SUVmax decrease rate of main tumor, pre-CCRT MTV, pre-CCRT TLG, and post-CCRT SUVmax were independent and significant predictors.

OC-005

## Quantification of “Regional Centiloid Scale” on 18F-florbetaben Images and Comparison to Visual Interpretation

Chih-Yi Lin, Chi-Lun Ko, Ruoh-Fang Yen, Mei-Fang Cheng,  
Ching-Chu Lu, Jei-Yie Huang, Chia-Ju Liu

*Department of Nuclear Medicine, National Taiwan University Hospital, Taipei, Taiwan*

**Introduction:** The standardized interpretation of 18F-florbetaben (<sup>18</sup>F-FBB) image was based on expert scoring of regional cortical tracer uptake (RCTU) to calculate brain amyloid plaque load, judging from four different regions. However, visual scoring relies on readers' experience. And the inter-reader agreements become worse in complex clinical scenario. A “standard” method of analyzing amyloid PET data, called Centiloid scale, help us standardize quantitative amyloid imaging measures by scaling the outcome to an unbounded 100-point scale. This study is aimed to propose a method for quantification of regional Centiloid scale (RCL) by extending the concept from Centiloid project. We also compare the result to visual interpretation.

**Methods:** We recruited 24 subjects of suspected mild cognitive impairment or Alzheimer's disease (AD) referred for <sup>18</sup>F-FBB imaging. The RCTU scores read by qualified experts were served as reference standard. We used MI Neurology software to automatically quantify standardized uptake value ratio (SUVR) of the four specific cortical regions with whole cerebellum as reference region. To convert <sup>18</sup>F-FBB SUVR to RCL, we first established the correlation between regional PiB SUVR and RCL by processing the calibration datasets from the Centiloid project's website. In each specific region, the average SUVR of young controls and AD patients were scaled to RCL = 0 and 100. And then, we calculated the correlation between <sup>18</sup>F-FBB SUVR and RCL by using the tracer-specific calibration dataset, which contained paired <sup>18</sup>F-FBB and PiB scans from 10 healthy young controls and 25 elderly subjects. Finally, we converted the SUVR to RCL using region-specific conversion factors. The quantified SUVR and RCL values were compared to RCTU scores. And we use ROC analysis to evaluate their predictive performance of positive scans.

**Results:** The Spearman's rank-order correlation coefficients with RCTU were 0.707 and 0.729 for SUVR and RCL respectively. The AUCs were 0.905 and 0.920 for SUVR and RCL, respectively ( $p = 0.09$ ). The best cutoffs of SUVR and RCL were 1.13 (sensitivity: 78%; specificity: 90%, accuracy = 85.4%) and 20.76 (sensitivity: 86%; specificity: 90%, accuracy = 88.5%).

**Conclusions:** In this pilot study, we found RCL slightly outperformed SUVR in prediction of positive readings with borderline statistics significance. We also found optimal cutoff values for RCL and SUVR. Because clinical use of <sup>18</sup>F-FBB is currently by visual interpretation. Quantitative cutoff may help physicians to arbitrate disagreement in borderline cases.

OC-006

## Left Ventricular Ejection Fraction Measured from Cardiac MRI, Echocardiography, and Coronary Angiography: Validation with Multi-gated Acquisition – the Gold Standard

Lien-Hsin Hu<sup>1,2</sup>, Wei-Ting Wang<sup>1,2</sup>, Yu Kuo<sup>1,2</sup>, Ruey-Hsing Chou<sup>1,2</sup>,  
Po-Hsun Huang<sup>1,2</sup>, Chien-Ying Lee<sup>1,2</sup>, Ko-Han Lin<sup>1</sup>, Liang-Chih Wu<sup>1</sup>,  
Wen-Sheng Huang<sup>1,2,3</sup>, Yuh-Feng Wang<sup>1</sup>, Nan-Jing Peng<sup>1,2</sup>

<sup>1</sup>Department of Nuclear Medicine, Taipei Veteran General Hospital, Taiwan

<sup>2</sup>School of Medicine, National Yang Ming Chiao Tung University, Taiwan

<sup>3</sup>Department of Nuclear Medicine, Cheng Hsin General Hospital, Taiwan

**Introduction:** The aim of this study is to analyse the correlation and agreement of left ventricular ejection fraction (LVEF) from cardiac MRI (cMR), echocardiography (ECHO), and contrast left ventriculography in coronary angiography (LVG) with multi-gated acquisition ventriculography (MUGA), the modality that is the gold standard of LVEF measurement.

**Methods:** Retrospectively, patients with both MUGA and the validation target study performed within 1.5 months (i.e.  $\pm 45$  days) were screened for inclusion. Patients who had any events between the 2 studies were excluded to avoid confounding effects. The excluding events are myocardial infarction, percutaneous intervention, coronary bypass surgery, new onset arrhythmia, acute decompensated heart failure, hospitalization from heart failure, adjustment of heart failure medications (adding or withholding ACEI, ARB, spironolactone, beta-blocker), implantation of pacemaker, cardiac resynchronization therapy device (CRT), or intra-aortic balloon pump (IABP). Correlation and agreement of the two studies were analyzed.

**Results:** Three cohorts of MUGA-cMR, MUGA-ECHO, and MUGA-LVG were established. Cardiac MR is performed infrequently and the number of patients with concomitant MUGA and cMR studies within the defined time interval is only 3. The other two cohorts of MUGA-ECHO and MUGA-LVG included 51 and 25 cases, respectively. The correlation coefficients for MUGA vs. cMR, MUGA vs. ECHO, and MUGA vs. LVG are 0.68, 0.83, and 0.73. Bland-Altman analysis reveals the mean difference and the standard deviation for the four groups are  $3.4 \pm 14.6$ ,  $0.6 \pm 6.8$ , and  $-0.1 \pm 11.0$ , respectively.

**Conclusions:** Among the three modalities being validated with MUGA, ECHO shows the higher linear correlation and the best agreement with MUGA. Cardiac MR, being another commonly considered gold standard cannot be fully evaluated due to limited number of cases.

OC-007

## Multimodality Validation of First-pass Radionuclide Angiography: Correlation and Agreement Analysis with Cardiac MRI, Echocardiography, and Coronary Angiography

Lien-Hsin Hu<sup>1,2</sup>, Yu Kuo<sup>1,2</sup>, Wei-Ting Wang<sup>1,2</sup>, Ruey-Hsing Chou<sup>1,2</sup>,  
Po-Hsun Huang<sup>1,2</sup>, Chien-Ying Lee<sup>1,2</sup>, Ko-Han Lin<sup>1</sup>, Liang-Chih Wu<sup>1</sup>,  
Wen-Sheng Huang<sup>1,2,3</sup>, Yuh-Feng Wang<sup>1</sup>, Nan-Jing Peng<sup>1,2</sup>

<sup>1</sup>Department of Nuclear Medicine, Taipei Veteran General Hospital, Taiwan

<sup>2</sup>School of medicine, National Yang Ming Chiao Tung University, Taiwan

<sup>3</sup>Department of Nuclear Medicine, Cheng Hsin General Hospital, Taiwan

**Introduction:** The aim of this study is to analyse the correlation and agreement of left ventricular ejection fraction (LVEF) in first-pass radionuclide angiography (FPRNA) with other clinically important modalities, the validation target studies, used to evaluate heart function including multi-gated acquisition ventriculography (MUGA), cardiac MRI (cMR), echocardiography (ECHO), and contrast left ventriculography in coronary angiography (LVG).

**Methods:** Retrospectively, patients with both FPRNA and the validation target study performed within 1.5 months (i.e.,  $\pm 45$  days) were screened for inclusion. Patients who had any events between the 2 studies were excluded to avoid confounding effects. The excluding events are myocardial infarction, percutaneous intervention, coronary bypass surgery, new onset arrhythmia, acute decompensated heart failure, hospitalization from heart failure, adjustment of heart failure medications (adding or withholding ACEI, ARB, spironolactone, beta-blocker), implantation of pacemaker, cardiac resynchronization therapy device (CRT), or intra-aortic balloon pump (IABP). Correlation and agreement of the two studies were analyzed.

**Results:** Four cohorts of FPRNA-MUGA, FPRNA-cMR, FPRNA-ECHO, and FPRNA-LVG were established with inclusion of 31, 13, 121, and 139 cases, respectively. The correlation coefficients for FPRNA vs. MUGA, FPRNA vs. cMR, FPRNA vs. ECHO, and FPRNA vs. LVG are 0.92, 0.76, 0.69, and 0.60. Bland-Altman analysis reveal the mean difference and the standard deviation for the four groups are  $-2.2 \pm 5.6$ ,  $-1.2 \pm 9.0$ ,  $-4.6 \pm 9.3$ , and  $-1.3 \pm 11.0$ , respectively.

**Conclusions:** Correlation and agreement analyses reveal the highest linear correlation and the best agreement between FPRNA and MUGA while comparing to other modalities.



OC-008

## Perspective from a Case Series – Is it Possible to Monitor Disease Activity or Therapeutic Response with Tc-99m Pyrophosphate Myocardial Scan in Patients with Transthyretin Amyloidosis Cardiomyopathy?

Lien-Hsin Hu<sup>1,2</sup>, Tse-Hao Lee<sup>1</sup>, Wei-Ting Wang<sup>1,2</sup>, Yu Kuo<sup>1,2</sup>, Ko-Han Lin<sup>1</sup>,  
Chen-Hao Chiang<sup>1</sup>, Wen-Sheng Huang<sup>1,2,3</sup>, Nan-Jing Peng<sup>1,2</sup>, Yuh-Feng Wang<sup>1</sup>

<sup>1</sup>Department of Nuclear Medicine, Taipei Veteran General Hospital, Taiwan

<sup>2</sup>School of Medicine, National Yang Ming Chiao Tung University, Taiwan

<sup>3</sup>Department of Nuclear Medicine, Cheng Hsin General Hospital, Taiwan

**Introduction:** Tc-99m pyrophosphate (PYP) myocardial scan emerged as an important study to diagnose transthyretin amyloidosis cardiac myopathy (ATTR-CM) but its role in monitor treatment response is unclear. The aim of the study is to describe the PYP scan result in patients with multiple times of scan and to correlate these results with their clinical profile and to see if it is possible to monitor disease activity or treatment response to ATTR-specific treatment.

**Methods:** Since Jan. 1, 2017, to Apr. 19, 2022, all patients who were referred to our department for PYP myocardial scan for diagnosis of ATTR-CM were screened. In the referred 306 patients, 12 patients and their correlated 25 PYP scans were identified. All scans including the SPECT images were evaluated with the standard method recommended by expert consensus. Patient's clinical information, Perugini score-based scan result, result of ATTR gene test, and medication history specific for ATTR treatment were collected from the electronic medical record. These patients were described in 3 groups based on their first scan result: Group 1-negative first scan; Group 2- equivocal first scan, and Group 3-positive first scan. The sequential scan results and the correlation to their clinical profile were described.

**Results:** Among the 12 patients, 11 patients had two scans and one patient had three scans. Except for one patient who has not been tested for ATTRv, the other 11 patients were all cases with ATTRv. The three groups include 3, 2, and 7 patients, respectively. Their clinical profile are as follows:

**Group 1:** Three cases were negative (score 0) in their first scan which are consistent with their status of asymptomatic carrier. Two of the three cases remained a negative result in their second scans and both are cases under diflunisal usage despite their asymptomatic status. The third one, who has no diflunisal usage, shows a score 1 result in the second study which is likely suggesting an evolving disease status.

**Group 2:** Two cases were equivocal (score 1) in their first scan and both patients remained equivocal result in their second scans. One of the two cases is the only case not confirmed with ATTRv and monoclonal protein has not been excluded. Therefore, a light chain cardiomyopathy cannot be excluded in this case. The other one case, under diflunisal, has borderline LVEF and LV hypertrophy in echocardiography but remains cardiac-symptoms free clinically. The stable scan result is consistent with the patient's clinical picture.

**Group 3:** Seven patients were positive (score 2 or 3) in their first scan. All cases started treatment with ATTR stabilizers (diflunisal or tafamidis) at some point after their first scan. All the seven patients show at least 1-level decrease in their second scan and relative stable clinical conditions under treatment.

**Conclusions:** In this 12-patient case series, serial scan results for each patient match their clinical profile in all 12 cases. Potential of PYP myocardial scan to monitor disease activity and treatment response is suggested. Further observation in a large cohort is needed.

OC-009

## The Clinical Significance of Retropharyngeal/Parapharyngeal Lymph Node Metastasis in Papillary Thyroid Cancer: A Single-Center Observational Study

Tsu-Kang Chen<sup>1</sup>, Yen-Hsiang Chang<sup>1</sup>, Pei-Wen Wang<sup>1,2\*</sup>

<sup>1</sup>*Department of Nuclear Medicine, Kaohsiung Chang Gung Memorial Hospital and Chang Gung University, Kaohsiung, Taiwan*

<sup>2</sup>*Division of Endocrinology and Metabolism, Department of Internal Medicine, Kaohsiung Chang Gung Memorial Hospital and Chang Gung University, Kaohsiung, Taiwan*

**Introduction:** Lymph node (LN) metastasis is common in papillary thyroid cancer (PTC) and accounts for 20%–50% of patients. However, the development of LN metastasis in retropharyngeal or parapharyngeal (RP/PP) space is rare. The objective of this study was to evaluate the clinical features and the prognosis of RP/PP LN metastasis in PTC.

**Methods:** A total of 18 PTC cases with RP/PP LN metastasis (17 retropharyngeal and 1 parapharyngeal) were retrospectively reviewed from July 2008 to June 2022 in our institute. The clinicopathologic and demographic features, including age, gender, tumor size, extrathyroidal extension, TNM staging, American Thyroid Association (ATA) risk, thyroglobulin (Tg) level, radioiodine avidity, F-18 FDG uptake, and time to progression, were recorded according to medical chart review. The progression-free survival (PFS) analyses were estimated using the Kaplan-Meier method.

**Results:** Among the 18 patients, 10 (56%) had RP/PP LN metastasis found at initial presentation. The median age at RP/PP LN diagnosis was 58 years (range 32-81 years). The median maximum diameter of a metastatic RP/PP LN was 0.9 cm (range 0.6-3.1 cm, 2 unmeasurable). Of the 18 patients, 4 underwent observation, 13 received non-surgical systemic treatment, and 1 had local treatment (radiofrequency ablation plus external beam radiation). At initial diagnosis, 15 patients (83%) had advanced T classification (T3 or T4); 11 patients (61%) had pathological N1b disease; 5 patients (28%) had distant metastasis (M1); 14 patients (78%) were classified as ATA high risk for recurrence. During the median follow-up of 23.3 months, 13 (72%) patients developed progressive disease, with a median PFS of 11.3 months (95% CI: 6.8-20.6). High Tg level (> 20 ng/ml) at RP/PP LN metastasis diagnosis was an independent risk factor of worse PFS ( $P = 0.03$ ).

**Conclusions:** RP/PP LN metastasis is rare but is often associated with unfavorable clinical features and poor outcomes. RP/PP LN metastasis may be implied as a poor prognosis marker in PTC patients.

OC-010

## Prognostic Factors and Survival Prediction in Breast Cancer with Latent Bone Metastases: A Single-center Retrospective Cohort Study

Hsin-Chang Chen, Yen-Hsiang Chang

*Department of Nuclear Medicine, Kaohsiung Chang-Gung Memorial Hospital  
and Chang-Gung University, Kaohsiung, Taiwan*

**Introduction:** Bone metastasis may develop years after primary surgery of breast cancer, which is called latent bone metastasis. Less is known about prognostic evaluation for breast cancer patients with latent bone metastasis. The aim of this study is to identify survival predictors among breast cancer patients with latent bone metastasis.

**Methods:** We retrospectively assessed a total of 114 breast cancer cases of latent bone metastases from Kaohsiung Chang Gung Memorial Hospital Database from 2008 to 2019. Both the demographic and clinical characteristics were included as follows: age at bone metastasis, initial stage, histopathological feature, and the presence of visceral metastasis. Laboratory data such as alkaline phosphatase, carcinoembryonic antigen, Cancer antigen 15-3 (CA15-3) were also included. According to the results of bone scintigraphy, the cohort was divided into 3 groups based on the number of bone metastasis: solitary, oligo-, and multiple metastasis. Cox proportional hazards regression models were used to determine factors associated with overall survival (OS) after bone metastasis diagnosed.

**Results:** The mean age of latent bone metastasis development were 55 years. In this population of latent bone metastasis, 92 (81%) died during the follow-up period, with a median OS of 33 months. Solitary, Oligo-, and multiple bone metastasis accounted for 21%, 32%, and 47%, respectively. Visceral metastasis was also identified in 75 patients (66%), and among them, lung was the most common site (60%). Multiple bone metastasis, visceral metastasis, and CA15-3 level were significant variables associated with worse overall survival, and visceral metastasis was identified as the independent factor (HR = 2.52, 95%CI 1.39 – 4.57, P = 0.002). In the subgroup survival analysis, the median survival was 26 months vs. 60 months in patients with and without visceral metastasis, respectively (P < 0.0001).

**Conclusions:** In this study, we demonstrate demographic and clinicopathological features of breast cancer patients with latent bone metastasis. Among them, patients with visceral metastasis, multiple bone metastasis, or high CA15-3 level have worse prognosis.

OC-011

## Comparison of 1 Hour Versus 3 Hours Planar and SPECT/CT in Visual Grading for Technetium Pyrophosphate Imaging for Transthyretin Amyloid Cardiomyopathy

Yi-San Shih<sup>1</sup>, Shan-Ying Wang<sup>1</sup>, Yen-Wen Wu<sup>1,2\*</sup>

<sup>1</sup>Department of Nuclear Medicine, Far Eastern Memorial Hospital, New Taipei City, Taiwan

<sup>2</sup>Division of Cardiology, Cardiovascular Medical Center, Far Eastern Memorial Hospital, New Taipei City, Taiwan

**Background:** We investigated the correlation between planar and single photon emission tomographic (SPECT) image visual grading, between 1 hour and 3 hours imaging time points, and other factors that may affect the imaging parameters for technetium-99m pyrophosphate (<sup>99m</sup>Tc-PYP) cardiac scintigraphy in patients with clinical suspicions for transthyretin amyloid cardiomyopathy (ATTR-CM).

**Methods:** Consecutive patients who underwent a <sup>99m</sup>Tc-PYP scan to diagnose suspected ATTR-CM were enrolled. Visual scores and heart to contralateral lung (H/CL) ratios on the planar anterior view were compared between 1- and 3-hours imaging time points as well as between planar and SPECT/CT acquisitions.

**Results:** A total of 70 patients (66% male, mean age, 67 years) were recruited; and 1- and 3-hour planar images were obtained for 69 patients and 1- and 3-hours SPECT/CT images were obtained for 67 patients. For planar imaging at 1 hour, there were 2, 41, 21, and 5 cases for grades 0, 1, 2, and 3, respectively, and there were 24, 35, 9, and 1 case for the same grades at 3 hours. Only 1 patient with grade 3 at both time points was ultimately diagnosed by genetic sequencing to have a TTR mutation. There was a significant difference between 1- and 3-hour planar image grading, with a downgrade in scores in 41/69 (59%) cases. 21/41 (51%) of these cases downgraded from grade 1 to grade 0; and there were similar findings in SPECT/CT images (all  $p < 0.05$ ). There was no significant difference between planar and SPECT/CT imaging grading at both imaging time points. For H/CL ratios at 1 hour, most of the cases had a ratio between 1-1.5 (62 cases [90%]). Out of these 62 cases, 57 (92%) cases downgraded to H/CL ratio below 1.3 at 3 hours. Other factors including age, sex, creatinine, or NT-ProBNP did not differ significantly between negatively (0,1) and positively (2,3) graded cases on planar imaging at 3 hours, as was the case between patients in different H/CL ratio groups at 1 and 3 hours. The downgrading of visual scores was also not significantly affected by these factors.

**Conclusion:** There is a significant downgrade in visual scoring in 3 hours imaging of both planar and SPECT imaging as compared with imaging at 1 hour. 3-hour imaging alone may suffice for an efficient protocol with a reduction in the potential for over-scoring and equivocal interpretations.

OC-012

## Prototype of Semi-quantification for Renography Analysis

Hsin-Ning Wang<sup>1</sup>, Jiun-Jr Wang<sup>2</sup><sup>1</sup>Department of Nuclear Medicine, Taipei Veteran General Hospital, Taipei, Taiwan<sup>2</sup>School of Medicine, Fu Jen Catholic University, New Taipei City, Taiwan

**Introduction:** Though various methods have been established for the dynamic view of renography, a reliable quantitative evaluation of the renal function through these images is still lacking. Renography image interpretations were commonly conducted through each clinician's narrative about the pattern and the "half time" of the renography image shape. However, such a "free evaluation of evidence" is highly subjective and interpreter-dependent that made cases discussions between institutions rather difficult. In this study, we proposed a simple quantities method to evaluate renography image acquisitions and established a reference of renography image for normal kidneys.

**Methods:** Twenty-one patients who conducted renography in the Taipei Veteran General Hospital and reported no renal obstruction were selected. The renography image recordings contained a distinct initial upstroke and an exponential decay for both kidneys in a unit of counts/min. Since the time of upstrokes were largely consistent among patients with and without obstruction, we regarded the exponential decay section contained crucial information and analyzed by fitting the curve with an exponential decay equation,  $y = a + b * e^{(-cx)}$  (Matlab 2018), where  $a$ ,  $b$  and  $c$  were the asymptotic value of exponential decay, the amplitude and the relaxation time constant, respectively.  $c$  is highly sensitive to the clearance capacity of renal function, namely the larger  $c$  the faster the clearance of renal radiotracer.

**Results:** In these 20 patients (40 left and right kidneys), 30 kidneys showed normal excretion function, 4 kidneys revealed equivocal results, 5 kidneys represent decreased urine excretion and 1 kidney showed nearly total obstruction.  $a + b$  and  $c$  were parameters best representing normal renal excretion function, whereas for normal kidney,  $a + b$  were averaged around 817 (+/-304) counts/second and  $c$  was averaged at 0.177 (+/-0.107). For those kidneys with decreased excretion,  $a + b$  was notably smaller (0.093+/-0.060) and also smaller  $c$  787.9 (+/-204.6), demonstrating slower clearance.

**Conclusions:** By means of a simple exponential function, we analyzed renal renography images, and provided an objective and quantities method describing renal function. Renal obstruction and decreased urine excretion was unequivocally associated with smaller  $a + b$  and smaller  $c$ . Apparently, larger  $c$  yielded by steeper decline represented faster clearance of radiotracer. We considered that these model parameters may have diagnostic significance and provide an objective tool for case discussions by different clinicians.

OC-013

## Coronary Arterial Disease Prediction in Single-Photon Emission Computed Tomography Myocardial Perfusion Imaging: A 3D Deep-Learning-Based Model

Jen Yang, Nan-Tsing Chiu, Pei-Shan Wu, Hsi-Huei Lu

*Department of Medical Imaging, National Cheng Kung University, Tainan, Taiwan*

**Introduction:** Recent computer-aided diagnosis (CADx) systems for coronary arterial disease prediction in single-photon emission computed tomography (SPECT) myocardial perfusion imaging (MPI) have widely adopted deep-learning-based methods. However, most studies use polar maps or 2D images of three axes as inputs, causing potential torsion of intrinsic volumetric information. This research develops a deep-learning-based model with 3D inputs and the corresponding preprocessing algorithm to handle the drawback.

**Methods:** The proposed model consists of layers of 3D convolutions and fully-connected layers. To feed 3D inputs into the model, we reconstructed volumetric arrays by cropping and concatenation image series of short-axis views. We remapped RGB color into grayscale representation through the look-up table of “warm metal” since there's no need for pre-trained weighting preservation. We applied data augmentation methods, including rotation and translation, to reduce potential overfitting. The more in-depth investigations of kernel size, ways of pooling, and the necessity of attention mechanism are performed and evaluated by performance metrics, including sensitivity, specificity, accuracy, and area under the curve (AUC) of receiver operating characteristics (ROC) on the dataset provided by Berkaya et al. (2020, PMID: 32768042) with 192 patients (age 26-96, average age 61.5, 38% men, 78% coronary artery disease, 83% training, and 17% testing).

**Results:** The AUC of the final model on the testing set is 0.913. The Youden's J index shows a sensitivity of 0.960 (95% CI: 0.805-0.993) and a specificity of 0.571 (95% CI: 0.250-0.842).

**Conclusions:** The proposed 3D model showed competitive performance, potential with dataset scaling, and generalizability to intrinsic volumetric imaging.

OC-014

## Impact of Three-Month Androgen Deprivation Therapy on Ga68-PSMA-11 PET/CT Indices in Men with Advanced Prostate Cancer

Szu-Han Chang<sup>1</sup>, Jing-Ren Tseng<sup>2,3</sup>, Feng-Yuan Liu<sup>1</sup>

<sup>1</sup>*Center for Advanced Molecular Imaging and Translation, Department of Nuclear Medicine, Linkou Chang Gung Memorial Hospital*

<sup>2</sup>*Department of Nuclear Medicine, New Taipei Municipal TuCheng Hospital (Built and Operated by Chang Gung Medical Foundation)*

<sup>3</sup>*School of Medicine, Chang Gung University*

**Introduction:** The purpose of this pilot prospective study is to examine the gallium-68-prostatespecific membrane antigen-11 (Ga68-PSMA-11) positron emission tomography/computed tomography (PET/CT) imaging response in patients with advanced or metastatic hormone-naïve prostate cancer (PC) after 3 months of androgen deprivation therapy (ADT).

**Methods:** We prospectively included men with untreated, clinical stage III or IV PC scheduled to receive ADT for at least 6 months. Ga68-PSMA-11 PET/CT images were obtained before the start of ADT and 10–14 weeks thereafter. The following indices were examined: maximum standardized uptake value (SUVmax), mean SUV, PSMA total volume, and PSMA total lesion values of the prostate, nodes, bones, and whole-body. The therapeutic response was assessed using the modified PET response criteria in solid tumors 1.0. A subgroup analysis of patients with the International Society of Urological Pathology (ISUP) grade group 5 versus < 5 was also performed. Results: A total of 30 patients were eligible. All PSMA PET/CT indices were significantly reduced ( $p < 0.001$ ) after 3 months of ADT. 24 patients (80%) showed partial response. Complete response, stable disease, and disease progression were observed in 2 patients each. 6 patients with ISUP grade group 5 showed a less prominent SUVmax reduction ( $p = 0.006$ ), and none of them reached complete response.

**Conclusions:** Three months of ADT in patients with untreated, advanced PC significantly reduced PSMA PET/CT indices. While most participants partially responded to ADT, patients with ISUP grade group 5 showed a less prominent SUVmax reduction. Collectively, our pilot results indicate that Ga68-PSMA-11 PET/CT imaging holds promise to monitor treatment response after the first three months of ADT.



OC-015

## Influence of Interval between Myocardial Perfusion Imaging and Coronary Angiography on Diagnostic Accuracy of Quantitative Analysis

Wei-Jheng Yen<sup>1</sup>, Chin-Chuan Chang<sup>1,2,3,4</sup>

<sup>1</sup>Department of Nuclear Medicine, Kaohsiung Medical University Hospital, Kaohsiung, Taiwan

<sup>2</sup>Department of Electrical Engineering, I-Shou University, Kaohsiung, Taiwan

<sup>3</sup>School of Medicine, College of Medicine, Kaohsiung Medical University, Kaohsiung, Taiwan

<sup>4</sup>Neuroscience Research Center, Kaohsiung Medical University, Kaohsiung, Taiwan

**Introduction:** Stress total perfusion deficit (sTPD) is an objective parameter derived from quantification of myocardial perfusion imaging (MPI). The aim of this study was to investigate the changes in diagnostic accuracy of sTPD with different interval between MPI and coronary angiography (CAG).

**Methods:** From January 2017 to December 2018, patients without previously known coronary artery disease (CAD), who underwent Tl-201 MPI and CAG within 3 months from MPI were enrolled. Initially, the optimal criteria and diagnostic accuracy of sTPD for detection of CAD was obtained by receiver operating characteristics (ROC) analysis of all enrolled patients. And then, the enrolled patients were classified into 4 groups by different interval between MPI and CAG. ROC analysis was used to determine the diagnostic accuracy of sTPD with the different interval, followed by paired comparison of different interval ROC curves.

**Results:** A total of 271 patients were enrolled. With the optimal cutoff value of 9, ROC analysis revealed that the area under curve (AUC), sensitivity and specificity of sTPD were 0.649, 0.326 and 0.971, respectively. Further ROC analysis for different interval between MPI and CAG revealed improved diagnostic accuracy of sTPD with the shorter interval. Although no statistical significance was observed from paired comparison of different interval ROC curves, there is a tendency for p-value to decline in the shorter interval between MPI and CAG.

**Conclusions:** In the current study, the diagnostic accuracy of sTPD varied with different interval between MPI and CAG, especially in sensitivity. We suggest that the interval between MPI and CAG is as shorter as possible.

PB-001

## Improving the Uptake of Tc-99 m-TRODAT-1 in an Animal Model by Mannitol Administration

Chi-Jung Tsai<sup>1</sup>, Kang-Wei Chang<sup>2</sup>, Yu-Hua Lin<sup>2</sup>, Wen-Sheng Huang<sup>1</sup>

<sup>1</sup>*Nuclear Medicine Division, Taipei Medical University Hospital*

<sup>2</sup>*Laboratory Animal Center, Taipei Medical University, Taipei, Taiwan*

**Purpose:** [<sup>99m</sup>Tc]TRODAT-1 is a convenient radioligand used in the clinic for early detection of dopaminergic disorders. It can pass through the brain blood barrier (BBB) and bind to presynaptic dopamine transporters (DATs) on the dopaminergic neurons in the human brain. However, the low permeability of [<sup>99m</sup>Tc]TRODAT-1 through the rat BBB limits its utility in animal models to study dopaminergic disorders. In this study, we used mannitol, an osmotic agent, to improve the uptake of [<sup>99m</sup>Tc]TRODAT-1 in the rat brain.

**Methods:** Sprague–Dawley rats were infused with 2 ml of 20% mannitol before [<sup>99m</sup>Tc]TRODAT-1 injection. Ex vivo autoradiography and nanoSPECT/CT imaging were employed to verify the uptake of [<sup>99m</sup>Tc]TRODAT-1 in the brain after mannitol administration.

**Results:** In ex vivo autoradiography, the uptake of [<sup>99m</sup>Tc]TRODAT-1 in the striatum was higher in the mannitol group than the control group. The specific binding ratios (SBRs) were 85.06% vs. 22.79% at 60 min post-injection and 129.60% vs. 50.26% at 120 min post-injection ( $p < 0.05$ ). In the nanoSPECT/CT dynamic image, [<sup>99m</sup>Tc]TRODAT-1 was at the highest level in the rat striatum 100 min post-injection. The SBRs of the striatum in the mannitol and control groups were 170.29% and 113.50%, respectively, at 100 min post [<sup>99m</sup>Tc]TRODAT-1 injection.

**Conclusion:** Pre-treatment with mannitol in a rat model significantly increased the uptake of [<sup>99m</sup>Tc]TRODAT-1 in the striatum. This method improved the brain images of a rat model to study the central DAT in vivo.

PB-002

## Identification of Metabolites of Fluor-nitrophenylallylideneindolinone Ligand, a PET Agent for Diagnosis of $\alpha$ -Synucleinopathies, in Mice Liver and Brain Using LC and Tandem Mass Spectrometry

Weihsi Chen\*, Kuanyin Chen, Shioushiow Farn

*Division of Isotope Applications, Institute of Nuclear Energy Research, Taoyuan City, Taiwan*

**Introduction:** The false folded protein of alpha ( $\alpha$ )-synuclein forms aggregation and causes neurodegenerative diseases known as  $\alpha$ -synucleinopathies, such as Parkinson's disease. A new designed F-18 labeled ligand, (Z)-[(fluoroethoxy)ethyl]-(E)-3-(4-nitrophenyl)-allylidene-indolin-2-one ( $\alpha$ -syn-<sup>18</sup>F), was tested as a positron emission tomography (PET) imaging agent for use in animal studies for the diagnosis of  $\alpha$ -synucleinopathies. In the study, we determine the metabolites of  $\alpha$ -syn-F in mice liver and brain tissues using high-performance liquid chromatography (HPLC) and tandem mass spectrometry.

**Methods:** Levels of  $\alpha$ -syn-F and thereof metabolites incubated in various tissues sample solutions for up to 150 min were analyzed via HPLC on a C18 column, with the identities determined via electrospray ionization-triple quadrupole tandem mass spectrometry.

**Results:** There were nine and six metabolites were identified in the liver and brain biomatrices, respectively. Biotransformation occurs in fluoroethoxyethyl, which results in the truncation and oxidation of the side chain and hydroxylation at the nitrophenylallylideneindolinone group before sulfonation, methylation, or glycine conjugation. A number of these metabolites lost their fluor and were not traceable on the PET graph.

**Conclusions:** The results suggest that PET imaging should be finalized within 30 min after intravenous administration of  $\alpha$ -syn-F into the body.

PB-003

## 腦神經退化造影劑前驅物 ( $\alpha$ -syn-3) 合成研究

施宗佑 張博智 陳冠因 樊修秀

原子能委員會核能研究所同位素應用組

**背景介紹：**巴金森氏症是第二種常見的神經退化疾病，其致病機轉與大量堆積 alpha-synuclein (突觸核蛋白) 錯誤摺疊有極大關聯。因此，以吡啶酮衍生物為基礎，我們設計了新穎性前驅物代號  $\alpha$ -syn-3。根據文獻上的合成程序，我們分別合成了步驟一產物 3a，產率 40%，步驟二產物 4，產率 11.2%，以及最終產物 5 ( $\alpha$ -syn-3)，產率有 14.2%，總產率達 0.6%。

**方法：**藉由現有的市售材料，第一，我們參考羰基縮合反應於加熱迴流的條件下，合成出步驟一產物 3a；第二，我們參考親核性取代反應於溫和的室溫條件下，合成出步驟二產物 4；最後，我們參考親核性取代反應於加熱迴流的高溫條件下，再經由再結晶方式得到前驅化合物 5。

**結果：**我們藉由光學儀器，高壓液相層析儀、質譜儀以及核磁共振光譜儀的幫助下，成功確認了化合物 3a (99.76%)、化合物 4 (95.39%) 與化合物 5 (96.24%) 的結構鑑定和純度。

**結論：**化合物 3a、化合物 4 與化合物 5，我們利用質譜與核磁共振光譜儀鑑定其結構，利用高壓液相光譜儀確認其純度，前驅化合物 5 的純度達到 95% 以上，總產率為 0.6%；雖然總產率偏低，但純度有符合預期，未來將針對三個步驟的個別產率做精進提升，以及配置最終產物 5 的 HPLC 溶液樣品做安定性測試。

PB-004

## Using High-frequency Correction for Harmonization of Inter-scanner Variance in PET Images

Shao-Yi Huang<sup>1</sup>, Kun-Ju Lin<sup>1,2</sup>, Ing-Tsung Hsiao<sup>1,2</sup>

<sup>1</sup>Department of Medical Imaging and Radiological Sciences, Chang-Gung University, Taoyuan, Taiwan

<sup>2</sup>Department of Nuclear Medicine, Lin-Kou Chang-Gung Memorial Hospital, Taoyuan, Taiwan

**Introduction:** In multicenter PET imaging trials for neurodegeneration studies, harmonization of imaging from different scanning sites and different imaging protocols is necessary to ensure consistent image quality for reliable comparison of images acquired from different places and protocols. For PET images, many factors affect final image quality including system intrinsic resolutions, reconstruction algorithms and post-reconstruction methods and parameters. In this work, to achieve harmonization of inter-scanner variance in tau PET images using <sup>18</sup>F-APN-1607 tracer, the optimization of parameters for high-frequency correction by using 3-D Hoffman phantoms was derived, and the resulted optimal correction parameters were applied to the normal control PET <sup>18</sup>F-APN-1607 images for validation.

**Methods:** Phantom images from 4 different PET/CT scanners were obtained by using FDG-PET scan of a 3-D Hoffman brain phantom. All PET images preprocessing was conducted by using PMOD 3.7 software. Phantom images were first normalized to the digital Hoffman phantom image with 8-mm-FWHM Gaussian kernel. Quantification was performed using the gray matter as reference regions. The optimal parameters of the high-frequency correction were derived for each scanner. After that, the derived correction parameters were applied to <sup>18</sup>F-APN-1607 normal control images. Root mean square error (RMSE) and coefficient of variation (CV) were used to evaluate the results after correction.

**Results:** After high-frequency correction, the RMSE (%) decreased approximately 20%-50% in phantom study and 10-30% in clinical data. There was a significant CV (%) decrease ( $p < 0.05$ ) in frontal, parietal, occipital, thalamus, precuneus and centrum in the phantom study. For the clinical data validation, the CV (%) of the quantitation was significantly reduced ( $p < 0.01$ ) after the high-frequency correction.

**Conclusions:** High-frequency correction can reduce the inter-scanner variance of multicenter PET images. From results of phantom images and clinical data, the image quantitation variance in the cortex decreased after the high-frequency correction. Essentially, harmonization of the image quality between each scanner is an important work before carrying out the subsequent comparison of quantification analysis.

PB-005

## 以運動行為模式與磁振造影分析脂肪源性幹細胞 對小腦萎縮症小鼠之療效研究

楊浚泓 詹振勳 于鴻文 簡傳益 王美惠

行政院原子能委員會核能研究所同位素應用組

**背景介紹：**脊髓小腦萎縮症 (SCA) 是一類會引發運動神經失調，嚴重甚至導致死亡的遺傳性神經退化性疾病，目前尚無有效的治療藥物，亦缺乏即時與高專一性的診斷方法。其中，第 17 型小腦萎縮症模式小鼠 (SCA17) 因具有人類 TBP 基因且在小腦表現 polyQ 蛋白，可導致小鼠產生神經退化與小腦細胞的死亡。我們使用脂肪組織源性幹細胞 (ADSCs) 進行小腦萎縮症模式小鼠的細胞治療療效研究。

**方法：**在尾靜脈注射  $1 \times 10^6$  ADSC cell/mice 之前，先進行小鼠滾輪試驗檢測其運動能力，並以 3T MRI head coil 掃描小鼠腦部，再於治療後每 10 天進行一次上述兩種檢測，造影條件使用 T2 加權 (T2-weighted) 影像，冠狀切面 (coronal section)，總切片數 15 張，厚度為 0.7 mm，FOV = 30，FOV = 0.875，Average = 5，Sequence = FSE25。造影結果使用 Pmod 軟體進行分析，透過比對 Allen Brain Atlas 網站上小鼠小腦之解剖結構，確定小腦之範圍後，以人工方式進行小腦體積之 ROI 圈選，並將圈選結果進行統計分析。

**結果：**在滾輪試驗中，無論有無接受 ADSCs 治療，小鼠的運動能力都有提升的趨勢，治療組與控制組間未顯示出顯著的差異。但在 MRI 小腦體積影像圈選定量結果，發現若以治療前的 MRI 定量結果作為基準，計算每次造影時間點的體積變化百分比進行校正後，治療後 20 天與 30 天治療組小鼠的小腦體積增加之比例都顯著高過於控制組 ( $p < 0.01$ )，而治療組的小腦體積相對於其治療前的體積變化百分比也同樣在這兩次造影中有顯著的增加，同時也可觀察到部分治療組小鼠小腦後葉的 T2-weighted 高訊號現象在治療後降低。治療組小鼠的小腦體積相較治療前增加至 114%~124%，而控制組則維持在 98%~100% 的水平。

**結論：**滾輪試驗可能因個體差異大、變因較複雜及過於密集的運動行為追蹤導致未顯示出顯著差異，但在 MRI 影像中則可顯著的發現治療組小鼠的小腦體積恢復與病理特徵減輕，因此我們認為 ADSCs 對於 SCA17 型的基因轉殖小鼠是有相當療效的，值得進行更進一步研究與分析。

PB-006

## I-131 廢水管路阻塞處理及改善

陸建華<sup>1</sup> 洪佑昇<sup>1</sup> 李將瑄<sup>2</sup>◎

<sup>1</sup> 奇美醫療財團法人柳營奇美醫院核子醫學科

<sup>2</sup> 奇美醫療財團法人奇美醫院核子醫學科

**背景介紹：**I-131 廢水管路為引流 I-131 治療病人排放之放射性廢液至廢水槽用，如病人於馬桶中意外投入異物（如：內褲、紙尿褲、衛生棉等）造成管路阻塞又無立即通知病房護理人員或核醫科輻防師（員）的話，將會造成管路無預警的阻塞，排放廢液會隨阻塞管路往上溢流至馬桶外，產生廢液外流之放射污染事件，為避免此類事件發生，故研究阻塞的改善方式。

**方法：**在廢水管路中間上方開一檢測口，放入異物阻塞檢測器，如遇管內廢液排放受阻無法正常流動時，當阻塞高度超過管內容量三分之二時，偵測器即發出阻塞訊號，訊號直接傳出告知相關人員手機，人員即可迅速至管路檢查，判斷是訊號異常或是確實阻塞，而給予立即性處理，即使在非工作時間內也可由值勤工務人員先行處理，而不致產生輻射廢液外流之污染性事件。

**結果：**檢測器安裝後，發生過幾次警報訊號，均能立即迅速處理，而無發生輻射廢液污染事件。

**結論：**I-131 廢液排放管路正常與否，可以直接影響到 I-131 病人之收置與治療，如廢水管路阻塞又無適時處理造成溢流情形，必須清理與除汙，勢必影響病人之收置與治療而延誤醫療作業。

PB-007

## Automatically Synthesis of [<sup>18</sup>F]AIF-NOTA-octreotide with TRACERlab FxFDG Module

Ching-Hung Chiu<sup>1</sup>, Yu-Ting Chien<sup>1</sup>, Pei-Yao Lin<sup>2</sup>, Mei-Fang Cheng<sup>1</sup>

<sup>1</sup>*PET Center, Department of Nuclear Medicine, National Taiwan University Hospital*

<sup>2</sup>*Department of Nuclear Medicine, National Taiwan University Cancer Center*

**Introduction:** Somatostatin analogue (SSA) labelled with gallium-68 from a germanium-68/gallium-68 generator was used as standard for somatostatin receptor (SSTR) PET imaging at present. However, it is limited by limited yield per elute (can only image 2-3 patients per day), short half-life of the <sup>68</sup>Ga isotope ( $t_{1/2} = 68$  min), and high cost of the generator that needs to be replaced annually, all which posed challenges for routine clinical use. Research collaborators have expressed high interest in fluorine-18-labelled alternatives that also target somatostatin receptor type 2, one of which is [<sup>18</sup>F]AIF-NOTA-octreotide([<sup>18</sup>F]AIF-OC). To implement GMP-compliant production in our laboratory (National Taiwan University Hospital, NTUH), an in-house automation of [<sup>18</sup>F]AIF-OC production is required prior to clinical use.

**Methods:** In this study, [<sup>18</sup>F]AIF-OC was full-automatic radiosynthesized with a synthesis module (GE TRACERlab FX<sub>FDG</sub>). Briefly, eluent solution (NaCl 0.9%/EtOH) was eluted into the reaction vessel. After [<sup>18</sup>F]AIF formed by mixed with 2 mM aluminum chloride (AlCl<sub>3</sub>), precursor solved in sodium acetate solution were added to the reaction vessel for chelation. When reaction was ended, the mixture was diluted with formulation solution and passed through the SPE (C18 light) for further purification. Finally, the product was eluted with EtOH into the product vial by passing through a sterile Millex-GV 0.22- $\mu$ m filter and diluted with sterile formulation solution. The radiochemical purity was determined with HPLC (column: ACE C18, 4.6 x 100 mm ; mobile phase: 0.1%TFA in MeCN/0.1%TFA in H<sub>2</sub>O).

**Results:** The fully automated syntheses of [<sup>18</sup>F]AIF-OC were successfully synthesized under GMP conditions, resulting in radiochemical yield of 5~8% (EOS) within 60 min (n > 3) of synthesis time. Radiochemical purity of each batch were  $\geq 95\%$ .

**Conclusions:** [<sup>18</sup>F]AIF-OC has been automatically manufactured at the NTUH PET center following GMP principles. The manufacture of [<sup>18</sup>F]AIF-OC on the GE Tracerlab FX<sub>FDG</sub> consistently satisfied the defined acceptance criteria. Each batch of [<sup>18</sup>F]AIF-OC will produce sufficient product activity for demand. Preclinical evaluation of [<sup>18</sup>F]AIF-OC as SSTR imaging agent is ongoing.



PB-008

## 銾 111 標誌 TLR9 活化劑及其於 CT26 腫瘤模式 小鼠造影與生物體分佈研究

游佳瑜<sup>1</sup> 張雅珍<sup>1</sup> 何宗澧<sup>1</sup> 林旻萱<sup>1</sup> 鄭凱鴻<sup>1</sup> 羅世偉<sup>1</sup>  
林昀生<sup>1</sup> 樊修秀<sup>1</sup> 余孟萍<sup>2</sup> 吳明錫<sup>2</sup>

<sup>1</sup>核能研究所同位素應用組

<sup>2</sup>工業技術研究院生醫與醫材研究所

**背景介紹：**TLR9 活化劑可活化樹突狀細胞分泌干擾素，進而活化 T 細胞並撲殺腫瘤，達到癌症治療效果。以放射性標誌 TLR9 活化劑可快速完整獲得其於體內的分佈影像及其於各器官的量化數據，進而評估其路徑。本研究利用螯合基修飾 TLR9 活化劑並順利標誌銾 111，再以銾 111 標誌 TLR9 活化劑進行 SPECT/CT 造影及生物體分佈試驗，可有效監測 TLR9 活化劑於體內動態分佈及定量各器官的蓄積量。

**方法：**於 TLR9 活化劑結構接上螯合基並進行銾 111 標誌後再複合於載體上，以完成銾 111 標誌 TLR9 活化劑製備。將 100 微升 300 微居銾 111 標誌 TLR9 活化劑以單一劑量靜脈注射方式投予 CT26 腫瘤模式小鼠，並於投藥後 1, 4, 24 小時以 nanoSPECT/CT 進行造影，再經影像重建獲得銾 111 標誌 TLR9 活化劑於小鼠體內隨時間分佈的影像數據；另將 CT26 腫瘤模式小鼠分為每組 5 隻，每隻小鼠分別以單一劑量靜脈注射方式予以 100 微升 45 微居銾 111 標誌 TLR9 活化劑，並於投藥後 1, 4, 24 小時犧牲小鼠，進行臟器採集與秤重，並測量採集臟器之放射性活度，以計算出藥物於各採集器官之蓄積量 (%ID/g)。

**結果：**銾 111 標誌 TLR9 活化劑標誌效率可達 97% 以上，且於 4°C PBS 及 37°C 大鼠血漿中 168 小時內穩定性達 95% 以上，複合於載體後藥物粒徑大小介於 100~200 nm，粒徑分佈均一 (PdI < 0.2)，界面電位可降至 20 mV。於影像結果顯示，藥物注射後 1 小時可分佈於肝臟、膀胱、腸道及腫瘤；於生物體分佈試驗結果顯示，標靶器官之腫瘤與淋巴結中的藥物濃度分別於給藥後 1 小時達最高值、脾臟中藥物濃度於 24 小時達最高值。其中腎臟給藥 24 小時後降低約 50%，推測藥物主要經由腎臟與尿液排出體外。

**結論：**核研所建立的 TLR9 活化劑放射性標誌技術，可快速評估 TLR9 活化劑於活體內隨時間的動態分佈情形，及精確定量 TLR9 活化劑於各主要器官分佈的蓄積量，有效評估 TLR9 活化劑於體內分佈代謝的表現。

PB-009

## 利用奧攝敏造影注射劑 執行正子造影之流程以中部某醫院為例

蔡沛君<sup>1</sup> 曾能泉<sup>1</sup> 歐宴泉<sup>2</sup>

<sup>1</sup> 童綜合醫療社團法人童綜合醫院核子醫學科

<sup>2</sup> 童綜合醫療社團法人童綜合醫院泌尿腫瘤中心

**目的：**奧攝敏造影注射劑 ( $^{18}\text{F}$ -Fluciclovine,  $^{18}\text{F}$ -FACBC, Axumin) 於 2016 年通過美國食品藥物管理局 (FDA)，2017 年通過歐洲藥品管理局 (EMA)，2020 年 9 月通過衛生福利部食品藥物管理署 (TFDA)。適用於先前接受治療完畢後，因 PSA 濃度上升而懷疑攝護腺癌復發之病患，輔以協助診斷攝護腺癌復發與否。參照 UK guideline 及 SNM guideline 執行檢查方針下，該區域醫院於 2020 年 12 月開始執行奧攝敏正子造影檢查至今已達 60 例，故將其造影流程報告之。

**材料方法：**正子造影儀為 GE Discovery MI。衛教患者於檢查前 24 小時停止劇烈運動，當日受檢前禁食 4 小時，若需服藥僅能配少量水。檢查前先衛教患者造影流程並請患者先行如廁，於如廁完畢計時 30 至 60 分鐘後執行造影，以降低尿液早期排至膀胱；同時照影前於患者右手放置留置針，並確認管路暢通。奧攝敏注射劑量為  $10 \text{ mCi} \pm 20\%$ ，於收到藥物後先檢測劑量。為確保檢查流程順暢進行我們安排二名人力，一名放射師負責注射藥物 (放射師 A)，另一名放射師負責操作儀器 (放射師 B)。病患平躺於檢查床雙手舉起先執行 CT Scout view，接著將檢查床退出，放射師 A 將患者右手放置注射檯面，確認管路暢通後隨即注射藥物，並由放射師 B 記錄注射時間；待奧攝敏注射完畢，以 20 毫升生理食鹽水沖洗管路再將患者右手放回原先舉手姿勢，持注射完畢空針離開造影室並檢測殘餘劑量；同時 B 放射師利用注射藥物空檔設定造影條件，圈選造影範圍。放射師 A 離開造影室，放射師 B 隨即執行 CT scan，流程進入 PET mode 時，再將奧攝敏注射時間與殘針劑量輸入電腦，待注射後 4 分鐘立即開始收集 PET 影像。正子造影條件為由骨盆掃描至頭頂，影像以 Q clear 方式重組。

**結果：**執行奧攝敏正子造影因注射藥物後 4 分鐘後立即開始執行正子掃描，故安排另外人力執行藥物注射、劑量檢測工作，以便放射師執行造影條件及範圍選定，在過程中也需記錄注射時間，以便輸入電腦掌握開始造影時間，降低放射師執行檢查之壓力。因二名人力配合得以讓檢查順利完成，至今沒有檢查失敗或重新掃描之案例，收集之影像也皆在二位以上專科醫師可接受範圍。

**結論：**由於此檢查對於每個時間點的掌控需精準，故檢查前衛教流程非常重要，讓患者明確了解檢查流程可提高受檢者的配合度。加上二位放射師相互合作，降低檢查過程中突發狀況並將檢查順利完成，以得到最佳化的操作流程與影像。

PB-010

## Novel Isotopes Labeling Compound for Bladder Cancer and Post-therapy Follow Up

Kang-Wei Chang<sup>1</sup>, Chi-Jung Tsai<sup>2</sup>, Yu-Hua Lin<sup>1</sup>, Wen-Sheng Huang<sup>2</sup>

<sup>1</sup>Laboratory Animal Center, Taipei Medical University, Taipei, Taiwan

<sup>2</sup>Nuclear Medicine Division, Taipei Medical University Hospital

**Purpose:** Nuclear medicine molecular imaging uses positron emission tomography (PET) and single-photon emission computed tomography (SPECT) with radiopharmaceuticals to reflect physiological and biochemical changes in vivo to achieve disease diagnosis and treatment evaluated. Using appropriate isotope on specific biomarker had developed into an important in vivo diagnosis and treatment tool. At present, the clinical diagnosis and treatment methods for bladder cancer are still improving, and a specific non-invasive early imaging assessment tool (fibroblast-activated protein inhibitor, FAPI) can be used to evaluate the efficacy of bladder cancer before and after treatment.

**Methods:** NOD/SCID mice orthotopic implanted bladder cancer cell line (T24 cell line) into bladder. The radioactivity of cell bound with [<sup>18</sup>F]FDG, [<sup>18</sup>F]FEPPA and [<sup>177</sup>Lu]FAPI and nanoPET and nanoSPECT/CT imaging were employed to verify the uptake of [<sup>18</sup>F]FDG, [<sup>18</sup>F]FEPPA and [<sup>177</sup>Lu]FAPI in the bladder after radiopharmaceutical administration.

**Results:** In in vitro cell bound of [<sup>18</sup>F]FDG, [<sup>18</sup>F]FEPPA and [<sup>177</sup>Lu]FAPI in T24 cell line shows positive correlation with cell number and radiopharmaceutical uptake. In nanoPET image of [<sup>18</sup>F]FDG and [<sup>18</sup>F]FEPPA (after squeezed urine from the mice), showed the higher accumulated trend between bladder cancer animal model than control group, but no statistically different. In [<sup>177</sup>Lu]FAPI/nanoSPECT/CT image, dynamic and static image showed the obvious image in bladder animal model.

**Conclusion:** There have been many literatures on FAPI for tumor theranostic application, but lack of research on bladder cancer. The presence of tumors image quality due to the high hydrophilicity of [<sup>177</sup>Lu]FAPI ( $\text{LogD}(7.4) = 10^{-2}$ ) still need continuous research and improvement. In future clinical application, clinical subjects could drinking water and urinate more before the nuclear medicine image (as F-18 FDG).

PB-011

## Preclinical Evaluation of Radiolabeled YKL40 Antibodies as Potential Theranostic Agents for Ovarian Cancer

Chun-Tang Chen, Ming-Cheng Chang, Ping-Fang Chiang,  
Yu-Jen Kuo, Cheng-Liang Peng

*Institute of Nuclear Energy Research, Taoyuan, Taiwan*

**Introduction:** To date, ovarian cancer remains the most devastating gynecological cancers and ranks seventh in cancer related deaths for women in Taiwan. Although patients diagnosed with early stage (I/II) ovarian cancer have an excellent prognosis, the majority of patients (~60%) are diagnosed in late stages (III/IV) and tend to have a poor prognosis. Chitinase-3-like protein 1 (CHI3L1), also known as YKL40, is associated with progression of ovarian cancer, and targeted imaging and therapy of YKL40 is a promising strategy. In this study, we developed radiolabeled antibodies target to YKL40 and evaluated for their applications as theranostic agents against ovarian cancer.

**Materials and Methods:** DTPA-YKL40 antibodies radiolabeled with Indium-111 ( $^{111}\text{In}$ ) or Lutetium-177 ( $^{177}\text{Lu}$ ), and then were subjected to preclinical evaluation *in vitro* (stability test and cell uptake analysis in CA5171 and OVCAR-3 cells) and *in vivo* (SPECT/CT imaging, bio-distribution and therapeutic responses in ovarian cancer xenograft mice).

**Results:**  $^{111}\text{In}/^{177}\text{Lu}$ -DTPA-YKL40 antibodies were achieved in high radiochemical yields and purities of > 95% as determined by radio-HPLC or TLC. *In vitro* stability study suggested that  $^{177}\text{Lu}$ -DTPA-YKL40 antibodies were highly stable for at least 168 hours in PBS at 4°C or human plasma at 37°C with radiochemical purity still above 90%. The cell surface binding rate of  $^{177}\text{Lu}$ -DTPA-YKL40 antibodies into CA5171 cells (YKL40<sup>pos</sup>) reached about 15% of total activity, whereas the internalization rate was < 2%. The cell uptake dropped about 2% when OVCAR-3 cells (YKL40<sup>neg</sup>) were used, which proves YKL40-specific uptake of radiolabeled antibodies. SPECT/CT imaging indicated that accumulation of radiolabeled YKL40 antibodies in tumor site of ovarian cancer xenograft mice at 24 hours. Tumor uptake were  $0.7 \pm 0.4$  %ID/g for  $^{111}\text{In}$ -DTPA-YKL40/c24 and  $4.1 \pm 3.8$  %ID/g for  $^{111}\text{In}$ -DTPA-YKL40/c41 at 48 hours. And lastly,  $^{177}\text{Lu}$ -DTPA-YKL40 antibodies significantly inhibited tumor growth in ovarian cancer xenograft mice, compared with the control group (PBS).

**Conclusions:** Our preliminary study demonstrated that  $^{111}\text{In}/^{177}\text{Lu}$ -DTPA-YKL40 antibodies could have the potential for the diagnosis and therapy of ovarian cancer in nuclear medicine.

PB-012

## A Dual-motif CAIX Probe as a Nuclear Imaging Agent for Hypoxic Colorectal Carcinoma Detection in Vivo

Siao-Syun Guan, Tse-Zung Liao, Kun-Liang Lin, Yi-Hua Cai, Shiou-Shiow Farn

*Institute of Nuclear Energy Research, Atomic Energy Council, Taoyuan, Taiwan*

**Introduction:** The tumor hypoxic microenvironment influences cancer treatment outcomes, which can be a target for precision medicine. Precision medicine is a biomedical health care strategy that provides personalized diagnosis and medical decision-making to improve quality of life. However, hypoxic molecular imaging can be essential in selecting treatments to match this landscape. Therefore, an accurate diagnosis of the hypoxic tumor microenvironment is urgent to increase the therapeutic effects and survival rate in hypoxic cancer. Carbonic anhydrase IX (CA9) is considered one of the reliable cellular biomarkers of hypoxia. Therefore, we aimed to utilize the CA9 inhibitor and anti-peptide as a dual-motif probe and label indium-111 for hypoxic colorectal cancer (CRC) imaging detection in vivo.

**Methods:** The CA9 targeted peptide (INER-GSS-01) and acetazolamide (AAZ) were conjugated with 1,4,7,10-Tetraazacyclododecane-1,4,7,10-tetraacetic acid (DOTA) and Indium-111 as a hypoxic tumor agent ( $^{111}\text{In-DOTA-AAZ-CA9}$ ) for labeling rate and stability assay. Then, the HCT-15-induced hypoxic animal model was established and intravenously injected with one mCi  $^{111}\text{In-DOTA}$  (control group) and  $^{111}\text{In-DOTA-AAZ-CA9}$  (experimental group). After 24 hours, nanoSPECT / CT was performed to observe the imaging of the radio-agent location. In addition, we also observed the distribution of drugs in animals. Finally, we compared the drug distribution of  $^{111}\text{In-DOTA-AAZ-CA9}$  and  $^{18}\text{F-MISO}$ .

**Results:** The labeling efficiency of  $^{111}\text{In-DOTA-AAZ-CA9}$  was more than 95%. The results displayed that the stability of  $^{111}\text{In-DOTA-AAZ-CA9}$  was preserved at more than 90% for 144 hours in human and mouse serum. The radionuclide imaging was significantly increased in  $^{111}\text{In-DOTA-AAZ-CA9}$ -treated mice compared to  $^{111}\text{In-DOTA}$ -treated mice. For the distributions of  $^{111}\text{In-DOTA-AAZ-CA9}$  in HCT15-induced xenograft mice, the tumor tissue possessed higher signals than the  $^{111}\text{In-DOTA}$ -treated group. Finally, we observed that the  $^{111}\text{In-DOTA-AAZ-CA9}$  tumor accumulative level was higher than  $^{18}\text{F-MISO}$  at 2 hours.

**Conclusions:** We considered that  $^{111}\text{In-DOTA-AAZ-CA9}$  might be applied in CRC patients for hypoxic tumor imaging toward precision medicine.

PB-013

## 基於氟 -18 氟代去氧葡萄糖正子斷層影像的放射組學分析對食道癌進行預後判斷

黃玉晴<sup>1</sup> 龔瑞英<sup>2</sup> 黃靖文<sup>3</sup> 林宜濤<sup>2</sup> 陳志成<sup>1\*</sup> 蔡世傳<sup>2\*</sup>

<sup>1</sup> 國立陽明交通大學 生物醫學影像暨放射科學系 (所)

<sup>2</sup> 台中榮民總醫院 核子醫學科

<sup>3</sup> 台中榮民總醫院 放射腫瘤部

**背景介紹：**食道癌在台灣十大癌症死因中名列第9，且於腸胃道癌症中預後不佳。氟 -18 氟代去氧葡萄糖正子斷層 (F-18 FDG PET/CT) 已廣泛應用於食道癌診斷、分期及追蹤，而放射組學 (radiomics) 則可以提供更多影像上肉眼無法識別的資訊以供分析。本研究採用放射組學分析食道癌的 F-18 FDG PET/CT 影像，以期提供更好的預後判斷，協助臨床進行處置。

**方法：**本研究為回溯性研究，共收集近十年內 (2010~2019) 食道癌治療前的 F-18 FDG PET/CT 影像 93 例並收集這群病人的性別、年齡、病理狀態、分期、處置等臨床資料。PET/CT 影像經人工半自動圈畫 PET 影像後，以 LIFE<sub>x</sub> 程式跑出影像特徵。再利用獨立樣本 T 檢定的方式選出能有效篩選預後之特徵，將影像特徵及臨床資料輸入機器學習模型進行學習，並判斷模型成效。以 5 年無惡化存活期 (Progression free survival) 及整體死亡率 (overall survival) 做為預後評估成效。

**結果：**我們選出 SUV peak in Sphere、Uniformity、GLZLM\_LZLGE 等 7 種可能有效篩選預後之影像特徵。在單獨使用影像特徵所建立的無惡化存活期模型的準確率 (accuracy) 來到 85%，與合併臨床特徵與影像特徵所建立的模型的準確率 85.5% 相近，比單獨使用臨床特徵的模型的 67.7% 來的佳。而後利用資料擴充 (data boost) 的方式可以獲得更好的準確率 93.4%。在整體死亡率模型中，合併臨床特徵與影像特徵建立的模型準確率來到 85.5%，單獨使用影像特徵的模型準確率 87%，均較單獨使用臨床特徵的 58% 為佳。另外在資料擴充後的整體死亡率模型準確率達 99.3%。

**結論：**經由我們選出的放射組學影像特徵及機器學習的結果顯示食道癌病患的治療前 F-18 FDG PET 影像特徵分析對於預後判斷有較高的利用價值。因此食道癌病患治療前的 F-18 FDG PET/CT 影像結合放射組學特徵分析建模應該可以有效增進病患預後之預測，並因此在病患處置上提供更適合的建議，提升對病患個人化醫療的效果。將來若能增加影像資料使模型基底之數據庫資料量提升，應可將模型準確率提升至臨床可用的程度。

PB-014

## Preclinical Selection Platform for Radiolabeled-FAPI Drugs by *in vitro* Binding and SPECT/CT Imaging

Liang-Cheng Chen, Wei-Lin Lo, Sheng-Nan Lo, Chu-Pang Yen,  
Yun-Sheng Lin, Shiou-Shiow Farn

*Institute of Nuclear Energy Research, Taoyuan, Taiwan*

**Introduction:** Cancer associated fibroblasts are one of the major components of stromal cells and they were presented in more than 90% of epithelial cancers (such as pancreatic cancer, colorectal cancer, and breast cancer). Fibroblast activation protein has been confirmed to be overexpressed in tumor-associated fibroblasts of many solid tumors, and its activity is related to cancer development, cancer cell migration and cancer spread. The aim of this study is to explore the *in vitro* binding and nano-SPECT/CT imaging of radiolabeled-fibroblast activation protein inhibitor (FAPI) in cancer cell line for evaluation of the new FAPI drugs.

**Materials and methods:** The precursors of FAPI-04 and FAPI-46 were purchased from NAMICROBIO Co., LTD. After labeled with Lu-177, the labeling efficiencies were analyzed by radio-TLC and radio-HPLC system. Cell binding studies with <sup>177</sup>Lu-radiolabeled FAPIs were performed using HEK-293 (low FAP expression) and HEK-293-FAP (FAP-transfected HEK-293 cells;  $3 \times 10^6$  cells/tube, n = 4). After incubation at 37°C for 4 h, the samples were centrifuged and washed twice with cold phosphate-buffered saline. Each sample was counted in a gamma-counter (Wizard 1480; Perkin-Elmer). Cell bound radioactivity (%) was calculated using cell bound radioactivity / total radioactivity x 100. HT-29 cells were subcutaneously inoculated in BALB/c nude mice. After intravenous injection of <sup>177</sup>Lu-FAPI-04 and <sup>177</sup>Lu-FAPI-46, the HT-29 tumor-bearing mice were anesthetized and imaged at 1, 4 and 24 h by nano-SPECT/CT, respectively.

**Results:** The labeling efficiencies of <sup>177</sup>Lu-FAPI-04 and <sup>177</sup>Lu-FAPI-46 were more than 90%. The cellular binding efficiency in HEK-293-FAP cells showed higher uptake than that of control groups (HEK-293) at 4 h. SPECT/CT images showed there were high uptake of <sup>177</sup>Lu-FAPI-04 and <sup>177</sup>Lu-FAPI-46 in bladder and HT-29 tumors at 1 h and 4 h; it revealed clearance in tumors at 24 h.

**Conclusions:** In our research, the radiolabeled FAPI molecules, <sup>177</sup>Lu-FAPI-04 and <sup>177</sup>Lu-FAPI-46, showed specific characteristics in *in vitro* cell binding and *in vivo* SPECT/CT in tumor-bearing model. We suggested that this selection platform may provide useful information for development new FAPI drug in the future in Taiwan.

PB-015

## Development and Evaluation of Luteinizing Hormone-releasing Hormone Antagonists on Triple Negative Breast Tumor-bearing Model by SPECT/CT Imaging

Mao-Chi Weng, Kai-Hung Cheng, Shiou-Shiow Farn

*Institute of Nuclear Energy Research, Taoyuan, Taiwan*

**Introduction:** Triple negative breast cancer (TNBC) that is lack of diagnostic and effective therapeutic agents was clinically considered a subtype with low survival rate of human breast cancer patients. As we know, agonists and antagonists specific for receptors of luteinizing hormone-releasing hormone (LHRH-R), which is reported as potential targets for TNBC, are still under investigation as yet. In previous study, we have evaluated a peptidic abarelix-based antagonist, DOTA-LHRH, which revealed specific uptake in TNBC tumors. In this study, a cetorelix-based antagonist, DOTA-LHRH-C, has been newly developed and also proved an effective strategy for in vivo uses by SPECT/CT imaging.

**Materials and methods:** The cetorelix antagonist was first conjugated with a DOTA chelator; after radiolabeled with In-111, the radiochemical purity (R.C.P.) was analyzed by a radio-TLC system. HCC 1806 cells were incubated and subcutaneously inoculated on mice. After intravenous (i.v.) injection of  $^{111}\text{In}$ -DOTA-LHRH-C, HCC 1806-bearing mice were anesthetized and imaged at 1, 4 and 24 h by a SPECT/CT, respectively. The bio-distribution test of  $^{111}\text{In}$ -DOTA-LHRH-C in HCC 1806-bearing mice was also investigated at 1, 4 and 24 h, respectively.

**Results:** The R.C.P. of  $^{111}\text{In}$ -DOTA-LHRH-C was determined  $> 90\%$  by radio-TLC. SPECT/CT imaging data showed that  $^{111}\text{In}$ -DOTA-LHRH-C was first collected in liver, kidney and tumors and retained in those within 24 h. In results of bio-distribution,  $^{111}\text{In}$ -DOTA-LHRH-C was mainly collected in lung, kidney, liver and HCC 1806 tumors at 1, 4 and 24 h. The tumor-to-muscle count ratio (T/M) is calculated as  $2.18 \pm 0.68$  and the tumor-to-brain count ratio (T/B) is  $4.33 \pm 1.05$  at 24 h, respectively; it also demonstrated similar results in comparison with those of DOTA-LHRH. (T/M is  $3.88 \pm 0.34$  and T/B is  $17.23 \pm 0.25$  at 24 h, respectively.)

**Conclusions:** This study has evaluated the characteristics of a cetorelix-based antagonist for LHRH-R over-expressive tumors in vivo. We suggested that DOTA-LHRH-C for further diagnostic research and comparing with DOTA-LHRH in vitro and in vivo, respectively. We think they may both provide innovative information for development of TNBC patient's treatment strategies in the future in Taiwan.



PB-016

## Scale-up and Purity Analysis of Lu-175-PSMA-INER-56

Su-Jung Chen, Sheng-Nan Lo, An-Chi Lu, Shiou-Shiow Farn

*Department of Isotope Application Division, Institute of Nuclear Energy research, Taoyuan, Taiwan*

**Introduction:** Lu-177-PSMA-INER-56 is a long-acting radiotherapy drug for prostate cancer, which can quickly reach the tumor location and accumulate for up to 96 hours. Based on the efficacy results in LNCaP and PC3 tumor-bearing animal models, Lu-177-PSMA-INER-56 can be accumulated in the liver and kidney, which were rapidly eliminated within 24 hours. Gram-level of Lu-175-PSMA-INER-56 will be synthesized for the GLP toxicology and safety test. This study aimed to develop the scale-up process and purity analysis of Lu-175-PSMA-INER-56 and evaluate it as a potential drug.

**Methods:** PSMA-INER-56, a long-circulation PSMA-targeted molecule, has high purity (> 95%) by HPLC quality control. The 100~900 mg amount of PSMA-INER-56, was incubated with 8-88 mg  $^{175}\text{LuCl}_3$  in 1 M sodium acetate solution (pH 5-6) at 95°C for 30-40 min. The crude Lu-175-PSMA-INER-56 was separated through the MPLC and C-18 columns. After purity analysis of the collected aqueous, samples were drying-freeze to get the powder. Final products of Lu-175-PSMA-INER-56 were quality controlled by HPLC and LC-Mass.

**Results:** The final amount of Lu-175-PSMA-INER-56 was 1100 mg, and that purity was greater than 95% by HPLC analysis. Sample recovery yield was from 45% to 65%. In chelation, the mole ration of PSMA-INER-56 / Lu-175 is 4.5 (with 100 mg precursors, 88 mg of  $^{175}\text{LuCl}_3$ , pH 5, at 95°C, reacting 40 min), and the total reacting volume can control to 6 mL. After LC-Mass analysis, the final product can be detected  $[\text{M} + \text{H}]^+ 1615$ , Lu-175-PSMA-INER-56.

**Conclusions:** The development of gram-level Lu-175-PSMA-INER-56 can apply to PSMA-targeted peptides. This amount of Lu-175-PSMA-INER-56 was used for the GLP toxicology & safety test, and that can be as a reference to the stability experiment in the future.

PB-017

## 利用田口方法分析 Tc-99m MDP 骨掃描最佳影像解析度參數

黃信慈<sup>1,2</sup> 潘榕光<sup>1</sup> 陳慶元<sup>2</sup>

<sup>1</sup> 中臺科技大學 醫學影像暨放射科學系

<sup>2</sup> 佛教慈濟醫療財團法人台中慈濟醫院核子醫學科

**目的：**核醫骨骼掃描具有高敏感度及早期偵測骨骼病灶的能力，因此廣泛應用於臨床鑑別診斷，亦為核醫檢查中最重要的項目之一。然核醫影像的空間解析度與對比度品質仍為成像時的缺口，因此，導入田口方法與使用塊規假體驗證，分析最佳化條件組合，以提升該品質，讓核醫骨骼掃描成為骨骼病變的最佳影像檢查方法。

**材料方法：**此實驗利用田口  $L_{18}$  直交表，進行 18 組實驗，臨床將骨掃描常用攝影參數選擇五個因子為 (距離、總計數、放大倍率、距陣大小、能窗) 及三個水準，將 1 mCi 的 Tc-99m MDP 加入 20 c.c. 的生理食鹽水內，用藍色墨水染色後，注入塊規假體內並進行攝影，使用儀器為 GE Discovery NM/CT 860。掃描影像收集共計十八張，以直觀影像品質分析法 (VGA)，邀請四位放射師進行影像品質排序，最優為 18 分，最低為 1 分進行評分。

**結果：**田口方法中信號 / 雜訊比 (SNR) 可作為參數設計對產品或製程品質改善之指標，進而提升品質及達到產品特性之目的。同仁評分出十八張中最優的影像結果為第七張，得出最佳化的條件參數為距離 (5 cm)、總計數 (225 k)、放大倍率 (1)、距陣大小 (256 x 256)、能窗 (5%)。

**結論：**此研究驗證田口方法可找出影像空間解析度最佳化之參數進行檢查，提升靜態取像時的影像品質，臨床上可輔助醫師判讀，提高診斷率並掌握病程的進展及預測。

PB-018

## 精準診療正子藥物調製之優良調劑作業策略

李銘忻 洪綾蔓 林亭君 楊詩涵 楊橙凌 黃玉儀

和信治癌中心醫院核子醫學科

**背景介紹：**‘See what you treat and treat what you see, at a molecular level’，腫瘤診療時代的新座右銘。精準診療創新藥物 (Theranostic Innovation) 主要為成對型診療核醫藥物 (Theranostic Pair Radiopharmaceutical) 所組構，治療前病患須先使用與治療藥物相同藥效團 (Pharmacophore Motif) 之正子診斷藥物進行診斷。為實踐精準診療於臨床應用，其相關藥物之調劑作業需符合醫療安全暨品質相關法規。2022 年起，正子中心藥物調劑由衛生福利部食品藥物管理署 (TFDA) 稽核管理，目前有北部 2 家與東部 1 家正子中心已經接受過稽核，相關待改善事項涵蓋無塵室動線設計、通風空調 HVAC 系統、生產 A/B/C 級區完整性與微粒子監控、產品製程確效與分析方法確效、原物料供應與儲存管理、CAPA/OOS、產品放行、資料完整性、文件作業與風險品質管理。其中 A 級無菌區品質系統與 PIC/S GMP 品質風險管理的執行，對 TFDA 每 2 年一次的正子中心例行查核或新藥物查核有決定性影響。

**方法：**為符合藥物之調劑作業所需符合品質相關法規，進行下列策略方法：

1. 建立正子藥物品質風險系統與確效布局：  
進行策略規劃擬定正子藥物生產用無菌無塵室設計及採購規劃，使之成為一個合法、安全、穩定的生產正子藥品場所。
2. 先期性方式運作品質風險系統與確效手段：  
每一個設備與程序步驟都經由品質風險的確效程序控管，使得正子藥物調劑在保證品質與風險控管情況下，不會造成交叉污染，對藥品及人員皆能獲得保障，並有效降低因設計不周而增加之確效程序與時間成本。
3. 回溯性方法運作品質風險系統與確效：  
使用知識管理系統與年度產品品質評估結果，進行藥物品質風險管制、溝通及檢討。
4. 引入創新技術增強品質風險系統管理：  
產線 B 級區合成後於 A 級區分裝，為增強產品品質與降低風險，任何進入 A 級區之物品與原料，均需在 prechamber 經過 H<sub>2</sub>O<sub>2</sub> 滅菌；在 B 級區自動化合成，純化後之藥物經由 closed tubing set 傳送至 A 級區正壓環境，進行 0.22 um 濾膜除菌，降低 A/B 級區汙染之風險。

**結論：**為提供癌症病人更精準的癌症診療技術，迎接核子醫學界最新的突破與契機，本機構建構藥廠等級的高規格正子藥物調製環境與品質風險管理系統，以因應 TFDA 之稽核管理。整廠系統流程設計與品質風險評估是其中最為艱難與複雜的部分。經由上述 4 策略之執行，發現 do the right thing 的策略規劃與創新技術的導入，有助於大量降低品質風險與確效成本，以新流程與新技術提升正子藥物調劑製程可靠度。

PB-019

## Fractionated Elution using the MON.TEK $^{99}\text{Mo}/^{99\text{m}}\text{Tc}$ Generator

Wen-Yi Chang, Yuan-Chung Wu, Hsin-Chun Lin, Nan-Jing Peng

*Department of Nuclear Medicine, Taipei Veterans General Hospital, Taipei, Taiwan*

**Introduction:** The MON.TEK  $^{99}\text{Mo}/^{99\text{m}}\text{Tc}$  generator was designed to allow dry column shipment and automatized conception. A high Tc-99m radioactive concentration is required in a subset of radiopharmacy procedures. Fractionated elution can be a useful tool to meet this requirement, especially when current elution is close to the generator expiration date. The aim of our study was to assess MON.TEK  $^{99}\text{Mo}/^{99\text{m}}\text{Tc}$  generator elution kinetics and to determine the optimal fractionated elution volume to fit with procedures requiring the highest Tc-99m radioactive concentration in clinical use.

**Methods:** After duplicate elution at several predetermined elution days, the activity of each eluate with same volume about 1 mL (total 6 mL) were measured which were assessed on MON.TEK  $^{99}\text{Mo}/^{99\text{m}}\text{Tc}$  generators calibrated at 30 or 50 GBq.

**Results:** The entire volume of 6 mL was collected and measure activity. The highest activity was obtained with the second elute. Radio-activity of elutions were plotted to obtain elution kinetics with the corresponding curve fitting.

**Conclusions:** Our study describes MON.TEK  $^{99}\text{Mo}/^{99\text{m}}\text{Tc}$  generators elution kinetics and provides data to easily handle fractionated elution in the context of radiopharmaceutical preparations for clinical use.

PB-020

## 固體胃排空檢查藥物與輔助食材製備之探討

林欣蕓 張文議 陳苓仕 吳元鍾 彭南靖

臺北榮民總醫院核醫部

**背景介紹：**胃腸道動力和功能的障礙，可能會導致胃排空時間的延遲或加速，造成包括噁心、嘔吐、易飽、飽脹、腹脹、腹部不適或疼痛等症狀，影響病人消化吸收與營養攝取。因此，評估病人胃排空的時間是重要的。測量胃排空的標準技術是透過放射性核種標記的輔助食材，進行閃爍攝影，以評估胃排空時間。本研究探討以鎝 -99m-MAA 與蛋白標記為輔助食材之製備程序。

**方法：**依據文獻將 3 顆雞蛋的液體蛋白 (約 118 mL) 與 1-1.5 mCi 鎝 -99m-MAA 混和，使用微波爐加熱至凝固。將兩片白吐司塗上 30 公克草莓果醬，與已結合鎝 -99m-MAA 之固體蛋白組成三明治，配合 120 mL 白開水一併服下。於攝入檢查餐後立即、以及每隔一小時 (1 小時、2 小時、3 小時、4 小時) 以 GE NM 870 CZT 進行動態或靜態造影。

**結果：**比較液體蛋白與鎝 -99m-MAA 混和後之攪拌時機；一、於二者混和後立即攪拌，微波加熱至凝固 (700 W，60 秒)。二、於混和後立即攪拌，微波加熱至半流體 (700 W，30 秒)，取出攪拌第二次，微波加熱至凝固 (700 W，40 秒)。比較二種製備方法，於攝取完後立即造影之影像。方法一取得之影像，胃部有斑駁顯像。方法二所取得之影像，為胃部完整之影像。

**結論：**液體蛋白與鎝 -99m-MAA 兩者有良好的結合，製備過程中經二次混和後，可取得胃部完整影像，為進一步胃排空時間之評估，提供更準確之結果。

PB-021

## 放射性物質安全管理\_iLab 系統

呂惠敏<sup>1</sup> 余誠泰<sup>2</sup> 郭婕<sup>2</sup> 黃淑慈<sup>2</sup> 魏玉雲<sup>3</sup>  
李岱芬<sup>4</sup> 陳建榮<sup>1</sup> 黃奕琿<sup>1</sup> 彭信逢<sup>1,5</sup>

<sup>1</sup> 國立臺灣大學醫學院附設醫院核子醫學部

<sup>2</sup> 國立臺灣大學醫學院附設醫院資訊室

<sup>3</sup> 國立臺灣大學醫學院附設醫院安全衛生室

<sup>4</sup> 國立臺灣大學醫學院附設醫院檢驗醫學部

<sup>5</sup> 國立臺灣大學醫學院

**背景介紹：**各類實驗場所經常被視為具有潛在危害風險的威脅之一，實驗場所的安全管理在本院專業分工的前提下，分屬多個單位負責，例如化學品由安全衛生室負責、感染性生物材料由檢驗醫學部負責、放射性物質由核子醫學部負責等，導致實驗場所的各項危害資訊分散，同時各個實驗場所具有的危害特性及現場狀況缺少整合機制，甚至對於場所在緊急應變的整備能力亦無明確資料，連帶影響院內危害風險的全面評估及控管措施，也造成針對全院實驗場所的安全管理成效難以綜觀掌握。

**方法：**本院安全衛生室、檢驗醫學部(生物安全會)、核子醫學部(輻射防護管理委員會)以及資訊室共同組成「實驗場所安全管理團隊」，以全面整合有關實驗場所安全管理事項，並重新檢討現行管理問題，訂定本院實驗場所安全管理策略目標：增強制度管理、強化危害風險管制、及加強場所災害預防整備能力，並自 2017 年起開始開發本院實驗場所 E 化管理系統－iLab 系統。

**結果：**2019 年正式上線啓用，藉由 iLab 系統加強各實驗場所的危害性物質運作安全控管、研究人員管理與其安全教育訓練資格查核以及環境設施安全稽查等管理措施，同時縮短院內危害物質請購，協助全院實驗場所提升安全維護成效，並提供有效率的研究支援服務，達成零災害、零罰鍰之目標。

**結論：**本院實驗場所安全管理團隊透過 iLab 系統的開發，應用資訊平台建立起管理的基礎架構，改善申請的審查時效，解決長期以來實驗場所危害資訊不明及人員安全維護的困擾，並嘗試強化實驗場所地理圖資功能，讓本院在各類實驗場所的安全管理獲得提升，配合本院地理資訊系統的開發期程，本院 iLab 系統的各項危害物資料，可望利用 web 版編輯功能，增設 GIS 圖層以顯示危害相對位置，可作為院區空間利用及再造之參考，對於醫療作業環境及病人安全維護更能獲得保障。

PB-022

## The Radiosynthesis of [ $^{18}\text{F}$ ] THK5351 by Eckert-Ziegler Modular-Lab System

Chun-Tse Hung, Geng-Ying Li, Chi-Wei Chang, Min-Tzu Ku,  
Shih-Pei Chen, Wen-Yi Chang, Nan-Jing Peng

*Department of Nuclear Medicine, National PET/Cyclotron Center, Veterans General Hospital, Taipei, Taiwan*

**Introduction:** [ $^{18}\text{F}$ ]THK5351 used in Neurofibrillary Pathology imaging must be highly sensitive and specific for tau protein fibrils in Alzheimer Disease. [ $^{18}\text{F}$ ]THK5351 was used for animal imaging study by using microPET/MR in out center. Reliable procedure of [ $^{18}\text{F}$ ]THK5351 in cGMP conditions was developed by Modular-Lab system.

**Methods:** For the radiosynthesis, cyclotron-produced [ $^{18}\text{F}$ ]fluoride ( $^{18}\text{O}(\text{p},\text{n})^{18}\text{F}$ ) was transferred to the Modular-Lab system and fixed on a QMA cartridge. The activity was eluted from the cartridge with 1.1 mL of a potassium carbonate (12 mg/mL water) and Kryptofix (12.5 mg/mL acetonitrile) solution in water / acetonitrile 1/4 and transferred to the reactor by nitrogen. The complex was azeotropically dried at 120°C by addition of 1.6 mL of acetonitrile. After complete drying, 5 mg of the THK5352 precursor in 0.6 mL of DMSO was added to the activated and dried [ $^{18}\text{F}$ ]fluoride/K2.2.2 complex and the reaction vessel was heated at 100°C for 10 min. The reaction was quenched with 1 mL of 1 N HCl and mixed with 1 mL 1 N AcOK and the crude product was purified by a semi-preparative HPLC column (YMC-Actus Triart C18 250 x 20 mm I.D S-5  $\mu\text{m}$ , 12 nm) and eluted with a solution of 20 mM  $\text{NaH}_2\text{PO}_4$  and acetonitrile (65/35, flow at 5 mL/min). The fraction containing the product was collected and mixed with 40 mL of water. Subsequently, [ $^{18}\text{F}$ ]THK5351 was trapped on a pre-conditioned (10 mL ethanol and 20 mL water) tC18plus SepPak cartridge and acetonitrile was washed off by rinsing tC18plus SepPak cartridge with water. The product ([ $^{18}\text{F}$ ]THK5351) was eluted with ethanol (0.9 mL) and formulated with normal saline (9 mL).

**Results:** The sterile [ $^{18}\text{F}$ ]THK5351 was produced in 120 min with greater than 99% radiochemical purity. The quality control was in accordance to the guidelines of the European Pharmacopoeia with a mean 8.11% EOS yield and 133.98 GBq/ $\mu\text{mol}$  ( $n = 4$ ).

**Conclusions:** The routine production of [ $^{18}\text{F}$ ]THK5351 proved to be reliable and stable. [ $^{18}\text{F}$ ]THK5351 of the Ph.Eur. quality could be used for clinical study by using PET/MR in the future.

PB-023

## Rapid and Convenient Production in a New Synthesizer, ORA Neptis Mosaic RS of $^{18}\text{F}$ -Choline, in GMP Compliance

Geng-Ying Li, Chun-Tse Hung, Wen-Yi Chang, Min-Tzu Ku,  
Shih-Pei Chen, Nan-Jing Peng

*Department of Nuclear Medicine, National PET/Cyclotron Center, Veterans General Hospital, Taipei, Taiwan*

**Introduction:** National PET/Cyclotron Center, Veterans General Hospital, Taipei (VTGH) installed a new synthesizer ORA Neptis Mosaic RS and Perform in May 2021 to replace Tracer-Lab MXFDG Coincidence synthesizer for  $^{18}\text{F}$ -FDG synthesis which synthesis and quality control are approval by the US FDA. In recent year prostate cancer is ranked in the chart of the top ten cancer mortality rate in Taiwan. Several studies have mentioned that  $^{18}\text{F}$ -Choline can effectively diagnose prostate cancer in positron emission tomography / computed tomography (PET/CT) modality. Different from the more complicated production process used in the past, We make  $^{18}\text{F}$ -Choline easy to obtain and comply with Good Manufacturing Practice (GMP) regulations.

**Methods:**  $^{18}\text{F}$ -Choline was prepared from nucleophilic substitution reaction and used dibromo methane (DBM) and N, N dimethylaminoethanol (DMEA) as primary and secondary precursors with ORA Neptis Mosaic RS System. [ $^{18}\text{F}$ ]fluoride was produced with a Scanditronix MC17F cyclotron by proton irradiation of 98% enriched [ $^{18}\text{O}$ ]water with 40  $\mu\text{Ah}$  beam current integration then transferred to the Mosaic RS system and trapped in a pre-conditioned QMA cartridge. Elution buffer containing 0.075 M tetrabutylammonium bicarbonate ( $\text{TBA.HCO}_3$ ) solution was used to elute the activity into reaction vial then water was evaporated azeotropically to dryness by adding acetonitrile. After completely drying, a solution of dibromo methane (0.1 ml) in 3 ml of acetonitrile was added to the dried residue, by maintaining a temperature of  $120^\circ\text{C}$  over 280 seconds to produce ( $^{18}\text{F}$ ) $\text{BrCH}_2\text{F}$ . The raw product purified by four Sep-Pak<sup>®</sup> Plus silica cartridges, and gone through a Sep-Pak<sup>®</sup> Plus C18 cartridge to react, which was loaded dimethylethanolamine (0.3 ml). At the final purification step, the raw was passed Sep-Pak<sup>®</sup> Plus CM cartridge and eluted with buffer and saline solution underwent a 0.22  $\mu\text{m}$  sterile filter to sterile vial. All cassettes and reagents were manufactured under GMP condition by ABX Advanced Biochemicals (Radeberg, Germany).

**Results:** The GMP-Compliant [ $^{18}\text{F}$ ]Choline was produced in 50 min, Overall yield was  $25 \pm 1\%$  ( $n = 5$ ) with greater than 99% radiochemical purity.

**Conclusions:** [ $^{18}\text{F}$ ]Choline of the cGMP quality could be promoted to clinical study for cancer diagnosis in the future.



PB-024

## 以加馬計數儀之品管計數值與各品管數據之相關性研究 —以南部某核醫科放射免疫分析實驗室為例

張淑芬 卓世傑 顏吉龍 張朝鈞 曾宜玲 段淑薰 李將瑄

奇美醫療財團法人奇美醫院核子醫學科

**背景介紹：**加馬計數儀是放射免疫分析室中，準確測量檢驗值以決定檢驗結果的重要儀器。因此為了確保加馬計數儀的準確，作業前必須對加馬計數儀進行 QC 測試。加馬計數儀的 QC 測試通常是以實驗室使用之同位素射源作為品管計數值之依據，再計算出相關之品管數據，例如 Peak Devition Resolution 及 Horrocks Efficiency 等。由於較低的放射性計數值會導致較高的隨機誤差，所以品管計數值之大小，即有可能影響各品管數據之高低。因此，究竟品管計數值之大小與品管數據之高低是否相關，是值得深入研究的。本文即為探討加馬計數儀品管計數值與各品管數據是否相關之研究。

**方法：**1. 以南部某醫院核醫科放射免疫分析室，Perkin Elmer 公司 Wizard-1470-020 型，序號 4702714 之加馬計數儀共 10 支計數管，作為研究分析之儀器數據來源。2. 紀錄自 111 年 1 月 3 日至 4 月 29 日止，將 10 支計數管，各分為 10 組資料，每組包含品管計數值與 Peak Devition Resolution 及 Horrocks Efficiency 等 4 類數據，各 78 筆。3. 整理、統計，品管計數值與 Peak Devition Resolution 及 Horrocks Efficiency 等品管數據之相關性，以提出結果。

**結果：**1. 所有 1 至 10 號管的品管計數值中，平均值依序為 61069,61215,61089, 61148,59506,60855,60204,60160,59755,59956。2. Peak Devition 之值由 1 至 10 號管的平均依序則為 3.61,2.65,3.89,5.39,3.89,2.05,3.15,4.85,3.46,4.15。3. Resolution 之數值，自 1 至 10 號管的平均值依序為 25.69,24.13,22.09,21.37,23.85,24.39,23.24, 22.52,22.29,24.31。4. Horrocks Efficiency 的數值中，1 至 10 號管的平均值依序為 83.39,83.01,83.48,83.56,81.37,83.26,82.28,82.34,81.72,82.23%。5. 品管計數值 1 至 10 號管與 Peak Devition 之相關性依序為 -0.06,0.18,-0.39,-0.50,-0.35,-0.65,-0.35, -0.44,-0.46,-0.04。6. 品管計數值 1 至 10 號管與 Resolution 之相關性依序為 -0.08, 0.41,-0.22,-0.10,0.04,0.11,-0.22,0.15,0.09,0.03。7. 品管計數值 1 至 10 號管與 Horrocks Efficiency 之相關性依序為 0.15,-0.13,-0.07,0.00,-0.10,0.15,0.00,-0.03,-0.06,0.20。

**結論：**研究顯示，南部某醫院核醫科放射免疫分析室之加馬計數儀，品管計數值與各品管數據間多無明顯之相關性，反而計數管各管間之平均計數值差距較為明顯，因此應加強調校各計數管之參數，使各計數管之計數值較為一致。

PB-025

## 作業量與放射性廢棄物產出暨輻射劑量率關係之研究 —以南部某醫院核醫科放射免疫分析室為例

張朝鈞 卓世傑 顏吉龍 張淑芬 曾宜玲 段淑薰 李將瑄

奇美醫療財團法人奇美醫院核子醫學科

**背景介紹：**放射免疫分析室之檢驗作業，將產出一定比例含輻射劑量之放射性廢棄物。此放射性廢棄物之多少與劑量率之高低，基於安全與法規規定，是放射免疫分析室作業安全與場所使用必要且關切的事項之一。依經驗法則來說，放射免疫分析室檢驗作業量之多寡，應該會直接影響放射性廢棄物產出之數量，以及輻射劑量率之高低。不過，究竟是否如此，則較少此類的研究可供參考。因此增進此方面之研究，應該是值得努力的。本文即為探討，作業量與放射性廢棄物產出暨輻射劑量率關係之研究。

**方法：**1. 紀錄 2020 年 12 月 4 日至 2022 年 6 月 30 日止，每次放射性廢棄物(試管)外釋之日期、重量與輻射劑量率(距離 5 公分處)，共 220 筆。2. 收集自 2020 年 12 月至 2022 年 6 月之每月檢體作業量共 19 筆，選取數量最少之月份設為 1，其餘各月份之數量依比例轉換。3. 將放射性廢棄物之重量與劑量率資料，分別依月份加總，重量部份則選取數量最少之月份設為 1，其餘各月份之數量依比例轉換。4. 整理、統計，前三項作業量、廢棄物重量與劑量率等相關數據，以提出結果。

**結果：**1. 作業量比值、廢棄物重量比值與劑量率依月份各加總為 19 筆，平均數分別為 1.54、1.38 與 3.16 uSv/h。2. 經相關性統計結果，發現作業量比值與廢棄物重量比值之相關性為 0.43，廢棄物重量比值與劑量率之相關性為 0.28，作業量比值與劑量率之相關性則為 0.32，三者均未達 0.5 以上之良好相關。3. 經迴歸統計結果，發現作業量比值與廢棄物重量比值之線性迴歸關係式  $f(x) = 0.32X + 0.89$ ， $R^2$  為 0.185，作業量比值與劑量率相應之線性迴歸關係式則為  $f(x) = 1.24X + 1.26$ ， $R^2$  為 0.102，顯示作業量比值不論是與廢棄物重量比值或劑量率方面之迴歸，均缺乏相關性。

**結論：**本研究顯示，南部某醫院核醫科放射免疫分析室之作業量多少與廢棄物重量或輻射劑量率可能並無明顯之相關性。但其作業量比值與廢棄物的產出重量比值，略高於與劑量率相關性之原因，可能是由於該實驗室作業量並未細分使用試劑輻射活度不同之檢驗項目所造成。

PB-026

## 釷 90 治療微球體之輻射防護研究 – 以 SIR-Spheres 為例

卓世傑 陳興隆 林凡珍 張南雄 鄭揚霖 顏玉安 李將瑄

奇美醫療財團法人奇美醫院核子醫學科

**背景介紹：**釷 90 治療，是使用帶有放射性物質釷 90 的「微球體」(microsphere)，注入病人體內，以進行治療的方法。由於釷 90 治療所使用的微球體直徑僅 20-60  $\mu\text{m}$ ，約為人類頭髮的 1/4 左右。因此乾燥的微球體即是所謂的懸浮粒子 (suspended particle)，為可懸浮在空氣中之粒狀物質。此與所謂的氣態放射性物質，例如 Xe-133 等的輻射防護要求與方法有很大的不同，頗值得探討。本文即是針對釷 90 治療微球體之輻射防護研究。

**方法：**1. 收集 SIR TeX 所生產之 SIR-Spheres 釷 90 微球體治療藥劑仿單。2. 收集釷 90 治療之輻射防護相關文獻。3. 收集釷 90 治療之輻射防護之實際經驗。4. 彙整提出輻射防護之可行原則。

**結果：**1. 微球體之材質為樹脂，直徑約 20-60  $\mu\text{m}$ ，可滾動且彈性良好，乾燥後可懸浮於空氣中，內含之釷 90 為純  $\beta$  射源，最大能量為 2.27 MeV，平均能量為 0.93 MeV，半衰期為 64.1 小時，於空氣中最大射程為 1062 cm。2. 每瓶藥劑含 3 GBq 之釷 90，每個微球體所含的比活度為 40-70 Bq，每瓶有 40-80\*10<sup>6</sup> 個微球體混合於 5 ml 之注射用水中。3. 據文獻估計，注射後病人可能造成的體外污染，最大約為注射劑量的 0.4%，即 12 MBq (3 GBq\*0.4%)。4. 進行釷 90 治療作業時，於藥劑調配與藥劑注射階段，也可能造成污染，經實際測量已經過約 11 個半衰期之釷 90 治療藥劑調配階段廢棄物，其 5 公分距離之輻射活度為 19862 CPM (已經儀器效率調整)，換算回藥劑調配階段之污染值約為 0.68MBq，低於文獻估計。

**結論：**依據結果所示，微球體雖為固態但由於質輕微小，可滾動且彈性良好，乾燥後並可懸浮於空氣中且極易造成污染之特性，因此歸納之可行輻射防護原則如下：一、工作人員應全身嚴密防護。二、盡量縮小必要之工作範圍，且需考慮密封及負壓作業之可能。三、因其為固態，除污應盡量以膠帶黏附或以 Scrubbing Bubbles 噴灑後以紙巾吸附移除。四、廢棄物應切實依照污染活度高低妥善分類，避免儲放時間不必要之增加。

PB-027

## 免疫放射分析法與化學冷光免疫分析法 測定促甲狀腺激素結果差異分析

陳佳伶 賴建甫 陳郁茵 汪姍瑩 蕭聿謙 吳彥雯

亞東紀念醫院核子醫學科

**目的：**促甲狀腺激素 (Thyroid-stimulating hormone; TSH) 是受腦部下視丘和血液中甲狀腺素所調控的，下視丘分泌的促甲狀腺素釋放激素 (TRH) 可以刺激腦下垂體前葉分泌 TSH，而 TSH 可以促使甲狀腺製造更多甲狀腺素，當血液中游離甲狀腺素 (free T4) 濃度升高時，會負回饋抑制腦下垂體 TSH 的分泌。TSH 的分泌對血液中游離甲狀腺素非常敏感，所以 TSH 的檢測已成為鑑別診斷 甲狀腺功能低下症和甲狀腺功能亢進症及其亞臨床甲狀腺疾病的主要試驗。由於發現臨床 TSH 的開單數以化學冷光免疫分析法佔大多數，所以本研究將分別用免疫放射分析法 (IRMA) 及化學冷光免疫分析法 (CLIA) 對 TSH 做檢測，並比較其結果。

**材料方法：**本實驗於 2022/08/24 至 2022/08/26 間，收集 53 支血液檢體，離心取上清液。分別使用 BECKMAN COULTER IMMUNOTECH TSH IRMA 試劑和 SIEMENS IMMULITE 2000 第三代 TSH 試劑進行檢測，並比較其結果。IRMA 試劑之量測區間為 0.04-50  $\mu\text{IU/mL}$ ，參考值 0.3-5.0  $\mu\text{IU/mL}$ ，分析敏感度 0.04  $\mu\text{IU/mL}$ ，校正物質已經利用國際標準品 WHO 3<sup>rd</sup> IS 2003 81/565 進行過校正。CLIA 第三代試劑之量測區間為 0.004-75  $\mu\text{IU/mL}$ ，參考值 0.4-4.0  $\mu\text{IU/mL}$ ，分析敏感度 0.004  $\mu\text{IU/mL}$ ，校正物質已經利用國際標準品 WHO 2<sup>nd</sup> IRP 80/558 進行過校正。

**結果：**本研究統計方法採用 Paired sample t-test，檢定結果 t 值為 7.226，顯著性 P 值為  $< 0.001$ ，其結果顯示 IRMA 和 CLIA 兩組數據具有顯著性的差異，且 IRMA 的值高於 CLIA。執行迴歸分析後，發現其判定係數  $R^2$  為 0.984，偏迴歸係數值為 1.575，且顯著，故建立迴歸模型為： $Y = 1.575(X) - 0.03$ ，此模型的解釋能力達 0.984，顯示兩種方法的檢測結果具有高度相關性。

**結論：**評估甲狀腺功能異常時，測量血清中的 TSH 是最佳的初步判斷的依據，通常 TSH 大於 0.1  $\mu\text{IU/mL}$  應該可以排除甲狀腺亢進的可能。而 TSH 值明顯升高大於 20  $\mu\text{IU/mL}$  則證實是原發性甲狀腺功能低下症。本研究所使用之試劑其敏感度皆小於 0.1  $\mu\text{IU/mL}$ ，最大可測量值皆大於 20  $\mu\text{IU/mL}$ ，故兩種分析方法都適用於臨床診斷。本實驗結果顯示 TSH 以 IRMA 檢測的值高於 CLIA 檢測結果且具有高度相關性，推測可能是因為兩種分析方法的校正物質濃度的差異所引起的，但由於樣本數較少且樣本未平均涵蓋低中高值，此結果仍需進一步研究證實。

PB-028

## 「核研心交碘 -123 注射劑」 臨床試驗用藥供應

彭正良 陳俊堂 唐一中 郭裕民 梁德生 張明誠 樊修秀

行政院原子能委員會核能研究所

**背景介紹：**核能研究所擁有國內唯一之 30 MeV 中型迴旋加速器，可以產製碘 -123 (I-123) 放射性同位素，遂投入 I-123 MIBG 注射劑之開發。本所也應用此合成系統，建立化學、製造與管制 (CMC) 文件等技術性文件，申請藥品查驗登記，並於 2019 年 9 月順利取得「核研心交碘 -123 注射劑」藥品許可證 (衛部藥製字第 R00037 號)。

**方法：**為研製國內首創之 I-123 MIBG 注射劑，本所開發放射性碘標誌研製技術，並開發出自動化合成系統，本合成系統已獲得中華民國、日本及美國的專利。由電腦控制自 / 半自動化操作，提高產物品質一致性，有效降低人員的輻射操作劑量，量產品質優良之核醫診斷製劑供應臨床使用。完成三批次製程確效與經時安定性試驗，藥物安定性已延長至 10 小時，並彙整相關資料送衛福部核定，已於 2022 年獲衛福部來函核定仿單變更與藥物有效期限延長至 10 小時。

**結果：**2022 年中起，正式供應國內四家醫院執行學術研究用臨床試驗，研究範圍包括路易氏體失智症、帕金森症、類澱粉心肌病變、心室頻脈與心房顫動等疾病。至今已供應醫院 12 批次，31 劑的「核研心交碘 -123 注射劑」。

**結論：**未來核能研究所會持續供應「核研心交碘 -123 注射劑」臨床試驗用藥供應，並積極建置另一條符合 PIC/S GMP 規範無菌注射液劑生產線，期能加入量產供應行列。另外，積極推動其他適應症之臨床試驗，擴大臨床使用的範圍。

PB-029

## 核醫部門女性輻射工作人員懷孕期間所接受的輻射劑量 是否會超過法規規定之劑量限度？ —以南部某 2 間醫院核醫部門為例

陳素英<sup>1</sup> 卓世傑<sup>2</sup> 陳宜伶<sup>1</sup> 蕭莉茹<sup>1</sup> 林秋美<sup>1</sup> 古琴鳳<sup>1</sup>  
陳怡如<sup>1</sup> 曾翠芬<sup>1</sup> 劉怡慶<sup>1</sup> 林家揚<sup>1</sup> 張晉銓<sup>1</sup>

<sup>1</sup> 高雄醫學大學附設中和紀念醫院核子醫學部

<sup>2</sup> 奇美醫院核子醫學科

**前言：**隨著醫療的進步，各項醫療診斷與治療儀器越來越普遍精密，尤其輻射相關診斷儀器與同位素治療項目是比較受到關切。而女性輻射工作人員如於懷孕期間所接受的職業曝露，是我們比較關切的議題。故本研究以南部 2 間醫院核醫部門女性輻射工作人員在懷孕期間，推估其與其胚胎或胎兒於工作中所接受的輻射劑量是否會超過原委所規定的劑量限度？是否有需要調整其工作性質？

### 方法：

#### 1. 評估依據：

- a. 每月人員全身有效劑量紀錄。
- b. 評估公式：(公式來源：游離輻射防護安全標準附表三。)

$$ET = Hp(d) + \sum_j h(g)j_{ing} \cdot I_{j,ing} + \sum_j h(g)j_{inh} \cdot I_{j,inh}$$

此為參考用之計算劑量，推估剩餘妊娠期間每月可能所接受的最大劑量。

2. 依據「游離輻射安全標準」第十一條法規規定：雇主於接獲女性輻射工作人員告知懷孕後，應即檢討其工作條件，使其胚胎或胎兒接受與一般人相同之輻射防護。前項女性輻射工作人員，其剩餘妊娠下腹部表面之等價劑量不得超過二毫西弗，且攝入體內放射性核種造成之約定有效劑量不得超過一毫西弗。

### 結果：

1. A~F 放射師與醫檢師工作性質為操作放射性同位素，其中 D~F 醫檢師因為工作環境有其他輻射作業造成劑量，有 2.445  $\mu\text{Sv}/\text{日}$  的輻射曝露劑量。A~F 剩餘妊娠期總劑量最高 432.5  $\mu\text{Sv}$ ，皆 < 1 mSv 其胚胎或胎兒之劑量限度。
2. G 為 RIA 書記，因為工作環境有其他輻射作業造成劑量，推估有 4.69  $\mu\text{Sv}/\text{日}$  輻射曝露劑量，其剩餘妊娠期總劑量為 774  $\mu\text{Sv}$ 。< 1 mSv。
3. H~I 護理師工作性質為穿鉛衣注射 Tl-201、Tc-99m 與 2 小時後 F-18 拔針，其剩餘妊娠期總劑量最高 461.2  $\mu\text{Sv}$ 。J 護理師工作性質為穿鉛衣且注射 20 mCi Tc-99m、Ra-223，其人員全身有效劑量紀錄有 0.23 mSv 之輻射劑量紀錄。其剩餘妊娠期總劑量為 177.6  $\mu\text{Sv}$ 。H~J 皆 < 1 mSv。
4. K~M 放射師工作性質為 Tl-201、Tc-99 m、Ga-67 檢查項目，穿 0.5 mm 鉛衣以距離 30 cm 進行擺位，

擺位時間每次上下共 3 分鐘計算。於控制台 5 mm 鉛屏蔽，以距離 200 cm，每人次 20-30 分鐘計算，其剩餘妊娠期總劑量為 174  $\mu\text{Sv}$ 。N 放射師工作性質為 PET/CT 注射 F-18 與擺位，其人員全身有效劑量紀錄有 0.31 mSv 之輻射劑量紀錄。其剩餘妊娠期總劑量為 958  $\mu\text{Sv}$ ，K~N 皆 < 1 mSv。

**結論：**推估 A~N 醫檢師、放射師、書記、護理師其剩餘妊娠期間可能所接受的輻射曝露劑量皆在法規劑量限度之內。依合理抑低精神，雖未超過法規劑量限度，仍盡可能減少其輻射劑量。如有可能超過法規劑量限度，仍須考量調整其工作性質與工作量。

PB-030

## Production of Gallium-68 Radionuclide for Biomedical Applications

Chia-Ling Tsai, Yu-Ting Chien, Wen-Shing Fu, Ching-Chu Lu, Mei-Fang Cheng, Steven Shinn-Fornng Peng, Chyng-Yann Shiue

*PET Center, Department of Nuclear Medicine, National Taiwan University Hospital, Taipei, Taiwan*

**Introduction:** Molecular theranostics create a new era in nuclear medicine [1]. In this regard, peptide drug labeled with a diagnostic or therapeutic radionuclide can be used as a diagnostic or targeting therapeutic drug. Gallium-68 ( $^{68}\text{Ga}$ ) and Lutetium-177 ( $^{177}\text{Lu}$ ) are two most commonly used radionuclides to serve this purpose. The purposes of this study are to synthesize three  $^{68}\text{Ga}$ -labeled radiopharmaceuticals, [ $^{68}\text{Ga}$ ]Ga-DOTA-TATE, [ $^{68}\text{Ga}$ ]Ga-DOTA-TOC and [ $^{68}\text{Ga}$ ]Ga-PSMA-11 for in-house pre-clinical and clinical studies, and to compare the pro and con of the  $^{68}\text{Ga}$  produced from different methods.

**Methods:** [ $^{68}\text{Ga}$ ]Ga-DOTA-TATE was automated synthesized with a commercial module (Modular-Lab Eazy, Eckert & Ziegler Eurotope GmbH). Briefly, the 5 ml of [ $^{68}\text{Ga}$ ]GaCl<sub>3</sub> was eluted out from the pharma-grade  $^{68}\text{Ge}/^{68}\text{Ga}$  generator with 0.1 N HCl and processed with a SCX cartridge. The buffer mixture of DOTATATE acetate and [ $^{68}\text{Ga}$ ]GaCl<sub>3</sub> was kept at 100°C for 8 minutes. After cooling, the final product was diluted with 5 mL of saline and then was sterilized by filtration online through a 0.22 μm filter. The purity of the final product was analyzed by TLC and HPLC. [ $^{68}\text{Ga}$ ]Ga-DOTA-TOC and [ $^{68}\text{Ga}$ ]Ga-PSMA-11 were synthesized similarly.

**Results:** The Activity of [ $^{68}\text{Ga}$ ]Ga-DOTA-TATE, [ $^{68}\text{Ga}$ ]Ga-DOTA-TOC and [ $^{68}\text{Ga}$ ]Ga-PSMA-11 synthesized by this method was 18 mCi, 13.5 mCi and 19.4 mCi, respectively. The Labelling time was about 8 mins.

Currently,  $^{68}\text{Ga}$  radionuclide can be produced by three methods: a) Solid target: enriched zinc-68 ( $^{68}\text{Zn}$ ) or  $^{nat}\text{Zn}$  target was bombarded with protons [2,3]. b) Generator:  $^{68}\text{Ga}$  is produced from a germanium-68/gallium-68 ( $^{68}\text{Ge}/^{68}\text{Ga}$ ) generator and c) Liquid target: a 1.0 M solution of [ $^{68}\text{Zn}$ ]Zn(NO<sub>3</sub>)<sub>2</sub> in dilute (0.2–0.3 M) HNO<sub>3</sub> was irradiated with proton beam [4]. Among these three methods,  $^{68}\text{Ge}/^{68}\text{Ga}$  generators are most commonly used. It is a convenient source of  $^{68}\text{Ga}$  and independent from  $^{68}\text{Ga}$  production centers. For novel radionuclides productions, solid targets are often used. Producing  $^{68}\text{Ga}$  with solid target gives high activity and high purity with long beam time.  $^{68}\text{Ga}$  produced using liquid target is fast and simple handling but having lower production yields than using solid target.

**Conclusions:** [ $^{68}\text{Ga}$ ]Ga-DOTA-TATE, [ $^{68}\text{Ga}$ ]Ga-DOTA-TOC and [ $^{68}\text{Ga}$ ]Ga-PSMA-11 have been synthesized in reasonable yields.  $^{68}\text{Ga}$  radionuclide could be generated through  $^{68}\text{Ge}/^{68}\text{Ga}$  generators, solid targets or liquid targets. Among them, generator is suitable for PET center without cyclotron facility. Solid target and liquid target are more satisfactory with small medical cyclotron in hospital. At NTUH, we could expand new target and relative facilities to our present cyclotron. Then  $^{68}\text{Ga}$ -based radiopharmaceuticals, i.e. [ $^{68}\text{Ga}$ ]Ga-DOTA-TOC, [ $^{68}\text{Ga}$ ]Ga-PSMA-11 or new tracer could be routinely and steadily produced.



PB-031

## 利用回收率方法來檢測方法之準確性

蕭莉茹 陳宜伶 陳素英 陳怡如 林秋美  
曾翠芬 劉怡慶 古琴鳳 林家揚 張晉銓

高雄醫學大學附設中和紀念醫院核子醫學部

**Introduction :** 檢驗方法測定結果之準確度分析中回收率 (Recovery ratio) 主要以已知檢體濃度加入低至高各不同濃度，以預測值比較。回收率 (Recovery Ratio) 可分為絕對與相對回收，絕對回收常用於分析藥品的比例，其樣本處理後回收比例。相對回收於已知濃度中再加入不同濃度後，其實際濃度與預測濃度之間的差異。而目的以回收率方式分析檢驗方法學來探討準確性。

**Design and methods :** 不同檢驗項目為  $\alpha$ -fetoprotein, AFP; Testosterone, TT 來評估。設計取五個已知參考值 A, B, C, D, E 與三種低中高 (L, M, H) 濃度總共 15 個組合。主要以相對回收率的數據來確認是否此方法之準確性。再以檢驗方法比較中常用相關係數 (correlation) 驗證之是否有差異，再以線性迴歸模式確認是否屬於正常分佈。

**Results :**  $\alpha$ -fetoprotein, AFP 與 Testosterone, TT 的 15 組合之回收率分別為 83.46~104.82; 92.60~147.99 代表。相關係數分析為 r 值分別為 0.994 & 0.976。線性迴歸模式主要探討是否符合常態性之檢定係數 F 值分別為 1003.063 & 258.472，其顯著性皆為  $< 0.01$ 。以殘差值使用 Shapiro-Wilk 檢定常態分佈其顯著性分別為 0.324 & 0.998。另外以常態機率圖的推論殘差成 45 度線兩者皆符合常態性假設。獨立性檢定利用 Durbin-Watson 判斷其數據為 1.899 & 2.005 查表後，Durbin-Watson 值  $> DU$  顯示獨立性成立。變異數同質性主要以殘差圖 (Residual Plot) 來探討，標準化殘差與預測值的散佈圖中發現數據均於 0 線上下，也符合變異數同質性假設。

**Conclusion :** 以兩個檢驗項目的回收率與相關係數來分析準確度。發現回收率範圍接近 100% 的 AFP 其相關係數 0.994 接近 1。另外 TT 回收率範圍較大其相關係數 r 值為 0.976。雖然兩者以線性迴歸討論其資料皆屬常態分佈且皆為獨立性而變異數同質性，所以不影響數據之判斷。因此回收率確實可以當作試劑方法評估準確性的依據。

PB-032

## 簡述 IVDR 歐盟體外診斷醫療器材法規 轉換對放射免疫分析實驗室之影響

楊宛甄 陳晴雅 李佳蓉 王昱豐 彭南靖

臺北榮總核醫部

**背景介紹：**在核子醫學領域中，放射免疫分析屬於體外分析方法，所用的試劑需仰賴國外廠商製造且通過相關國際認證及規範，然而現在歐盟針對體外醫療診斷器材制定了詳細的監管法規，即為 IVDR (In-Vitro Diagnostic Regulation (EU) 2017/746) 歐盟體外診斷醫療器材法規，將取代 IVDD (In-Vitro Diagnostic Directive 98/79/EC) 歐盟體外診斷醫療器材指令，成為歐洲體外診斷醫療器材市場最新的監管基礎。

**IVDR 變更與影響：**醫療器材製造廠須重新建立品質管理系統及新的產品風險分級，並建立醫療器材單一識別碼方便上市後追蹤監視；此外，對於產品查核機構 (Notified Body) 之認定更加警慎且擴大須受評估之產品範圍。

**結果：**由於受到 COVID-19 疫情的影響且查核機構不足，使得多數製造廠無法在期限內完成審查。因此，歐盟委員會 (European Commission) 根據不同的風險等級分階段延後施行 IVDR，針對 Class B (甲狀腺檢測試劑) 及 Class C (腫瘤檢測試劑) 之轉換過渡期將在 2027 年 05 月及 2026 年 05 月到期，屆時市場將可能有巨大轉變。

**結論：**新版的法規公布之後，對於產品上市前後都有比以往嚴格之規範，對製造商無疑是一種衝擊，也對實驗室及整個醫療界造成不同層面之影響，使用單位需思考將來若廠商無法再生產銷售試劑時，實驗室是否已經有面臨試劑轉換時的處置方式及評估標準。

PB-034

## Synthesis and Radioiodination of $^{131}\text{I}$ -CXCR4 Tracer as an CXCR4 Expression Theranostic Agent

Yun-Tang Lu<sup>1</sup>, Hui-Ting Chen<sup>2</sup>, Chai-Lin Kao<sup>3</sup>, Chuan-Lin Chen<sup>1,\*</sup>

<sup>1</sup>Department of Biomedical Imaging and Radiological Sciences,  
National Yang Ming Chiao Tung University, Taipei, Taiwan

<sup>2</sup>Faculty of Pharmacy, National Yang Ming Chiao Tung University, Taipei, Taiwan

<sup>3</sup>Department of Medicinal and applied Chemistry, Kaohsiung Medical University, Kaohsiung, Taiwan

**Introduction:** The chemokine receptor CXCR4 plays a vital role in multiple biological processes including tumor proliferation and metastasis. The novel potent CXCR4 antagonist Arg-Ala-[D-Cys-Arg-2-Nal-His-Pen]-COOH, displayed nanomolar affinity toward CXCR4, with a significant selectivity over CXCR3 and CXCR7. It might represent the good candidate for the development of novel theranostic probe for nuclear medicine in CXCR4 overexpressing cancers. Here, the novel radioiodinated  $^{131}\text{I}$ -CXCR4 was synthesized and evaluated in A549 cell line and SAS cell line.

**Methods:** An alkyne-bearing precursor was commercial available and subjected to click chemistry-based prosthetic group modification for authentic compound preparation and radioiodination. The new radioiodinated  $^{131}\text{I}$ -CXCR4 was synthesized with suitable yield. In vitro experiments were performed with A549 cell line and SAS cell line.

**Results:** The radiochemical chemical yield of  $^{131}\text{I}$ -CXCR4 was  $50 \pm 5\%$  and a high radiochemical purity of  $> 95\%$ . It showed high hydrophilicity ( $\log P = -1.63 \pm 0.1$ ), the  $^{131}\text{I}$ -pentixather was less polar ( $\log P = -1.12$ ). The  $^{131}\text{I}$ -CXCR4 showed high stability in FBS after incubation for 96 h of  $> 90\%$ . The cellular uptake showed that the uptake with  $^{131}\text{I}$ -CXCR4 by A549 cell line CXCR4 (+) was higher than SAS cell line CXCR4 (-).

**Conclusions:** The cold I-CXCR4 and  $^{131}\text{I}$ -CXCR4 were obtained with acceptable yield and moderated radiolabeling yield with high radiochemical purity. The selective uptake in CXCR4 (+) A549 cell line was showed that might be a potent theranostic probe in high CXCR4 expression tumor.

PB-035

## The Validation of HPLC Analytical Method of [<sup>18</sup>F]PSMA-1007 in Taipei Veterans General Hospital

Shih-Pei Chen<sup>1,2</sup>, Wen-Yi Chang<sup>1,2</sup>, Chun-Tse Hung<sup>1,2</sup>,  
Geng-Ying Li<sup>1,2</sup>, Min-Tzu Ku<sup>1,2</sup>, Nan-Jing Peng<sup>1,2</sup>

<sup>1</sup>Department of Nuclear Medicine, Taipei Veterans General Hospital, Taipei, Taiwan

<sup>2</sup>National PET/Cyclotron Center of Taipei Veterans General Hospital, Taipei, Taiwan

**Introduction:** [<sup>18</sup>F]PSMA-1007 is a radio pharmaceutical for showing the distribution of prostate specific membrane antigen (PSMA) by positron emission tomography (PET) imaging. Quality control (QC) tests of [<sup>18</sup>F]PSMA-1007 and their acceptance criteria were compliant with European Pharmacopoeia (Ph. Eur.) Supplement (10.5) standards. The radiochemical purity and chemical impurities of [<sup>18</sup>F]PSMA-1007 were evaluated by high performance liquid chromatography (HPLC). The HPLC analytical method of [<sup>18</sup>F]PSMA-1007 should be validated by sensitivity, specificity, accuracy, and reproducibility before applying in clinic.

**Methods:** Three kinds of standard solution used in this study were impurities which forming from the manufacture of [<sup>18</sup>F]PSMA-1007, such as [<sup>19</sup>F]PSMA-1007, OH-PSMA-1007 and the precursor of [<sup>18</sup>F]PSMA-1007. They were mixed in the same concentration then diluted into five concentrations in turn, each was ten times to the next. All concentration of standard solutions would be injected three repeats. Sensitivity was evaluated by the minimum detection limit of concentration of standard solution in HPLC, it should be less than the lower limitation of QC. Specificity was evaluated by the resolution between three signals from the standard solution and by the relative standard deviation (RSD) of retention time (Rt) from the specific signal of three repeats injection. Accuracy was evaluated by all injections of standard solution, all 15 signals should be linear. Reproducibility was evaluated by the RSD of signal from [<sup>19</sup>F]PSMA-1007 of three different lots.

**Results:** The minimum detection limit of [<sup>19</sup>F]PSMA-1007 in HPLC was 0.000005 (mg/mL). The resolutions between three components were 3.34 and 16.47 in average (lower limit: 2). The RSD values of Rt from all components were 3.93%, 3.18% and 0.99% (upper limit: 5%). The values of RSD of signal to noise ratio (SNR) of [<sup>19</sup>F]PSMA-1007 from three repeat injections were 0.14%, 0.41%, 2.14%, 4.51% and 0% (upper limit: 5%). The RSD values of height of [<sup>19</sup>F]PSMA-1007 signal from three repeat injections were 2.31%, 1.29%, 0.84%, 2.04% and 0% (upper limit: 5%). The value of r-square of 15 signals was 1.0 (lower limit: 0.98). The RSD value of signal from [<sup>19</sup>F]PSMA-1007 of three different lots was 0.45 (upper limit: 5%).

**Conclusions:** The HPLC analytical method of [<sup>18</sup>F]PSMA-1007 in Taipei Veterans General Hospital had passed the validation of sensitivity, specificity, accuracy and reproducibility. It had been ready for clinical use.

PC-001

## 運用 QR CODE 多媒體呈現方式在核醫之應用

謝文彬 王欣寧 姚珊汎

臺北榮總核醫部

**目的：**近年來環保意識逐漸成爲趨勢，讓核醫藥物負荷心肌灌注掃描檢查說明書上的文字解說簡單無紙化。使得複雜冗長的說明文字，改變爲影片解說。利用 QR CODE 圖像轉換，讓原有紙上解說瞬間變成無紙化。一般而言，文字冗長通常民眾較不會花費時間來讀取，隨者手機普及化的發展，民眾可直接掃描 QR CODE，直接連結到影片解說，將核醫藥物負荷心肌灌注掃描檢查項目解釋更有效率，也更親民。

**方法：**當受檢者在門診看完診後，紙上的預約門診單附有 QR code。使用者利用智慧型手機使用 QR Code 掃描器，便能直接連結到預設拍好的解說影片。

**結果：**本部在服務受檢者做藥物負荷心肌灌注掃描檢查，七月到檢人次爲 516 人，影片觀看人次數約 548 次 / 月，觀看人次占比到檢人次爲 106%，超過 100%。代表幾乎每位心肌灌注掃描檢查的受檢者都有觀看，甚至有另外的家屬協助觀看。此外，此影片的平均觀看時間長度爲 2.05 分鐘，而影片總長 3.26 分鐘，占比 62.8%，表示大多數的病人，都有把前半段的檢查說明看完。此數據顯示，此影片提升病人理解檢查流程之效果，病人配合檢查預備停藥流程，提升檢查的準確率。

**結論：**由於智慧型手機的使用普及化以及網際網路在教學上的廣泛運用，希望藉由多媒體呈現方式講解的方式來輔助傳統紙本，增加學習的效果。以往，許多受檢者都困於文字紙本呈現，而導致理解困難，而必須到專程至本部櫃台，由櫃檯工作人員重新講解數次之後，民眾才得以了解檢查方式。自有了 QR CODE 多媒體呈現方式輔助，除了能夠使醫療人員負擔減輕，也能夠使民眾更加了解藥物負荷心肌灌注掃描檢查內容，並且提高影像檢查的品質和準確率。

PC-002

## 針對劑量不足之病人利用增加造影時間 以改善鉈 -201 心肌灌注掃描之影像品質

李柏葦 張哲瑋 陳雅鳳 賴佳玟 黃兆駿 吳彥雯 蕭聿謙 汪姍瑩

亞東紀念醫院核子醫學科

**背景介紹：**心肌灌注掃描檢查通常需合併壓力測試，利用心臟處於壓力下時需氧量會增加，正常冠狀動脈血流量會增加，而阻塞的冠狀動脈血流量只少許增加或甚至不增加，以便區分正常或缺氧的心肌。壓力測試的方法有運動（如運動心電圖）或藥物注射（如 Dipyridamole, Adenosine, Dobutamine）等。若病人罹患關節炎、中風、臥床無法運動時，則只能選擇藥物式。其中利用血管擴張劑 Dipyridamole (persantin) 來增加冠狀動脈的流量的方法最為常用，一般正常人的血管會因為冠狀動脈擴張劑的作用而擴張；相反的，有問題的血管則比較不會，配合核子醫學血流灌注影像，我們可以找到異常的冠狀動脈血管。

**病例報告：**病人為一名 54 歲男性，患有糖尿病、高脂血症、心臟疾病。在亞東紀念醫院核子醫學科採用心臟專用半導體掃描儀 (CZT camera, Discovery NM 530c - GE Healthcare) 執行心電圖門控式鉈 -201 心肌血流灌注檢查，注射放射性同位素鉈 -201 時，因病人靜脈血管較脆弱導致部分藥物滲漏在注射處，進行造影時發現影像計數值明顯較少，以致影像品質不佳，為改善此問題而將造影時間調整為原來的兩倍來改善計數值不足的問題，原先 stop conditions 為 stop on time : 300 sec，將其改為 600sec，其餘造影條件、病人擺位皆不改變的情況下再次進行造影，並將結果分析比對。

**結果：**將兩次造影結果進行切面排列，分別排列成 short axial、vertical axial、horizontal axial，上排為使用一般造影條件的影像 (300 sec)，下排為增加造影時間的影像 (600 sec)，兩者比較可明顯發現增加造影時間之影像解析度較佳，心肌部分攝取更為明顯，背景雜訊較少。

**結論：**經過此次案例經驗，我們若在藥物發生滲漏且因藥物短缺而無法再注射的情況下，增加造影時間對影像品質是有幫助的，也不會增加病人輻射劑量，進而提供較好的影像品質能幫助醫師做出更精確的診斷。

PC-003

## 以 MUGA 檢查追蹤乳癌病人接受化學治療藥物 對於 LVEF 之影響

林昱璉<sup>1</sup> 莊紫翎<sup>1,2</sup> 劉芳馨<sup>1\*</sup>

<sup>1</sup> 佛教慈濟醫療財團法人大林慈濟醫院核子醫學科

<sup>2</sup> 慈濟學校財團法人慈濟大學醫學院醫學系

**背景：**本篇利用多頻道血池分析 multigated blood pool analysis (MUGA) 追蹤乳癌病人接受化學治療前、後 left ventricular ejection fraction (LVEF) 之變化。

**材料與方法：**本研究共納入 69 位乳癌病患來追蹤化療藥物對於心臟之心毒性影響，分別在化療之前以及開始化療後的 3 個月與 6 個月以 MUGA 檢查，評估不同時間點 LVEF 的變化，之後將 3 次檢查的 LVEF 利用 SPSS Statistics 18.0 (SPSS Inc., Chicago, IL, USA) 軟體，使用單因子相依變異數分析 (repeated measured ANOVA) 統計，評估 LVEF 在使用化療藥物後是否因心毒性而有變化。

**結果：**經由統計結果得出在化療前 baseline 的 LVEF 為  $66.54 \pm 8.27\%$ ，在 3 個月後的檢查結果 LVEF 為  $64.59 \pm 6.77\%$ ，6 個月時為  $64.09 \pm 6.66\%$ ，經由單因子相依變異數分析計算後得出在化療之前與開始化療後的 3 個月及 6 個月，其 LVEF 之間有顯著性差異 ( $p = 0.003$ ) (如 Table 1)，可看出在使用化療藥物之後因心毒性的影響，造成 LVEF 下降 (如 Figure 1)。

**結論：**乳癌治療所使用的化療藥物還有一些免疫療法，可能導致心臟長期損害造成充血性心衰竭，影響 LVEF 功能。MUGA 可用於評估化學治療後因為心毒性所造成的 LVEF 降低，提供臨床使用化學治療藥物時重要的參考指標。

PC-004

## Myocardial Perfusion Imaging in Patient with Ebstein's Anomaly

Ya-Min Chi, Wen-Ling Hsu, Wei-Jheng Yen, Chin-Chuan Chang

*Department of Nuclear Medicine, Kaohsiung Medical University Chung-Ho Memorial Hospital, Kaohsiung, Taiwan*

**Introduction:** Ebstein's anomaly is a rare heart disease that accounts for less than one percent of all congenital heart defects. It is a complex disorder with a broad clinical manifestation that is characterized by malformation of the tricuspid valve and right ventricle. In myocardial perfusion imaging (MPI), Ebstein's anomaly cause decreased counts on ventricular septum, which might bring about a false positive interpretation of coronary artery disease (CAD). Previous studies have reported possible reasons of decreased counts: 1. decreased uptake of radiotracer due to fibrosis of ventricular septum; 2. partial sampling due to exaggerated motion of the septum; or 3. increased attenuation due to enlarged right atrium. However, Ebstein's anomaly with coronary artery disease is rarely reported.

**Case Report:** A 80-year-old woman with history of Ebstein's anomaly was referred for MPI due to suspect of CAD. Her electrocardiogram (ECG) exhibited anteroseptal myocardial ischemia. Transthoracic echocardiography revealed Ebstein's anomaly with severe tricuspid regurgitation; markedly enlarged right atrium and ventricle; and small left ventricle chamber. Rest/stress  $^{99m}\text{Tc}$ -sestamibi MPI with dipyridamole was done. Planar image showed mildly reduced heterogeneous uptake on left ventricle myocardium and mild heterogeneous uptake on right ventricle wall. Single-photon emission computed tomography (SPECT) imaging demonstrated slight reversibility in the proximal to mid septal wall. However, taking into account of patient's history, the likelihood of CAD was low. Thus, the patient continues to follow up at our cardiovascular clinic with medication control.

**Conclusions:** Although only slight reversibility was noted in proximal to mid septal wall in our patient, whereas previous cases reports showed significant reversibility, careful review of the patient's history and through knowledge of Ebstein's anomaly help with proper interpretation of MPI.



PC-005

## 心肌灌注掃描在使用衰減校正功能後的心得分享

曾柏銘<sup>1</sup> 呂建璋<sup>2</sup> 沈淑禎<sup>2</sup> 門朝陽<sup>1</sup> 林雅婷<sup>2</sup> 蕭聿謙<sup>3</sup>

<sup>1</sup> 天主教中華聖母修女會醫療財團法人天主教聖馬爾定醫院正子造影中心

<sup>2</sup> 天主教中華聖母修女會醫療財團法人天主教聖馬爾定醫院核子醫學科

<sup>3</sup> 亞東紀念醫院核子醫學科

**前言：**心肌灌注掃描為一無侵入性檢查之造影，臨床上可使用  $^{201}\text{Tl}$  或  $^{99\text{m}}\text{Tc}$  MIBI 進行掃描，在心肌冠狀動脈疾病的診斷和管理中成為心臟內科不可或缺的一項檢查，然而使用  $^{201}\text{Tl}$  進行心肌灌注掃描因能量較低，容易出現下壁衰減，如儀器配備有電腦斷層則可使用衰減校正輔助成像。然科內於 2020 裝機後使用電腦斷層的衰減校正（以下簡稱 CTAC）來進行心肌灌注掃描的頻率較低，顯示科內醫師對於 CTAC 在心肌灌注掃描中的常規使用上仍有疑慮，在進行討論後，將科內醫師的使用心得並針對 4 例同時進行 CTAC 及心導管檢查案例進行分析。

**方法：**我們搜集了 2020-2022 年共 15 位患者，使用  $^{201}\text{Tl}$  進行 CTAC 的心肌灌注掃描，比較 AC (attenuation correct) 與 NAC (unattenuation correct) 影像其中差異，並對其 15 例中之 4 例在掃描後進行心導管檢查相互比對。

**討論：**在我們討論的 15 個案例中，有 4 位在接受 CTAC (Resting phase) 的心肌灌注掃描後並心導管檢查，其中有 3 位在 NAC 時下壁均呈現缺損但在 AC 後均得到補償，此 3 位在進行心導管檢查後發現有 2 位病患於 RCA 有動脈粥狀硬化現象（狹窄 70%），另外 1 位 RCA 30% 動脈粥狀硬化狹窄，顯示經過衰減校正後影像在判定動脈動脈硬化能力並不顯眼。第 4 例則因 NAC 及 AC 下壁均呈現缺損狀態，經心導管檢查後確認其 LAD、LCX 均有 90% 的狹窄，RCA 則有 80% 的狹窄。由於 CTAC 後的心肌灌注掃描影像下壁會顯的更加飽滿，其影像可以用來輔助因橫隔膜衰減造成的計數下降，我們認為如 AC 與 NAC 在 Stress 或 Resting 均無缺損的情況下發生狹窄的機率較低，但在狹窄超度超過 70%，AC 與 NAC 於 Resting 均無恢復即可判定為狹窄或壞死；若 AC 有恢復但 NAC 卻顯示無恢復時則需參考病患病史來綜合判斷。

**結論：**雖然目前還不清楚 CTAC 對影像質量的影響，但文獻對於 CTAC 能提高診斷的準確性仍具爭議。由於科內醫師較習慣使用 NAC 當成判讀標準，如未來想使用 CTAC 來幫助提高影像品質及診斷率，則醫事放射師的和醫師的培訓和經驗是確定診斷準確性時應考慮的一個重要因素。核醫科團隊的經驗愈豐富，則診斷的準確性就越高。

PC-006

## The Pre-evaluation of the Quality of First Pass Radionuclide Angiography

Hsin-Ning Wang, Yao Shan-Fan

*Department of Nuclear Medicine, Taipei Veteran General Hospital, Taipei, Taiwan*

**Introduction:** First pass radionuclide angiography (FPRA) provides a fast and accurate assessment of both the right and left ventricle ejection fraction, for pre-operation survey and heart function evaluation. One of the critical quality control parameters is total count. However, this parameter only generated after imaging processing by experienced technicians. At the time unqualified images found, patients usually have left. Therefore, we would like to have indicators to evaluate the quality of the first pass radionuclide angiography image while the patient still on the examination table.

**Methods:** We collected 138 patients underwent first pass radionuclide angiography. During the exam, we also collected the peak and plateau gamma count rate. Peak gamma count rate was identified as the maximum number of gamma count rate during the injection; plateau gamma count rate was identified as the count rate at 40th second. Owing to the circulation is completed within 7-10 seconds in normal patients, at the 40th second after injection, the count rate was almost stable.

**Results:** The correlation of the peak and total count is 0.58; and the correlation of plateau and total count is 0.61. As we set X as plateau value and Y as total count, the regression curve function is  $y = 31.435x + 216.88$ . We usually set threshold button limit of total count as 400 thousand. Therefore, as the plateau above 5.8 thousand counts/second, the image quality may be acceptable.

Compatible with our clinical experience, there seems almost no effect of superior vena cava mean transit time (SMTT) with right ventricular ejection fraction (RVEF), the correlation between them was 0.06. However, indeed, we found there is negative correlation between pulmonary mean transit time (PMTT) and left ventricular ejection fraction (LVEF) but surprisingly, the correlation is relatively weak ( $R = -0.19$ ).

**Conclusions:** Plateau value might provide first line doctors a good predictor to waive the trouble while we found the unqualified images after patients had left. As we notice the plateau value below 5.8 thousand counts/second at the 40<sup>th</sup> second, we might repeat the process once again even before we remove the catheter from the patient. As the result, we might say the plateau value might serve as the pre-evaluation parameter of the quality of first pass radionuclide angiography.

PC-007

## The Proportion Difference of Myocardial Perfusion Imaging Before and After the COVID-19 Pandemic in Taiwan

Hsin-Ning Wang<sup>1</sup>, Nan-Jing Peng<sup>1,2</sup>

<sup>1</sup>Department of Nuclear Medicine, Taipei Veteran General Hospital, Taipei, Taiwan

<sup>2</sup>School of medicine, National Yang Ming Chiao Tung University, Taiwan

**Introduction:** Myocardial perfusion imaging (MPI) serves as a gate keeper before invasive intervention of suspected coronary artery diseases (CAD). After the COVID-19 pandemic, the amount of MPI and catheterization seems be changed. In this study, we hope to obtain the difference of proportion of the catheterization in MPI before and after the COVID-19 pandemic outbreak.

**Methods:** We collected all patients who received MPI before 90 days of the catheterization date within Dec. 2020 to Nov. 2021. Python 3.9 and Excel 2021 were used as matching tool and analysis software. Chi-squared test was used to examine the differences between groups. Differences were considered to be significant at  $p < 0.05$ . Taking the catheterization result into as our gold standard, cross-comparison of myocardium perfusion imaging and coronary angiography was also conducted.

**Results:** In total of 911 MPI patients collected, 498 and 413 received catheterization before and after May 2021, respectively. For those who underwent catheterization before May 2021, accuracy was 59.2% with positive predict value was 59.0%; chi-square p-value is 0.69. On the other hand, for those who underwent catheterization after May 2021, accuracy was 60.5% with positive predict value was 64.2%. In the proportion analysis, there was 30.7% and 24.9% of patients who received MPI before 90 days of catheterization before and after the pandemic ( $p = 0.000179$ ); while there was 9.5% and 7.9% of the patient who received catheterization within 90 days after MPI ( $p = 0.003339$ ).

**Conclusions:** Although there were more and more patients bring complaint of atypical chest pain into the clinic and underwent MPI exam before further intervention, the MPI accuracy hadn't changed. However, interestingly, in our analysis, we found the proportional of the catheterization within MPI significantly shrink from 30.7% to 24.9% with p-value 0.000179 of chi-square; on the other hand, the proportional of the MPI before catheterization also shrink from 9.5% to 7.9% with p-value 0.003339. Although the stricter admission policy, such like PCR negative proof, vaccine injection proof, during the pandemic period in Taiwan, the result reveals that MPI served more important as a gate keeper to exclude patients who were not necessarily have to undergo catheterization.

PC-008

## Incidental Uptake at Shoulder Joint on Raw Data of Myocardial Perfusion Imaging

Shih-Fu Wang, Yu-Ling Hsu

*Department of Nuclear Medicine, Ditmanson Medical Foundation Chia-Yi Christian Hospital*

**Case:** A 61-year-old male patient was arranged myocardial perfusion scan to track any possible ischemic heart disease. On the exam day, the patient told that there was pain over right shoulder therefore he couldn't raise his arm. So he put down the right arm during the scan, and we found that there was a strip of uptake activity in the right arm area during the scan, similar to the activity caused by the injection. However, we confirmed that the injection site was at the left forearm. Also, the patient had orthopedic sonography due to the rupture of the rotator tendon of the right shoulder joint six months ago. The uptake was suspiciously related to the inflammation of the right shoulder joint.

**Discussion:** After searching of literature, we found that in addition to known tumor uptake, bone sarcoidosis, hereditary multiple exostoses, pulmonary edema, and recently discovered Moderna COVID-19 vaccination-related axillary lymphadenopathy activity was all possibly can be seen in Tl-201 myocardial perfusion imaging. In this case, Tl-201 uptake may be related to high vascularity due to inflammation.

In such case, it is necessary for us to confirm the injection site, also to find out all the possibilities of any unusual radioactivity.

PC-009

## 以不同血流模型參數分析心肌血流與血流儲備

魏文祺 王昱豐 彭南靖

臺北榮民總醫院核醫部

**背景介紹：**核子醫學檢測心肌缺血的主要方法目前是採用心肌血流灌注造影 (myocardial perfusion imaging, MPI)，而使用動態 SPECT 方式對心肌進行血流定量是評估心肌缺血的一種新方法。血流動力模型有隔室模型 (compartmental model) 與淨保留模型 (net retention model)，本研究的目的是使用不同的血流動力模型參數分析左心室的血流儲備 (myocardial flow reserve, MFR) 與心肌血流 (myocardial blood flow, MBF) 並比較其結果。

**方法：**31 位病人接受動態 SPECT 心肌血流定量檢查，Rest 及 Stress 分別注射 18 mCi 及 36 mCi 的 Tc99m-MIBI，先執行 Rest 造影，3 個小時後再執行 Stress 造影，影像採集時間皆為 10 分鐘，使用的造影設備為 GE NM 53°C，另以 GE NM/CT 870 執行胸腔部位電腦斷層掃描以做為心肌血流定量分析時之衰減校正用。定量分析軟體使用 Corridor4DM，血流模型參數採用 INVIA Medical Imaging Solutions 於 2021 年發佈，建議適用於 GE NM 53°C 動態 SPECT 心肌血流分析的參數：AC-1TCM (1-tissue compartmental model), NC-1TCM, AC-Netret-2 (net retention model) 及 NC-Netret-2。分析左心室的 MFR 與 MBF。統計分析軟體使用 MedCalc，統計方法採用相關性、線性回歸分析及 Bland-Altman 法。

**結果：**在相關性及線性回歸分析方面，有做衰減校正 (attenuation correction, AC) 的組別：AC-1TCM 與 AC-Netret-2 其在 MFR 的相關係數 (r) 為 0.96，判定係數 ( $R^2$ ) 為 0.92；MBF 的相關係數 (r) 為 0.97，判定係數 ( $R^2$ ) 為 0.93。在未做衰減校正 (no attenuation correction, NC) 的組別：NC-1TCM 與 NC-Netret-2 其在 MFR 的相關係數 (r) 為 0.95，判定係數 ( $R^2$ ) 為 0.9；MBF 的相關係數 (r) 為 0.95，判定係數 ( $R^2$ ) 為 0.91。以上結果皆呈現高度相關。在 Bland-Altman 一致性評價方面，MFR 在 AC 組有 97%，NC 組有 94%，MBF 在 AC 組有 97%，NC 組有 95% 的數據落在 95% 的一致性界限內 (95% limits of agreement, 95% LoA)，差值平均值分別為 0.2、-0.18、0.03 與 -0.02。

**結論：**使用不同的血流模型參數及操作技術，在分析心肌血流與血流儲備，一般結果都會呈現不同程度的差異。在 INVIA Imaging Solutions 所建議的模型參數中，不論選用隔室模型或淨保留模型，在分析心肌血流與血流儲備皆可得到相近結果。

PC-010

## The Evaluation of Post COVID-19 Vaccination Patients with Presenting Cardiac-Like Symptoms on $^{201}\text{Tl}$ Myocardial Perfusion Imaging

Hung-Pin Chan<sup>1</sup>, Fu-Ren Tsai<sup>1</sup>, Ming-Hui Yang<sup>2</sup>, Wen-Chun Lin<sup>1</sup>,  
Daniel Hueng-Yuan Shen<sup>1</sup>

<sup>1</sup>Department of Nuclear Medicine, Kaohsiung Veterans General Hospital

<sup>2</sup>Department of Medical Education and Research, Kaohsiung Veterans General Hospital

**Introduction:** SARS-CoV-2 is a highly transmission disease with coronavirus in late 2019 that has caused pandemic outbreak of acute respiratory disease and human health threatening. There are several COVID-19 vaccines with Emergency Use Authorization that were injected to patients by different Mechanism during this time. However, some patients complained persistent cardiac-like symptoms after COVID-19 vaccination, including chest tightness, chest pain and dyspnea. The purpose of this study is to evaluate the results of those patients who presented cardiac-like symptoms while post COVID-19 vaccination on  $^{201}\text{Tl}$  Myocardial Perfusion Imaging (MPI).

**Methods:** The patients were enrolled to this study who complained persistent symptoms within 6 months post COVID-19 vaccination, the symptoms included chest tightness, chest pain and dyspnea. They were referred to our department for MPI survey by cardiologist. Dipyridomale-stress (2~3 mCi  $^{201}\text{Tl}$ ) imaging at first and then 3 hours later for redistribution imaging that were performed on a dedicated Siemens Symbia-T2 SPECT system. Statistical analysis included Pearson's chi-square test by commercially available soft ware (SPSS) and  $P < 0.05$  was considered statistically significant.

**Results:** There were 63 patients who were referred from Cardiologist from 2019-Jun to 2022-Feb. We found 15 patients (15/63; 24%) with positive MPI who had injected by BioNTech (BNT; 5 pts) and Moderna (10 pts) and 7 patients had no any prior CAD history. Six patients of these 15 patients (6/15) had positive PCI results. Only one AstraZeneca (AZ)-injected patient had positive PCI but with negative MPI. Interesting, the incidental finding of  $^{201}\text{Tl}$  axillary lymphadenopathy avidity due to post COVID-19 vaccination was noted, mainly while patients injected with BNT and Moderna. The duration time of axillary avidity was about 1.5 months post vaccination. No statistically significant correlation was noted between axillary avidity to sex, positive MPI, or CAD history.

**Conclusions:** According to our study:

1. Some patients were fresh cases of CAD due to post vaccination symptoms and positive MPI/PCI result, mostly in Moderna group. However, there are need more study for discussion the relationship of MPI perfusion abnormality and COVID-19 vaccines.
2.  $^{201}\text{Tl}$  axillary lymphadenopathy avidity was found mainly in BNT and Moderna vaccination groups and the duration time of avidity about 1.5 months post injection.

PC-011

## Persantin 對不同核種心肌灌注掃描檢查 病人血壓影響之研究—以南部某醫院核醫科為例

江佳諭<sup>1</sup> 丁瑞玫<sup>2</sup> 鄭揚霖<sup>1</sup> 卓世傑<sup>1</sup> 張虹麗<sup>1</sup> 顏玉安<sup>1</sup> 李將瑄<sup>1</sup>

<sup>1</sup> 奇美醫療財團法人奇美醫院核子醫學科

<sup>2</sup> 奇美醫療財團法人奇美醫院護理部

**背景介紹：**Persantin 是目前台灣以藥物介入法，執行心肌灌注掃描檢查 (Myocardial Perfusion Imaging, MPI)，取代跑步，使病人心肌血流呈現壓力相最常使用的藥物之一。由於 Persantin 的藥理作用是擴張冠狀動脈血管以增加血流量，因此施打後經常導致檢查病人血壓下降，必須密切注意，以免發生危險。而核子醫學科執行心肌灌注掃描檢查，經常使用的放射性同位素核種，卻有 Tl-201 及 Tc-99m+MIBI 兩種。所以注射 Persantin 後，施打不同核種對施行心肌灌注掃描檢查病人之血壓影響，顯值得進一步瞭解。

**方法：**1. 收集南部某醫院核醫科，自 2022 年 1 月 10 日至 4 月 29 日止，分別紀錄 371 位施打 Tl-201 之病人及 119 位施打 Tc-99m+MIBI 病人，共 490 位接受心肌灌注掃描檢查病人之有效血壓數據。2. 以 Welch Allyn 牌 53N00 型電子血壓計，於每位病人靜脈注射 Persantin (劑量為體重 \*0.56) 前與後，分別測量其收縮及舒張血壓值共 4 筆資料並予記錄。3. 整理、統計前項數據，以提出結果及結論。

**結果：**1. Tl-201 與 Tc-99m+MIBI 之病人，注射前之收縮壓平均為 132.4 與 129.5 mmHg，舒張壓平均為 75.1 與 73.2 mmHg。2. Tl-201 與 Tc-99m+MIBI 組之病人，注射 Persantin 後之收縮壓平均為 116.3、114.8 mmHg，舒張壓平均為 66.7、64.8 mmHg。3. 注射 Persantin 後之收縮壓相較注射前，Tl-201 與 Tc-99m+MIBI 組最高分別下降了 63、43 最低為 -11、16，平均下降 16.0、14.7 mmHg。4. 注射 Persantin 後之舒張壓相較注射前，Tl-201 與 Tc-99m+MIBI 組其最高分別下降了 45、34 最低為 -27、-19，但兩組平均皆為下降 8.4 mmHg。5. 注射 Persantin 後之收縮壓相較注射前之比率，Tl-201 與 Tc-99m+MIBI 其最高分別下降了 77.8、41.7 最低為 -13.4、-11.6，平均下降 14.3、13.7%。6. 注射 Persantin 後之舒張壓相較注射前之比率，Tl-201 與 Tc-99m+MIBI 組其最高分別下降了 109.8、55.7 最低為 -37.5、-21.7，平均下降 13.8、14.0%。

**結論：**本研究數據顯示，Tl-201 與 Tc-99m+MIBI 兩組病人，於注射 Persantin 後之收縮壓與舒張壓，其數值差與數值比率，平均值差異均不大。

PC-012

## Deep Learning with Generative Adversarial Networks for the Prediction of Obstructive Coronary Artery Diseases from Myocardial Perfusion Image

Chu-Pin Lo<sup>1</sup>, Yi-Ching Lin<sup>2</sup>, Yu-Cheng Hsieh<sup>3,4\*</sup>, Shih-Chuan Tsai<sup>2\*</sup>

<sup>1</sup>Department of Data Science and Big Data Analytics, Providence University, Taichung, Taiwan

<sup>2</sup>Department of Nuclear Medicine, Taichung Veterans General Hospital, Taichung, Taiwan

<sup>3</sup>Cardiovascular Center, Taichung Veterans General Hospital, Taichung, Taiwan

<sup>4</sup>Department of Internal Medicine, Faculty of Medicine, Institute of Clinical Medicine  
National Yang Ming Chiao Tung University, Hsinchu and Taipei, Taiwan

\*Corresponding author

**Introduction:** Myocardial perfusion imaging (MPI) is widely used for the diagnosis of obstructive coronary artery disease (OCAD). Deep learning (DL) with standard framework (Multilayer Perceptrons [MLPs] and Convolutional Neural Network [CNN]) using large MPI database (raw polar map, blackout, total perfusion deficit [TPD]) has been employed to predict OCAD. Deep learning models with generative adversarial networks (GAN) might generate similar accuracy with limited and unbalanced MPI database. We would like to investigate the accuracy of DL with GAN framework in predicting OCAD using limited and unbalanced MPI database (only raw polar map).

**Methods:** Patients with angina underwent stress and rest 99mTc-sestamibi MPI with SPECT, and coronary angiographies (CAG) were performed within 6 months of MPI. Left ventricular myocardium was segmented and perfusion defect areas were identified using nuclear cardiology software. Polar map samples derived from the raw images were used to generate raw polar maps showing radiotracer count distributions normalized to the maximal counts. Deep learning models with generative adversarial networks (GAN) were trained using combined resting and stress raw polar maps of MPI for 3 major coronary arteries (LAD, LCX, RCA) territories. The evaluations for prediction of OCAD were on a per-patient and per-vessel basis. The training labels were annotated by cardiologist from the correlating CAG. For patient scale, obstructive disease was defined as at least 70% narrowing of one of the 3 major coronary arteries or at least 50% for the left main coronary artery. For vessel scale, obstructive disease was defined as at least 70% narrowing.

**Result:** A total of 102 of 222 (45.9%) patients and 171 of 666 (25.68%) arteries had OCAD. For per-patient scale, the areas under the receiver-operating characteristic (ROC) curve and precision-recall (PR) curve for OCAD prediction by GAN model were 0.78 and 0.74, respectively. For per-vessel scale, the areas under ROC curve and PR curve were 0.72 and 0.86, respectively. These values were comparable with previous studies using large amount of patient's MPI data.

**Conclusions:** DL with GAN framework using limited and unbalanced MPI database generated similar accuracy in predicting OCAD compared to that generated by conventional DL. DL with GAN framework might be an alternative method to predict OCAD when the MPI data were limited and unbalanced. This proposed approach using only raw polar map can be clinically implemented more easily especially for the case of lacking population statistical information of polar maps of MPI, since mean and standard deviation are needed for the derivation of blackout and total perfusion deficit (TPD).



PC-013

## The Correlation Between First Pass Radionuclide Angiography and Multi-Gated Acquisition

Hsin-Ning Wang<sup>1</sup>, Lien-Hsin Hu<sup>1,2</sup>

<sup>1</sup>Department of Nuclear Medicine, Taipei Veteran General Hospital, Taipei, Taiwan

<sup>2</sup>School of medicine, National Yang Ming Chiao Tung University, Taiwan

**Introduction:** Although first pass radionuclide angiography (FPRA) provides a fast and accurate assessment of both the right and left ventricle ejection fraction, for pre-operation survey and heart function evaluation. There are several conditions generate unqualified images or even the examination cannot be done. For those whose vessels are hard to approach to a have a bolus injection, and for those images having prolonged vena cava mean transit time (SMTT) and pulmonary mean transit time (PMTT), multi-gated acquisition (MUGA) is one of the suggested alternatives. In this study, we would like to investigate the correlation between MUGA and FPRA.

**Methods:** We collected all the patients who underwent both FPRA and MUGA during Jan. 2022 to Aug. 2022 and taking left ventricular ejection fraction (LVEF) into comparison. We used Matlab 3.9 as our matching tool and Excel as our analysis software. Cross-comparison of FPRA and MUGA was conducted.

**Results:** Selected criteria of the window of FPRA and MUGA was constrained into one week (7 days). After removing incomplete data, 21 patients were taken into our analysis. The average of the difference between the two methods is 3.5% with the standard deviation 5.2. Even with various PMTT and SMTT, the correlation between LVEF from the two methods were extremely high, 0.956, while, in paired-t test, the p-value was 0.0085.

**Conclusions:** In conclusion, the results produced by FPRA and MUGA are highly correlated. Although p-value 0.0085 in paired-t test indicated the existence of the significant difference between two methods, the difference was only 3%. The analytic significance difference does not necessary lead to clinically difference. By reviewing the difference data, there was only two patients with higher LVEF by FPRA than by MUGA while all other patients had higher MUGA results. In these two patients, one difference is only 1 and the other was 10. The later patient had 33% of LVEF by FPRA and 23% by MUGA. Therefore, we could conclude that FPRA and MUGA are basically described the same thing with certain accuracy but with 3% of analytic difference. However, weather a patient with unqualified image in FPRA needs an alternative examination like MUGA, has to evaluate the different clinical scenario.

PC-014

## Hyperphosphatemia Related False Positive Tc-99m Pyrophosphate Myocardial Scan: A Case Report with Endomyocardial Biopsy Result

Lien-Hsin Hu<sup>1,2</sup>, Tse-Hao Lee<sup>1</sup>, Fu-Pang Chang<sup>1</sup>, Fa-Po Chung<sup>1,2</sup>,  
Yu Kuo<sup>1,2</sup>, Ko-Han Lin<sup>1</sup>, Chen-Hao Chiang<sup>1</sup>, Wen-Sheng Huang<sup>1,2,3</sup>,  
Nan-Jing Peng<sup>1,2</sup>, Yuh-Feng Wang<sup>1</sup>

<sup>1</sup>*Department of Nuclear Medicine, Taipei Veteran General Hospital, Taiwan*

<sup>2</sup>*School of Medicine, National Yang Ming Chiao Tung University, Taiwan*

<sup>3</sup>*Department of Nuclear Medicine, Cheng Hsin General Hospital, Taiwan*

**Introduction:** We report a case of extensive score 3 myocardial uptake in 3-hour pyrophosphate (PYP) myocardial SPECT that the followed endomyocardial biopsy revealed no amyloid deposition. The potential cause of false positive in this case was also discussed.

**Case report:** A 30-year-old man underlying with end-stage renal disease (ESRD) under peritoneal dialysis was referred for PYP myocardial scan due to LVEF decreased from 52% to 36% within one year. LV hypertrophy with 18 mm of interventricular thickness was noted. The PYP scan show extensive score 3 uptakes in the myocardium with apical region relative spared. Endomyocardial biopsy was performed and no amyloid deposit was noted. Serum immunofixation and free light chain assay did not reveal monoclonal protein. Myocardial perfusion scan revealed no apparent ischemia but an uptake pattern of dilated left ventricle. The patient did not have history of myocardial infarction, hypercalcemia, or history of radiation therapy, which are the known causes of false-positive. However, a long-standing hyperphosphatemia is noted which is related to his ESRD. By reviewing literature, several patterns of extra-skeletal uptake, including extensive myocardial uptake, in Tc-99m hydroxyl-diphosphonate bone scans have been reported. These uptakes in the extra-skeletal regions are considered to relate to metastatic calcification in patients with hyperphosphatemia.

**Conclusions:** Despite the documented 100% specificity of PYP scan to diagnose ATTR-CM in patients with monoclonal gammopathy excluded, false-positive scan still happens incidentally. With this case, our experiences of the potential causes of false-positive result are further expanded.

PC-015

## Referral Profile and Scan Results of Tc 99m Pyrophosphate Myocardial Scan for Diagnosis of Transthyretin Amyloidosis Cardiomyopathy: Experiences from Taipei Veterans General Hospital

Lien-Hsin Hu<sup>1,2</sup>, Tse-Hao Lee<sup>1</sup>, Wei-Ting Wang<sup>1,2</sup>, Yu Kuo<sup>1,2</sup>,  
Ko-Han Lin<sup>1</sup>, Wen-Sheng Huang<sup>1,2,3</sup>, Nan-Jing Peng<sup>1,2</sup>, Yuh-Feng Wang<sup>1</sup>

<sup>1</sup>Department of Nuclear Medicine, Taipei Veteran General Hospital, Taiwan

<sup>2</sup>School of Medicine, National Yang Ming Chiao Tung University, Taiwan

<sup>3</sup>Department of Nuclear Medicine, Cheng Hsin General Hospital, Taiwan

**Introduction:** Tc 99m pyrophosphate (PYP) myocardial scan emerged as an important study to diagnose transthyretin amyloidosis cardiac myopathy (ATTR-CM) in the recent years. Understanding of the referral source and the whole picture of the scan results of this group of patients is lacking. The aim of the study is to describe the referral source, the positive rates of different referral source, and the dynamic change of the scan pattern between the 1 hour and the scan result of the entire cohort of patients who were referred to our department for ATTR-CM diagnosis since 2017.

**Methods:** Since Jan. 1, 2017, to Apr. 19, 2022, all patients who were referred to our department for PYP myocardial scan for diagnosis of ATTR-CM were included. Anterior, left anterior oblique (LAO), and lateral planar images at 1 hour and 3 hour post-injection were obtained in all studies. A SPECT of the chest at 3 hour post injection were also obtained for each study. All scans were scored with the Perugini 4-point scale. In addition to assigning a final score with the standard method (i.e. scoring the entire study including SPECT information), the Perugini score was also applied to the 1 hour planar image and a score was also assigned separately in order to clarify the dynamic relationship between 1 hour planar image and the final scan result. According to the 1 hour and the final score, all patients were categorized into 4 groups: negative in both 1 hour & the final score (NN), negative in 1 hour but positive in the final score (NP), positive in the 1 hour but negative in the final score (PN), and positive in both 1 hour and final score (PP). Patient's referral information and scan result were collected from the electronic medical record of our site.

**Results:** A total number of 306 patients were referred to our hospital and 319 scans were performed. Among the 306 patients, 12 patients were referred for scans more than once per clinical need. In the 319 scans, 24% revealed positive results. Positive rates were 47% and 14% for patients referred from neurologists and from cardiologists. In the whole population, the four groups are 71%, 0%, 5%, and 24% for NN, NP, PN, and PP group, respectively.

**Conclusions:** A profile of the referral source, the relationship between the referral source, the positive rate, and the dynamic change between the 1 hour image and the final scan result is described.

PC-016

## 心肌灌注影像標準化後重組條件優化問題 — 案例報告

李建穎

臺北榮民總醫院核醫部

**背景介紹：**心肌灌注影像 (Myocardial perfusion imaging, MPI) 診斷主要是利用放射性追蹤藥物於心臟肌肉細胞吸收與分佈的狀態，來判定是否有無缺損決定。但其缺損大小與分佈受其影像重組所使用的濾波器強度與種類不同會有所變化。本部於今年 5 月訂定心肌灌注影像品質標準化定量造影條件，排除病患體型與劑量設限，統一收取影像標準，休息相 - 壓力相影像總計數量 (rest-stress total counts) Tl-201 為 1.2 Mcounts，Tc-99m-MIBI 為 2 Mcounts。

**病例報告：**一位 62 歲女性，身高 158 公分，體重 62 公斤。使用 QPS/QGS 分析處理影像時發現心臟短軸切面影像呈現模糊的現象 (smooth)，將此問題提出與醫師討論後懷疑所使用的重組條件中的巴特沃斯濾波器 (BW) 是否也無法適用於現在的臨床標準，於圖中紅色箭頭處標示出。建議增加其截斷頻率 (Cut-off frequency)，發現明顯改善其影像品質與其定量數值。

**結論：**在影像品質標準化定量造影條件下，之前的臨床重組條件已經不復使用，須建立出應對於其標準化條件下的重組參數。這是目前迫切所需，未來希望利用系統性比較找出最適化的條件。

PC-017

## F18-FDG PET/CT Imaging for Cerebellar Ataxia with Anti-glutamic Acid Decarboxylase Antibodies – A Case Report

Chi-Che Ho<sup>1\*</sup>, Yen-Hsiang Chang<sup>2†</sup>, Yung-Cheng Huang<sup>2</sup>

<sup>1</sup>*Department of Neurology, Chi Mei Medical Center, Tainan, Taiwan*

<sup>2</sup>*Department of Nuclear Medicine, Kaohsiung Chang-Gung Memorial Hospital, Kaohsiung, Taiwan*

*\*CC Ho and YH Chang are Equal Contributors to this Work*

*†Correspondence*

**Introduction:** Cerebellar ataxia (CA) with anti-glutamic acid decarboxylase antibodies (GAD-Ab) is a form of cerebellar dysfunction developed through immune-mediated mechanism, which affects mostly women in the sixth decades of life. The features on Fluorine-18 fluorodeoxyglucose positron emission tomography/computed tomography (F18-FDG PET/CT) of CA has rarely been discussed in literature. Herein, we report a case of CA with GAD-Ab and the presence of FDG uptake in the cerebellum.

**Case Presentation:** A 60-year-old man developed a subacute onset gait disturbance 4 months before his first examination. Autoimmune laboratory examinations showed increased serum and cerebrospinal fluid GAD-Ab levels. Brain magnetic resonance imaging (MRI) showed diffuse cerebellar volume loss inappropriate to the patient's age. Diffuse hypometabolism in the cerebellum was observed on F18-FDG PET/CT. The final diagnosis was cerebellar ataxia with GAD-Ab. The patient was treated with intravenous methylprednisolone for 3 days and then maintenance therapy with oral prednisolone and azathioprine. After 6 months of follow up, there had been no improvement in his neurological abnormalities, but his gait disturbance did not worsen.

**Conclusions:** F18-FDG PET/CT can potentially aid in the differential diagnosis of cerebellar diseases and may be useful in the detection of coexisting autoimmune diseases and unknown underlying malignancy.

PC-018

## Brain Perfusion Image in Transient Alcoholic Cerebellar Degeneration

Tzyy-Ling Chuang<sup>1,2</sup>, Yuh-Feng Wang<sup>3</sup>

<sup>1</sup>*Department of Nuclear Medicine, Dalin Tzu Chi Hospital, Buddhist Tzu Chi Medical Foundation, Chiayi, Taiwan;*

<sup>2</sup>*School of Medicine, Tzu Chi University, Hualien, Taiwan*

<sup>3</sup>*Department of Nuclear Medicine, Taipei Veterans General Hospital, Taipei, Taiwan*

**Introduction:** We present a case with transient alcoholic cerebellar degeneration who demonstrated frontal hypoperfusion and cerebellar hyperperfusion in Tc-99m ECD SPECT/CT instead of cerebellar hypoperfusion.

**Case report:** A 55-year-old male had alcohol consumption about 10 units daily for 25 years and developed social withdrawal after retiring. In recent two months, he started walking diagonally to the right, with his right shoulder drooping. He spoke and walked slowly, but his speech was clear. He was scared and stopped drinking for 20 days. His symptoms are better and he walks more steadily. His brain MRI showed no specific finding. Brain perfusion scintigraphy with Tc-99m ECD showed hypoperfusion in the prefrontal, frontal and left anterior temporal lobes, left thalamus, hyperperfusion in posterior white matter, parietal-occipital cortical regions, pons and cerebellum in two-tailed view display in eZIS.

**Discussion:** Cerebellar/cortical perfusion ratios in the subgroups of young alcoholics were diminished, compared with young controls. Alcoholics often suffer from motor incoordination resulting from alcohol-related cerebellar damage. Alcoholic cerebellar degeneration is clinically characterized by cerebellar ataxia predominantly in the lower extremities. Gait problems caused by brain degeneration are usually called frontal gait. The most common ones are like slower walking, smaller pace, cautious walking, unsteady or uncoordinated walk with a wide gait. Slow and slurred speech (dysarthria) are also occurred. Two-thirds of patients with active chronic alcoholism exhibited frontal lobe impairment demonstrated by neuropsychological testing and SPECT, which suggested the disruption of frontocerebellar circuitry and function. The cerebellar hyperperfusion instead of hypoperfusion in our case, probably implied that tissue shrinkage without permanent cell loss may account for variance in the correlation between cerebellar structural and functional impairment and might represent the potential for recovery.

PC-019

## 利用全角度連續掃描模式優化 縮減 TRODAT-1 斷層的掃描時間

陳至豪 丁建鑫 李哲皓 姚珊汎 彭南靖 黃文盛

臺北榮民總醫院核子醫學科

**背景介紹：**以單光子掃描 (SPECT) 進行 TRODAT-1 斷層掃描，是帕金森氏症 (Parkinson's disease) 的常規鑑別診斷檢查。現行標準程序是採用步進拍攝 (Step-and-Shoot) 進行 20 秒 × 120 取樣 (3°/View) × 雙頭 360° 掃描，總掃描時間需時 46 分鐘。如此長的掃描時間對於患者是很痛苦的經歷，也是影像品質下降的重要因素。本研究是嘗試利用全角度連續掃描模式 (full-angle continuous mode) 來優化縮減 TRODAT-1 scan 的掃描時間。

### 方法：

1. Jaszczak SPECT Phantom：準備注射了塔 -99m 的高劑量狀態假體 (6.17 mCi 計數率約 5 kcts/s) 和低劑量狀態假體 (0.7 mCi 計數率約 0.8 kcts/s)，進行步進拍攝掃描程序 (46 分鐘) 和全角度減時連續掃描程序 (30 分鐘)。而臨床 TRODAT-1 掃描計數率約 0.7~1.0 kcts/s。
2. Skull phantom：將 5 mCi 的塔 -99m 注射入 skull phantom，並在注射後第 0、1、6、7、12、13、18、19 小時 (計數率由 4 kcts/s 到 0.5 kcts/s)，進行步進拍攝掃描程序和全角度減時連續掃描程序取像。
3. 臨床影像：回溯分析 2016 年 8 位同時進行步進拍攝掃描程序和全角度減時連續掃描程序造影的臨床影像。

**結果：**更多的取樣數有助於提升在低計數率 (< 1.0 kcts/s) 造影影像的辨識。以每取樣 5 秒進行全角度連續掃描造影所得影像全計數 (total counts) 約為原程序所得影像的 76%~82%，若改為每取樣 6 秒影像全計數則為原程序所得影像的 96%~108%，全掃描時間分別為 30 分鐘和 36 分鐘，而且兩者在定性診斷和半定量分析方面與原程序造影結果趨勢一致。

**結論：**在不會改變診斷結果的前提下，更多的影像取樣角度和比較短的造影時間能有效的減少病患躁動對影像的影響，和減少病患造影的不適感，對於提升 TRODAT-1 斷層掃描造影品質有明顯的幫助。

PC-020

## The Rational of TRODAT-1 Uptake and Swallow Tail Sign on Parkinson Disease and Dementia with Lewy Bodies

Yu Kuo<sup>1,2</sup>, Tse-Hao Lee<sup>1,2</sup>, Wan-Tien Hsieh<sup>1</sup>,  
Nan-Jing Peng<sup>1,2</sup>, Wen-Sheng Huang<sup>1,2</sup>

<sup>1</sup>Department of Nuclear Medicine, Taipei Veterans General Hospital, Taipei, Taiwan

<sup>2</sup>School of Medicine, National Yang Ming Chiao Tung University, Taiwan

**Introduction:** The swallow tail sign describes the normal axial imaging appearance of nigrosome-1 within the substantia nigra. Absence of the sign is reported to have a diagnostic accuracy of greater than 90% for Parkinson disease and dementia with Lewy bodies. Brain SPECT with <sup>99m</sup>Tc-TRODAT-1 (SPECT-TRODAT) has been used as a useful tool in the differential diagnosis of Parkinsonism. This study is performed to analyze the relational of <sup>99m</sup>Tc-TRODAT-1 pattern and swallow tail sign on Parkinson disease and dementia with Lewy bodies.

**Methods:** Patients with both MR and SPECT-TRODAT in Taipei Veterans General Hospital performed within 3 months were recruited. The results were analyzed on the basis of imaging reports. Chi-squared test and Student's t test were used to examine the differences between groups. Differences were considered to be significant at  $p < 0.05$ .

**Results:** Of 122 patients, 23 had normal swallow tail on MR (Group 1) and 99 abnormal (Group 2). Ten of 23 (43.5%) in Group 1 showed symmetric caudate, putamen and striatal uptake on SPECT-TRODAT, whereas 23 of 99 (23.2%) in Group 2 did ( $p = 0.0490$ ). The ratios of striatal, caudate and putamen uptake on SPECT-TRODAT in Group 1 patients were higher than those in Group 2, although they didn't reach the statistical significance ( $p > 0.05$ ).

**Conclusions:** Abnormal swallow tail sign may represent loss of substantia nigra dopaminergic neurons and reduce specific binding of dopamine transporter. We found patients with loss of swallow tail sign had more asymmetric and lower ratios of striatal uptake than those preserved.



PC-021

## Relationship Between the Metabolic and Structural Changes of Thalamic Subnuclei and the Cognitive Performances in Temporal Lobe Epilepsy

Syu-Jyun Peng<sup>1</sup>, Hsin Tung<sup>2,3,4,5</sup>, Shih-Chuan Tsai<sup>6,7</sup>, Pu-Jung Huang<sup>6</sup>

<sup>1</sup>Professional Master Program in Artificial Intelligence in Medicine, College of Medicine, Taipei Medical University, Taipei, Taiwan

<sup>2</sup>Institute of Clinical Medicine, National Yang Ming Chiao Tung University, Taipei, Taiwan

<sup>3</sup>Center of Faculty Development, Taichung Veterans General Hospital, Taichung, Taiwan

<sup>4</sup>Division of Epilepsy, Neurological Institute, Taichung Veterans General Hospital, Taichung, Taiwan

<sup>5</sup>College of Medicine, National Chung Hsing University, Taichung, Taiwan

<sup>6</sup>Department of Nuclear Medicine, Taichung Veterans General Hospital, Taichung, Taiwan

<sup>7</sup>Department of Medical Imaging and Radiological Technology, Institute of Radiological Science, Central Taiwan University of Science and Technology, Taiwan

**Introduction:** [18F]-FluoroDeoxyGlucose positron emission tomography ([18F]-FDG-PET) is a common tool for epileptogenic zone identification, which presented an area with hypometabolism. Extratemporal hypometabolism was observed in temporal lobe epilepsy (TLE) patients, and thought as the network disorder. Besides, epilepsy patients usually have declined cognitive function, which might be related to both metabolic and structural changes of the cortexes. However, whether the deep grey matter, thalamus, related to cognitive performances in epilepsy patients had not been identified.

**Methods:** We retrospectively collected the TLE patients, who received brain MRI and PET for presurgical survey between Jun, 2020 and Feb, 2022 in Veteran Taichung General Hospital. There were 15 right-TLE (7 female, 8 male) and 21 left-TLE (8 female, 13 male) cases enrolled. The PET images were acquired by the GE Healthcare Discovery STE PET/CT system, while MR images were collected by Simens Magnetom 1.5T system. The grey matters were segmented and then registered to the PET images. The whole brain grey matter was chosen as a reference for intensity normalization. The SUV map was spatially smoothed with Gaussian smoothing kernel of 6 mm full width at half maximum. The volumes and the SUVs of each thalamic subnuclei (anterior, lateral, ventral, intralaminar, medial, posterior) were calculated. The asymmetrical index [(L-R)/(L+R)] was used to study the relationship between the metabolic/structural images and five indices of cognition (Full-Scale IQ: FSIQ; Verbal IQ: VIQ; Performance IQ: PIQ; Working Memory Index: WMI; Processing Speed Index: PSI). P value less than 0.01 was thought as statistically significant.

**Results:** Five aspects of intelligence quotient did not show obvious difference between left-TLE and right-TLE. In left-TLE, only the asymmetrical index of anterior nucleus volume was related to VIQ. PSI was negatively related to the asymmetrical index of lateral, intralaminar, and the whole thalamic SUV. The longer seizure duration, the smaller left subnuclei volume than the right corresponding areas. In right-TLE, only PSI was correlated with the asymmetrical index of anterior nucleus volume. However, the cognitive function

was not related to any SUV asymmetrical index. The SUV of the right thalamic subfield is relatively stronger than the left corresponding site in the cases with longer seizure duration.

**Conclusions:** Our study suggested thalamus participate in the network of cognitive function of TLE patients, presenting structural and metabolic changes. Seizure duration was related to the thalamic structural changes of left-TLE and metabolic changes of right-TLE. It suggests left-TLE induces ipsilateral thalamus atrophy, while right-TLE relatively enhance the ipsilateral thalamus metabolism. Among all cognitive aspects, PSI is well reflected by the imaging. PSI is maintained in left-TLE when contralateral thalamic SUV is preserved. In contrast, processing speed is kept in right-TLE when contralateral anterior thalamic nuclei volume is relatively larger.

PC-022

## Semi-quantitative Values of TRODAT in Patients with Clinically Diagnosed Secondary Parkinsonism in Taipei Veterans General Hospital

Nan-Jing Peng<sup>1,2</sup>, Yu Kuo<sup>1</sup>, Wan-Tien Hsieh<sup>1</sup>,  
Tse-Hao Lee<sup>1</sup>, Wen-Sheng Huang<sup>1,2</sup>

<sup>1</sup>Department of Nuclear Medicine, Taipei Veterans General Hospital, Taipei, Taiwan

<sup>2</sup>School of Medicine, National Yang Ming Chiao Tung University, Taiwan

**Introduction:** Secondary Parkinsonism refers to a group of disorders that have features similar to those of Parkinson's disease but have a different etiology. SPECT with <sup>99m</sup>Tc-TRODAT-1 (TRODAT) was mainly useful in differentiating between secondary Parkinsonism and synucleinopathies. This study is performed to analyze the semi-quantitative values of TRODAT in patients with clinically diagnosed secondary Parkinsonism.

**Methods:** Patients with SPECT-TRODAT performed from Jan. 2021 to Jun. 2022 in Taipei Veterans General Hospital were recruited. The results were analyzed on the basis of clinical diagnosis. Student's t test was used to examine the differences between groups. Differences were considered to be significant at  $p < 0.05$ .

**Results:** Of 122 patients, 61 were diagnosed secondary Parkinsonism (Group 1) and 61 synucleinopathies (Group 2). The semi-quantitative TRODAT values of caudate, putamen and striatum in Group 1 were  $1.09 \pm 0.43$ ,  $0.79 \pm 0.35$  and  $0.87 \pm 0.36$  on the left, and  $1.06 \pm 0.46$ ,  $0.78 \pm 0.37$  and  $0.85 \pm 0.39$  on the right, respectively, whereas those in Group 2 were  $0.80 \pm 0.32$ ,  $0.53 \pm 0.27$  and  $0.59 \pm 0.26$  on the left and  $0.76 \pm 0.32$ ,  $0.50 \pm 0.28$  and  $0.56 \pm 0.27$  on the right, respectively. The values in Group 1 were significantly higher than those in Group 2 ( $p < 0.001$ ). Group 1 patients showed more symmetric TRODAT ratios on both sides of caudate, putamen and striatum than Group 2 patients ( $p = 0.034$ ,  $0.004$  and  $0.029$ , respectively).

**Conclusions:** Semi-quantitative values of TRODAT could make a good differentiation between secondary Parkinsonism and synucleinopathies. Patients with secondary Parkinsonism demonstrate rather symmetric ratios than those with synucleinopathy.

PC-023

## Discussion on eZIS Analysis Differences when Reducing Raw Images

Chia-Hao Chang<sup>1</sup>, Yu-Sheng Hung<sup>1</sup>, Chiang-Hsuan Lee<sup>2\*</sup>

<sup>1</sup>*Division of Nuclear Medicine, Department of Medical Imaging, Chi Mei Medical Center, Liouying, Tainan, Taiwan*

<sup>2</sup>*Division of Nuclear Medicine, Department of Medical Imaging, Chi Mei Medical Center, Tainan, Taiwan*

**Introduction:** Taiwan is likely going to become a “hyper-aged” society within 3 years. Using ECD cerebral perfusion by SPECT to assess dementia is more common. Because patients symptoms include memory loss, mood changes, and being confused about time and place, we often have to stop scan in middle time and restart the whole scan when patients forget exam is going. If the scan time can be shortened, this situation might be avoid. We try to reduce the number of views and explore the difference.

**Methods:** The raw images (matrix size: 128 x 128; zoom: 1.45; Both detectors; Degrees of Rotation: 360; Number of Views: 60) in previous patients exams taken by E.CAM, Siemens. We use Siemens image processing activity named “Series Arithmetic” to separate the images series by two detectors, from 1 subset to 2 subsets. And then we use 10 patients complete images and the separated images to analyze by eZIS respectively.

**Results:** Compared to the eZIS reports by complete images, 30% severity in separated images reports have be changed from being lower than the cutoff value to higher, 10% extent, 15% Ratio as well.

**Conclusions:** There is a apparent difference between using separated images and complete images in eZIS analyze report. But all the difference is value changed from being lower than cutoff value to higher. It means blood flow decreases in memory regions of brain are more likely to be highlighted. If scan time can be shortened by scanning with 2 detectors rotate 180 degrees, patients with memory loss are more easier to finish this exam.

PC-024

## Seizure Operation in Patients after Pre-surgical Workups with $^{18}\text{F}$ -FDG Brain PET in Taipei Veterans General Hospital

Tse-Hao Lee<sup>1</sup>, Wan-Tien Hsieh<sup>1</sup>, Nan-Jing Peng<sup>1,2</sup>, Wen-Sheng Huang<sup>1,2,3</sup>

<sup>1</sup>Department of Nuclear Medicine, Taipei Veterans General Hospital, Taipei, Taiwan

<sup>2</sup>School of Medicine, National Yang Ming Chiao Tung University, Taiwan

<sup>3</sup>Department of Nuclear Medicine, Cheng Hsin General Hospital, Taipei, Taiwan

**Introduction:**  $^{18}\text{F}$ -FDG brain PET (PET scan) might be helpful in defining the epileptogenic zone, especially when MRI findings are negative. This study is performed to analyze the seizure operation in patients after pre-surgical workups in Taipei Veterans General Hospital.

**Methods:** Patients with PET scan performed for defining the epileptogenic zone for surgery in Taipei Veterans General Hospital were recruited. The results were analyzed on the basis of clinical follow-up. Chi-squared test was used to examine the differences between groups. Differences were considered to be significant at  $p < 0.05$ .

**Results:** In total, 80 consecutive patients underwent PET scan, including 39 adults and 41 children. Sixty-eight PET scans (85%) were abnormal (33 adults and 35 children), including focal hypometabolism in 26 (19 temporal lobes, 7 frontal lobes) (32.5%) and bilateral hypometabolism in 42 (52.5%). Six of the 12 (50%) normal, 16 of 26 (65.4%) focal hypometabolism and 30 of 42 (71.4%) bilateral hypometabolism on PET scans underwent operation for seizures. Thirteen of 19 patients (68.4%) with temporal focal hypometabolism and 3 of 7 patients (42.9%) with frontal focal hypometabolism did undergo seizure operation ( $p < 0.05$ ). Overall, no significant difference was found between adults and children.

**Conclusions:** PET scan can help decision making in 67.6% seizure patients for pre-surgical workups. Patients with temporal focal hypometabolism show more prevalent and higher chance of undergoing seizure operation than those with frontal focal hypometabolism.

PC-025

## 核醫 L-P Shunt 檢查在新型腰椎腹腔引流管經驗分享

張添信 陳慶元

佛教慈濟醫療財團法人台中慈濟醫院核子醫學科

**背景介紹：**水腦症主要好發在老年人身上的疾病，指在腦脊髓液異常堆積在腦部，俗稱腦積水，成人腦室每天大約產生 300 ~ 500 c.c. 的腦脊髓液，具有緩衝保護和代謝循環等功能，正常人每天腦脊髓液量所產生的與被吸收的量幾乎是平衡的，一旦腦脊髓液無法正常在腦室系統內流動或吸收出現障礙時，就會演變成水腦症，以前治療方式多為腦腹腔引流 (V-P Shunt) 需要開腦手術，現今新型腰椎腹腔引流是這幾年新術式，此手術是在腦水循環會經過的腰椎處放置細細的引流軟管，將腦室內的脊髓液排至腹部，使擴大的腦室變小，不需要開顱手術，手術傷口小、恢復較快，安全性也提高，且腰椎腹腔引流管還設有一個非侵入性的調節壓力裝置，本篇主要探討與分享核醫 L-P Shunt (Lumbar-Peritoneal Shunt) 檢查在新型腰椎腹腔引流管的如何施行及注意事宜。

**案例報告：**本案例為一名 74 歲女性，有水腦症病史 (2020 年) 且有施行過傳統腦腹腔引流手術，有放置 V-P Shunt 紀錄因阻塞關係，於 2022 年 1 月重新放置新型腰椎腹腔引流管，近期因復健療程有退化及意識狀況不清楚現象產生，神經外科醫師懷疑 L-P Shunt 再次阻塞因此安排核醫 L-P Shunt Scan，給藥位置由神經外科醫師確認腹部調壓閥門處，注射  $^{99m}\text{Tc-DTPA}$  1mCi 進行動態 (1 張 / 3 秒) 與靜態造影分別為 5 分、10 分、30 分、1H、2H、6H，阻塞位置確認會施行 SPECT/CT 進行定位，最後分析結果於 L-P Shunt 腹腔末端處阻塞導致病人右側腦室擴大，並再次手術更換 L-P Shunt，後續追蹤病人復健，該病患有好轉情況並持續進步。

**結論：**核醫 V-P Shunt 與 L-P Shunt Scan 皆可以幫助臨床科判定管路通暢與否，協助後續醫療處置，在 L-P Shunt Scan 注射時則無需按壓近端與遠端問題，給藥位置需與神經外科醫師進行確認，因為調壓閥門裝置因素，最後阻塞處可以進行 SPECT/CT 定位，給予臨床科阻塞精確位置。

PC-026

## Voxel-wise Image Analysis of $^{18}\text{F}$ -florbetaben Brain Amyloid PET from GAAIN Database

Tse-Hao Lee<sup>1</sup>, Syu-Jyun Peng<sup>2</sup>, Nan-Jing Peng<sup>1,3</sup>

<sup>1</sup>Department of Nuclear Medicine, Taipei Veterans General Hospital, Taipei, Taiwan

<sup>2</sup>Professional Master Program in Artificial Intelligence in Medicine, College of Medicine, Taipei Medical University, Taipei, Taiwan

<sup>3</sup>School of Medicine, National Yang Ming Chiao Tung University, Taiwan

**Introduction:**  $^{18}\text{F}$ -florbetaben is a commercially available radiotracer for beta-amyloid brain PET. Visual assessment brain PET presentation is based on regional cortical tracer uptake (RCTU) and brain amyloid plaque load (BAPL) score.

However, equivocal situation might be encountered when visual assessment of mild uptake in the grey matter. In our study, we conducted a voxel-wise image processing to highlight whether the grey matter uptake higher than white matter uptake in voxel-based level

**Methods:** Images of thirty-five subjects from a publicly available Global Alzheimer's Association Interactive Network (GAAIN) database were used for analysis. Each subject had  $^{18}\text{F}$ -florbetaben brain PET and 1mm slice thickness T1WI MRI, respectively. Image processing was conducted by SPM software and the steps were: (1) Spatial normalization of brain MRI to MNI space; (2) Co-registration of PET and T1WI MRI; (3) Segmenting MRI into grey matter, white matter and CSF space using brain tissue probability map (using 0.5 as threshold); (4) PET image smoothing with kernel of 6 mm full width at half maximum; (5) MRI-derived ROI<sub>grey matter</sub> and ROI<sub>white matter</sub> were superimposed on the PET image; (6) Set the voxel with maximum intensity in white matter (WMmax) as reference; (7) The voxels in grey matter with higher intensity than WMmax are highlighted as clusters superimposed on MRI. Besides, the voxel numbers were also calculated for group comparison between AD patients and health controls.

**Results:** Twenty-five of 35 subjects were elderly (> 60 years old) and the other 10 subjects were young health controls. For 25 elderly, 8 were AD patients, 9 were MCI patients, 2 were FTD patients and 6 were elderly health control. We found that the numbers of grey matter voxel with high uptake (higher than white matter uptake) is significantly higher in AD patients than that in 6 elderly health control ( $p < 0.05$ ).

**Conclusions:** Voxel-wise image processing of  $^{18}\text{F}$ -florbetaben brain PET might accurately compare the uptake between the grey matter and white matter in the cerebrum and could be used for distinguishing images of AD and health control.

PC-027

## 初步探討血液中尿酸濃度與骨骼強度之相關性

蔡依良<sup>1,2</sup> 王昱豐<sup>3</sup> 廖建國<sup>1</sup> 莊紫翎<sup>1,4</sup>

<sup>1</sup> 佛教慈濟醫療財團法人大林慈濟醫院核子醫學科

<sup>2</sup> 佛教慈濟醫療財團法人大林慈濟醫院醫學研究部

<sup>3</sup> 台北榮民總醫院核子醫學部

<sup>4</sup> 慈濟學校財團法人慈濟大學醫學系

**背景介紹：**體內氧化壓力上升被認為是骨量下降的機制之一。痛風是一種因嘌呤代謝障礙導致尿酸 (Uric acid, UA) 累積而引起的疾病，長期以來尿酸一直被認為是一種代謝廢物。然而，越來越多的證據表明，UA 可作為一種抗氧化劑，在神經系統中發揮保護作用。由於其抗氧化特性，UA 也被認為可透過抑制破骨細胞的活性和促進成骨細胞分化，助於骨骼密度 (Bone mineral density, BMD) 的增加。

雖然目前已有許多探討 UA 與 BMD 的相關性研究。然而骨骼是由皮質骨與骨小樑所構。現今測量 BMD 的儀器 DXA 只能檢測出骨骼的「量」，尚不能直接檢測「質」。因此我們藉由 TBS iNsight 軟體評估腰椎的骨骼紋理，得到骨小樑指數 (Trabecular bone score, TBS)，進而推測骨骼強度與 UA 的關聯。

**方法：**回溯性收集本院預防醫學中心，受試者為 2014 年 6 月至 2020 年 7 月間接受健康檢查的人。統計方法使用 t-test 比較男性和女性的計量資料。並使用簡單線性回歸分析因子 (x) 和 TBS (y) 的相關性；當因子與 TBS 有相關時 ( $p < 0.05$ )，將進一步使用多項式線性回歸分析所有相關因子 (x) 和 TBS (y) 的相關性。

**結果：**收案男性平均年齡為  $56.0 \pm 12.2$  歲，女性平均年齡為  $55.8 \pm 11.0$  歲，年齡在不同性別間沒有差異 ( $p = 0.484$ )。男性的平均 UA 與 TBS 分別為  $6.03 \pm 1.35$  mg/dL 及  $1.387 \pm 0.091$ ；而女性則分別為  $4.56 \pm 1.12$  mg/dL 及  $1.339 \pm 0.109$ 。

TBS 與 UA 之簡單線性回歸，男性結果顯示為正相關 ( $r = 0.027$ ,  $p = 0.026$ )；女性為負相關 ( $r = -0.070$ ,  $p < 0.001$ )。但加入年齡及身體質量指數兩個因子，進行模型的調整後，不論男女其 TBS 與 UA 之多項式回歸結果皆顯示為正相關 ( $p < 0.05$ )。

**結論：**在我們初步探討 UA 與 TBS 的相關性，其結果與大多 UA 和 BMD 的研究結果相同，發現尿酸除了有助於骨骼密度的增加外，尿酸同樣也與骨骼強度呈現正相關的關係。



PC-028

## 使用骨小樑指數預測作為判定骨質疏鬆症的可能性行性評估

蔡依良<sup>1,2</sup> 王昱豐<sup>3</sup> 廖建國<sup>1</sup> 莊紫翎<sup>1,4</sup>

<sup>1</sup> 佛教慈濟醫療財團法人大林慈濟醫院核子醫學科

<sup>2</sup> 佛教慈濟醫療財團法人大林慈濟醫院醫學研究部

<sup>3</sup> 台北榮民總醫院核子醫學部

<sup>4</sup> 慈濟學校財團法人慈濟大學醫學系

**背景介紹：**骨質疏鬆症 (Osteoporosis) 是一種沈默的疾病，症狀可能只有身高變矮的變化。但是只要一個突然的外力就可能造成骨折。骨折後引發嚴重的後遺症，可能影響患者的生活品質，甚至是死亡。

然而現今測量骨骼密度 (Bone mineral density, BMD) 的儀器 DXA 只能檢測出骨骼的「量」，尚不能直接檢測「質」。骨小樑指數 (Trabecular bone score, TBS) 可以作為骨骼微結構的替代品，評估腰椎的骨骼紋理，進而推測骨骼的強度。

因此本篇研究目的在於探討 TBS 是否可預測骨質疏鬆症，以及其分界點 (Cut-off point) 為何。由於 TBS 是透過評估腰椎的骨骼紋理所得之數據，因此我們進一步探討以腰椎 T 分數 - 2.5 為界時，TBS 的分界點為何。

**方法：**回溯性收集本院預防醫學中心，受試者為 2014 年 6 月至 2020 年 7 月間接受健康檢查的人。並採用兩種方式進行分組：一、參考國際臨床骨密檢測學會 (the International Society for Clinical Densitometry, ISCD) 的骨質疏鬆症標準，腰椎、左右兩邊的總髖骨或股骨頸其中一個部位的 T 分數  $\leq -2.5$ ，即被診斷為骨質疏鬆症。骨質疏鬆症患者分入骨質疏鬆組，骨質流失和骨質正常者則分入非骨質疏鬆組；二、直接以腰椎 T 分數 - 2.5 為界，分為腰椎 T 分數  $\leq -2.5$  組和 T 分數  $> -2.5$  組。

統計分析使用 t-test 和 chi-square 比較非骨質疏鬆組和骨質疏鬆組的差異。以 ROC curve 分析 TBS 預測骨質疏鬆症和以腰椎 T 分數 - 2.5 為界時，他們的曲面下面積 (Area under curve, AUC)、特異性 (Specificity)、靈敏度 (Sensitivity) 以及分界點。當  $p$  值小於 0.05 時，視為有統計上的意義。

**結果：**如 (表一) 所示，總共收案 17,574 名受試者，平均 TBS 為  $1.357 \pm 0.105$ 。被診斷為骨質疏鬆的病患有 3,542 位，占總收案人口的 20.2%；而腰椎 T 分數  $\leq -2.5$  的人有 2,026 名，占總收案人口的 11.5%。如 (表二) 所示，分別以 TBS 預測骨質疏鬆症和以腰椎 T 分數 - 2.5 為界分組的 AUC 為 83.3% 及 86.4%；特異性為 76.8% 及 84.6%；靈敏度為 75.3% 及 74.0%，分界點各為 1.319 及 1.311。最後 AUC 的結果，如 (圖一) 所示。

**結論：**可表示骨骼強度的 TBS，降低至 1.319 以下時，患者須留意本身的骨骼健康，是否罹患了骨質疏鬆症。

PC-031

## 良性攝護腺肥大與腰椎區域骨質密度增加 對骨骼強度之影響

陳保良<sup>1,2</sup> 王昱豐<sup>3</sup> 廖建國<sup>1</sup> 莊紫翎<sup>1,4\*</sup>

<sup>1</sup> 佛教慈濟醫療財團法人大林慈濟醫院核子醫學科

<sup>2</sup> 佛教慈濟醫療財團法人大林慈濟醫院醫學研究部

<sup>3</sup> 台北榮民總醫院核子醫學部

<sup>4</sup> 慈濟學校財團法人慈濟大學醫學系

**目的：**本篇研究想探討良性攝護腺肥大與與腰椎骨質密度增加是否對骨骼強度有影響。

**材料方法：**這是一篇回溯型研究，從台灣南部某區域教學醫院收集研究個案，個案於本院預防醫學中心接受健康檢查之男性受檢者，收集個案從 2014 年 06 月至 2020 年 12 月，年齡介於 50-98 歲，排除曾經罹患癌症的個案、抑或實驗室數據資料不完整、或骨質密度有任何一個區域部位無法量測，這些我們都把他們排除不列入本篇研究中。最後有 4,697 位個案納入研究，良性攝護腺肥大 (benign prostatic hyperplasia, BPH) 影像判讀是利用彩色 Doppler 超音波，分成正常組與 BPH 組。

**結果：**個案平均年齡  $61.73 \pm 7.59$  歲，身高  $166.38 \pm 5.80$  cm，體重  $68.73 \pm 9.94$  kg，身體質量指數  $24.80 \pm 3.13$  kg/m<sup>2</sup>，TBS  $1.374 \pm 0.088$ 。平均腰椎骨質密度 (bone mineral density, BMD) 為  $0.983 \pm 0.156$  g/cm<sup>2</sup>，平均右側股骨頸 BMD 為  $0.712 \pm 0.113$  g/cm<sup>2</sup>，平均右側全髖 BMD 為  $0.884 \pm 0.126$  g/cm<sup>2</sup>，平均左側股骨頸 BMD 為  $0.719 \pm 0.113$  g/cm<sup>2</sup>，平均左側全髖 BMD 為  $0.854 \pm 0.126$  g/cm<sup>2</sup>，平均骨小樑指數 (Trabecular bone score, TBS) 為  $1.374 \pm 0.088$ 。最後發現，腰椎 BMD 區域，BPH 組為正常組的 1.068 倍，有顯著 ( $p = 0.038$ )，但腰椎 TBS，BPH 組為正常組的 1.033 倍，但無顯著 ( $p = 0.324$ )。

**結論：**我們利用 BMD 搭配 TBS，能進一步確認 BMD 數值增加是否是增加骨頭中的骨小樑還是外面皮質骨，結果發現 BPH 與腰椎 BMD 增加的區域不是在骨小樑，增加區域為皮質骨，至於皮質骨量增加多寡，我們還要進一步研究。

PC-032

## 探討臨床上常見腰椎骨質密度增加之原因

陳保良<sup>1,2</sup> 王昱豐<sup>3</sup> 廖建國<sup>1</sup> 莊紫翎<sup>1,4\*</sup>

<sup>1</sup> 佛教慈濟醫療財團法人大林慈濟醫院核子醫學科

<sup>2</sup> 佛教慈濟醫療財團法人大林慈濟醫院醫學研究部

<sup>3</sup> 台北榮民總醫院核子醫學部

<sup>4</sup> 慈濟學校財團法人慈濟大學醫學系

**目的：**本篇研究為探討，骨質密度腰椎區域 T-score  $\geq 2.6$  的受檢者，搭配腰椎 X-ray 相關影像，整理出常見腰椎骨質密度增加之因素。

**材料方法：**收集，2014 年 11 月至 2022 年 3 月，於本院門診與住院執行骨質密度檢查之受檢者，當 T-score  $\geq 2.6$  我們就納入研究，但有部分受檢者有二次以上的數據，我們僅採 T-score 最高的數值，此外，有 30 位因無腰椎相關影像，我們也排除在本篇研究中，最終收集 107 位受檢者 男性 65 位與女性 42 位。

**結果：**整體平均年齡  $69.89 \pm 12.06$  歲，平均身高  $159.73 \pm 7.99$  cm，平均體重  $67.18 \pm 11.69$  kg，平均身體質量指數  $26.32 \pm 4.16$  kg/m<sup>2</sup>，平均腰椎骨質密度  $1.390 \pm 0.142$  g/cm<sup>2</sup>，平均腰椎 T-score  $3.4 \pm 0.8$ 。歸納出一般常見導致腰椎骨質密度增加之因素（包括：滑脫 53 位 (49.5%)、血管鈣化 20 位 (18.6%)、壓迫或狹窄 69 位 (64.5%)、退化性病變 96 位 (89.7%)、增生 94 位 (87.8%)、脊柱曲線改變 37 位 (34.6%)、手術後 6 位 (5.6%)）。有些受檢者，會有二種以上腰椎問題，而這種狀況我們將分別列入各細項中。

**結論：**臨床上骨質密度增加因素探討甚少，本篇研究整理出臨床上常見因骨質密度增加的相關疾病，簡單總結增加之因素（包括：滑脫、血管鈣化、壓迫或狹窄、退化性病變、增生、脊柱曲線改變、手術後）；其中以退化性改變，造成骨質密度增加為最多，未來我們將進一步分析相關數據與因素，提供臨床參考。

PC-033

## 全身骨骼掃描 (Tc-99m MDP) 顱骨異常攝取之探討 — 案例報告

李佩璇 楊朝瑋

澄清綜合醫院中港院區核子醫學科

**背景介紹：**全身骨骼掃描是核醫科應用非常廣泛的檢查項目之一。透過靜脈注射 Tc-99m MDP 來進行造影。Tc-99m MDP 為磷酸鹽類似物，與骨骼中的結晶羥基磷灰石結合。Tc-99m MDP 與成骨細胞活性成比例，因此骨骼修復較多的部位就會吸收較多的磷酸鹽，而在全身骨骼掃描上呈現放射性攝取增高的影像。臨床上造成攝取增高的原因，包含骨折、感染、骨轉移和不太常見的骨病，如佩吉特病、尿毒症性骨病等。

**病例報告：**一名 68 歲女性，有乳癌與末期腎臟疾病 (end stage renal disease, ESRD) 病史，每周三次進行血液透析。抽血報告顯示有異常高的血中尿素氮 (Blood urea nitrogen ; BUN) 26 mg/dL 及肌酐酸 (Creatinine) 5.06 mg/dL。2021 年 3 月骨密度檢測為骨質疏鬆症。於 2021 年 4 月進行核醫全身骨骼掃描 (Tc-99m MDP)，影像呈現整個顱骨、面部骨骼和整個下頷骨有瀰漫性放射性攝取增高。

**討論：**造成顱骨瀰漫性攝取增高的原因，可能有骨轉移、佩吉特病及尿毒症性骨病等。本案例為 ESRD 患者，疑似為尿毒症性骨病。由於 ESRD 患者繼發性的副甲狀腺功能亢進導致顱骨過度生長，表現方式為下頷骨和上頷骨擴大以及其他顱骨變形等。全身骨骼掃描 (Tc-99m MDP) 的攝取主要取決於成骨細胞活性，在骨骼修復時成骨細胞大增，骨骼攝取 Tc-99m MDP 增加，在影像以熱區呈現。

**結論：**尿毒症性骨病是一種慢性疾病，在慢性腎病、繼發性的副甲狀腺功能亢進和腎性骨營養不良患者中普遍存在。因此，當全身骨骼掃描呈現顱骨異常攝取時，需考慮是因尿毒症而引起的。

PC-034

## Bone Scintigraphy in Patients with Osgood-Schlatter Disease

Ya-Wen Chuang, Ying-Fong Huang, Chia-Yang Lin,  
Chin-Chuan Chang, Hsiu-Lan Chu

*Department of Nuclear Medicine, Kaohsiung Medical University Hospital, Kaohsiung, Taiwan*

**Introduction:** Osgood-Schlatter disease (OSD) is a traction apophysitis of the tibial tubercle commonly occurring in preadolescents and adolescents. It is sometimes difficult to differentiate infrapatellar bursitis from OSD on clinical examination, as the pain localises to or near the patellar tendon attachment to the tibial tuberosity. Bone scintigraphy of the disease has rarely been reported.

**Methods:** The authors demonstrate 2 teenagers presented with anterior knee pain, without antecedent trauma, was referred to our department for detecting occult bone lesions.

**Results:** Focal areas of increased tibial tubercle uptake were found in one case on the routine bone scan, consistent with avulsion fracture of the tibial tuberosity following OSD. On the contrary, the bone scan of the other case showed negative finding and OSD superimposed inflammatory process could be ruled out.

**Conclusions:** This study demonstrates that the bone scan appears to have some diagnostic utility in patients with markedly symptomatic OSD, and may better correlate with clinical activity although the diagnosis is provided by the clinical and radiological findings.

PC-035

## 全身骨掃描之造影方式與影像品質探討

張哲璋 李柏葦 陳雅鳳 賴佳玟 黃兆駿 吳彥雯 汪姍瑩 蕭聿謙

亞東紀念醫院核子醫學科

**背景介紹：**全身骨掃描是一項可以用來評估多種骨骼病變的檢查，包含有骨折、癌症骨轉移等，而 Tc-99m MDP 是目前骨骼掃描常用的核醫藥物，經靜脈注射後 3-4 小時進行全身骨頭的造影。對於造影方面，使用兩種 scan mode，分別是 continuous 和 step and shoot，在收像時間相近的條件下，比較兩種模式之影像品質差異。

**方法：**本案收集了四位病人的造影，分別針對這四位病人使用了兩種 scan mode 做 whole Body Bone Scan 來比較，第一種 Continuous 操作的條件為：一 . Exposure time per pixel 120 sec 二 . Speed in 20 cm/min，此為連續式的造影 table 以每分鐘移動 20 cm 的速度造影，第二種 Step and shoot 的條件為：Stop on time per step 80 sec，此為分段式的造影，每段掃描範圍為 35 公分、收集 80 秒的時間，overlap 為 5 公分。

**結果：**收集的前兩位病人與第四位病人在影像上並沒有太大的差異，但在第三位病人的 anterior 影像上發現在由於此病人的 lesion 在 L spine (L4-L5) 的位置，剛好電腦重組影像時 L5 為交疊處，造成 L5 的位置在影像上相較於第一種 scan mode 看起來更深，而因對比的關係造成 L4 的位置相較變淺，此原因可能會導致醫師的誤判。

**結論：**第二種 scan mode (step and shoot) 電腦在重組影像時，由於 overlap 的關係，若 lesion 的位置剛好在 overlap 的交界處，影像交疊在一起，會造成 lesion 的位置在影像上看起來更深，而因對比關係造成周圍的 lesion 變淺，相較於第一種連續式造影在影像品質方面較不理想。

PC-036

## 利用 SPECT/CT 鑑別 AED 在全身骨頭掃描影像上之影響 – Case Report

許文齡 張淑敏 莊雅雯 張晉銓 王榛婷

高雄醫學大學附設中和紀念醫院核子醫學部

**背景介紹：**Automated External Defibrillator 簡稱 AED，是一台能夠自動偵測心律脈搏，並施以電擊使心臟恢復正常運作的儀器，其使用能大幅增加施救的成功率。然而除顫和胸部按壓過程可能會造成電燒傷及胸骨、肋骨骨折，在全身骨頭掃描影像上呈現異常的活性累積，傳統平面影像在區別病兆上有其限制，妥善使用 SPECT/CT 將能改善其限制。

**Case report：**一位 65 歲男性，有膽管癌病史，在全身骨頭掃描正面影像顯示：右上胸骨旁區域及左下胸壁有放射性示蹤劑累積，胸骨下部有放射性活性增加，雙側肋軟骨連接處可見熱點 (hot spot)。而胸部局部側面影像顯示：胸骨放射性活性增加及左下側一局部區域活性累積。因無法準確分辨其吸收為軟組織或骨頭，進而執行斷層影像。而在斷層影像中則能清楚分辨右上胸骨區其吸收為軟組織之吸收，左下胸壁亦為軟組織之吸收。經查詢相關病例發現病患幾天前因心搏停止而使用 AED 進行急救。

**討論：**全身骨頭掃描廣泛應用於癌症骨轉移及相關骨骼疾病診斷上，<sup>99m</sup>Tc-MDP 為最常使用之示蹤劑，除了骨骼會吸收外，亦有其他因素可使骨骼以外組織放射性聚集應加以鑑別，如游離的 Tc 會使腺體顯影，軟組織的發炎、損傷、鈣化亦會造成放射性積累，而影響判讀。平面影像判讀有其限制，SPECT/CT 的使用能補其不足，相關的病史詢問亦是重要的判讀根據。

PC-037

## 氟 -18 氟化鈉正子電腦斷層骨頭掃描 在攝護腺癌之應用—病例報告

王雅萍<sup>1</sup> 曾能泉<sup>1</sup> 歐宴泉<sup>2</sup>

<sup>1</sup> 童綜合醫療社團法人童綜合醫院核子醫學科

<sup>2</sup> 童綜合醫療社團法人童綜合醫院泌尿腫瘤中心

**簡介：**攝護腺癌是全球男性中第二大最常被診斷癌症，也是第六大癌症死因。攝護腺癌即使是早期發現仍有 10% 的骨轉移比例，晚期發現的骨轉移比例甚至高達 70%，是造成攝護腺癌死亡率高升的重要原因。骨轉移的檢查對於攝護腺癌的分期、處置和預後都非常重要。使用放射性同位素的骨骼造影可追蹤成骨細胞新生骨骼的狀況，這讓核子醫學在偵測骨轉移比起其他醫學影像更能早期發現，具有很大的優勢。目前臨床上常用的骨轉移檢查為 Tc-99m 亞甲基二磷酸鹽 (methylene diphosphonate MDP) 搭配閃爍攝影機的全身骨骼掃描；本病例所使用的氟 -18 氟化鈉正子電腦斷層 (<sup>18</sup>F sodium fluoride positron emission tomography/computed tomography <sup>18</sup>F-NaF PET/CT) 骨頭掃描在影像呈現上有更好的空間解析度與敏感度。

**病例報告：**本病例是 59 歲男性患者，2021 年 1 月發現攝護腺癌並施作根治性攝護腺切除術併雙側骨盆腔淋巴切除術，每隔 3 個月定期至核醫追蹤，全身骨頭掃描結果皆無骨轉移產生，因前列腺特異抗原 (prostate specific antigen PSA) 數值持續升高 (PSA: 3.301 ng/mL)，主治醫師 2021 年 6 月安排氟 -18 氟化鈉正子電腦斷層骨頭掃描，在此檢查之前給予 400 毫升白開水，檢查流程使用儀器 GE-Discovery MI PET-CT 靜脈注射 5 mCi <sup>18</sup>F-NaF，60 分鐘後進行氟 -18 氟化鈉正子電腦斷層骨頭掃描。掃描結果為右側坐骨活動性骨病變，右側坐骨高度攝取 (SUV<sub>max</sub> 18.31) 懷疑骨轉移，後續安排患者已接受完整放射治療，2022 年 6 月追蹤氟 -18 氟化鈉正子電腦斷層骨頭掃描，右側坐骨攝取已減少許多 (SUV<sub>max</sub> 4.72)，PSA 數值指數已下降 (0.008 ng/mL)。

**結論：**Tc-99m MDP 骨骼掃描為平面影像容易因相對位置重疊而不容易發現微小骨轉移，氟 -18 氟化鈉正子電腦斷層骨頭掃描在注射藥物後 1-2 小時即可得到最佳品質影像，比起 Tc-99m MDP 需 3-4 小時的骨骼造影更加縮短病患等候時間，<sup>18</sup>F-NaF 的生物分佈與血流量有很大的關係，其與血漿結合率很低，且在單次血液通過後就被骨吸收的比例接近 100%，吸收量可達到 Tc-99m MDP 的兩倍。氟 -18 氟化鈉正子電腦斷層骨頭掃描為 3D 立體影像可以提供更好的空間解析度與敏感度，所以可偵測微小骨骼轉移病灶，提供臨床醫師針對攝護腺癌早期骨轉移檢查更好的選擇。



PC-038

## 不同腎絲球過濾率下貧血與否和骨質疏鬆的關係

莊紫翎<sup>1,2</sup> 王昱豐<sup>3</sup>

<sup>1</sup> 慈濟醫療財團法人大林慈濟醫院核子醫學科

<sup>2</sup> 慈濟學校財團法人慈濟大學醫學系

<sup>3</sup> 臺北榮民總醫院核子醫學部

**目的：**貧血 (anemia) 和腎病變都是骨質疏鬆的潛在因子，文獻上之前的研究發現貧血與腎絲球過濾率 (eGFR) 結果之間存在 U 型關係，本研究目的為闡明貧血族群和正常非貧血族群在不同 eGFR 時，其與骨質疏鬆的關係。

**材料方法：**本篇為回溯性研究，收集 2014 年 6 月至 2020 年 7 月於本院預防醫學中心接受健康檢查之成年人。利用雙能量 X 光能量吸收儀 (dual-energy X-ray absorptiometry, DXA) (Hologic Inc., Discovery QDR series. Marlborough, MA, USA)，分析腰椎 (第一至四節) 與雙側髖部 (股骨頸與全髖部) 區域之 BMD 與 T-score，BMD 以絕對值表示，單位以  $\text{g/cm}^2$  表示，T-score 為低於年輕正常參考組 BMD 的標準偏差數 (亞洲數據庫)。所有受檢者均使用相同的 DXA 儀器來確保研究的相較間的正確性。骨質疏鬆組定義為 T-score  $\leq -2.5$ ，以三個區域中 T-score 最低為最終判定骨質疏鬆與否。並計算腎絲球過濾率 (eGFR)，分成八組 (< 60、60-69、70-79、80-89、90-99、100-109、110-119、 $\geq 120$  mL/min/1.73m<sup>2</sup>)。依血紅素 (hemoglobin) 分成正常組與貧血組，男性血紅素小於 13 g/dL、女生血紅素小於 12 g/dL，判定為貧血。並進行正常與貧血兩組間骨質疏鬆的比例的卡方檢定 (Chi-square)。

**結果：**所有人中，貧血組骨質疏鬆的比例較正常組高，有統計差異。進一步根據 eGFR 進行分組，在 eGFR 為 < 60、60-69、70-79、80-89 的組別，貧血組骨質疏鬆的比例較正常組高，有統計差異。在 eGFR 為 90-99 的組別，兩組間的骨質疏鬆比例無統計差異。在 eGFR 為 100-109、110-119、 $\geq 120$  的組別，正常組骨質疏鬆的比例較貧血組為高，有統計差異。

**結論：**貧血組和正常非貧血組骨質疏鬆的比例，在不同 eGFR 組別 (< 90 和  $\geq 100$ )，有所不同，潛在原因可能是 eGFR 高低的主要貧血原因不同，但真正的因素需要進一步研究分析。

PC-039

## 肝臟轉移性微鈣化在全身骨骼掃描表現

陳薇璇<sup>1</sup> 許幼青<sup>1</sup> 莊紫翎<sup>1,2</sup><sup>1</sup> 佛教慈濟醫療財團法人大林慈濟醫院核子醫學科<sup>2</sup> 慈濟學校財團法人慈濟大學醫學系

**影像報告：**一位 61 歲女性，經臨床證實為左側乳癌，醫師安排進行全身骨骼掃描檢查，影像結果顯示在腰椎和骶骨邊界有活性攝取，為退化性變化；另外，在前位像的胸椎第十一節前側和上腹部也有局部活性攝取，經單光子電腦斷層 / 電腦斷層造影 (SPECT/CT) 顯示皆為肝臟微鈣化。回溯之前的檢查結果，電腦斷層攝影 (CT) 檢查報告顯示肝臟低密度病灶，經病理切片證實為肝臟轉移性腺癌。而 FDG PET/CT 掃描，亦在肝臟發現局部高代謝病灶活性攝取。

**討論：**乳癌最常轉移至骨頭，其次是肝臟和肺臟，因此在完成一次常規的全身骨骼掃描後，在影像上任何活性攝取都會被注意，藉由 SPECT/CT 掃描，意外發現肝臟微鈣化，而後病理切片證實為肝臟轉移性腺癌。在全身骨骼掃描中肝臟局部的活性攝取常見為肝轉移，此外臨床上乳癌合併肝臟轉移預後較差，所以 SPECT/CT 可協助醫師早期發現病灶，及早治療。在全身骨骼掃描中有時候會發現腹部區域有異常的活性攝取，這時候要先判別是哪個區域，如果在右季肋區與腹上區，可能要注意肝臟的問題；在左、右腰區和臍區則是腸道；而活性攝取和脊椎重疊時會懷疑是骨骼。因為 Tc-99m MDP 的藥物機轉是與鈣進行結合，所以可以看到骨骼上的變化，包括器官上的微鈣化，因此可以協助臨床找出一些還未發現的病癥，SPECT/CT 可以有效的提供醫師準確的定位。

**結論：**全身骨骼掃描的骨外攝取增加可能由許多不同的病因引起。我們的案例表明肝臟微鈣化是骨外攝取的其中一個原因。SPECT/CT 對於評估肝臟意外的局部活性攝取很有價值。

PC-040

## 比較 18F-NAF 及 Tc-99m MDP 在偵測攝護腺癌的骨轉移—案例分析

曾柏銘<sup>1</sup> 呂建璋<sup>2</sup> 沈淑禎<sup>2</sup> 門朝陽<sup>1</sup> 林雅婷<sup>2</sup> 蕭聿謙<sup>3</sup>

<sup>1</sup>天主教中華聖母修女會醫療財團法人天主教聖馬爾定醫院正子造影中心

<sup>2</sup>天主教中華聖母修女會醫療財團法人天主教聖馬爾定醫院核子醫學科

<sup>3</sup>亞東紀念醫院核子醫學科

**前言：**Tc-99m MDP 全身骨骼掃描為一種低成本、高靈敏度的檢查方法，目前經常被使用在各類癌症合併骨轉移的術前評估及術後追蹤。而 18F-NaF 亦為核醫科近期較熱門用來檢測骨骼轉移的藥物，具有高能量、高靈敏度，低半衰期的藥物，是未來核醫在檢測骨骼轉移的一大利器，有報告顯示 18F-NaF 檢測骨病變的敏感性和特異性分別為 96% 和 98%，而 Tc-99m MDP 前列腺骨掃描的敏感性和特異性分別為 57% 和 98%。

**案例分析：**有一 64 歲男性受檢者因攝護腺癌至本院就診，PSA 指數為 167，泌尿科醫師為受檢者安排 Tc-99m MDP 骨骼掃描，在 Tc-99m MDP 骨骼掃描影像中僅發現在右髌骨有一病灶，臨床上並診斷不確定是否為骨轉移，遂安排該受檢者進行 NAF 正子骨骼掃描檢查，在 18F-NAF 影像上發現除原骨骼掃描發現的病灶點外，另外還發現了 3 個病灶點。對照 CT 影像因此可確定為多處骨骼轉移。

**討論：**在許多的研究報告中顯示，18F-NAF 比起 Tc-99m MDP 在診斷骨骼轉移上有著更好的靈敏度，其中 PSA < 10 在臨床上就該考慮有骨轉移，此案例的受檢者 PSA 雖高達 167，在 Tc-99m MDP 全身骨骼掃描卻只有一處病灶點，而 18F-NAF 骨骼掃描卻能顯影四個病灶處，並且對照 CT 可更準確診斷為骨骼轉移，顯示當 PSA 較高而 Tc-99m MDP 骨骼掃描無法確定為骨轉移時，18F-NAF 是一個較好的選擇。

**結論：**不同的藥物及儀器導致了其診斷性能的差異，18F-NaF 對於識別骨轉移有很好的診斷性能，能給于臨床醫師較高的參考價值甚至是改變了受檢者後續的治療方針。但 18F-NAF 仍然存在一些挑戰：成本高、稍高的輻射、缺乏廣泛的供應，以及易形成假陽性。但隨著 PET/CT 儀器掃描效率的提高，以及新的掃描和後處理技術的發展，未來 NAF 不管有無走向健保，應該都是一項偵測骨骼掃描的一項重要利器。

PC-041

## 氟-18 氟化鈉全身骨骼正子電腦斷層掃描案例分析

林娜宜 陳慶元

佛教慈濟醫療財團法人台中慈濟醫院

**背景介紹：**骨掃描是早期診斷轉移性骨病最常見的檢查，也是癌症治療前一個重要評估步驟。最常用的法是  $^{99m}\text{Tc}$ -MDP 骨頭掃描，因為  $^{99m}\text{Tc}$ -MDP 是一種價錢合理且容易獲得的放射性藥物，能敏感的偵測到成骨細胞的活性和活動力；氟-18 去氧葡萄糖正子電腦斷層全身掃描 ( $^{18}\text{F}$ -FDG PET/CT) 在骨轉移灶中的攝取機制取決於惡性細胞糖酵解活性的病理性增加，因此可以評估骨病灶的蝕骨細胞的葡萄糖的代謝情況；氟-18 氟化鈉全身骨骼正子電腦斷層掃描 ( $^{18}\text{F}$ -NaF PET/CT Bone scan) 氟離子通常大量聚積於中軸骨骼及骨關節處，不管是成骨性或蝕骨性的轉移病灶，都有更高的準確性，更容易區別良性與惡性骨骼病灶。與  $^{99m}\text{Tc}$ -MDP 相比，骨骼中  $^{18}\text{F}$ -NaF 的吸收更高，血液清除速度更快，在更短的時間內產生更好的目標與背景比。此外，與傳統的骨骼掃描相比，輻射暴露劑量無明顯差別。

**案例報告：**該案例為 69 歲男性，在它院做過頭頸部磁振造影、電腦斷層掃描和病理切片檢查，證實為下咽的鱗狀細胞癌並懷疑有肺部、T4 及 L5 骨頭轉移，而轉至本院治療，術前評估  $^{18}\text{F}$ -FDG PET/CT 和  $^{99m}\text{Tc}$ -MDP 全身掃描檢查，在  $^{18}\text{F}$ -FDG PET/CT 發現肺轉移，T4、L5 和骶骨處有骨硬化病變，但無蝕骨細胞不正常吸收，但在  $^{99m}\text{Tc}$ -MDP 骨骼掃描沒有看到 T4、L5 和骶骨處不正常吸收增加，進而安排了  $^{18}\text{F}$ -NaF PET/CT 掃描。

**結果：** $^{18}\text{F}$ -NaF 經靜脈注射 10 mCi 放射性追蹤劑後 1 小時掃描，影像顯示 T4、L5 和骶骨處的骨硬化病灶無異常放射藥物吸收，建議此骨病灶為良性變化。

**結論：** $^{18}\text{F}$ -NaF PET/CT 在腫瘤的分期之骨轉移檢測具有良好的診斷性能，且優於  $^{99m}\text{Tc}$ -MDP 及  $^{18}\text{F}$ -FDG，但因  $^{18}\text{F}$ -NaF 費用高於  $^{99m}\text{Tc}$ -MDP 數倍，在健保給付上有所限制，就以病人為中心角度來看，希望未來能夠更放寬健保適應症，以提昇臨床診斷和治療之品質。

PC-042

## A Benign Radiouptake on $^{99m}\text{Tc}$ -MDP Whole Body Bone Scintigraphy Mimicking Malignancy

Ya-Cing Hsu, Yu-Ling Hsu

*Department of Nuclear Medicine, Ditmanson Medical Foundation Chia-Yi Christian Hospital*

**Case:** A 54-year-old man suffered from left knee pain for several weeks. The X-ray exam showed an osteolytic lesion over left distal femur. Later on,  $^{99m}\text{Tc}$ -MDP whole body bone scan showed increased radioactivity at the same position. The differential diagnosis of medical imaging including solitary bone cyst, aneurysmal bone cyst, multiple myeloma, metastasis, or other nature. As the result, the pathological study revealed it was giant cell tumor of bone.

**Discussion:** Giant cell tumor (GCT) of bone is generally a benign tumor composed of mononuclear stromal cells and characteristic multinucleated giant cells that exhibit osteoclastic activity. It usually develops in long bones but can occur in unusual locations. The typical appearance is a lytic lesion with a well-defined but nonsclerotic margin that is eccentric in location, extends near the articular surface, and occurs in patients with closed physes.

Bone scan is one of the most common and oldest examinations among all nuclear medicine procedures. It is used in the evaluation of benign bone disease like infection/inflammation and also is the standard of care for evaluating metastatic disease in the breast, prostate, and lung cancer.

Though the reported sensitivity of bone scan is high, its specificity is low due to increased metabolic activity seen in benign disease such as trauma, infection, inflammation, and degenerative joint diseases. Widespread involvement usually suggests metastatic disease. A single focal lesion is almost always a cause of dilemma in reporting. In all such cases, the dilemma can be solved by a correlative CT or magnetic resonance imaging (MRI). In our case, it is truly difficult to differentiate from benign lesions from malignancy. Therefore, we should use multiple imaging method (including CT and MRI) to try to make optimal diagnosis.

PC-043

## Colon Visualization on $^{99m}\text{Tc}$ -MDP Whole Body Bone Scan

Juang-Wei Hsieh, Yu-Ling Hsu

*Department of Nuclear Medicine, Ditmanson Medical Foundation Chia-Yi Christian Hospital*

**Case:** The patient is a 52 year old female. She was hospitalized because of chest pain and gastroesophageal reflux disease. She was diagnosed by chest computed tomography as intraluminal esophageal tumor and a lot of ground glass opacity pattern in left upper lung. Surgical removal of part of the left lung and partial esophageal smooth muscle was performed. She came to the nuclear medicine department for yearly follow-up  $^{99m}\text{Tc}$ -MDP whole body bone scan.

After recent  $^{99m}\text{Tc}$ -MDP whole body bone scan, the first impression was suspicious  $^{99m}\text{Tc}$ -MDP uptake on right ilium at anterior view. When we took right anterior oblique position, we found that the increased uptake was probably over colon.

**Discussion:** The radiopharmaceutical  $^{99m}\text{Tc}$ -MDP was metabolized through the urinary system, and usually not visualized in the gastrointestinal tract. As literature revealed, most of the reasons for the radioactivity of the gastrointestinal tract are as follows: the gastrointestinal tract or urinary system is open up after tumor or surgical treatment, so the urine with  $^{99m}\text{Tc}$ -MDP flows to the gastrointestinal tract to be visualized. Or, the patient has acute or chronic gastroenteritis causing small bowel or colon ingest lots of  $^{99m}\text{Tc}$ -MDP. More unusual, the patient ingested urine with  $^{99m}\text{Tc}$ -MDP due to folk customs or mistaken knowledge, resulting in bowel activity. As in this case we have learned, in addition to the need of paying attention to the effect of different patient positions, it is also necessary to understand the patient's possible tumor location, treatment sequelae, and consider overall conditions.

PC-044

## 利用 SPECT/CT 診斷肺、胃攝取 Tc99m-MDP 一病例討論

王榛婷 許文齡 莊雅雯 張淑敏 張晉銓

高雄醫學大學附設中和紀念醫院核子醫學科

**背景介紹：**骨骼掃描常用於檢測癌症骨轉移、骨髓發炎、原發性骨腫瘤、骨折或是代謝性的骨病變，臨床應用非常廣泛。骨骼掃描主要是以平面影像做呈現，當病灶位置難以區別時，可配合單光子電腦斷層 SPECT/CT，得到的三度空間影像有助於發現病灶之相對位置。

**案例報告：**一位 56 歲女性患有左右側乳房惡性腫瘤，兩年前發現骨轉移，來院進行定期追蹤，發現整個中軸骨骼和兩年前相比，有放射性活性增加。特別的是，此病人這次的影像發現雙側肺以及胃，有明顯的放射性同位素積聚，已排除放射性藥物含有過量的游離 Free Tc 的可能。此病人先前患有高血鈣，推估是此原因造成軟組織攝取 Tc99m-MDP。經醫師評估，決定配合單光子電腦斷層 SPECT/CT，看能否將肋骨上的病灶與肺的活性積聚分別辨識。利用電腦後處理，得到病人軸向、橫向、縱向的三組影像，發現結合後的影像，肺的活性實在太高，導致影像太亮，無法分辨肋骨上是否有病灶。

**結論：**使用單光子電腦斷層 SPECT/CT，功能性的核醫影像可以與電腦斷層 CT 的解剖影像結合，解剖資訊增加了影像結果的特異性及敏感性。但此病例因軟組織攝取放射性藥物過多，單光子電腦斷層 SPECT/CT 也無法將影像上肋骨與肺的亮處分開，可以知道單光子電腦斷層 SPECT/CT 在骨骼掃描中還是有其限制。

PC-045

## 3-Phase $^{99m}\text{Tc}$ -MDP Bone Scan in Pigmented Villonodular Synovitis: A Case Report

Fang-Shin Liu<sup>1</sup>, Yuh-Feng Wang<sup>2</sup>

<sup>1</sup>Department of Nuclear Medicine, Dalin Tzu Chi Hospital, Buddhist Tzu Chi Medical Foundation, Chiayi, Taiwan

<sup>2</sup>Department of Nuclear Medicine, Taipei Veterans General Hospital, Taipei, Taiwan

**Introduction:** We present a case of pigmented villonodular synovitis (PVNS) and discuss the appearance on 3-phase  $^{99m}\text{Tc}$ -MDP bone scan.

**Case report:** The 63-year-old female was diagnosed with right knee PVNS in 2019 and status post right knee arthroscopic treatment. However, bilateral knee pain, more severe over right side, occurred more than 2 years ago. In Feb. 2022, she came to orthopedic outpatient department for help. Blood tests revealed elevated ESR (26 mm/hr) and joint aspiration showed turbid fluid and higher leukocytes without calcium pyrophosphate dihydrate nor uric acid crystals. Right knee joint MRI showed multiple synovial masses, effusion, femoral and tibial erosions, which was compatible with PVNS. 3-phase  $^{99m}\text{Tc}$ -MDP bone scan was also arranged and showed intense metabolic activity with increased vascularity at the site of right knee, more likely degeneration at L1/2 and L3/4 and probable arthritis at right elbow. No definite metastatic lesions were noted. Therefore, she underwent tumor resection of posterior knee on 2022/04/15, and received right TKR on 2022/07/14. Histopathology revealed compatible with PVNS.

**Discussion:** PVNS is a proliferative disorder of unknown etiology originating from synovial membranes of joints, tendon sheaths, and bursae. It causes significant swelling, pain, limited movement and even hemarthrosis. In 80% of cases, PVNS was found in one of the knee joints. Some develops in joints that have been damaged in previous injuries. Surgery is the main treatment to relieve the symptoms and prevent further damage to the joint. 3-phase  $^{99m}\text{Tc}$ -MDP bone scan is used to assess these lesions, and different patterns have been described. Typically, increased blood flow, blood pool and delayed radiotracer uptake were found. However, some reports demonstrated normal perfusion and blood pool images with only slightly increased radiotracer uptake on delayed images. SPECT/CT also provides valuable information by delineating the abnormality and revealing the extent of involvement, and is sometimes helpful in differentiating PVNS from other etiologies.



PC-046

## 在全身骨骼掃描中 發見少見的輸尿管結石活性攝取

張秀瑛<sup>1</sup> 莊紫翎<sup>1,2</sup>

<sup>1</sup> 佛教慈濟醫療財團法人大林慈濟醫院核子醫學科

<sup>2</sup> 慈濟學校財團法人慈濟大學醫學系

**背景介紹：**利用 Tc-99m MDP 來執行全身骨骼掃描可用以檢查骨頭是否有惡性轉移、發炎及骨折等情形。在全身骨骼掃描中發現結石有異常活性攝取是較為少見的，因為通常結石並不會吸收放射性藥物。在此篇病例報告中我們介紹一位在全身骨骼掃描結果中意外發現結石有活性攝取的病例。

**影像報告：**一名 74 歲，攝護腺特定抗原為 48.1 ng/mL，格里森分數為 4+4/10，左側輸尿管結石大小有 1.5 公分的男性攝護腺癌患者，於今年 5 月由外院轉至本科進行全身骨骼掃描。除常規的平面全身骨骼掃描之外，因檢查時發現肋骨、脊椎及骨盆處呈現異常的活性攝取增加，故針對脊椎及骨盆處加照 SPECT/CT。檢查結果發現第十胸椎及第三、第四腰椎左側的異常活性攝取是由退化性變化所造成，而右側第五肋骨及右側恥骨的異常的活性攝取可能是惡性骨轉移所造成。除此之外在左側腎水腫與左側輸尿管結石也有異常的活性攝取。

**結論：**全身骨骼掃描對於評估骨骼是否異常是一項很好的診斷工具，所使用的 Tc-99m MDP 會經由泌尿系統排泄，所以腎臟、輸尿管、膀胱等尿液聚積處可能會有正常活性攝取的現象，而結石組織通常不會吸收 Tc-99m MDP，根據文獻指出，結石產生活性聚積的機制可能是因放射性藥物在其晶體表面緩慢流動形成吸附所導致。此次所介紹的病例是在針對骨骼病灶加照 SPECT/CT 時意外發現輸尿管結石有異常活性攝取，藉此與大家分享。

PC-047

## 50 歲以上男性良性前列腺增生 與腰椎骨質密度分界點相關性探討

陳保良<sup>1,2</sup> 王昱豐<sup>3</sup> 廖建國<sup>1</sup> 莊紫翎<sup>1,4</sup>

<sup>1</sup> 佛教慈濟醫療財團法人大林慈濟醫院核子醫學科

<sup>2</sup> 佛教慈濟醫療財團法人大林慈濟醫院醫學研究部

<sup>3</sup> 臺北榮民總醫院核子醫學部

<sup>4</sup> 慈濟學校財團法人慈濟大學醫學系

**背景：**本研究目的為找出 50 歲以上男性良性前列腺增生 (benign prostate hypertrophy; BPH) 在腰椎骨質密度 (bone mineral density; BMD) 及 T-score 的分界點。

**方法：**這是一篇回溯分析，收集區間 2014 年 06 月至 2021 年 12 月於台灣南部某教學醫院預防醫學中心接受健康檢查之男性。排除年齡小於 50 歲、癌症、BMD 三個部位判斷為骨質流失、骨質疏鬆、或數據不完整的個案。最終共收集 1,993 位男性。

**結果：**平均年齡：60.63 ± 7.36 歲，平均身高：168.04 ± 5.69 公分，平均體重：73.68 ± 10.19 公斤，身體質量指數：26.06 ± 3.16 kg/m<sup>2</sup>，腰椎 BMD：0.171 ± 1.938 g/cm<sup>2</sup> (範圍 1.113 – 0.135)，腰椎 T-score：0.8 ± 1.1 (範圍 -0.9 – 7.8)。本篇研究數據分析顯示，腰椎 BMD 區域：曲線下面積 (area under curve, AUC) 為 54.1%，95% 信賴區間 (Confidence interval, CI) 為 0.513 – 0.570，靈敏度 44.4%，特異性 62.8%，p = 0.004，分界點為 1.128 kg/m<sup>2</sup>。腰椎 T-score 數值：AUC 54.1%，95% CI 0.513-0.569，靈敏度 61.3%，特異性 45.7%，p = 0.005，分界點為 0.5。

**結論：**雖然腰椎 BMD 與 T-score 對預測 BPH 的相關性偏低，但我們先前研究發現 BPH 會造成腰椎 BMD 增加之狀況，由於本篇研究是納入 50 歲以上的受檢者，分界點分別當腰椎 BMD 1.128 g/cm<sup>2</sup> 與腰椎 T-score 0.5 時，可以懷疑此受檢者能有 BPH 的問題，當然 T-score 大於 0.5 的時候 BPH 可能性一定會更高。未來我們將進一步利用高於分界點以上的受檢者同時又有 BPH 的受檢者，來進一步分析其相關性。

PC-048

## 比較癌症患者與非癌症受試者的股骨頸骨骼密度與十年骨折風險

蔡依良<sup>1,2</sup> 劉芳馨<sup>1</sup> 廖建國<sup>1</sup> 莊紫翎<sup>1,3</sup><sup>1</sup> 佛教慈濟醫療財團法人大林慈濟醫院核子醫學科<sup>2</sup> 佛教慈濟醫療財團法人大林慈濟醫院醫學研究部<sup>3</sup> 慈濟學校財團法人慈濟大學醫學系

**背景介紹：**癌症和用於治療癌症的療法都可能對骨骼產生重大的有害影響，增加骨質流失和骨折發展的風險。轉移性乳腺癌、前列腺癌、肺癌和其他癌症通常會影響骨骼，導致疼痛和骨折風險增加。十年骨折風險 FRAX<sup>®</sup> 是一種骨折風險的計算法，透過雙能 X 射線骨密度儀 (DXA) 測得的股骨頸骨骼密度，加上年齡、身高體重、病史以及生活史等因子的輸入計算而來。本篇的研究目的為比較癌症患者與非癌症受試者的股骨頸骨骼密度與十年骨折風險是否會因罹患癌症而有差異。

**方法：**收案受試者為回溯性收集本院預防醫學中心，於 2014 年 6 月至 2020 年 12 月間接受骨骼密度檢查的人。收集受試者利用 DXA 測得的左右二側股骨頸，利用 DXA 測得的骨骼密度來計算十年骨折風險，並且進一步再加入骨小樑分數 (TBS) 計算得到調整過後的十年骨折風險。受試者族群將不論癌症的種類或分期，只依照罹患癌症的與否，分為非癌症組和癌症組兩個組別。統計方法採用 t-test 比較二組的計量資料。以非癌症組作為基準組，使用二元羅吉斯回歸 (Binary logistic regression)，分析癌症 (y) 與左右兩側股骨頸骨骼密度、十年主要骨鬆性骨折機率 (MOF)、十年髕骨骨折機率 (HF)、TBS 調整後的十年主要骨鬆性骨折機率 (TBS-adjusted MOF) 及 TBS 調整後的十年髕骨骨折機率 (TBS-adjusted HF) (x) 之相關性。當  $p$  值小於 0.05 時，視為有統計上的意義。

**結果：**總共收集 18,668 名受試者，具有癌症病史的人有 674 名，占總受試族群的 3.6%。癌症組左右兩側股骨頸的骨骼密度明顯低於非癌症組，且兩側的 MOF、HF、TBS-adjusted MOF 以及 TBS-adjusted HF，皆顯著高於非癌症組 ( $p < 0.001$ )。癌症與十年骨折風險之二元羅吉斯回歸結果，不論加入 TBS 調整與否，癌症組所有的十年骨折風險皆高於非癌症組，勝算比 (Odds ratio, OR) 介於 1.049 至 1.060 間 ( $p < 0.001$ )。

**結論：**雖然十年骨折風險的計算中並未將癌症病史列入風險因子，但透過二元羅吉斯回歸比較癌症患者與非癌症受試者的十年骨折風險，結果顯示癌症是增加骨折風險的因素之一。建議癌症患者平時可適量的補充鈣質與維生素 D，定期追蹤骨骼密度的變化及治療，以延緩病理性骨折的發生。

PC-049

## 初步探討貧血女性平均紅血球容積與骨骼密度和骨小樑分數之相關性

蔡依良<sup>1,2</sup> 劉芳馨<sup>1</sup> 廖建國<sup>1</sup> 莊紫翎<sup>1,3</sup>

<sup>1</sup> 佛教慈濟醫療財團法人大林慈濟醫院核子醫學科

<sup>2</sup> 佛教慈濟醫療財團法人大林慈濟醫院醫學研究部

<sup>3</sup> 慈濟學校財團法人慈濟大學醫學系

**背景介紹：**血紅素 (hemoglobin) 是一種富含鐵的蛋白質，可以幫助紅血球將氧氣從肺部輸送到身體其他部位。假若無法為身體提供氧氣，可能會出現虛弱、嗜睡、頭暈、頭痛、呼吸急促或心律失常等症狀。此外長期貧血是心力衰竭的危險因子之一，不足的血紅素無法供應細胞足夠的氧氣外，同時易增加罹患骨質疏鬆症的風險。貧血依據平均紅血球容積 (mean corpuscular volume, MCV) 可分為小球性貧血、正球性貧血和大球性貧血。本篇研究欲透過 MCV 來探討貧血女性的骨骼密度與強度。

**方法：**回溯性收集本院預防醫學中心，受試者為 2014 年 6 月至 2021 年 11 月間接受健康檢查的貧血女性。貧血的定義為血紅素小於 12 g/dL，並進一步以 MCV 細分成三組，有小球性貧血 (< 80 fl) 組、正球性貧血 (80~100 fl) 組和大球性貧血 (> 100 fl) 組，作為變項 MCV group (小球性貧血 = group 1；正球性貧血 = group 2；大球性貧血 = group 3)。

統計方法使用 One-way ANOVA 比較三組不同 MCV 組別的計量資料，當組間有差異時 ( $p < 0.05$ )，使用事後檢定 Tukey test 進行兩兩比較。並使用簡單線性回歸分析 MCV group (x) 和骨骼密度及骨小樑分數 (y) 的相關性；當 MCV group 與骨骼密度及骨小樑分數有相關時 ( $p < 0.05$ )，將進一步使用多項式線性回歸分析 MCV group 與相關因子 (x) 和骨骼密度及骨小樑分數 (y) 的相關性。

**結果：**小球性貧血組的平均年齡為 50.3 ± 10.9 歲；正球性貧血組的平均年齡為 56.8 ± 12.8 歲；大球性貧血組的平均年齡為 61.9 ± 7.2 歲，MCV 較小的組別有較年輕的趨勢。且骨骼密度與骨小樑分數將隨著 MCV 的上升而下降 ( $p < 0.001$ )。

MCV group 與骨骼密度與骨小樑分數之簡單線性回歸結果，顯示所有變項皆與 MCV group 呈現負相關。加入年齡及身體質量指數兩個因子，進行模型調整後的多項式回歸結果，顯示除了腰椎骨骼密度外，其他部位的骨骼密度和骨小樑分數皆與 MCV group 呈現負相關 ( $p < 0.05$ )。

**結論：**初步探討 MCV 與骨骼密度和骨小樑分數的相關性，結果顯示雖然貧血女性的腰椎骨骼密度未隨著 MCV 上升而降低，但透過骨小樑分數顯示骨骼強度會隨著 MCV 上升而降低。因此建議罹患大球性貧血的女性應比小球性貧血女性多留意自身的骨骼健康，並建議可多攝取葉酸與維生素 B12。

PC-050

## Asymptomatic Intervertebral Disc Calcification on Tc-99m MDP Bone SPECT/CT Scan: A Case Report

Chao-Wei Tsai, Shih-Chuan Tsai, Shin-Yi Wang, Yi-Jing Lin, Jing-Uei Hou

*Department of Nuclear Medicine, Taichung Veteran's General Hospital, Taichung, Taiwan*

**Introduction:** Intervertebral disc calcifications can occur due to a variety of conditions, and back pain can occur. Only a few cases of symptomatic intervertebral disc calcification have been reported on Tc-99m MDP bone scans. We reported a case of intervertebral disc calcification without any symptom diagnosed by Tc-99m MDP bone SPECT/CT scan.

**Case Presentation:** We described a case report of a 52-year-old patient with nonkeratinizing carcinoma of nasopharynx, whom a new area of increased MDP uptake at the junction between the T9 and T10 vertebral bodies was found when receiving Tc-99m MDP bone scintigraphy for tumor restaging. The patient had no history of trauma or surgery at the thoracic spine, and there were also no local fever, pain and other symptoms and signs of systemic infection. An SPECT/CT was arranged for further evaluation, and intervertebral disc calcification was diagnosed due to the characteristics of CT images.

**Conclusion:** Intervertebral disc calcification may mimic different bone pathologies, including bone metastases, on planar images of Tc-99m MDP bone scan. An SPECT/CT scan will help physicians make differential diagnoses.

PC-051

## Evaluation of the Discharge Time of Patients with Differentiated Thyroid Cancer After Taking Large Doses of I-131

Chien-Hua Lu<sup>1</sup>, Chiang-Hsuan Lee<sup>2\*</sup>

<sup>1</sup>*Division of Nuclear Medicine, Chi Mei Medical Center, Liouying, Tainan, Taiwan*

<sup>2</sup>*Division of Nuclear Medicine, Chi Mei Medical Center, Tainan, Taiwan*

**Purpose:** Patients with well-differentiated thyroid cancer must be hospitalized after taking high-dose I-131 drugs, and can be discharged from the hospital when the body radiation exposure rate falls below a certain standard value. There is currently no domestic standard for this radiation exposure rate. The appropriate discharge time of patients treated with I-131 can be assessed by referring to the external release criteria.

**Methods:** This study was a retrospectively analyzed data from 106 patients (22 males, and 84 females, mean age, 51 years) who received 3.7 GBq (34 patients), 4.45 GBq (26 patients), 5.55 GBq (35 patients), 6.7 GBq (5 patients), 7.4 GBq (1 patient) of I-131 from June 2018 to December 2019. 24 hrs and 41 hrs after taking the medicine, the radiation dose was detected by the ATOMTEX AT1121 scintillation detector at 1 m. The length of hospital stay was evaluated according to the NRC criterion. The 10CFR35.75 "Restriction on Release of Patients Injected with Radiopharmaceuticals" of the US NRC stipulates that the patient's injection activity is  $< 30 \text{ mCi}$  or  $< 5 \text{ mrem/h}$  ( $50 \mu\text{Sv/h}$ ) You can be discharged without restrictions.

**Results:** By the NRC criterion ( $< 5 \text{ mrem/h}$  ( $50 \mu\text{Sv/h}$ ) 1 m away from the patient, 98 of 106 (92.5%) could have been discharged without isolation and within 24 hrs, and 8 of 106 (7.5%) Can be discharged without isolation within 41 hrs.

**Conclusions:** Referring to this standard to assess the appropriate discharge time, there are almost similar differences in different countries. Most patients can be discharged without isolation after 24 hrs, and all patients can be discharged after 41 hrs.

PC-052

## Utility of F-18 FACBC PET/CT Before Salvage Radiotherapy in a Prostate Cancer Patient with Biochemical Recurrence: A Case Report

Yi-Hsien Chou<sup>1</sup>, Shi-Wei Huang<sup>2</sup>, Chia-Ju Liu<sup>3</sup>, Mei-Fang Cheng<sup>3</sup>

<sup>1</sup>Department of Nuclear Medicine, National Taiwan University Hospital Yun-Lin Branch, Yunlin, Taiwan

<sup>2</sup>Department of Urology, National Taiwan University Hospital Yun-Lin Branch, Yunlin, Taiwan

<sup>3</sup>Department of Nuclear Medicine, National Taiwan University Hospital and  
National Taiwan University College of Medicine, Taipei, Taiwan

**Introduction:** Prostate cancer (PCa) is the fifth-most common cancer for male in Taiwan, with increased incidence and mortality rate in last decade. After PCa patients receive definitive therapy, up to half those experience biochemical recurrence (BCR). It is important to identify early lesion to initiate salvage treatment despite not all patients with BCR proceed to develop disease progression.

**Case Report:** The initial presentations of our patient were difficult voiding, urine retention, serum PSA 38.351 ng/ml plus hard nodule through digital rectal exam. Under the impression of very high risk group, TRUSP biopsy was executed and the result was Gleason score 3 + 4 adenocarcinoma. He decided to accept RALRP plus bilateral pelvic LND, and the pathology showed pT3bN0 with multifocal positive margin. Following serum PSA levels was an upward trend, and reaching the criteria of BCR in later half year. <sup>18</sup>F-FACBC PET/CT was suggested before scheduled salvage radiotherapy to postoperative prostate bed.

<sup>18</sup>F-FACBC PET/CT was arranged for the indication of BCR, and the images displayed focal hot spots at para-rectal, right internal iliac and left common iliac nodes. Therefore, salvage radiotherapy to prostate bed, pelvic lymph nodes and lymphatic instead of prostate bed alone was performed in accordance with modified RT plan.

**Conclusion:** This case report demonstrates the necessity of PET agents like <sup>18</sup>F-FACBC, which may lead to RT plan change, before salvage radiotherapy for PCa patients with BCR.

PC-053

## 在乳癌患者全身正子造影中發現疑似 mRNA 疫苗引起淋巴結及脾臟影像異常一案例報告

李佩璇 楊朝瑋

澄清綜合醫院中港院區核子醫學科

**背景介紹：**全身正子造影檢查常應用在乳癌的偵測及確定復發的範圍、乳癌的轉移、腋下淋巴結分期以及治療的反應。腋下淋巴結轉移是早期乳癌病人最重要的預後因子，因為淋巴結轉移範圍將影響治療方式的選擇。肌肉注射 COVID-19 mRNA 疫苗，可能會誘發同側腋下淋巴結反應。臨床上可能被錯誤認為是癌症轉移造成，或被歸類於因疫苗接種後的反應，而導致延誤治療。

**病例報告：**一名 37 歲女性為初診斷右側乳癌患者，在接受全身正子檢查前 4 天，於左上臂接種第二劑 COVID-19 mRNA 疫苗 (Moderna)。使用 Siemens Biograph Horizon，靜脈注射 10 mCi F-18 FDG 後 60 分鐘造影。全身正子檢查發現右側乳房腫瘤及右側腋下淋巴結 (level I-II) 的 SUVmax 分別為 17.4 及 3.0；同時在左側鎖骨上窩、左側腋下淋巴結 (level I-III) 及脾臟也有高度 FDG 攝取，SUVmax 分別為 4.7、15.9 及 3.5。

**討論：**研究顯示 FDG 全身正子檢查對腫大的淋巴結反應非常敏感，且肌肉注射 COVID-19 mRNA 疫苗後常見同側腋下淋巴結反應，接種第二劑後比第一劑更常見 [1]。此案例左側觀察到的鎖骨上窩、腋下淋巴結 FDG 攝取增加，需考量可能是由於對疫苗的炎症免疫反應造成。另有研究顯示，脾臟瀰漫性高度攝取與注射 COVID-19 mRNA 疫苗後造成全身免疫反應有關 [2]。

**結論：**執行 FDG 全身正子檢查前應記錄 COVID-19 疫苗注射史，包含注射日期、疫苗種類 (第一劑、第二劑及以上) 及注射位置，以協助報告判讀。



PC-054

## Evaluation of Radiomic Features Reliability in Lower Resolution Images Using Reduced-matrix-size $^{18}\text{F}$ -FDG PET

Yu-Hung Chen<sup>1,2,3</sup>, Kun-Han Lue<sup>3</sup>

<sup>1</sup>*School of Medicine, Tzu-Chi University, Hualien, Taiwan*

<sup>2</sup>*Department of Nuclear Medicine, Hualien Tzu-Chi Hospital, Buddhist Tzu Chi Medical Foundation, Hualien, Taiwan*

<sup>3</sup>*Department of Medical Imaging and Radiological Sciences, Tzu Chi University of Science and Technology, Hualien, Taiwan*

**Background:** Quantification of small lesions on PET is complicated by partial volume effect owing to limited spatial resolution. The effect of limited PET image resolution on the reliability of radiomic features is yet to be studied.

**Methods:** We prospectively analyzed  $^{18}\text{F}$ -FDG PET images from 27 lung cancer patients. The study has been approved by the local Institutional Review Board and Ethics Committee. We reconstructed standard, high ( $256 \times 256$  and  $384 \times 384$ ), and reduced matrix-size ( $128 \times 128$ , represented the low-resolution images) images from each patient. Fifty radiomics features (13 first-order or shape features, 17 GLCM features, 8 GLRLM features, 8 GLSZM features, and 4 NGTDM features) were extracted from the primary tumor. Intra-class correlation coefficient (ICC) was used to represent the reliability of radiomic features under the effect of image resolution differences.

**Results:** Eighteen radiomic features showed a high ICC  $> 0.9$  (11 first-order or shape features, 4 GLCM features, 2 GLRLM features, and one GLSZM feature). Although these 18 features generally showed lower ICCs when metabolic volumes  $< 10$ , the ICCs in 13 features still exceeded 0.9, and the remaining five demonstrated an ICC of 0.75-0.9.

**Conclusions:** First-order and shape features are generally less affected when matrix size is reduced, suggesting they may be less sensitive to image resolution reduction. Although small lesion size negatively affects the reliability, the effect is inconsequential for those 18 high-reliable features.

PC-055

## The Combination of Systemic Inflammation Marker and Tumor Glycolytic-volumetric Product as Prognostic Models in NSCLC Patients with Regional Lymph Node Metastasis

Chung-Ying Huang<sup>1</sup>, Yu-Hung Chen<sup>1,2,3</sup>, Kun-Han Lue<sup>3</sup>,  
Yi-Feng Wu<sup>1,4</sup>, Sung-Chao Chu<sup>1,4</sup>

<sup>1</sup>*School of Medicine, Tzu-Chi University, Hualien, Taiwan*

<sup>2</sup>*Department of Nuclear Medicine, Hualien Tzu-Chi Hospital, Buddhist Tzu Chi Medical Foundation, Hualien, Taiwan*

<sup>3</sup>*Department of Medical Imaging and Radiological Sciences, Tzu Chi University of Science and Technology, Hualien, Taiwan.*

<sup>4</sup>*Department of Hematology and Oncology, Hualien Tzu Chi Hospital, Buddhist Tzu Chi Medical Foundation, Hualien, Taiwan.*

**Background:** The survival outcomes of nodal positive non-small cell lung cancer (NSCLC) varied widely, and, a better survival stratification tool is an unmet need. To date, <sup>18</sup>F-FDG PET-derived features and systemic inflammatory markers are helpful in predicting survival of these patients. However, the effect of combining the two has not been thoroughly investigated.

**Methods:** We retrospectively reviewed 85 NSCLC patients with regional nodal metastasis. We used the Cox regression model to seek the independent prognosticators of overall survival (OS) and progression-free survival (PFS). Afterwards, we compared our devised survival stratification models based on the independent prognosticators to the traditional staging system using Harrell's concordance index (c-index).

**Results:** Age and total lesion glycolysis (TLG) > 81 independently predicted unfavorable PFS (HR = 1.026, p = 0.048; HR = 2.910, p = 0.001) and OS (HR = 1.043, p = 0.006; HR = 7.873, p < 0.001). Lymphocyte-to-monocyte ratio (LMR) < 3.4 and ECOG of at least 1 independently predicted poor OS (HR = 2.402, p = 0.003; HR = 2.855, p = 0.049). We integrated the independent predictors into survival prediction models. The integrative models attained c-indices of 0.784 and 0.683 in predicting PFS and OS respectively, outperformed the traditional staging system (c-indices of 0.527 and 0.550, both p < 0.001).

**Conclusions:** Our results indicate that the combination of LMR, total TLG and clinical risk factors enables better prognostic stratification in NSCLC patients with nodal metastasis. Our models may facilitate tailored therapeutic strategies in these patients.

PC-056

## Correlation of $^{18}\text{F}$ -FDG PET Features with Glucose Metabolic Signature Gene Mutation in Non-small Cell Lung Cancer

Yu-Hung Chen<sup>1,2,3</sup>, Kuang-Chi Chen<sup>4</sup>, Kun-Han Lue<sup>3</sup>, Sung-Chao Chu<sup>1,5</sup>

<sup>1</sup>*School of Medicine, Tzu-Chi University, Hualien, Taiwan*

<sup>2</sup>*Department of Nuclear Medicine, Hualien Tzu-Chi Hospital, Buddhist Tzu Chi Medical Foundation, Hualien, Taiwan*

<sup>3</sup>*Department of Medical Imaging and Radiological Sciences, Tzu Chi University of Science and Technology, Hualien, Taiwan*

<sup>4</sup>*Department of Medical Informatics, Tzu-Chi University, Hualien, Taiwan*

<sup>5</sup>*Department of Hematology and Oncology, Hualien Tzu Chi Hospital, Buddhist Tzu Chi Medical Foundation, Hualien, Taiwan*

**Background:**  $^{18}\text{F}$ -FDG PET has been widely used to evaluate the disease extent of non-small cell lung cancer (NSCLC). Its radiomic features also provide prognostic values. However, the genotypes that associate with glycolytic phenotype on  $^{18}\text{F}$ -FDG PET remain elusive.

**Methods:** We prospectively recruited patients with NSCLC who received pre-treatment  $^{18}\text{F}$ -FDG PET. Our study has been approved by a local Institutional Review Board and Ethics Committee. We select 73 glucose metabolic signature genes from the whole-exome sequencing (WES) for analysis. The gene mutation status is compared with the primary tumor  $^{18}\text{F}$ -FDG PET features.

**Results:** We analyzed the  $^{18}\text{F}$ -FDG PET and WES data from 29 NSCLC patients. In the 73 glucose metabolic signature genes, the mutation status of phosphofructokinase muscle gene (PFKM, 6 cases showed this mutation) correlates with  $^{18}\text{F}$ -FDG PET-derived features. Tumors with mutated PFKM showed a lower primary tumor  $\text{SUV}_{\text{max}}$  (8.3 versus 12.9,  $p = 0.02$ ) and  $\text{SUV}_{\text{mean}}$  (5.2 versus 8.2,  $p = 0.03$ ) are found in tumors with mutated PFKM. Furthermore, lower first-order entropy (3.8 versus 4.3,  $p = 0.16$ ) and entropy<sub>GLCM</sub> (4.6 versus 5.1,  $p = 0.10$ ) showed a statistical trend for patients with mutated PFKM.

**Conclusions:** Our preliminary results show a correlation between  $^{18}\text{F}$ -FDG PET-derived glycolytic phenotype and mutation of PFKM, which encodes a glycolytic regulatory enzyme. Further studies correlating PFKM and  $^{18}\text{F}$ -FDG PET features with clinical information may help discover their biological and pathophysiologic meanings.

PC-057

## Unusual Gliomatosis Peritonei Identified by 18F-FDG PET/CT: A Case Report

Shih-Ya Ma, Tzu-Ting Huang

*Department of Nuclear Medicine, Yuan's General Hospital, Kaohsiung, Taiwan*

**Introduction:** Gliomatosis peritonei is the implantation of glial tissue in the peritoneal cavity and a rare condition followed by treatment for immature teratoma. We report a case of ovarian immature teratoma with gliomatosis peritonei which had accumulation of FDG on a FDG PET/CT scan mimicking peritoneal metastases.

**Case Report:** A 29-year-old woman had history of left ovarian immature teratoma of stage IA and received left salpingo-oophorectomy followed by six cycles of chemotherapy with etoposide and cisplatin. At the 6 months follow-up, FDG PET/CT revealed a right ovarian cystic tumor (2.2 cm), containing fluid and a little fatty tissue without FDG accumulation and suspected to be a dermoid cyst. Additionally, there were numerous tiny soft tissue nodules at mesentery and omentum with mild FDG accumulation (the sizes of 0.4~1.0 cm; standard uptake value, SUVmax, early: 2.5 and delayed 3.5), and was suspicious for peritoneal metastases. Serum level of AFP, CA-199, Ca-125 and CEA were within normal limits. Second surgery found right ovarian tumor and numerous military nodules at mesentery and omentum. The final pathology demonstrated the presence of right ovarian mature teratoma, and mature glial tissue elements without immature tissues in mesenteric and omental nodules. A diagnosis of gliomatosis peritonei (GP) was made.

**Conclusions:** We report a case of gliomatosis peritonei with accumulation of FDG that developed after treatment for immature teratoma, mimicking peritoneal metastasis. In the follow-up examination after treatment for immature teratoma, we should consider that gliomatosis peritonei, which cannot be completely differentiated from metastases by imaging tests alone. In such a case, we should consider surgery and pathological examination to obtain an accurate diagnosis.

PC-058

## Dermatomyositis in a Patient with Newly Diagnosed Nasopharyngeal Carcinoma: A Case Report

Xuan-Ping Lu, Jui-Hung Weng, Pan-Fu Kao

*Department of Nuclear Medicine, Chung Shan Medical University Hospital, Taichung, Taiwan*

**Introduction:** Dermatomyositis is a kind of idiopathic inflammatory myopathy and is recognized as a paraneoplastic syndrome in adults. The risk of malignant tumors in the patients of dermatomyositis is approximately 1.8-3.6 folds of the general population. Cancer screening is usually recommended in these patients, but there is no consensus now. FDG-PET/CT may help tumor detection.

**Methods:** We reported a nasopharyngeal carcinoma patient who was referred for FDG PET/CT scan for staging. FDG-PET scan was performed after fasting for 6 hours with a GE Discovery MI PET/CT scanner at 60 min after intravenous injection of F-18- FDG. The CT scan is low-dose without contrast enhancement. The scan area covers vertex to above knees. Images are reconstructed iteratively with attenuation correction.

**Results:** FDG-PET/CT scan demonstrated diffusely increased FDG uptake in all skeletal muscles of the whole body. Tracing back his history, he suffered from skin rashes over face and chest with positive V-sign, Shawl's sign, Gottron papules, and heliotrope sign. Also, blood test revealed strong positive of TIF-1. Dermatomyositis was then impressed by the rheumatologist. Due to the patients also suffered from throat bleeding, he was referred to an otolaryngologist and nasopharyngeal carcinoma was diagnosed.

**Conclusions:** Although this case is first diagnosed with nasopharyngeal carcinoma and then referred for FDG PET/CT scan. Early detection and treatment of occult malignancies is important for patients with dermatomyositis. Patients with dermatomyositis may be recommended to receive FDG PET/CT scan for cancer survey.

PC-059

## Comparative Accuracy of FDG PET/CT and Endoscopic Ultrasound for Preoperative T-staging of Esophageal Squamous Cell Carcinoma

Yung-Cheng Huang<sup>1</sup>, Shau-Hsuan Li<sup>2</sup>, Hung-I Lu<sup>3</sup>, Chien-Chin Hsu<sup>1</sup>

*Department of <sup>1</sup>Nuclear Medicine, <sup>2</sup>Hematology-Oncology, and <sup>3</sup>Thoracic & Cardiovascular Surgery, Kaohsiung Chang Gung Memorial Hospital, Chang Gung University College of Medicine, Kaohsiung, Taiwan*

**Introduction:** The overall survival of esophageal cancer is dismal despite advances in the diagnostic methods and multimodal therapies in recent decades. Accurate assessment of T-stage is crucial to treatment planning and is one of the keys to individualizing therapy selection. FDG PET/CT with thresholded-SUVmax was found useful for classifying the T-stage. We further aimed to investigate comparative accuracy of FDG PET/CT and endoscopic ultrasound (EUS) for preoperative T-staging of esophageal squamous cell carcinoma (ESCC).

**Methods:** Patients diagnosed of ESCC underwent FDG PET/CT and EUS followed by surgical resection of the tumor were included for the analysis. The FDG PET/CT for T-stages were using thresholded-SUVmax classifications according to our previous report. The EUS for T-stages were classified as the depth of the primary tumor invasion by gastroenterologists with expertise in endosonography. The diagnostic performances of FDG PET/CT and EUS were calculated using pathological results as the gold standard according to the 8th American Joint Committee on Cancer (AJCC) staging system and overall accuracies were compared using McNemar's chi-square test.

**Results:** Among the totally 38 eligible patients included, pathology T-stages were 2 in T0, 22 in T1, 7 in T2, 6 in T3, and 1 in T4. The overall accuracy of the FDG PET/CT for predicting pathology T-stage was higher than the accuracy of our EUS results (76.3% vs. 57.9%,  $P = 0.09$ ). Using FDG PET/CT, the T-stage was understaged for 1 (2.6%) and overstaged for 8 of the patients (21.1%). Using EUS, the T-stage was understaged for 6 (15.8%) and overstaged for 10 of the patients (26.3%).

**Conclusion:** For preoperative T-staging of ESCC, the FDG PET/CT using thresholded-SUVmax classifications could achieve a higher accuracy than EUS.

PC-060

## I131 掃描發現膽囊活性之影像探討

朱秀蘭<sup>1</sup> 許文齡<sup>1</sup> 游慧貞<sup>2</sup> 繆孝謙<sup>3</sup>

<sup>1</sup> 高雄醫學大學附設中和紀念醫院核子醫學部

<sup>2</sup> 高雄醫學大學附設中和紀念醫院影像醫學部

<sup>3</sup> 高雄醫學大學附設中和紀念醫院心導管中心

**背景介紹：**以放射性碘 (I-131) 治療甲狀腺癌，透過  $\gamma$  及  $\beta$  兩種放射線，可以從體外偵測甲狀腺功能，並進行近距離的放射線標靶治療，以破壞癌細胞。且 I-131 只會經由甲狀腺細胞上的碘分子通道進入細胞，對於非甲狀腺細胞並無破壞力，除了療效顯著外，副作用也較一般化學治療藥物小，另外在服用後的第 8 天，利用  $\gamma$  射線的高穿透性做 I-131 掃描檢查，以鑑定治療效果如何。

**病例報告：**一位 73 歲女性患者於超音波檢查發現左側有巨大甲狀腺腫塊，確診為乳突性甲狀腺癌，因乳突性甲狀腺癌容易經由淋巴轉移，不易以手術根除。因此，甲狀腺癌病患在手術切除甲狀腺組織後，I-131 成為治療癌細胞的最佳選擇。

患者經過數週低碘飲食及甲狀腺素停藥後，於隔離病房給予 100 mCi 口服 I-131，在服用後第 8 天進行 I-131 掃描檢查，以偵測有無明顯轉移。在平面半身掃描及靜態掃描中，發現除了正常聚集在甲狀腺切除的殘餘組織、鼻骨、口腔黏膜、唾液腺、腸胃道和膀胱之外，在肝臟附近有異常的放射性活性聚集，因在平面影像上無法確認病灶位置，便進一步搭配使用單光子電腦斷層掃描，藉由 SPECT/CT 的影像中可以確認並不是在肝臟的位置上，而是在膽囊中。

**結論：**對於乳突性甲狀腺癌病患來說，利用甲狀腺癌可專一攝取 I-131 的特性，能得到相當好的治療品質。在 I-131 掃描檢查中，分化良好型甲狀腺癌轉移至肝臟的機率並不高，轉移的機率約只有 0.1%~0.97%，且大部分都是伴隨其他器官的轉移，較少單一轉移肝臟，因此有些關於肝臟附近偽陽性的病歷報告，如肝囊腫、肝內膽管擴張使放射線活性滯留於肝臟，而在聚積於膽囊內的原因可能因異常膽囊型態或生理功能造成，即像是急性或慢性膽囊炎或甲狀腺功能低下造成的膽汁鬱積等等，抑或是正常膽囊也可能有放射性碘攝取，但因身體前後器官重疊，在平面影像上無法區分病灶位置，進而造成偽陽性，這時可藉由 SPECT/CT 的影像，將傳統閃爍造影機與單光子電腦斷層掃描進行影像結合，提供解剖定位更精確之融合影像，提高判讀的正確性及臨床價值。

PC-061

## “FDG-devoid” Recurrent Low-grade Endometrial Stromal Sarcoma

Chin Hu, Shen DH

*Department of Nuclear Medicine, Kaohsiung Veteran General Hospital, Taiwan*

**Introduction:** Endometrial stromal sarcoma (ESS) is a very rare uterine mesenchymal neoplasm, accounting for only 0.2% of uterus malignancy, and low-grade, high-grade and undifferentiated subtypes is classified according to World Health Organization (WHO). We described the findings of FDG PET/CT in a case of recurrent ESS.

**Case Report:** In this report, we presented a 37-year-old female with endometrial stromal sarcoma, cT2bNxM0, pT1bNxM0, FIGO stage IB, s/p abdominal total hysterectomy, bilateral salpingectomy with ovary preservation on 2020-05-14 at other hospital. However, during asymptomatic routine follow-up, the MRI on 2022-01-21 showed one 2.8 cm enhancing lesion in pelvis adjacent to vagina stump, in suspicion of local recurrence. The FDG PET/CT performed later on the same day showed that “absent” FDG uptake in the lesion, which might be interpreted as negative result if not knowing the MRI information. This patient received excision of pelvic peritoneal tumor on 2022-01-28, and the pathology showed recurrent low-grade endometrial stromal sarcoma.

**Conclusion:** The FDG PET/CT of low-grade ESS is difficult to interpret correctly in the absence of MRI or other clinical information. The low-glucose-metabolism on imaging could be explained by the indolence of tumor, which may limit the utility of FDG PET/CT in detecting recurrence and metastasis.



PC-062

## Signet Ring Cell Carcinoma of Descending Colon Metastases to the Left Kidney and Ureter after Complete Resection Detected by FDG PET/CT

Li-fang Lin, Chiao-Yu Huang, Pei-Hua Li

*Division of Nuclear Medicine, Taoyuan General hospital, Ministry of Health and Welfare, Taiwan*

**Introduction:** Colorectal Signet ring cell carcinoma (SRCC) is a rare subtype of adenocarcinoma and accounts for around 1% of colorectal cancer. Hence, articles on colorectal SRCC FDG PET images are scarce. The incidence of ureteral metastases is about 1% in autopsy studies. Because most patients are asymptomatic, ureteral metastases are usually found incidentally or on autopsy. Herein, we present a case of colorectal SRCC, with ureteral and renal metastases 15 months after complete resection.

**Case report:** The 85-year-old woman has a history of signet ring cell carcinoma of descending colon complicated with bowel obstruction and received complete resection for 15 months. She took oral tegafur-uracil maintenance therapy and regularly visited the out-patient department. Nine months later, due to the elevated serum CEA level (7.2 ng/mL), F-18 FDG PET/CT was requested but the result was negative. After 6 months, there was a near triple increase of serum CEA (19.5 ng/mL). Besides, GFR decreased from 74.60 mL/min/1.732 to 33.28 mL/min/1.732. F-18 FDG PET/CT was requested for suspected recurrence and showed intense FDG activity in the dilated left ureter but very faint FDG activity in the urine of the renal pelvis. The CT showed a soft tissue tumor occupying the lower pole of the left kidney and left ureter. Referring to elevated tumor markers and image finding, recurrence in the left kidney and left ureter was diagnosed clinically. Then the patient received palliative chemotherapy due to old age and poor performance status.

**Conclusion:** Because of urinary FDG excretion and nonspecific symptoms, ureteral metastases might be overlooked on FDG PET/CT. Besides, in cancer patients, renal function deterioration with newly developed hydronephrosis in a short period might be a sign of ureteral recurrence or metastases. To avoid misinterpretation, referring with clinical history, tumor markers, renal function tests and previous medical images are crucial.

PC-063

## Hepatic Cysts Mimicking Hepatic Metastases in I-131 WBS and SPECT/CT

Tzyy-Ling Chuang<sup>1,2</sup>, Yuh-Feng Wang<sup>3</sup>

<sup>1</sup>Department of Nuclear Medicine, Dalin Tzu Chi Hospital, Buddhist Tzu Chi Medical Foundation, Chiayi, Taiwan

<sup>2</sup>School of Medicine, Tzu Chi University, Hualien, Taiwan

<sup>3</sup>Department of Nuclear Medicine, Taipei Veterans General Hospital, Taipei, Taiwan

**Introduction:** We present a case with well-differentiated thyroid cancer whose hepatic cysts mimic hepatic metastasis in I-131 whole-body scintigraphy with SPECT/CT.

**Case report:** A 58-year-old female had previous history of left breast cancer, s/p total mastectomy and sentinel lymph node biopsy. She had body weight loss 5-6 kg in past 6 months. Thyroid sonography showed one 11.0 x 9.0 mm ill-defined hypoechoic tumor with central calcification. Frozen biopsy showed papillary carcinoma. Bilateral total thyroidectomy showed papillary carcinoma of right lobe of thyroid gland, with Hashimoto's thyroiditis of both lobes, tumor staging: pT3 (AJCC, 2010). After operation, 116 mCi radioiodine was administered, and the whole body I-131 cancer work up with SPECT/CT showed tracer is seen in the region of sublingual area and two foci at the liver. Hepatic metastases are suspected due to the two unclear hypodense lesions seen at the 2.5 mA low energy CT of SPECT/CT (Infinia Hawkeye 4 System, GE Healthcare, Milwaukee, WI, USA). However, diagnostic contrast-enhanced CT showed multiple liver cysts, and the largest is 64.2 mm in diameter.

**Discussion:** Although diagnostic and post-therapy I-131 whole-body scintigraphy is a sensitive tool for depicting metastatic diseases after thyroidectomy in patients with well-differentiated thyroid cancer. There has been false-positive radioiodine uptake in cystic lesions in the literature, such as breast cyst, sebaceous cyst, pleuropericardial cyst, renal cyst, liver cyst, hepatic hydatid cyst, bronchogenic cyst, and parotid gland benign lymphoepithelial cyst. The main benefit of hybrid SPECT/CT is that it can improve the localization and characterization of the cause of uptake. However, in our case scanned with Infinia Hawkeye 4, CT energy with 4 slice, 140 kVp and 2.5 mA is not sufficient, and diagnostic CT, even contrast-enhanced CT, is required to provide the CT number (Hounsfield unit) for differential diagnosis. Moreover, the possibility and patterns of false positive in I-131 cancer work up should be always kept in mind.

PC-064

## Comparison of Pre and Post-doses of Hepatic Tumors Treated by Y90 Glass TheraSpheres SIRT

MennaAllah Mahmoud<sup>1,2</sup>, Ko-Han Lin<sup>2</sup>, Chien-An, Liu<sup>1</sup>, Rheun-Chuan Lee<sup>1</sup>,  
Yuh-Feng Wang<sup>2</sup>, Nan-Jing Peng<sup>2</sup>

<sup>1</sup>Department of Radiology, Taipei Veterans General Hospital

<sup>2</sup>Department of Nuclear Medicine, Taipei Veterans General Hospital

**Introduction:** Selective internal radiation therapy (SIRT) for liver cancers patients has been operated using Y90 theraspheres. Pre and post-dosimetric calculation was performed with 99mTc-MAA SPECT/CT and 90Y-PET/CT in 21 patients treated with 90Y glass microspheres using Simplicit90Y™ software (Boston Scientific). Dose-volume histograms were obtained. Doses at volumes 100%, 90%, 80%, 70%, 60%, 50%, 40%, 30%, 20%, 10% and 5% compared pre and post-treatment. And liver functions compared pre and post-treatment.

**Methods:** A cohort of 21 patients (one case of Neuroendocrine tumors (NET), one case of metastatic colorectal cancer (mCRC), two cases of Cholangiocarcinoma (CCA), and 17 cases of Hepatocellular carcinoma (HCC)) were included in this study. All patients underwent a diagnostic angiogram and administration of technetium-99m macro aggregated albumin (99mTC MAA), followed by planar and SPECT/CT acquisitions. The lung shunt fraction was calculated from planar imaging during treatment planning. After glass-based Y90 radioembolization post-Y90 RE bremsstrahlung PET was obtained.

**Results:** According to paired t-test, the absorbed tumor doses were statistically stable at pre and post doses, tumor to normal tissue and whole liver normal tissue dose were variable through pre and post-treatment with significance values = 0.0432 and 0.0417 respectively. Liver functions compared pre and at 6 weeks, 3 months, and 6 months post-treatment all functions were statistically stable pre and post-treatment. The Spearman correlation coefficient was used to study the correlation between liver functions and tumor and normal tissue post-absorbed dose. All factors have low correlation factors with pos tumor dose where Albumin and creatinine show a medium correlation.

**Conclusions:** Pre and post-absorbed tumor doses and liver functions are statistically stable for hepatic lesions treated through Y90 glass TheraSpheres SIRT.

PC-065

## Yttrium-90 Microsphere Selective Internal Radiation Therapy for Hepatocellular Carcinoma with Portal Vein Tumor Thrombosis: A Case Report

Chun-Pang Huang, Chien-Chin Hsu, Hong-Jie Chen

*Department of Nuclear Medicine, Kaohsiung Chang Gung Memorial Hospital, Kaohsiung, Taiwan*

**Introduction:** Selective internal radiation therapy (SIRT) with yttrium-90 (Y-90) loaded microsphere has been used as a locoregional therapy for unresectable hepatocellular carcinoma (HCC). We present a case of advanced HCC with PVTT treated with Y-90 SIRT followed by transarterial chemoembolization (TACE) and atezolizumab plus bevacizumab.

**Case report:** A 72-year-old man is a case of multiple bilobar HCCs (number more than 10 and size ranged from 1.3 cm to 7.0 cm) with right PVTT. His initial alpha-fetoprotein was 358.7 ng/ml. The clinical stage was cT4N0M0. After one cycle of atezolizumab plus bevacizumab, Y-90 SIRT was performed with SIR-Sphere (1.0 GBq via right hepatic artery and 0.5 GBq via S4 hepatic artery). The post-therapy Y-90 positron emission tomography revealed Y-90 microsphere distribution over right lobe and S4 liver tumors and right PVTT. Two months later, he underwent additional TACE with Tandem via S4 hepatic artery and left hepatic artery for left lobe liver tumors. The patient also received atezolizumab plus bevacizumab every 3 weeks. At the 24-week follow up after Y-90 SIRT, his alpha-fetoprotein was 12.2 ng/ml, and computed tomography demonstrated complete resolution of the HCC and PVTT.

**Conclusion:** Y-90 SIRT is a safe and effective treatment for advanced HCC with PVTT.

PC-066

## Outcome of Radium-223 Treatment for Patients with Metastatic Castration-resistant Prostate Cancer: A Single-Center Analysis

Pei-Ing Lee, Yu-Yi Huang, Bor-Tau Hung

*Department of Nuclear Medicine, Koo Foundation Sun Yat-Sen Cancer Center, Taipei, Taiwan*

**Introduction:** Radium-223 is a targeted alpha emitter that selectively binds to sites of high bone turnover resulting from bone metastasis. In the ALSYMPCA trial, Ra-223 had shown to prolong overall survival in metastatic castration-resistant prostate cancer (mCRPC) patients with symptomatic bone metastasis but no visceral metastasis. In our study, we aim to evaluate the effectiveness of Ra-223 in mCRPC patients treated at our center.

**Methods:** This retrospective review included 44 mCRPC patients with bone metastases who were treated with Ra-223 at our center between June 2016 and May 2021. Primary endpoint was the effect of Ra-223 on patient prognosis. Overall survival (OS) was estimated from the date of Ra-223 initiation. Factors including number of Ra-223 doses and prior chemotherapy use were also correlated with overall survival.

**Results:** In total, 70% (n = 31) of patients completed Ra-223 treatment, defined as receiving 5-6 Ra-223 doses. The most frequent reason for discontinuation of Ra-223 treatment was disease progression (n = 5). Other reasons included hematological adverse events (n = 4), infection (n = 3), and cardiac attack (n = 1). Multivariate analysis showed that patients with higher baseline hemoglobin (11.9 mg/dL) were more likely to complete Ra-223 injections (p = 0.013). At a median follow-up time of 9 months (range 1.1-29.8 months), 23 patients had died. Median OS from Ra-223 initiation was 11.95 months. Patients who received 5-6 Ra-223 doses (n = 31) had a longer median OS than those receiving 1-4 doses (n = 13). There was no observed difference in OS between patients with prior chemotherapy (n = 16) and chemo-naïve group (n = 28). Using ROC analysis, serum PSA level higher than 170 ng/ml at Ra-223 initiation predicted a poorer prognosis, with AUC of 0.7 (p < 0.01). There was a decrease in serum alkaline phosphatase (ALP) in 84% of patients throughout treatment. Bone symptoms were stable or improved in 82% of patients.

**Conclusions:** Completion of Ra-223 treatment was associated with better overall survival in mCRPC patients with bone metastases. Earlier timing of Ra-223 (prior to chemotherapy) did not affect patient prognosis.

PC-067

## Chordoid Meningioma Initially Presented as an Intraconal Tumor with Heterogenous Gallium Uptake

Sin-Di Lee<sup>1-3</sup>

<sup>1</sup>Department of Nuclear Medicine, Pingtung Veterans General Hospital, Pingtung, Taiwan

<sup>2</sup>Department of Nuclear Medicine, Kaohsiung Veterans General Hospital, Kaohsiung, Taiwan

<sup>3</sup>College of Artificial Intelligence, National Yang Ming Chiao Tung University

**Introduction:** Chordoid meningioma is a rare type of meningioma. Herein, we report a case of chordoid meningioma with initial presentation as an intraconal tumor with heterogenous gallium uptake.

**Case:** This 77-year-old woman was referred from ophthalmology to receive a Ga-67 scan because of blurred vision in the left eye for months. Physical examination showed disc edema. CT showed intraconal soft tissue infiltration. Ga-67 scan with SPECT/CT for head and neck showed that the mass is gallium-avid with extension to the left central skull base, temporal lobe, and left midbrain. Endoscopic endonasal tumor biopsy 6 days later revealed chordoid meningioma, WHO type 2. Orbital decompression was performed as well. She refused the further surgical procedure. Therefore, she received definite radiotherapy. No evidence of recurrence is noted during the 8-month follow-up.

**Discussion:** Chordoid meningioma is a rare type of meningioma, with a high proliferative index, aggressive behavior, and high recurrent rate. To our best knowledge, chordoid meningioma noted on the Ga-67 scan was reported only once in 1993. In our case, it presented with heterogenous gallium uptake.

PC-068

## <sup>18</sup>F-FDG PET/CT Limitations in Evaluation of Mucinous Adenocarcinomas

Yi-Hsun Chen, Yu-Ling Hsu

*Department of Nuclear Medicine, Ditmanson Medical Foundation Chia-Yi Christian Hospital*

**Case report:** A 67-year-old woman presented to the out-patient-clinic with body weight loss. Lab data showed elevated CEA levels. Abdominal CT disclosed peritoneal and omental hypodense nodules, ascites, and dilated appendix with wall thickening. Initially, the impression was cecal cancer with peritoneal carcinomatosis. However, <sup>18</sup>F-FDG PET/CT yielded no abnormal FDG uptake. This patient received a surgical biopsy, and the histopathology report confirmed to be mucinous adenocarcinoma.

**Discussion:** Mucinous adenocarcinoma is a common gastrointestinal tract cancer that accounts for about 17% of colorectal tumors. The tumor cells contain clear, gelatinous mucin, which may be intracellular or extracellular. Mucins are high-molecular-weight glycoproteins resulting in an unusually high percentage of false-negative results. Lower levels or absence of FDG uptake in mucinous tumors might be due to a reduced number of tumor cells, replaced by mucin in the microenvironment, resulting in a decreased tumor cellular density. In our case, the histological showed mucin pools containing neoplastic glands lined by atypical epithelium. Therefore, it may lead to false negative FDG PET/CT imaging results. Awareness of the potential limitations of FDG PET with histological subtypes is essential for adequately applying this technique.

PC-069

## Post COVID-19 Pneumonitis Mimicking Lung Metastases of Lymphoma on $^{18}\text{F}$ -FDG PET/CT: A Case Report

Hsi-Huei Lu, Nan-Tsing Chiu

*Division of Nuclear Medicine, Department of Medical Imaging,  
National Cheng Kung University Hospital, Tainan, Taiwan*

**Introduction:** Coronavirus disease 2019 (COVID-19) pneumonia could present as various computed tomography (CT) findings, including ground-glass opacities, consolidations, and septal thickening, which may resemble other infectious, non-infectious diseases, or even neoplasm. Here we present a case of COVID-19 lung sequelae that mimics lymphoma metastases on FDG-PET/CT.

**Case Report:** This is a 42-year-old woman with underlying disease of asthma. She had been diagnosed with follicular lymphoma, grade 3A, Lugano stage 4, and had received chemotherapy with rituximab plus cyclophosphamide, doxorubicin, vincristine, and prednisone for six cycles in 2020. The mass showed partial remission and she was then given rituximab maintenance. However, follow-up CT scan revealed newly-developed ground glass densities over bilateral lungs, and serology showed elevated lactate dehydrogenase (525 U/L, reference range 135-225 U/L).  $^{18}\text{F}$ -fluorodeoxyglucose positron-emission tomography/computed tomography was arranged and showed bilateral consolidative pulmonary patches with intense FDG uptake (maximum standardized uptake value, 14.50), predominantly in subpleural locations. Tracing back her medical history, she was infected with COVID-19 which was confirmed with reverse transcription polymerase chain reaction testing 2 months ago, with symptoms of cough and sore throat, but recovered well without antiviral medication or hospitalization. Repeated bone marrow aspiration was negative for malignancy. Under the impression of infectious lung disease, active surveillance was suggested. A subsequent chest x-ray showed gradual regression of lung infiltrates.

**Conclusion:** The imaging features of COVID-19 pneumonia could mimic other pathologies presenting with lung disease. FDG PET/CT has potential utility in aiding diagnosis and monitoring of disease. Previous studies have shown high FDG uptake is often observed in the associated lung lesions during acute infection, but less is known about the presentation of post-acute sequelae of COVID-19 pneumonia on PET/CT. We present a case with lung patches demonstrating intense FDG uptake in the subacute phase 8 weeks after infection, which mimicked metastases of underlying lymphoma.



PC-070

## Primary Squamous Cell Carcinoma of the Thyroid: A Case Report

Hsin-Chang Chen, Yen-Hsiang Chang

*Department of Nuclear Medicine, Kaohsiung Chang-Gung Memorial Hospital  
and Chang-Gung University, Kaohsiung, Taiwan*

**Introduction:** Primary squamous cell carcinoma of the thyroid (PSCCT) is a rare and rapidly progressive neoplasm of the thyroid gland with a very poor prognosis. Due to the aggressiveness of primary tumor, enlarging anterior neck mass is the most prevalent initial presentation of PSCCT. Herein, we report an uncommon case of PSCCT with advanced metastatic disease despite a small primary tumor.

**Case presentation:** A 77-year-old woman presented with a progressively painful neck mass and local swelling for 2 weeks. She had a history of total thyroidectomy several months ago and the pathology revealed a small SCC component surrounded by Hurthle cell tumor, without extrathyroidal extension or capsular invasion. Computed tomography (CT) showed multiple enlarged left neck lymph nodes (LNs) with carotid artery encasement. The core-needle biopsy of neck LNs was applied and the results confirmed the diagnosis of SCC. The SCC components of both thyroid tumor and LN metastasis were found to be PAX8 (Paired Box 8) positive in immunohistochemical expression. Furthermore, no occult head and neck cancers were detected by otorhinolaryngology examination and F-18 FDG PET/CT study. Thus, the diagnosis of PSCCT was established by the consensus of multidisciplinary teams. The patient was then referred to oncology for platinum-based concurrent chemoradiotherapy.

**Conclusions:** PSCCT typically presents with rapidly aggressive disease. Tissue biopsy with immunohistochemistry is currently the preferred examination for the diagnosis. A complete otorhinolaryngology inspection accompanied by image studies assists the diagnosis. It is important for assessing the possibility of curative surgery. F-18 FDG PET/CT plays a pivotal role for detecting/excluding SCC from other origin and for PSCCT staging.

PC-071

## Metastatic Thyroid Cancer in the Lungs and the Cervical Vertebrae with Benign Thyroid Disease: A Case Report

Tsu-Kang Chen, Yen-Hsiang Chang\*

*Department of Nuclear Medicine, Kaohsiung Chang Gung Memorial Hospital  
and Chang Gung University, Kaohsiung, Taiwan*

**Introduction:** Ectopic thyroid tissue is rare in patients with a history of benign thyroid disease. However, with multisystem involvement of the ectopia, the behavior of the thyroid tissue raises the concern of malignant metastases. Herein we present a case of metastatic thyroid cancer in the lungs and cervical vertebrae with a history of benign thyroid disease of multinodular goiter.

**Case Report:** A 71-year-old woman with a history of total thyroidectomy for multinodular goiter presented with bilateral pulmonary nodules. Thoracoscopic excisional biopsy was performed for the largest nodule, and pathological examinations showed features of the benign thyroid tissue. Radioiodine (RAI) therapy was administered for the remaining pulmonary nodules. However, the post-therapy whole body scan revealed multiple RAI-avid foci in the cervical vertebrae and sternal manubrium, in addition to the pulmonary nodules. Positron emission tomography-computed tomography also showed hypermetabolism of the bone lesions. She underwent wide tumor excision for the cervical vertebral lesions, and pathological examination revealed metastatic carcinoma, consistent with thyroid origin. Repetition of radioiodine therapy was performed later and the post-therapy whole body scan showed persistent RAI-avid lesions in the lung and sternum.

**Conclusions:** This is a rare case of metastatic thyroid cancer without evidence of malignancy in the thyroid gland. Although the pathologic features of metastatic tumors mimic benign thyroid tissue, aggressive management and intensive follow-up should be considered in such cases.

PC-072

## FDG-PET/CT 掃描在葡萄膜黑色素瘤的應用 — 案例報告

劉宛茹 陳慶元

佛教慈濟醫療財團法人中慈濟醫院核子醫學科

**背景介紹：**黑色素瘤，是一種從黑色素細胞發展而來的癌症，絕大多數黑色素瘤發生在皮膚，是致死率很高的皮膚癌，但也可能出現在口腔、腸道或眼睛。葡萄膜黑色素瘤是一種罕見的疾病，每年每百萬人中有 5.1 例，但卻是成人中最常見的原發性眼部惡性腫瘤，也稱為眼內黑色素瘤。葡萄膜黑色素瘤最常見於脈絡膜黑色素細胞 (85%–90%)，但也可能來自虹膜 (3%–5%) 和睫狀體 (5%–8%)。葡萄膜黑色素瘤具有很高的轉移傾向，診斷為葡萄膜黑色素瘤的患者有 50% 會發生遠端轉移，常見於肝臟 (91%)、肺 (28%)、骨骼 (18%) 和皮膚 (12%) 等。

**病例報告：**患患者為 48 歲男性，因覺得視力下降、視野變窄至眼科檢查，經眼科檢查後，眼科醫師懷疑為在脈絡膜的惡性黑色素瘤，因此安排正子檢查。在注射 10 mCi 的 F-18 FDG 藥物 60 分鐘後，請患者至正子掃描室執行檢查，使用 GE Discovery ST PET-CT 儀器做約 30 分鐘全身的掃描。

**結果：**在影像中發現左眼球脈絡膜內側有一個小結節性病變，其 FDG 吸收上升，並針對該部分再進行延遲攝影，其他部位無異常發現。測量 SUVmax 值，左眼球脈絡膜內側的病變在初始掃描的 SUV 值為 2.33，在延遲攝影時該部位的 SUV 值上升為 2.77。

**結論：**FDG-PET/CT 提供的代謝和結構信息相結合，提高了腫瘤分期、復發檢測的準確性，並對患者診斷及治療提供較充分的訊息。因為葡萄膜黑色素瘤遠端轉移的風險很高，因此可透過 FDG-PET/CT 有效評估患者是否有遠端轉移。

PC-073

## 利用奧攝敏正子造影偵測攝護腺癌病人之肺部轉移 —病例報告

蔡沛君<sup>1</sup> 曾能泉<sup>1</sup> 歐宴泉<sup>2</sup>

<sup>1</sup> 童綜合醫療社團法人童綜合醫院核子醫學科

<sup>2</sup> 童綜合醫療社團法人童綜合醫院泌尿腫瘤中心

**簡介：**根據衛福部 110 年統計，攝護腺癌為十大癌症死因中死亡率排名第五名的癌症，其發生率與死亡率有逐年上升之趨勢。攝護腺癌常復發轉移的部位包含攝護腺床、骨骼、肝臟、肺部等。當兩次血中攝護腺特異抗原 (prostate specific antigen, PSA) 皆超過 0.2 ng/ml，或是相較於最低點，PSA 上升超過 2 ng/ml 時，即稱作生化性復發 (Biochemical recurrence, BCR)。奧攝敏正子造影 (<sup>18</sup>F-Fluciclovine PET/CT scan)，適用於先前接受治療後因 PSA 濃度上升而懷疑攝護腺癌復發之病患，以協助診斷攝護腺癌之復發。

**病例報告：**病患為 72 歲攝護腺癌男性，初期 PSA 為 10 ng/ml 於達文西機器手臂攝護腺根除手術 (RARP)，治療後 PSA 恢復正常值小於 0.008 ng/ml，並持續追蹤，但二年後 PSA 數值上升至 0.425 ng/ml 卻不到原因，故安排奧攝敏正子造影檢查。病患空腹 4 小時，於右手注射 <sup>18</sup>F-Fluciclovine，劑量 10 mCi，正子造影掃描儀型號為 GE Discovery MI，注射完畢 4 分鐘後立即進行造影。造影範圍為骨盆至頭頂，並於電腦斷層部分預設一組肺部電腦斷層影像供醫師閱片。造影結果發現左上肺葉 (LUL) 有一藥物聚集，為 0.68 公分結節，標準攝取值 (SUVmax) 為 1.38，參考點第三腰椎 SUVmax 值為 4.27。隨後安排手術，病理報告表示腫瘤細胞顯示 α- 甲基醯基輔携 A 消旋携 (AMACR) 和攝護腺特定細胞膜特定抗原 (PSMA) 陽性，故判斷為轉移性攝護腺癌，並持續追蹤。

**結論：**一般正子示蹤劑不易於太小之肺結節聚積，但在本次檢查肺部卻能有藥物的聚積，在臨床上具有相當的意義。再者奧攝敏影像判讀常與遠端腹主動脈、骨髓 (L3 椎骨) 和肝臟之攝取值比較，對於小病灶 (< 1 cm) 其攝取值大於血池或骨髓應被懷疑為惡性。雖然該病患肺部攝取值沒有大於血池或骨髓，但醫師依據奧攝敏影像及以重組肺部電腦斷層影像輔助判斷為肺部轉移且經手術證實。奧攝敏正子造影檢查能協助醫師更精準的判別病灶位置，並可以讓臨床醫師及病患獲得更完整訊息，得以及早調整後續治療計畫。

PC-074

## Clinical Nuclear Medicine Comparison of the Detection Performance Between FAP and FDG PET/CT in Various Cancers: A Systemic review and Meta-analysis

Li-Yu Chen<sup>1</sup>, Wen-Yi Chang<sup>2†</sup>, Neng-Chuan Tseng<sup>3,4</sup>, Chi-Wei Chang<sup>1,2,5</sup>,  
Ya-Yao Huang<sup>1,6,7</sup>, Ya-Ting Huang<sup>1,8\*</sup>, Yen-Chuan Ou<sup>9,10\*</sup>, Nan-Jing Peng<sup>2,11\*</sup>

<sup>1</sup>Primo Biotechnology Co., Ltd, Taipei, Taiwan

<sup>2</sup>Department of Nuclear Medicine, Taipei Veterans General Hospital, Taipei, Taiwan

<sup>3</sup>Division of Nuclear Medicine, Tungs' Taichung Metro Harbor Hospital, Taichung, Taiwan

<sup>4</sup>Department of Public Health, China Medical University, Taichung, Taiwan

<sup>5</sup>Department of Biomedical Engineering and Environmental Sciences,  
National Tsinghua University, Hsinchu, Taiwan

<sup>6</sup>Institute of Medical Device and Imaging, National Taiwan University College of Medicine, Taipei, Taiwan

<sup>7</sup>Molecular Imaging Center, National Taiwan University, Taipei, Taiwan

<sup>8</sup>Department of Medical Education and Research, Camillian Saint Mary's Hospital Luodong, Yilan, Taiwan

<sup>9</sup>Division of Urology, Department of Surgery, Tungs' Taichung Metro Harbor Hospital, Taichung, Taiwan

<sup>10</sup>Department of Research, Tungs' Taichung Metro Harbor Hospital, Taichung, Taiwan

<sup>11</sup>School of Medicine, National Yang-Ming Chiao Tung University, Taipei, Taiwan

<sup>†</sup>These authors have contributed equally to this work and share first authorship

**Introduction:** [<sup>18</sup>F]F-fluorodesoxyglucose (FDG) is the dominant radiotracer in oncology; however, it has limitations. Novel labeled fibroblast activation protein (FAP) radiotracers have been developed and published in several studies. Thus, this meta-analysis aimed to compare the detection rates of FDG and FAP, based on previous studies from a systematic review.

**Methods:** PubMed/MEDLINE and Cochrane library databases were used to perform a comprehensive and systematic search and are updated to April 30, 2022. After 192 articles were retrieved, and 54 full-text articles were assessed for eligibility after screening titles and abstracts and removing duplicate records. Finally, 30 studies were included. The detection rate (DR), relative risk (RR), and the maximum standardized uptake value (SUVmax) were calculated between the FAP and FDG tracers for the primary tumor and lymph node metastasis.

**Results:** The DR of FAP tracer for primary tumor and LN metastasis per patient and per lesion both were higher than FDG tracer, that the RR for primary tumor per patient and per lesion was respective 1.13 (95% CI 1.73-6.10,  $p = 0.0013$ ) and 1.14 (95% CI 1.07-1.22,  $p < 0.0001$ ), as well as, for LN metastasis per patient and per lesion was respective 1.13 (95% CI 1.03-1.24,  $p = 0.007$ ) and 1.12 (95% CI 1.10-1.15,  $p < 0.0001$ ).

**Conclusions:** FAP is an extremely potential radiotracer to replace most of the use of FDG in oncology.

PC-075

## Intense Diaphragmatic Uptake in a Sedated Patient Experienced of Desaturation and Dyspnea During PETCT Examination

Ya-Ju Tsai

*Department of Nuclear Medicine, Taipei Medical University Hospital*

**Introduction:** Unilateral or bilateral diaphragmatic and crural FDG uptake could be a kind of physiologic distribution. But intense diaphragmatic uptake to a large extent is unusual. We reported a case of significant diaphragmatic activity related to desaturation and dyspnea during PETCT acquisition.

**Case report:** A 77-year-old male is a case of B-cell lymphoma over thoracic spine status post total laminectomy of T1 and T2 vertebrae, with partial laminectomy and tumor removal of T3 vertebra. FDG-PETCT was further arranged and revealed residual malignancy at upper thoracic spine with intense & bilateral diaphragmatic activity, but only mild FDG uptake of neck & intercostal muscles. The patient was under sedation due to agitation and desaturation was noted during PETCT examination. Oxygen supply with mask was given for hypoxemia.

**Discussion:** Whole body FDG-PETCT is a common imaging modality for staging, therapy response and detecting recurrence disease in oncology. Familiarity of physiologic conditions and benign diseases is important for nuclear medicine physician to diminish false positive or borderline reports. FDG uptake of diaphragmatic crura is not rare in clinical practice. But intense diaphragmatic uptake to a large extent is unusual. High glucose metabolism in the crura, unilateral or bilateral diaphragm secondary to hyperventilation and hiccups has been reported. In our case, a rare presentation of significant diaphragmatic uptake without corresponding activity in neck and intercostal muscles raised the suspicion of lymphoma disease involvement. But after consideration of the patient's condition about desaturation during examination and under sedation, physiologic muscular uptake of diaphragm was considered first.

**Conclusion:** Significant diaphragmatic uptake without corresponding activity in neck and intercostal muscles could be a physiologic distribution in a sedated patient experienced of desaturation and dyspnea. Clinical correlation with the patient's condition during PETCT examination is mandatory for differential diagnosis.

PC-077

## Using F-18 Fluciclovine as a Substitute for F-18 Boronophenylalanine (FBPA) Before Boron Neutron Capture Therapy – A Preliminary Experience

Ko-Han Lin<sup>1</sup>, Wen-Yi Chang<sup>1</sup>, Yi-Wei Chen<sup>2</sup>, Nan-Jing Peng<sup>1</sup>, Wen-Sheng Huang<sup>3</sup>

<sup>1</sup>Department of Nuclear Medicine, Taipei Veterans General Hospital, Taipei, Taiwan

<sup>2</sup>Department of Oncology, Taipei Veterans General Hospital, Taipei, Taiwan

<sup>3</sup>Department of Nuclear Medicine, Cheng Hsin General Hospital, Taipei, Taiwan

**Introduction:** Boron neutron capture therapy (BNCT) is a promising cancer treatment method which relies on the absorption of a nonradioactive boron-10 isotope of tumor cell and the nuclei fission reaction induced by thermal neutron, then inducing an intracellular high linear-energy-transfer alpha particle and a recoiling lithium particle to kill the tumor cell. A successful BNCT treatment not only requires a tumor-specific boron-10 carrier to accumulate in the tumor, but also needs a theranostic probe to predict the boron-10 carrier concentration inside tumor before BNCT.

Currently, a theranostic combination of boronophenylalanine (BPA) and Fluoro-18 labeled boronophenylalanine (FBPA), which are absorbed through L-type amino-acid transporter 1 (LAT-1) by tumor cell, has been conducted in most clinical settings. Unfortunately, the producibility and dispensability of FBPA always limit the use of this crucial probe of BNCT. Thus, we conducted a study of using F-18 Fluciclovine, which also enters the tumor cell through LAT-1 like FBPA, as an alternative probe and compared with FBPA.

**Methods:** Preliminarily, we recruited one patient of brain stem glioma and one patient of maxillary sinus carcinoma and performed F-18 Fluciclovine PET and FBPA PET on a hybrid GE SIGNA PET/MRI scanner. Both images were acquired at 60 minutes after radioisotope injection. The interval between two scans were within one week. The images were reviewed on a GE Advanced Workstation. The tumor-to-normal-tissue (T/N) ratio was determined using auto-segmentation based on a SUV threshold fitting the tumor contour on simultaneous MRI images.

**Results:** In both patients, F-18 Fluciclovine accumulated in the tumors quite significantly and the images were similar compared to the FBPA PET. The T/N ratio from Fluciclovine PET and FBPA PET were 3.10 and 3.44 in the brain stem tumor, respectively. In the patient of maxillary sinus carcinoma, the T/N ratio were 3.58 and 3.12 from Fluciclovine PET and FBPA PET, respectively. The SUV thresholds to draw tumor contours for both imaging modalities were different and might need to be determined by physicians.

**Conclusion:** For the first impression, the F-18 Fluciclovine PET images and the T/N ratio results mimicked FBPA PET quite well. However, due to uncertain pathways of F-18 Fluciclovine in tumor cells, larger scale of patient recruitment is warranted for further confirmation.

PC-078

## Compared with the Difference in Detection Performance Between $^{68}\text{Ga}$ -PSMA-PET/CT and Multi-parametric MRI in Prostate Cancer: A Systematic Review and Meta-analysis

Ya-Ting Huang<sup>1,2</sup>, Li-Yu Chen<sup>1</sup>, Chih-Yi Wu<sup>1</sup>, Ya-Yao Huang<sup>1,3</sup>, Yuh-Feng Wang<sup>4</sup>

<sup>1</sup>*Primo Biotechnology Co., Ltd, Taipei, Taiwan*

<sup>2</sup>*Department of Medical Education and Research, Camillian Saint Mary's Hospital*

<sup>3</sup>*Molecular Imaging Center, National Taiwan University, Taipei, Taiwan*

<sup>4</sup>*Department of Nuclear Medicine, Taipei Veterans General Hospital, Taipei, Taiwan, R.O.C*

**Introduction:** The incidence of prostate cancer is fourth place in the world, but the diagnostic tools for early detected prostatic cancer have limitations due to poor diagnostic performance. Multiparametric magnetic resonance imaging (mpMRI) has been promoted as an auxiliary diagnostic tool before prostate biopsy. Currently, prostate-specific membrane antigen (PSMA) such as  $^{68}\text{Ga}$ -PSMA-11 combined with positron emission tomography/computed tomography (PET/CT) are another acquaintance tool for detecting prostate cancer staging. The current meta-analysis aimed to compare the difference in diagnostic performance of  $^{68}\text{Ga}$ -PSMA-11 PET and mpMRI for localized prostatic tumors and T-staging.

**Methods:** This meta-analysis perform a systematic literature search from PubMed/MEDLINE and Cochrane liberatory databases and is updated to May 25, 2022. The pooling detection rate and related risk (RR) of PSMA and mpMRI were calculated. Subsequently, the pooling sensitivity and specificity of PSMA and mpMRI by the verified pathological analysis were calculated and used RR to compare the differences between the two imaging tools.

**Results:** 26 studies were included (3614 patients in total) from 2016 to 2022 in the current meta-analysis and found that the pooling RR of detection rate for localized prostatic tumors and T-staging (T3a and T3b) was 0.99 (95% CI 0.97- 1.00,  $p = 0.83$ ), 0.85 (95% CI 0.59- 1.23,  $p = 0.39$ ), and 1.04 (95% CI 0.77-1.41,  $p = 0.97$ ), respectively. The pooled sensitivity for localized prostatic tumors and T-staging (T3a and T3b) of PSMA-PET was respective 0.88 (95% CI 0.84-0.91), 0.63 (95% CI 0.44-0.80), and 0.70 (95% CI 0.64-0.86), while that of mpMRI was found to be 0.85 (95% CI 0.76-0.91), 0.55 (95% CI 0.43-0.67), and 0.65 (95% CI 0.39-0.84), without significant differences, either ( $p > 0.05$ ).

**Conclusions:** There was a consistent detection performance between  $^{68}\text{Ga}$ -PSMA-11 PET and mpMRI for localized prostatic tumors and T-staging.



PC-079

## 鎳 - 前列腺特異性膜抗原 (Lu-177-PSMA) 靶向治療之 輻射安全措施及實測劑量一個案報告

林亭君 洪綾蔓<sup>1</sup> 張筱琪<sup>1</sup> 楊詩涵<sup>1</sup> 李銘忻<sup>1</sup> 黃玉儀<sup>1,2</sup>

<sup>1</sup> 和信治癌中心醫院核子醫學科

<sup>2</sup> 國立陽明交通大學醫學院醫學系

**背景介紹：**Lu-177-PSMA，前列腺特異性膜抗原 (PSMA) 靶向治療。此治療在台灣屬於全新治療方式，在此提出第一個臨床個案治療經驗，提供治療中環境輻射偵測及工作人員接收之輻射劑量，以及住院期間放射廢棄物的處置。

**個案報告：**64 歲男性，患有轉移性去勢療法抗性攝護腺癌，大量淋巴結、肝、骨、腹膜轉移，經 Ga-68-PSMA-11 正子掃描後進行 200 mCi Lu-177-PSMA-617 之治療。

- 一、Lu-177-PSMA-617 治療：採重力法靜脈輸注，給藥前置作業時間約 30 分鐘，給藥過程約 30 分鐘，治療後放射性廢棄物處理約 30 分鐘。
- 二、輻射偵測項目及使用設備：監控給藥過程之人員劑量、治療後 3 天之病房護理人員劑量、病人離開病房後的環境監測、住院期間病人產生廢棄物的量測、病人治療後之體外輻射劑量率。人員劑量監控使用個人輻射警報器 (Thermo, Electronic Personal Dosimeter)，環境及廢棄物的監測使用 Atomtex AT1121 偵檢儀。

### 三、各項測量結果：

#### (一) 工作人員：

1. 治療期間 (D0)：核醫醫師、藥師、放射師、核醫護理人員及同位素治療病房護理師監控結果分別為 10、3、9、1、2  $\mu\text{Sv}$ 。

2. 一般護理師照護劑量：D1~D3 共 3 天，由 4 位護理人員輪值，進入病房次數 22 次，平均一位護理師進入 5.5 次，一次照護約接受 2.27  $\mu\text{Sv}$ 。

(二) 藥物注射完畢時距離病人腹部體表、30 公分、100 公分量測之輻射劑量率分別為 296、44、11.1  $\mu\text{Sv/hr}$ 。

(三) 治療後第二、七、十七天，病人腹部體表其輻射劑量率分別為：320、111、15  $\mu\text{Sv/hr}$ ；距離 30 公分其輻射劑量率分別為：39、9.8、3.1  $\mu\text{Sv/hr}$ ；距離 100 公分其輻射劑量率分別為：6.6、1.75、0.5  $\mu\text{Sv/hr}$ 。

(四) 病房環境及廢棄物監測：過程中量測到床單 2.33  $\mu\text{Sv/hr}$ ，生物醫療廢棄物 0.08  $\mu\text{Sv/hr}$ 。尿布相關廢棄物 31  $\mu\text{Sv/hr}$ 。

**結論：**本次治療時主要操作人員輻射暴露都可控制在 10  $\mu\text{Sv}$  以內。若依此類推，一般醫護人員年劑量限度小於 1 mSv，可容許每年執行 1250 次此治療。輻射工作人員以一年不超過 20 mSv，可容許醫師每年執行 2000 次；放射師每年執行 2222 次此治療。

PC-080

## Survival Analysis of Liver Cancer Patients Treated by Y90 Glass TheraSpheres SIRT

MennaAllah Mahmoud<sup>1,2</sup>, Ko-Han Lin<sup>1</sup>, Chien-An Liu<sup>2</sup>, Rheun-Chuan Lee<sup>2</sup>

<sup>1</sup>Department of Nuclear Medicine, Taipei Veterans General Hospital, Taipei, Taiwan

<sup>2</sup>Department of Radiology, Taipei Veterans General Hospital, Taipei, Taiwan

**Introduction:** Selective internal radiation therapy (SIRT) for liver cancers patients has been operated using Y90 theraspheres. Pre- and post-dosimetric calculation was performed with 99mTc-MAA SPECT/CT and 90Y-PET/MRI in 21 patients treated with 90Y glass microspheres using Simplicit90Y™ software (Boston Scientific). Tumor response to treatment was assessed through up to 12 months according to Response Evaluation Criteria in Solid Tumors (RECIST) and progression free survivor (PFS) was calculated.

**Methods:** The study included 21 patients: one with neuroendocrine tumors (NET), one with metastatic colorectal cancer (mCRC), two with cholangiocarcinoma (CCA), and 17 with hepatocellular carcinoma (HCC). All patients had a diagnostic angiogram and technetium-99m macro aggregated albumin (99mTc MAA) administration, followed by planar and SPECT/CT acquisitions. During treatment planning, the lung shunt fraction was calculated using planar imaging. Post-Y90 RE PET was obtained following glass-based Y90 radioembolization on a GE hybrid SIGNA PET/MRI.

**Results:** Treatment responses were compared as two groups: disease-progression group and treatment-responder group. The relation between treatment response and post tumor doses (TD) up and lower than 200 Gy was studied using Kaplan-Meier analysis. For post-TD higher than 200 Gy, mean survival time was 10.71 months and (95% CI, 8.42-11.92). For post-TD lower than 200 Gy, mean survival time was 10.2 months and (95% CI, 7.3-13.09). Log-rank test static = 0.048,  $p = 0.83$ .

**Conclusions:** Post-absorbed tumor doses show a progression free survivor higher than 10 months is post tumor doses higher and lower than 200 Gy. According to log rank test there are no significant difference between doses higher and lower than 200 Gy.

PC-081

## Prognostic Evaluation of $^{18}\text{F}$ -BPA-PET on Malignant Tumors

Nan-Jing Peng<sup>1,2</sup>, Yi-Wei Chen<sup>3</sup>, Ling-Wei Wang<sup>3</sup>, Jia-Cheng Lee<sup>3</sup>,  
Wan-Tien Hsieh<sup>1</sup>, Ko-Han Lin<sup>1</sup>

<sup>1</sup>Department of Nuclear Medicine, Taipei Veterans General Hospital, Taipei, Taiwan

<sup>2</sup>School of Medicine, National Yang Ming Chiao Tung University, Taiwan

<sup>3</sup>Department of Oncology, Taipei Veterans General Hospital, Taipei, Taiwan

**Introduction:** Boronophenylalanine (BPA) is a tumor-specific probe of L-type amino acid transporter 1 (LAT1). The system LAT1 imports BPA mainly into proliferating cells. Therefore, the expression of the LAT1 may play a significant role in tumor progression. This study is performed to analyze the relation of  $^{18}\text{F}$ -BPA PET on malignant tumors associated with their patient survival.

**Methods:** Patients with malignant tumors underwent  $^{18}\text{F}$ -BPA PET were divided into two groups: the T/N ratios derived from  $^{18}\text{F}$ -BPA PET  $\geq 2.5$  (Group 1) or those  $< 2.5$  (Group 2). The results were analyzed on the basis of clinical follow-up. Chi-squared test was used to examine the differences between groups. A cumulative survival curve was derived using the Kaplan–Meier method. Differences were considered to be significant at  $p < 0.05$ .

**Results:** In total, 146 patients with T/N ratios derived from  $^{18}\text{F}$ -BPA PET (55 in Group 1 and 91 in Group 2) were enrolled. Those were 106 brain tumors, 38 head and neck tumors, 1 renal tumor and another adrenal tumor. Mortality were observed in 91 patients. The survival of patients in Group 1 was slightly higher than that in Group 2 [(43.64% (24/55) vs. 34.07% (31/91),  $p = 0.1023$ ]. There is also no significant difference of cumulative survival between patients with the brain tumors and the other tumors [38.68% (41/106) vs. 35.00% (14/40),  $p = 0.2260$ ].

**Conclusions:** In this study, we found T/N ratios derived from  $^{18}\text{F}$ -BPA PET might not be related to the patient survival. BPA uptake was not associated with the outcome among different type of malignant tumors.

PC-082

## Demonstration of a Pheochromocytoma of Adrenal Using Low-dose of I-123 MIBG Scan: A Case Report

Shiou-Chi Cherng<sup>1,2</sup>, Yu-Hsiang Chou<sup>1</sup>, Tsung-Han Yang<sup>1</sup>

<sup>1</sup>Department of Nuclear Medicine, Taipei Tzu Chi Hospital, Buddhist Tzu Chi Medical Foundation, Taiwan

<sup>2</sup>School of Medicine, Buddhist Tzu Chi University, Hualien, Taiwan

**Abstract:** Iodine-123 metaiodobenzylguanidine (I-123 MIBG) scan has been used for localization of pheochromocytoma since 1981. The dose of 185-370 MBq (5~10 mCi) of I-123 MIBG for imaging is commonly recommended. In Taiwan, the availability of I-123 MIBG, however, still is limited due to lack of the tracer. We demonstrate a pheochromocytoma of adrenal in an adult male patient using low-dose (111 MBq; 3 mCi) of I-123 MIBG scan.

**Case Report:** A 67-year-old male patient was referred for I-123 MIBG scan because of suspicion of an adrenal pheochromocytoma. The 24-hours urinary excretion of vanillyl mandelic acid (VMA; 11.02 mg/24 h, normal range: 1.00-7.50) and norepinephrine (166  $\mu$ g/24 h, normal range: < 97.0) were elevated. An abdomen CT revealed a 2.9 cm nodule at the right adrenal gland. Lugol's solution 2% (potassium iodide 4% and iodine 2%), 7.5 mL daily, was given for 3 days (1 day before tracer injection and continuing for 3 days). A low-dose of 111 MBq of I-123 MIBG was injected intravenously. Whole body planar imaging was performed, which were obtained by collecting 500 K counts in both anterior and posterior views 24 hours after tracer injection. SPECT/CT of abdomen/pelvis images were obtained subsequently. The images of I-123 MIBG showed increased tracer uptake in the right adrenal tumor. A right adrenalectomy was performed; pathological examination confirmed the diagnosis of pheochromocytoma.

**Conclusion:** Oral taking thyroid blockade of Lugol's solution for 3 days and intravenous injection of 111 MBq of I-123 MIBG to an adult male suspected a victim of pheochromocytoma of right adrenal, whole body planar followed by SPECT of abdomen/pelvis images were obtained 24 hours after tracer injection. The images may show the pheochromocytoma distinctly.

PC-083

## Performance of Different Image Reconstruction Parameters in F-18 Fluciclovine Brain PET/MR

Yi-Lun Chen<sup>1,2</sup>, Bang-Hung Yang<sup>1,2</sup>, Ko-Han Lin<sup>1,2</sup><sup>1</sup>Department of Nuclear Medicine, Taipei Veterans General Hospital, Taipei, Taiwan<sup>2</sup>Integrated PET/MR Imaging Center, Taipei Veterans General Hospital, Taipei, Taiwan

**Introduction:** F-18 Fluciclovine is a new synthetic non-metabolic leucine derivative, which not only is used in prostate cancer imaging but also is able to accumulate in glioma cells through a large amount of transporter that evaluates the malignant level of glioma. Q.Clear is a block sequential regularized expectation maximization penalized-likelihood reconstruction algorithm. Compared to ordered subset expectation maximization (OSEM), Q.Clear can achieve full convergence and control noise level, so that it can provide a more accurate quantitative value and higher SNR. Therefore, we will evaluate performance of F-18 fluciclovine Brain PET in different image reconstruction parameters by using simultaneous PETMR scanner.

**Methods:** There were 10 patients who were diagnosed glioma and underwent F-18 Fluciclovine brain PET/MR in this study, retrospectively. The image reconstruction used OSEM and Q.Clear algorithms. Q.Clear algorithm was reconstructed with different  $\beta$  values (from 200 to 1000) to evaluation performance and find an optimal beta value. All image was analyzed by AW server. The volume of interests (VOIs) were drawn on the tumor, normal cerebellum tissue and muscle by referring to MRI image (T1 BRAVO and T2 FLAIR) and calculated the noise level and signal to noise ratio (SNR).

**Results:** Regardless of the image reconstruction methods, it was showed a significant accumulation of activity in gliomas, but low uptake in normal cerebellum tissue. Compared with the OSEM method, the higher the  $\beta$  value of the Q.Clear image reconstruction method, the lower the Noise level ( $P < 0.005$ ). And the SNR in Q.Clear is higher than that in OSEM, but there is no obvious trend. When the  $\beta$  value was set to 500, there was the most suitable noise level and SNR, which reduced the noise level by an average of 0.98 times and improved the SNR by 1.13 times.

**Conclusions:** F-18 Fluciclovine brain PET/MR can effectively evaluate the malignancy of glioma. Furthermore, the use of Q.Clear image reconstruction method can reduce the Noise level and improve the SNR and we recommend optimal  $\beta$  value is set at 500 for F-18 Fluciclovine brain PET/MR.

PC-084

## 回溯分析腋下前哨淋巴結定位檢查經驗分享

張添信 陳慶元

佛教慈濟醫療財團法人台中慈濟醫院核子醫學科

**背景介紹：**根據衛生福利部資料統計顯示，女性癌症位居首位依就是乳癌，然而政府每年投入大量的人物力資源，進行大規模施行乳房篩檢業務，進而提早發現提早治療，以降低未來的社會醫療費用，乳房前哨淋巴結定位是乳癌定義是否有癌細胞淋巴轉移的指標，常為乳房手術的參考，本篇主要探討腋下前哨淋巴結定位檢查靈敏度與經驗分享。

**方法：**利用回溯分析探討 2021 年 1 月至 2022 年 3 月，本科室施行前哨淋巴結定位檢查共 139 位，平均每月執行 9.4 位病人數，每位病人皆為淋巴手術前施行核醫腋下前哨淋巴結定位檢查，由核醫科醫師進行給藥，給藥位置依病人病灶位置，分為四象限乳頭處進行皮下給藥，但如病人病灶是在乳房體表淺處，則改施打於病灶位置上給藥，給藥後請病人順時鐘按摩乳房三分鐘後進行造影，動態造影每 3 秒 / 張共 30 張，靜態 10 分鐘後加上鈷 -57 平面密封性射源增加病人輪廓外觀影像，然後加上一張靜態側位照，造影結束後請專科判定是否加一小時後延遲靜態像，最後由核醫專科醫師報告判定前哨淋巴結是否顯影。

**結果：**此研究總共收集，施行 139 位腋下前哨淋巴結定位檢查，偵測前哨淋巴結定位敏感度為 98.5% (137/139)，是一個非常有效率的檢查，協助乳房外科勾勒出定位前哨淋巴結的位置。

**結論：**現今機器更新造影的品質效率與速度行遠自邇，能有好的偵測效能提高準確度，也讓病人可以得好的術後生活品質，減少病人不必要的淋巴水腫現象發生，雖然敏感度接近百分之百但也有可能出現偽陰性發生要特別注意根據前哨淋巴結定位檢查準則，必要時可以增加電腦斷層攝影增加確認位置，提升檢查完整度。

PC-085

## 使用不同儀器測量 I-131 膠囊計數之比較探討

吳忠順 郭建璋 譚鴻遠

高雄榮民總醫院核醫科

**目的：**臨床於執行甲狀腺攝取率時須先測量 I-131 膠囊計數，此計數對於計算甲狀腺攝取率的影響極大。本研究目的在比較使用本科 4 台不同儀器測量 I-131 膠囊計數，對於每台儀器之偵測效率與偵測距離對計數之影響進行比較探討。

**材料方法：**使用本科 4 台儀器 Siemens EVO、Siemens Symbia S、GE DR-870 及 Philips Bright view 搭配中能量準直儀，統一使用矩陣 128\*128、能窗 364 keV $\pm$ 10%、偵測時間 1 分鐘及倍率 1 倍進行收集，偵測距離分別為偵測器距離假體 5、10、15 及 20 公分，另分別收集 Siemens Symbia S 搭配 Pinhole collimator 偵測器距離假體 1、2、3、4、5 及 6 公分之影像。分析影像時以不圈選 ROI 及圈選 10000 mm<sup>2</sup> ROI 進行比較探討。

**結果：**每台儀器之偵測效率皆有不同，使用中能量準直儀時偵測距離對於計數於不圈選 ROI 時之變化較小（每增加 5 公分時約減少 5-6.8%），但圈選 ROI 時變化會變大（增加 5 公分時約減少 14.5-17.3%）。使用 Pinhole collimator 偵測時是否圈選 ROI 對計數之影響並不顯著，但偵測距離對計數之影響相較中能量準直儀則更為顯著（每增加 1 公分約減少 17.2-22.8%）。不圈選 ROI 時偵測計數由高到低為 EVO、Bright view、Symbia S、DR-870。但圈選 ROI 時計數由高到低為 EVO、Symbia S、Bright view、DR-870。DR-870 之計數值相較其他儀器明顯較低（約 40-50%）。

**結論：**使用 Gamma Camera 執行甲狀腺攝取率，宜事先建立不同儀器 I-131 膠囊計數之轉換率，以備儀器故障時替換，如使用 Pinhole collimator 測量 I-131 膠囊計數宜嚴格管控測量距離，使誤差降到最低。

PC-086

## SUVmax = 3.5 May not be Directly Applied as the Domestic Diagnostic Criterium to Differentiate Whether Lymph Node Metastasis or not on FDG PET/CT Scan in Squamous Cell Carcinoma of Oral Cavity Patients

Jui-Hung Weng<sup>1,2</sup>, Pan-Fu Kao<sup>1,2</sup>

<sup>1</sup>Department of Nuclear Medicine, Chung Shan Medical University Hospital, Taichung, Taiwan

<sup>2</sup>School of Medicine, Chung Shan Medical University, Taichung, Taiwan

**Introduction:** SUVmax has long been a simple and important parameter on FDG PET in oncology. When being applied to stage oral cancer, a SUVmax between 2.5 to 4.0, most often 3.5, had been suggested as a criterium to differentiate whether lymph node metastasis or not. The purpose of this study was to retrospectively collect SUVmax of suspicious lymph nodes on staging FDG PET/CT images of oral squamous cell carcinoma patients, correlated them with pathological reports of lymph node dissection, and determined cutoff of SUVmax that provided the highest diagnostic accuracy. The given objective criterium could be referred to in clinical practice.

**Methods:** SUVmax values of suspicious lymph nodes in total 162 FDG PET/CT reports of 151 patients of oral squamous cell carcinoma who were diagnosed during Jan. 2018 to Jun. 2021 were retrospectively recorded. Positive or negative for pathological metastasis of dissected corresponding lymph nodes were then recorded. The cutoff of SUVmax that yielded the highest accuracy to differentiate metastasis or not was identified by receiver-operating curve (ROC) with the largest area under curve (AUC).

**Results:** When SUVmax = 5.25, the AUC = 0.644 was the largest, with a resultant sensitivity of 0.533, and specificity of 0.851.

**Conclusions:** As the result, SUVmax = 5.25 as the cutoff seemed higher than ever reported in the literature. Owing to racial and geographic differences, SUVmax = 3.5 may not be directly applied as the domestic diagnostic criterium to differentiate whether lymph node metastasis or not on FDG PET/CT scan in squamous cell carcinoma of oral cavity patients.



PC-087

## Dual Time Point Imaging with Retention Index of SUVmax of Lymph Node on FDG PET/CT Scan Does not Help to Differentiate Positive from Negative Metastasis in Squamous Cell Carcinoma of Oral Cavity Patients

Jui-Hung Weng<sup>1,2</sup><sup>1</sup>*Department of Nuclear Medicine, Chung Shan Medical University Hospital, Taichung, Taiwan*<sup>2</sup>*School of Medicine, Chung Shan Medical University, Taichung, Taiwan*

**Introduction:** SUVmax has long been an important and simple parameter on FDG PET in oncology. Retention index (RI), acquired by dual time point imaging (DTPI) of PET, was defined as (SUVmax delay–SUVmax early)/ SUVmax early. SUVmax had been suggested as a helpful parameter to differentiate positive from negative metastasis in certain malignancies, e.g. lung cancer and breast cancer. It has been known that DTPI increases sensitivity to detect malignancy, but whether RI helpful to differentiate lymph node metastasis seemed uncertain in some cancers. This study retrospectively compared corresponding RI on staging FDG PET/CT images of dissected lymph nodes in oral squamous cell carcinoma patients. If there was statistically significant difference between pathologically positive (pN[+]) and negative (pN[-]) nodes, a quantitative analysis may be conducted to determine an optimal cutoff.

**Methods:** Total 162 FDG PET/CT reports of 151 patients of oral squamous cell carcinoma who were diagnosed during Jan. 2018 to Jun. 2021 were enrolled. RI of suspicious lymph nodes on staging FDG PET/CT images of oral squamous cell carcinoma patients were recorded. For dissected corresponding lymph nodes, mean  $\pm$  SD of RI of pathologically positive and negative lymph nodes were computed respectively.

**Results:** 100 RI were available with mean  $\pm$  SD =  $0.30 \pm 0.33$ . The RI of (pN[+]) group was  $0.32 \pm 0.35$ , while RI of (pN[-]) group was  $0.20 \pm 0.22$ . The p value = 0.079 by using an independent sample t test.

**Conclusions:** No significant difference of RI between pathologically positive and negative lymph nodes was noted. RI does not help to differentiate whether lymph node metastasis or not. Dual time point imaging had better be reserved in selected clinical scenarios otherwise.

PC-088

## Rapid Extensive Dissemination from Sarcomatoid Renal Cell Carcinoma: Detection with F-18 FDG PET/CT

Bor-Tau Hung, Pei-Ing Lee, Yu-Yi Huang

*Department of Nuclear Medicine, Koo Foundation Sun Yat-Sen Cancer Center*

**Introduction:** Sarcomatoid renal cell carcinoma (SRCC) is relatively rare, characterized by the transformational growth pattern of epithelial carcinomas into malignant spindle-shaped cells and exhibiting aggressive characteristics. F-18 FDG PET/CT, a noninvasive molecular imaging modality, has been extensively applied in clinical practice. However, the application of F-18 FDG PET/CT in the preoperative evaluation of SRCC is limited, primarily due to the physiological excretion of FDG from the kidneys. We herein present a rare case of SRCC detected with F-18 FDG PET/CT.

**Case presentation:** A 56-year-old man presented with rapid growing soft tissue mass in right arm and body weight loss two weeks before having a biopsy to rule out sarcoma. MRI of upper extremity revealed a 23 x 18 mm enhanced subcutaneous tumor in right upper posterior arm with indeterminate nature. Preoperative staging F-18 FDG PET/CT was performed for systemic survey and demonstrated multiple hypermetabolic lesions in right kidney, bilateral lungs, small intestine, peritoneum, lymph nodes, bones, and multiple soft tissue masses and nodules of variable size, suggesting malignant disease with multiple metastases. Further workup with contrast-enhanced CT of chest and abdomen disclosed right arm soft tissue mass (39 mm), right renal mass (69.7 mm), multiple lung nodules (up to 14.5 mm), peritoneal nodule (11 mm), and multiple intramuscular and subcutaneous soft tissue masses and nodules in chest wall, abdominal wall, and buttock. Increased size and number of lesions were noted, indicating rapid progressive disease. Histopathologic examination of right arm mass and second portion of duodenum confirmed the diagnosis of metastatic sarcomatoid renal cell carcinoma after multidisciplinary team discussion.

**Conclusion:** Our case presents a SRCC with rapid extensive dissemination and preoperative identification of this subtype of RCC with F-18 FDG PET/CT had helped determine the therapeutic strategies. In opposite to the conventional RCC, which may not always demonstrate avid FDG activity, SRCC shows intense FDG uptake on PET. This case highlights the role of F-18 FDG PET/CT in staging this uncommon subtype of RCC. Further studies and a larger case series will be required to fully clarify SRCC imaging features by CT, MRI, as well as F-18 FDG PET/CT.

PC-089

## Subcutaneous Panniculitis-like T-cell Lymphoma on F-18 FDG PET/CT: A Case Report

Chao-Jung Chen<sup>1</sup>, Er-Jung Hsueh<sup>2</sup>, Chang-Che Wu<sup>3</sup>

*Departments of <sup>1</sup>Nuclear Medicine, <sup>2</sup>Haematology-Oncology, and <sup>3</sup>Pathology, Yuan's General Hospital, Kaohsiung, Taiwan*

**Introduction:** Subcutaneous panniculitis-like T-cell lymphoma, a subtype of cutaneous T-cell lymphoma, is a rare disorder that is often confused with panniculitis. It is usually confined to the subcutaneous tissue, but rare cases have disseminated to involve the lymph nodes, blood, and bone marrow. The mean age at diagnosis was 24.2 years (age range: 13-48 years). Most cases have an excellent prognosis and follow an indolent clinical course. We herein present a case of subcutaneous panniculitis-like T-cell lymphoma on F-18 FDG PET/CT.

**Case report:** A 16-year-old male patient suffered from fever, productive cough, and sore throat for 2 weeks. No definite abnormal finding can be found in chest X-ray, abdominal ultrasonography, and abdominal CT. Gallium inflammation scan showed suspicious multiple subcutaneous tissue lesions all over the body. Biopsy showed subcutaneous panniculitis-like T-cell lymphoma. The F-18 FDG PET/CT image confirmed subcutaneous panniculitis-like T-cell lymphoma at the neck, thorax, abdomen, pelvis, and bilateral upper & lower extremities. Follow-up image six months later after treatment showed almost complete resolution except few residual tumors.

**Conclusion:** The presented case showed a rare case of subcutaneous panniculitis-like T-cell lymphoma. F-18 FDG PET/CT imaging seems helpful in staging and therapeutic assessment.

PC-090

## FDG PET-CT in Evaluation of Recurrence in Patients with Head and Neck Cancer after Therapy

Dung-Ling Yu<sup>1</sup>, Jun-Hong Juo<sup>2</sup>, Hsin-Wen Huang<sup>3</sup>

<sup>1</sup>Department of Nuclear Medicine, <sup>2</sup>Department of Medical Oncology,  
<sup>3</sup>Department of Radiology, Mennonite Christian Hospital, Hualien, Taiwan

**Introduction:** The purpose of the study was to evaluate the clinical value of FDG PET-CT in patients with head and neck cancer (HNC) after therapy.

**Methods:** The study collected 78 patients (Male: Female = 61:17; age range 35-86 yrs mean 61.6 yrs) with HNSCC. All of patients received surgery, radiotherapy or chemotherapy. FDG PET-CT was performed on all of the patients 3-24 months after completion of treatment. Regional recurrence or distant metastasis was confirmed by either histological proof or clinical or imaging follow-up. The diagnostic accuracy of FDG PET-CT was compared to conventional imaging studies.

**Results:** Nine out of 78 (11.5%) patients showed regional recurrence or distant metastasis on FDG PET-CT. The sensitivity and specificity of FDG PET-CT was 85% and 95% respectively. Conventional imaging studies showed sensitivity of 62% and specificity of 97% respectively. FDG PET-CT had similar specificity but higher sensitivity.

**Conclusions:** The study revealed FDG PET-CT had higher sensitivity than conventional imaging studies in evaluation of recurrence in patients with HNC after therapy, and suggested FDG PET-CT should be used in clinical follow-up in patients with HNC after therapy.

PC-091

## The Value of Data-Driven Respiratory Gated Acquisition in Patients Referred for F-18 FDG PET/CT Scan

Yi-Chieh Chen, Yih-Hwen Huang, Chia-Ju Liu

*Department of Nuclear Medicine, National Taiwan University Hospital  
and National Taiwan University College of Medicine, Taipei, Taiwan*

**Introduction:** Respiratory motion in  $^{18}\text{F}$ -FDG PET/CT may degrade image quality and leads to inaccurate quantification of tracer uptake or potentially lower detection rates for malignancies. This study aims to evaluate the feasibility and quantitative impact of a data-driven respiratory gated (DDG) acquisition with continuous-bed-motion scan in unselected patients referred for FDG PET/CT, without increasing acquisition time.

**Methods:** This study retrospectively enrolled 109 patients referred for FDG PET/CT from March 2022 to August 2022. Non-gated, hardware device respiratory gated (HDG) and DDG PET/CT images were reconstructed from the same data recorded using Biograph Vision PET/CT scanner with continuous table speed of 1.4 mm/sec. The lesions of thoracic and abdomen were identified and measured with the parameters of volume,  $\text{SUV}_{\text{max}}$ ,  $\text{SUV}_{\text{mean}}$  and total lesion glycoses (TLG).

**Results:** A total number of 167 lesions uptake were analyzed from the 109 patients. The lesion locations were classified into five groups: upper lunglobe (n = 57), middle lung lobe (n = 21), lower lung lobe (n = 34), liver (n = 24) and abdomen region except the liver (n = 31). For lesion quantification, HDG and DDG images had significantly greater  $\text{SUV}_{\text{max}}$  and  $\text{SUV}_{\text{mean}}$  values and smaller volumes than non-gated images, while no statistically significant difference between HDG and DDG. The median (IQR) percentage changes in  $\text{SUV}_{\text{max}}$  between DDG and non-gated images was 10.41 (4.52 to 18.54), 27.5 (7.78 to 63.35), 29.32 (12.07 to 64.00), 23.48 (15.77 to 39.59) and 14.32 (4.20 to 25.16) for upper lung, middle lung, lower lung, liver and abdomen region except liver, respectively. The median (IQR) percentage changes in lesion volume between DDG and non-gated images was -12.5 (-25.16 to -3.55), -26.09 (-58.01 to -3.26), -43.44 (-61.86 to -20.00), -34.87 (-62.29 to -23.50) and -27.59 (-38.32 to -11.26) for upper lung, middle lung, lower lung, liver and abdomen region except liver, respectively.

**Conclusions:** This study showed data-driven respiratory gated PET/CT technique is feasible in a daily routine use with improved PET quantification and could be an alternative to HDG without increasing acquisition time.

PC-092

## Prognostic Factors of Patient Survival for Radium-223 Treatment of Metastatic Castration-resistant Prostate Cancer

Shan-Fan Yao<sup>1</sup>, Willam-J Huang<sup>2</sup>, Tzu-Chun Wei<sup>2</sup>,  
Wan-Tien Hsieh<sup>1</sup>, Nan-Jing Peng<sup>1,3</sup>

<sup>1</sup>Department of Nuclear Medicine, Taipei Veterans General Hospital, Taipei, Taiwan

<sup>2</sup>Department of Urology, Taipei Veterans General Hospital, Taipei, Taiwan

<sup>3</sup>School of Medicine, National Yang Ming Chiao Tung University, Taiwan

**Introduction:** Radium-223 (Ra-223) has been proven significantly prolong overall survival (OS) in patients with metastatic castration-resistant prostate cancer (mCRPC) and symptomatic bone metastases. However, the outcomes may vary among individuals. This study is performed to evaluate the prognostic factors associated with patient survival.

**Methods:** Patients with mCRPC treated with Ra-223 in Taipei Veterans General Hospital were recruited. The clinical outcome was determined using medical records. Potential prognostic factors for survival were evaluated by univariate analysis. Chi-squared test was used to examine the differences between groups. A cumulative survival curve was derived using the Kaplan–Meier method. Differences were considered to be significant at  $p < 0.05$ .

**Results:** Seventy-seven patients have received Ra-223 therapy. Mortality was observed in 37 patients. Factors significantly associated with survival included  $< 5$  bone metastases ( $p = 0.0271$ ), baseline prostate-specific antigen (PSA)  $< 36$  ng/ml ( $p = 0.0170$ ), baseline alkaline phosphate (ALP)  $< 115$  U/L ( $p = 0.0337$ ), baseline hemoglobin (Hb)  $> 12$  g/dl ( $p = 0.0010$ ), PSA  $< 36$  ng/ml after Ra-223 therapy ( $p = 0.0063$ ), ALP  $< 115$  U/L after Ra-223 therapy ( $p = 0.0442$ ) and Hb  $> 12$  g/dl after Ra-223 therapy ( $p = 0.0014$ ).

**Conclusions:** Ra-223 could prolong the survival of patients with mCRPC. The outcomes might be associated with the some prognostic factors including the number of bone metastases, and the values of PSA, ALP and Hb before and after Ra-223 therapy.

PC-093

## Cytomegalovirus Colitis Virus (CMV) Infection Mimic Lymphoma Relapse: A Case Report

Lien-Hsin Hu<sup>1,2</sup>, Yi-Chen Yeh<sup>1,2</sup>, Chun-Kuang Tsai<sup>1,2</sup>, Yu Kuo<sup>1,2</sup>,  
Ko-Han Lin<sup>1</sup>, Wen-Sheng Huang<sup>1,2,3</sup>, Jyh-Pyng Gau<sup>1,2,4</sup>

<sup>1</sup>*Department of Nuclear Medicine, Taipei Veteran General Hospital, Taiwan*

<sup>2</sup>*School of Medicine, National Yang Ming Chiao Tung University, Taiwan*

<sup>3</sup>*Department of Nuclear Medicine, Cheng Hsin General Hospital, Taiwan*

<sup>4</sup>*Taipei Medical University Hospital*

**Introduction:** We report a case of diffuse large B cell lymphoma with Cytomegalovirus (CMV) Colitis mimicking lymphoma relapse.

**Case report:** A 56-year-old man has history of stage IV diffuse large B cell lymphoma with initial presentation of a bulky mass at ascending colon, lymphadenopathies on both sides of diaphragm, and peritoneal seedings. Despite serial treatment including right hemicolectomy and chemotherapy, the patient had the first relapse as a bulky mass right lower quadrant abdomen one year after initial diagnosis. Salvage therapy including and auto peripheral blood stem cell transplantation (PBSCT) were conducted. However, a follow-up F-18 FDG PET revealed abnormal uptake in the surgical anastomotic site suspected to be the second time of relapse. Colonoscopy biopsy at the anastomotic site revealed CMV infection. After valganciclovir treatment, the follow-up PET revealed regression of the previous abnormal uptake.

**Conclusions:** Despite the suspicion of lymphoma relapse is reasonable, in patients of lymphoma who are immunocompromised, CMV colitis/ileitis should be included in the differential diagnosis for abnormal bowel uptake.

PC-094

## Diagnostic and Prognostic Roles of Perioperative F18-FDG PET/CT for Differentiated Thyroid Cancer

Yen-Hsiang Chang<sup>1</sup>, Pei-Wen Wang<sup>1,2</sup>

<sup>1</sup>Department of Nuclear Medicine, Kaohsiung Chang Gung Memorial Hospital  
and Chang Gung University, Kaohsiung, Taiwan

<sup>2</sup>Division of Endocrinology and Metabolism, Department of Internal Medicine, Kaohsiung Chang Gung Memorial  
Hospital and Chang Gung University, Kaohsiung, Taiwan

**Introduction:** F-18 FDG PET/CT has a valuable role in the initial workup for solid tumors, such as head and neck cancer, lung cancer, etc. However, the role of F-18 FDG PET/CT for staging in thyroid cancer patients is still under debate. In the current guidelines, F-18 FDG PET/CT is considered for detecting recurrent disease in those with negative radioiodine whole body scan but elevated serum thyroglobulin. Routine F-18 FDG PET for initial workup is not recommended. The aim of this study is to evaluate the diagnostic performance and prognostic value of perioperative F-18 FDG PET/CT in newly diagnosed differentiated thyroid cancer (DTC).

**Methods:** We retrospectively analyzed perioperative F-18 FDG PET/CT scans of 49 patients with newly diagnosed DTC from January 2018 to June 2021 in our institute. The clinicopathologic and demographic characteristics were recorded. Imaging findings were compared with clinical follow-up and histopathologic results. Each patient's status at the last follow-up was also classified according to the dynamic risk stratification.

**Results:** The sensitivity, specificity, and diagnostic accuracy of F18-FDG PET/CT for the entire patient group were 90.0%, 83.3%, and 87.5%, respectively. However, in the patients with high risk of recurrence (N = 36), the sensitivity, specificity, and diagnostic accuracy were 92.9%, 87.5%, and 91.7%, respectively. In patients with negative FDG PET/CT results (N = 18), 15 (83.3%) had excellent response at the end of follow-up, and no one had structural incomplete response. While the other 31 had positive FDG PET/CT results, only 3 (9.7%) had excellent response and 24 (77.4%) had structural incomplete response at the end of follow-up. The risk of incomplete response was significantly higher in patients with positive FDG PET/CT results ( $p < 0.0001$ ).

**Conclusions:** Perioperative F-18 FDG PET/CT demonstrates good diagnostic and prognostic values for patients with newly diagnostic DTC.



PC-095

## 乳房前哨淋巴造影中未發現淋巴結顯影 與淋巴侵犯是否有關？

呂建璋<sup>1</sup> 林雅婷<sup>1</sup> 曾柏銘<sup>2</sup> 沈淑禎<sup>1</sup> 門朝陽<sup>2</sup> 蕭聿謙<sup>3</sup>

<sup>1</sup>天主教中華聖母修女會醫療財團法人天主教聖馬爾定醫院核子醫學科

<sup>2</sup>天主教中華聖母修女會醫療財團法人天主教聖馬爾定醫院正子造影中心

<sup>3</sup>亞東紀念醫院核子醫學科

**目的：**乳癌手術治療的包含乳房切除及腋下淋巴廓清，腋下淋巴清除術可減少未來復發的風險。惟腋下清除可能會導致肩關節僵硬或患側上肢淋巴水腫等後遺症。乳房前哨淋巴造影藉著放射性同位素定位出前哨淋巴結，術中將前哨淋巴結摘除並做切片檢查，並由病理科醫師初步分析檢查是否有癌細胞，再決定是否進行腋窩淋巴結清除術。前哨淋巴結造影並非每次皆可定位出前哨淋巴結。本篇針對前哨淋巴造影未發現淋巴結案例進行研究。

**方法：**本研究案例收集期間自 2015 年 12 月至 2021 年 2 月，共 315 例，患者皆經病理切片確認為乳房惡性腫瘤。所有患者皆於術前接受乳房前哨淋巴造影，前哨淋巴造影使用 <sup>99m</sup>Tc- Phytate (0.25 mCi×4 支，共 1 mCi，常規使用 3 支)，以皮下方式注射於乳暈周圍，然後收集平面影像 (1-10 分鐘 Dynamic view，10 分至 5 小時期間收集 anterior and lateral static views)，造影結束 (結束時間依淋巴結出現時而定)，病患隨後接受手術，術中以加馬探針定位取出淋巴結，由病理科切片判讀淋巴結是否遭受侵犯。如前哨淋巴造影未能完成 (未發現淋巴結顯影)，會採用藍染方式找出淋巴結。病理報告決定是否進行腋窩淋巴結廓清，淋巴侵犯為陽性進行廓清手術，陰性則保留。

**結果：**315 例前哨淋巴結造影，301 例於造影期間發現淋巴結顯影，造影成功率為 95.5%。301 例成功造影，病理報告陽性者有 75 例 (24.9%)，14 造影未成功案例，病理報告陽性有 4 例 (28.5%)。

**結論：**根據上述結果得知，乳房前哨淋巴攝影未發現淋巴顯影的機率會因淋巴是否遭受侵犯而增加。

PC-096

## Bremsstrahlung Image Condition of Ra-223 Distribution of Prostate Cancer Patient

Ming-Hsien Lin<sup>1</sup>, Pei-Wen Liu<sup>1</sup>, Ya-Yueh Hsu<sup>1</sup>, Lin-Fu Yeh<sup>2</sup>, I-Ling Shih<sup>2</sup>

<sup>1</sup>*Department of Nuclear Medicine, Camillian Saint Mary's Hospital, Luodong, Taiwan*

<sup>2</sup>*GE Healthcare*

**Introduction:** Radium-223 (Ra-223) brachytherapy is indicated for patient suffer from prostate cancer with bone metastasis. For precision medicine, the precise Ra-223 distribution is important to make sure target to bone metastatic lesion and the possibility of extravasation injection of Ra-223. Bremsstrahlung image can visualize the Ra-223 distribution. But the image condition for GE 850 SPECT/CT is not well established.

**Methods:** Two kind of collimator (LEHRS & MEGP) under different energy PHA (84 Kev & 255 Kev) for whole body scan in 5 cm/min speed were obtained at 24-hour post injection. For local static views (360 sec image time), we performed four sets (LEHRS 84 Kev, MEGP 84 Kev, MEGP 255 Kev and MEGP 84 Kev + 255 Kev) images for comparison. We gradually adjust the condition set by set to get the best condition.

**Results:** For Bremsstrahlung image condition of Ra-223 distribution of prostate cancer patient, 84 Kev with MEGP collimator get the best image quality for GE 850 SPECT/CT.

**Conclusions:** Radium-223 brachytherapy is painless & high-quality treatment for prostate cancer. The precise Ra-223 distribution after injection offer the precision medicine care. For GE 850 SPECT/CT, bremsstrahlung image of Ra-223 under 84 Kev with MEGP collimator can get the best image quality.

PC-097

## 正子斷層造影顯示頭頸癌患者術後單側活性攝取增加與唾液腺代償性增生有關

蔡豪軒 謝宏仁

林新醫療社團法人林新醫院核子醫學科

**簡介：**氟 18 去氧葡萄糖正子斷層造影 (F-18 Fluorodeoxyglucose Positron emission tomography, F-18 FDG PET) 應用在頭頸癌患者，其影像判讀往往是較具挑戰性的。頭頸部複雜的解剖構造歷經手術及放射治療後，更呈現多變異的影像表現。本科報告一位右側頰癌 (buccal cancer) 病例，在治療後數年期間，對側出現放射活性升高疑似腫瘤病灶。

**案例報告：**一位 57 歲右頰癌男性病人，於四年前接受手術及同步化學放射治療 (concurrent chemoradiotherapy, CCRT)。本次 FDG PET 追蹤檢查發現左側頸部疑似腫瘤病灶併有瀰漫性放射活性升高。然而病人於此處並無症狀且理學檢查外觀無異常。詳細比對歷年檢查圖術前影像可見右側頰癌及頸淋巴結轉移。術後追蹤影像圖顯示右側頰癌及淋巴結均已去除，右側腮腺活性消失，但左側腮腺於四年間逐漸增大，併有中等程度放射活性攝取升高並達到穩定狀態。

對照 FDG PET/CT 橫斷層影像，此放射活性位在左側廣泛增生之腮腺組織且並無局部異常病灶。綜合以上推論得知由於右側唾液腺功能缺失，左側腮腺代償性增生導致此種特殊的影像表現，並非真正的頸部腫瘤。

**結論：**先天性唾液腺缺失的情況並不多見，而更常見於頭頸癌經手術或放射線治療後的患者。單側唾液腺功能缺失可能造成同側或對側不同部位的唾液腺代償性增生。其機轉可能藉由咀嚼運動刺激細胞體積增大，以及經由交感 / 副交感神經調節腺泡細胞數目及體積增加。唾液腺增生症可能以疑似頸部腫瘤來呈現，透過謹慎的臨床觀察追蹤及仔細比對各種成像技術，包括 CT、MRI 排除腫瘤可以達到鑑別診斷。目前文獻上仍缺少唾液腺增生在 FDG PET 疑似頸部腫瘤的影像報導。藉由此病例提醒吾人對此現象保持警覺，以避免對此種良性變化進行不必要的手術、切片、或侵入性檢查。

PC-098

## 降低自動化清洗儀之潛在風險確保檢驗品質

邱祖廷<sup>1</sup> 方雅潔<sup>1</sup> 余景陽<sup>1</sup> 韓璞<sup>1</sup> 陳芄嘉<sup>1</sup> 林慶齡<sup>1,2</sup><sup>1</sup> 國泰綜合醫院放射免疫實驗室<sup>2</sup> 國泰綜合醫院內分泌新陳代謝科

**背景介紹：**目前臨床上的放射免疫分析是透過抗原抗體的特異性結合反應並加上放射性同位素標記作為示蹤劑，在體外實驗中實現微量生物活性物質的檢測，藉此協助診斷各種臨床疾病。實驗原理可區分為兩類：競爭法 (Radioimmunoassay ; RIA) 及三明治法 (Immunoradiometric assay ; IRMA)。然而無論執行哪種實驗原理皆需將待測物加入試管中，並於反應後將未發生特異性結合之物質洗去，再以標準劑量反應曲線 (standard-dose response curve) 和內插法計算出各試管中的放射活性 (radioactivity) 以測得待測物之含量。本實驗室以往所有實驗清洗步驟皆以手工方式操作，但因實驗室業務量增加、欲降低手工清洗之差異及自動化趨勢日益興盛，因此引進 TW-300 全自動試管清洗儀器取代手工操作清洗步驟，以提升檢驗效率及品質。為恪守實驗室之品質政策：確保環境安全，報告正確迅速；此次自動化之改變如何在檢驗效率提升下，顧及報告正確性為本篇探討要點。

**方法：**TW-300 全自動試管清洗儀器共有四個程式設定，依照不同實驗之清洗步驟設定清洗液種類及毫升量、吸取秒數與清洗次數。將欲清洗之試管排上儀器，選擇清洗之程式設定，使其自動清洗。一排試管數為 20 支：吸取針及分注針各 20 支，三排為一架，最多裝載五架，故一次清洗之試管數量為 300 支。

**結果：**試用 TW-300 全自動試管清洗儀器後，分析在清洗過程執行不善而導致報告錯誤之可能如下，1. 程式設定之選擇：由於實驗室操作項目眾多，實驗室人員透過製作操作小卡放置儀器週邊之方法，使不同實驗項目正確選擇其清洗之程式設定。2. 試管順序之排列：於試管架清楚標示第一支起始方向，並以 20 支檢體抽樣一次以避免每排之間順序錯誤。3. 吸取針及分注針頭之通暢：實驗前執行 PRIMING 確認吸取針及分注針頭無堵塞。4. 試管內 <sup>125</sup>I 之殘留：若實驗需於振盪器上反應，容易在試管壁上方殘留 <sup>125</sup>I，可藉由增加清洗液之毫升量來避免此狀況發生。

**結論：**執行以上預防措施後，實際使用 TW-300 全自動試管清洗儀器尚未發生因自動化清洗導致報告錯誤之事件。自動化清洗不僅降低了實驗室人員的工作量以及手工清洗之差異，更帶領本實驗室順利銜接自動化趨勢，提升了檢驗量能及檢驗品質。

PC-099

## 庫存管理系統新革命

陳芄嘉<sup>1</sup> 方雅潔<sup>1</sup> 余景陽<sup>1</sup> 韓璞<sup>1</sup> 邱祖廷<sup>1</sup> 林慶齡<sup>1,2</sup><sup>1</sup> 國泰綜合醫院放射免疫實驗室<sup>2</sup> 國泰綜合醫院內分泌新陳代謝科

**背景介紹：**依據 ISO15189 條文規範，實驗室應建立試劑與耗材的庫存管制系統。落實庫存管理可以定期了解試劑及耗材的消耗量以控管成本，且能避免庫存過少導致無法執行檢驗作業而遲發報告，或庫存過多造成試劑過期而浪費的情形。尤其以 RIA 實驗室來說，各項目試劑大多內含 I-125，其效期只有短短的一個多月，良好的庫存管理更顯重要。然而，一間臨床實驗室需管理的試劑及耗材種類繁多，從入庫到出庫，實驗室同仁需一筆一筆以手工謄寫方式記錄，在繁忙的檢驗工作中，每日庫存量都會更動，偶有疏於記錄的情況，造成管理不利。於是庫存管理系統的革新，儼然成為本 RIA 實驗室的一大課題。

**方法：**經實驗室同仁們一同討論，決議將原本試劑、耗材的紙本入出庫表單汰除，改使用電子化的庫存管理系統。同仁將需求整理出一份簡報，提供給本院資訊室，但資訊室方表示短時間內建構一套庫存管理系統網頁有難度。故本實驗室另尋方法，直接購買一套已建置完成的庫存管理軟體。軟體功能包括掃描條碼出入庫、查詢出入庫記錄、訂單記錄、品管驗證記錄、庫存總表、各項目庫存明細表、低於安全庫存清單及即期品警示清單等，在確認軟體功能符合評鑑條文規範後，透過同仁們實際使用情形，陸續向軟體工程師提出需修改之處，使軟體使用起來更加順手。

**結果：**此系統比紙本庫存管理更具效率的功能，一為試劑耗材進貨入庫時，系統會自動將不同項目、不同批號做分類，使同仁們可以更快速注意到同項目有不同的批號；二為訂單紀錄能同時顯示於入庫頁面右方，使同仁們更易於核對進貨量與訂單量是否相符。除此之外，更增進管理庫存的便利性，一是出庫時，當舊批號試劑尚未出庫完畢，刷讀條碼後會彈出警示視窗，提醒同仁注意還有舊批號試劑尚未使用；二是出庫完畢後，會顯示低於安全庫存量的項目清單，提醒同仁們應訂貨及節約用量，避免庫存不足導致報告延遲。種種優點，有助於本實驗室維持更穩定的檢驗品質。

**結論：**與舊時紙本管理不同，使用電子化的庫存管理系統後，不僅大幅省去了盤點試劑及耗材的時間，能即時掌握庫存量、各試劑耗材的出入庫情形，還多了警示系統，提醒同仁注意即期試劑或有無庫存不足的情形。它的出現改變了同仁們登記庫存的習慣，並大幅改善了試劑耗材出庫紀錄的疏漏情況，為本實驗室帶來革命性的影響，也帶領本實驗室邁向新的里程碑。

PC-100

## 藉由試劑清洗溶液之統一以提升實驗室工作效率

余景陽<sup>1</sup> 方雅潔<sup>1</sup> 韓璞<sup>1</sup> 邱祖廷<sup>1</sup> 陳芄嘉<sup>1</sup> 林慶齡<sup>1,2</sup>

<sup>1</sup> 國泰放射免疫實驗室

<sup>2</sup> 國泰綜合醫院內分泌新陳代謝科

**背景介紹：**抗原抗體結合反應後之清洗步驟，為放射免疫分析中常見之重要實驗步驟之一。Beckman RIA 試劑之檢驗項目，各項目標準作業程序中之清洗溶液多達 4 種，包含 Distilled water、需將原廠清洗濃縮液用 Distilled water 泡製稀釋 20 倍、50 倍、500 倍之不同濃度清洗液。礙於實驗室空間及實驗清洗儀數量之限制，且醫檢師需額外花費時間泡製不同濃度之清洗液。基於以上之原因，本篇將探討以不影響各項目之準確度為前提下，簡化檢驗清洗溶液之種類，以提升實驗室整體工作效率。

**方法：**使用校正液，品管液及病人檢體，針對需將原廠清洗濃縮液用 Distilled water 泡製成 20 倍，500 倍之清洗液與 Distilled water 做相關性比對。

**結果：**相關性比對結果以各項目  $R^2 \geq 0.95$  及  $\text{Bias}\% < \text{TEa}\%$  為允收標準。20x 清洗液與 Distilled water 比對結果：AFP  $R^2 : 0.99$ ， $\text{Bias}\% : 7.73\% < \text{TEa}\% : 21.9\%$ 。CA125  $R^2 : 0.99$ ， $\text{Bias}\% : 2.09\% < \text{TEa}\% : 35.40\%$ 。CEA  $R^2 : 0.99$ ， $\text{Bias}\% : 1.14\% < \text{TEa}\% : 24.70\%$ 。500x 清洗液與 Distilled water 比對結果：PSA  $R^2 : 0.99$ ， $\text{Bias}\% : 3.97\% < \text{TEa}\% : 33.60\%$ 。FPSA  $R^2 : 0.99$ ， $\text{Bias}\% : 8.65\% < \text{TEa}\% : 17.52\%$ 。20x，500x 清洗液與 Distilled water 比對之相關性，皆符合實驗室設定之允收標準。且自更換清洗液後之外部能力試驗結果 (Randox Cycle 20 sample 4,5,6)，均為合格。

**結論：**實驗室以病人報告之準確度為前提下，思考如何統一清洗溶液的種類，及簡化醫檢師需泡製清洗溶液之時間，有效的利用有限的空間，及人員工作時間，讓實驗室發揮最大之效益。

PC-101

## Hook effect 對 RIA 實驗的影響 — 以 Beckman CEA 為例

余景陽<sup>1</sup> 方雅潔<sup>1</sup> 韓璞<sup>1</sup> 邱祖廷<sup>1</sup> 陳芄嘉<sup>1</sup> 林慶齡<sup>1,2</sup>

<sup>1</sup> 國泰放射免疫實驗室

<sup>2</sup> 國泰綜合醫院內分泌新陳代謝科

**背景介紹：**實驗中 Hook effect 是指當待測物的濃度過高，高到超過了固相上抗體所能夠接合的數目，因為抗體量不足無法與抗原結合而呈現反常的下降的曲線，導致檢驗人員低估待測抗原真正的濃度。此反映在結果實際上是超過了偵測的範圍，因此必須要將檢體先作稀釋，才可確保有足夠的抗體可結合所有的抗原，以避免造成檢測數據過低。就臨床經驗看來，最高濃度校正液之 7 成至 8 成左右，即有可能發生 Hook effect。實驗室人員如何避免因為待測物抗原過高，或不同品牌試劑抗原抗體結合反應程度的差異，導致發生 Hook effect 而釋出錯誤報告，實為臨床檢驗上值得謹慎之事。

**方法：**Beckman CEA 校正液最高濃度為 345.0 ng/ml。某病患檢驗數值原倍為 91.5 ng/ml (其後標示為檢體 A)。此為連續追蹤病例，前一月 (其後標示為檢體 B) 及前 2 月 (其後標示為檢體 C) CEA 數值皆需稀釋 100 倍。於是將原倍 91.5 ng/ml 之檢體，稀釋 10 倍，100 倍，1000 倍觀察其結果。

**結果：**檢體 A 原倍：91.5 ng/ml，稀釋 10 倍：> 3450.0 ng/ml，稀釋 100 倍：22860.0 ng/ml，稀釋 1000 倍：19900.0 ng/ml。回溯此病患前 2 次原始紙本報告數據，檢體 B 原倍：109.3 ng/ml，稀釋 10 倍：> 3450.0 ng/ml，稀釋 100 倍：18380.0 ng/ml，稀釋 1000 倍：21200.0 ng/ml。檢體 C 原倍：142.4 ng/ml，稀釋 10 倍：> 3450.0 ng/ml，稀釋 100 倍：16210.0 ng/ml，稀釋 1000 倍：16400.0 ng/ml。

**結論：**由此次稀釋結果看來，待測檢體抗原越高，顯示出的原倍數值越低，僅達到最高濃度校正液 3 成左右之數值。如根據以往經驗僅篩選最高校正液濃度之 7~8 成數值，很容易將原倍數據發出，造成臨床上之誤判。本院檢驗資訊系統 (LIS) 有瀏覽前次檢驗結果的功能，本實驗室常規性於核發報告前，查詢病患歷次報告合併瀏覽後，確認無疑再發出報告。此外也針對互有相關生理機制之檢驗項目報告一起檢視當作參考。此次即是透過此機制，將有疑慮和有需要稀釋之檢體，於報告核發前再次覆檢，以減少發出錯誤的報告。

PC-102

## 建立適當的 CEA 生物參考區間

方雅潔<sup>1</sup> 余景陽<sup>1</sup> 韓璞<sup>1</sup> 邱祖廷<sup>1</sup> 陳芄嘉<sup>1</sup> 林慶齡<sup>1,2</sup>

<sup>1</sup> 國泰綜合醫院放射免疫實驗室

<sup>2</sup> 國泰綜合醫院內分泌新陳代謝科

**背景介紹：**接獲胸腔外科醫師抱怨：「更換 CEA 試劑後，生物參考區間從小於 5.0 ng/mL 調降至小於 2.5 ng/mL。追蹤的病患 3.0 ng/mL 於先前告知正常，現在 2.8 ng/mL 需告知為不正常，與病人解釋有所困難，並需安排多項檢查。這樣的調整是否恰當？」實驗室將此事件列為不符事件進行分析討論。

**方法：**1. 確認實驗室依據試劑書說明書提供之生物參考區間設定之正確性。2. 主動諮詢其他使用醫師：「更換試劑後生物參考區間的調整是否對臨床判讀造成影響。」3. 收集醫療專業團體、學會或文獻建議之生物參考區間。4. 詢問使用該試劑的其他醫院設定之生物參考區間 5. 評估是否修正現行使用之生物參考區間。

**結果：**BECKMAN COULTER CEA IRMA KIT 試劑說明書，內容載明來自 500 名健康人之 (Probability95%) 統計數值小於 2.5 ng/mL，設定無誤。主動諮詢臨床使用醫師，一位醫師希望延續先前使用之 Cis-bio 試劑，提供抽菸族群、不抽菸族群及涵蓋兩者的生物參考區間，因原廠並無建立抽菸族群數據。原廠提供相關參考文獻，建議設定為小於 5.0 ng/mL。另一位醫師回應因新舊試劑做出的數值相似，但生物參考區間設定之差異會引起臨床判讀的困難，建議詢問其他醫院因應對策。Cis-bio 與 BECKMAN COULTER 試劑比對相同檢體，相關係數  $R^2 = 0.998$ ，數值 Bias% 皆小於實驗室設定之 TEa，95% 比對數值差距，皆落於所有差距的正負 2 個標準差之內，證明兩家品牌檢測出的數值相近。詢問其他使用醫院超過 2 分之 1 的家數，沿用 Cis-bio 廠牌設定涵蓋抽菸與不抽菸之健康族群的參考值小於 5.0 ng/mL，且符合目前 CLIA 88 建議 CEA 之臨床決策值為 5.0 ng/mL。綜合上述原因，實驗室決議沿用之前設定涵蓋抽菸人口的生物參考區間：小於 5.0 ng/mL。

**結論：**新舊試劑校正品之計量追朔皆為 1st IRP 73/601，相同檢體比對數值相近，但兩家試劑設定之生物參考區間有所差距，導致追蹤病患於臨床判讀有困難及疑問。自行建立實驗室之生物參考區間是最好的方法，但在收集檢體的程序複雜繁瑣，執行上有困難。因此實驗室依據臨床醫師的臨床診斷情形及建議，進行收集醫療專業團體、學會或文獻等提出建議之生物參考區間，並依文獻建議沿用舊試劑之生物參考區間和比對方法來確認其適當性，以建立最適合的生物參考區間。



PC-103

## 四種治療藥物在臨床注射後 病人照護之輻射防護注意事項

張桂蘭 李岱恩 顏維徵 張淑敏 張晉銓

高雄醫學大學附設中和紀念醫院核醫部

**目的：**核醫放射線治療藥物屬非密封放射線物質，所以在臨床場所的使用，存放棄置，及工作人員操作中的輻射安全都要密切監測，以符合法規規定。

目前核醫用到的四種放射線同位素為對於各項癌症有其治療的功效；碘 -131；鐳 -223；釷 -90，鐳 -177；依據其各放射核種衰變時產生能量分率如碘 -131，釷 -90，鐳 -177 以  $\beta$  射線做治療，鐳 -223 則以  $\alpha$  射線治療，但同時若伴隨著穿透的  $\gamma$  射線是病人及照護者在臨床環境要注意的輻射防護。因此量測記錄這四種核種注射時之表面劑量率及距離 1 米處之表面劑量率，了解並注意之輻射防護安全。

**研究方法：**目前核醫放射標靶藥物治療，能夠定位腫瘤位置，將標靶藥物遞送至腫瘤位置，從而提供腫瘤治療。

先了解核醫注射放射治療藥物使用的核種物理特性；(1) 碘 -131 半衰期為 8.02 天是  $\beta$  衰變核素，發射  $\beta$  射線 (99%) 和  $\gamma$  射線 (1%)， $\beta$  射線最大能量為 0.6065 兆電子伏，主要  $\gamma$  射線 (2) 釷 -90 半衰期約 2.5 天以  $\beta$  射線 92% 粒子射出，射程為 3.6 mm (3) 鐳 -177 半衰期為 6.6 天是， $\beta$  衰變 (發射  $\beta$  射線 (78.6%) 和  $\gamma$  射線 (11%) (4) 鐳 -223 放射半衰期為 11.43 天，主要是經由  $\alpha$  衰變 ( $\alpha$  衰變：95.3%， $\beta$  衰變：3.6%， $\gamma$  或  $\chi$  射線衰變：1.1%)。

對此依據各項放射線物質之物理特性，於注射後或服用後做近距離及 1 米處的量測，可了解住院與否或回家後與家人及群眾之安全距離，做適當的輻防衛教。

**結論：**將各項治療核種列表顯示其半衰期、能量、組織穿透深度即  $\alpha$  或  $\beta$  一粒子的平均射程；並考慮  $\gamma$  射線的射程，依據其注射或服用劑量量測距離表面劑量率及距離 1 米處之表面劑量率如 (1) 碘 -131 因能量較強需住院隔離 2-3 天 (2) 釷 -90 於人體組織內發射距離較短的  $\beta$  射線，注射後即可回病房 (3) 鐳 -177 須輻射隔離病房住院 4-8 小時 (4) 鐳 -223 衰變釋放主要為  $\alpha$  粒子，注射後即可回家。

依據病人病程給予各項治療藥品劑量，如需繼續住院建議給予單人房，量測距離 1 米處之劑量率約 20-30  $\mu\text{Sv/h}$ ，如可以直接回家之病人，距離 1 米處之劑量率約 10-20  $\mu\text{Sv/h}$ ，皆低於法規規定之釋回劑量。

PC-104

## COVID-19-associated Pulmonary Cryptococcosis Presented as Necrotic Lung Mass on FDG PET/CT

Li-Fang Lin, Bo-Yu Chu

*Division of Nuclear Medicine, Taoyuan General hospital, Ministry of Health and Welfare, Taiwan*

**Introduction:** With the epidemic of COVID-19, COVID-19-associated pulmonary cryptococcosis (CAPC) gradually emerged. However there are merely a few case reports in the literature. Pulmonary cryptococcosis (PC) typically appears as clustered nodules on CT and manifests as necrotizing pneumonia seldomly. Here we report a case with CAPC presenting as necrotizing pneumonia.

**Case presentation:** The 53 year-old man had a history of Type 2 diabetes mellitus, chronic kidney disease and hypertension. He was transferred from a local clinic for unresolved fever, chest pain, productive cough and weight loss of 10 Kg after recovery from COVID-19 infection for one month. Results of laboratory studies were leukocytosis and elevated serum C-reactive protein level. COVID-19 rapid antigen test was negative. CT showed a huge hypoenhancing mass occupying the left upper lobe of the lung and massive pleural effusion. Brain MRI was negative. Serum of CEA and SCC were within reference range. Because necrotic lung cancer can not be excluded, ultrasound-guided transthoracic needle biopsy (US-TTNB) and F-18 FDG PET/CT were performed. F-18 FDG PET/CT revealed heterogeneous FDG hypermetabolism in the left lung mass and mediastinal lymph nodes. Whereas the histology of the lung specimen demonstrated numerous encapsulated yeasts with positive mucicarmine stain, which is consistent with cryptococcosis. But he was not a pigeon breeder and denied exposure to pigeons. To exclude AIDS, HIV antigen and antibody tests were performed and results were negative. Besides, the results of serum IgG, IgA, C3 and C4 were within normal reference. After discharge, he received oral fluconazole 200 mg daily and regular visits to the outpatient department.

**Conclusions:** COVID-19-associated pulmonary cryptococcosis (CAPC) may be encountered more and more frequently in the post-edemic era. CAPC could presented as necrotic lung mass on FDG PET/CT and possibly be confused with lung cancer. However, in a review of 13 published CAPC cases, the duration from diagnosis to death is just 23 days and mortality of patients under treatment is up to 45.4%. Attributed by rapid disease progression and high mortality of CAPC, early diagnosis and timely treatment is critical to improve survival. Thus, familiarity with image manifestations and keeping the differential diagnosis in mind are important.

PC-105

## Urogenital Tuberculosis in a Immunocompetent Host: Image Manifestation on FDG PET/CT

Li-Fang Lin, Hsiu-Ting Su, Su-Min Lin

*Division of Nuclear Medicine, Taoyuan General hospital, Ministry of Health and Welfare, Taiwan*

**Introduction:** Urogenital tuberculosis (UG-TB) accounts for 15~20% of extrapulmonary tuberculosis, but it's unusual in immunocompetent hosts without a history of pulmonary tuberculosis. What is more, CA-125 is found to be elevated in patients with pulmonary and extrapulmonary tuberculosis. Here we present a patient with GUTB, who was misdiagnosed as cancer due to elevated CA-125 and abdominopelvic lymphadenopathies on FDG PET/CT.

**Case report:** The 39-year-old woman without underlying disease suffered from dysuria for 2 months and a fever for 7 days. She visited the local clinic and received antibiotics, but the symptoms did not improve, hence she was transferred to the regional hospital. Physical examinations revealed bilateral knocking pain. Results of laboratory studies indicated neutrophilic leukocytosis, pyuria and hematuria. Under the impression of acute pyelonephritis, she was hospitalized. Abdominal CT showed bilateral hydronephrosis, a hypodense mass in the left kidney and lymphadenopathies in the para-aortic, pelvic and bilateral inguinal regions. Serum levels of CA-125 (70.6 U/mL) and IgG (1900 mg/dL) were elevated. Besides, F18 FDG PET/CT showed FDG hypermetabolism in the bilateral kidneys and FDG-avid lymphadenopathies in the para-aortic, mesenteric, bilateral iliac chains and bilateral inguinal regions.

To exclude cancer, biopsy of ureter, urinary bladder, urethra and right inguinal lymph nodes were performed. Surprisingly, the pathology of all specimens was granulomatous inflammation containing acid-fast bacillus. Under the impression of tuberculosis, chest CT, repeat sampling of sputum smear with PCR analysis were performed but results were all negative. Finally she received anti-tuberculosis therapy and ureteral stent insertion.

**Conclusion:** Urogenital tuberculosis (UG-TB) is uncommon and rare in immunocompetent hosts without a history of pulmonary tuberculosis. Symptoms of UG-TB are similar to urinary tract infection. UG-TB is FDG-avid and would cause elevated CA-125 level, so differentiating from malignancy is very important.

PC-106

## 建立機器手臂 Carry-over test 與允收標準

韓璞<sup>1</sup> 方雅潔<sup>1</sup> 余景陽<sup>1</sup> 邱祖廷<sup>1</sup> 陳芄嘉<sup>1</sup> 林慶齡<sup>1,2</sup>

<sup>1</sup> 國泰綜合醫院放射免疫室

<sup>2</sup> 國泰綜合醫院內分泌新陳代謝科

**背景介紹：**隨著實驗室自動化的發展，不僅改善流程提升檢測效率及品質，並減輕人員工作負荷，而其中採用機器手臂提升檢體量取樣的準確度及實驗操作速率。然而自動化之虞，仍需考量實驗成本與報告準確度，因此實驗室採用重覆清洗檢體探針之機器手臂，而不同以往的是實驗流程中人工操作方式以每吸取一次檢體便更換一支 Tip，機器手臂則以檢體探針吸取一次檢體便清洗一次再吸取下一支檢體的方式進行檢體量取樣，當前一檢體為高值時，易可能發生清洗不完全導致殘留在檢體探針上，發生 carry-over effect，進而干擾其他檢體之報告數值，不易察覺。如何在自動化的流程下，同時兼顧報告之準確度為本次討論主題。

**方法：**為了避免機器手臂因 carry-over effect 的發生，影響報告之準確度。實驗室採取模擬機器手臂可能會發生 carry-over effect 的情境，並比較目前檢體探針清洗一次與清洗兩次之差異。實驗室使用 Beckman 之 PSA total IRMA 試劑進行試驗，挑選已知高、低濃度之檢體，機器手臂依序吸取已知低濃度之檢體作為 control 組，再吸取已知高濃度之檢體後，清洗一次與兩次檢體探針，再吸取已知低濃度之檢體，加入 <sup>125</sup>I 抗 PSA 單株抗體，培育 2 小時，以 RIA 試管洗滌儀清洗後，放上  $\gamma$ -counter-2470 WIZARD 儀器計讀 CPM 數值與計算成 PSA 之濃度。

**結果：**實驗室 carry-over effect 模擬實驗之允收參考，依據實驗室  $\gamma$ -counter-2470 WIZARD 儀器標準操作手冊，背景值允收為 CPM < 50，表示不影響報告之準確度，另外根據 Westgard Quality requirements Desirable Biological Variation Database specifications 表單中提供之 TEa%，若相同檢體兩次作出之報告數值計算 bias%  $\leq$  TEa% (PSA TEa% 數值為 33.60)，則比對結果為可接受。故將檢體探針清洗一次與清洗兩次計算出之 CPM 數值和 control 組之 CPM 數值相減，可發現檢體探針清洗一次與清洗兩次中，各有一個 CPM 數值相減差異 > 50。另外，將 control 組之濃度與檢體探針清洗一次之濃度計算出之 bias% 和 control 組之濃度與檢體探針清洗二次之濃度計算出之 bias% 皆 < TEa% = 33.60，同時，檢體探針清洗一次之濃度與檢體探針清洗二次之濃度計算出之 bias% 也 < TEa% = 33.60。

**結論：**在 carry-over effect 模擬實驗中，發現雖然有 CPM 數值相減差異 > 50，但計算出 bias% 皆 < TEa%，表示病人數值比對結果為可接受，由此可顯示，CPM 數值相減差異 > 50，並不影響病人報告。另外，因檢體探針清洗一次與兩次之濃度計算 bias% 皆 < TEa%，故可說明檢體探針清洗一次與兩次並無明顯差異，由以上可證明機器手臂檢體探針清洗一次無 carry-over effect 之發生，同時，實驗室 carry-over effect 模擬實驗之允收能以 TEa% 作為允收標準。在自動化的流程中，機器手臂提高檢驗速率的同時，仍能兼顧報告之準確度。

PC-107

## 使用癌症類別來分析腸道顯影原因

曾柏銘<sup>1</sup> 呂建璋<sup>2</sup> 沈淑禎<sup>2</sup> 門朝陽<sup>1</sup> 林雅婷<sup>2</sup> 蕭聿謙<sup>3</sup>

<sup>1</sup> 天主教中華聖母修女會醫療財團法人天主教聖馬爾定醫院正子造影中心

<sup>2</sup> 天主教中華聖母修女會醫療財團法人天主教聖馬爾定醫院核子醫學科

<sup>3</sup> 亞東紀念醫院核子醫學科

**前言：**FDG PET/CT 目前在癌症及健檢的應用上非常廣泛，除了術前評估及術後追蹤，還可發現未知的轉移區域。但在造影的過程中卻經常發現大腸有許多的良性顯影，這些良性顯影可能為腸壁攝取或腸蠕動的吸收現象，受檢者未必有便秘、腹瀉或發炎等情況，而良性的腸道顯影若出現在大腸直腸、子宮頸癌、卵巢癌及淋巴癌的病人則會提高診斷難度。本研究分析了癌症的類別、血糖、性別、BMI、排便習慣及服用軟便劑來分析造成腸道顯影的原因。

**方法：**我們搜集了 2022 年 4-9 月共 209 位受檢者。受檢者於檢查前至少禁食 8 小時，使用 Siemens biograph 16 PET/CT 並於注射 FDG 後 60 分鐘攝影。由於 FDG 於腸道的良性顯影會以各種型態進行吸收，我們將取標準攝取值 (SUVmax) 於肝之 1.5-2 倍間，且顯影面積超過一個腸彎曲稱為腸道顯影；排便習慣以 48 小時為基準值，癌症類別由於種類較多，在統計上較為困難，故選擇會影響飲食的頭頸部癌為一類 (口腔、舌頭、食道、咽喉)，其它則以另一類進行統計。

**討論：**FDG 腸壁吸收可能與腫瘤、腸蠕動、便秘、腹瀉、或未停用 meformine 有關，研究結果發現，頭頸癌病人對於腸道顯影達統計上顯著差異，這類病人的 FDG 腸道顯影較為正常 ( $P = 0.007$ )。在使用軟便劑 ( $P = 0.821$ )、血糖 ( $P = 0.941$ )、BMI ( $P = 0.233$ ) 在統計上皆無顯著關係，但在性別 ( $P < 0.05$ ) 與癌症類別 ( $P < 0.05$ ) 卻有顯著關係，推測是因為頭頸部癌症的比例為男性較高，且這些癌症因手術完肌肉走向、體質及飲食習慣改變導致進入困難，腸蠕動也跟著較差，FDG 在腸道壁上較不易吸收。

**結論：**實驗結果我們發現部分頭頸部癌之受檢者因手術完後進食困難，大多會選擇減少食物攝取、低渣或流質食物，導致這類受檢者在腸道顯影的情況並不明顯。因不同的癌症類型可能有著不同的飲食形態，若能在進行正子掃描前實施低渣飲食，則腸道顯影的問題可能得到更好的結果。雖然腸道顯影大部份為良性變異，但仍有部分文獻指出過多的腸道 FDG 吸收也有病變的可能，若能降低 FDG 正常腸道顯影，則醫師在進行診斷則可更加準確。

PC-108

## 用 LUTATHERA<sup>®</sup> 進行胜肽受體放射性藥物治療 (PRRT) 之工作流程、病人身上的輻射曝露狀況 —以北部某醫院為例

林培堯<sup>1</sup> 黃奕琿<sup>2</sup> 呂惠敏<sup>2</sup> 鄭媚方<sup>2</sup> 柯冠吟<sup>1</sup>

<sup>1</sup> 國立臺灣大學醫學院附設醫院癌醫中心分院核子醫學部

<sup>2</sup> 國立臺灣大學醫學院附設醫院核子醫學部

**背景介紹：**LUTATHERA<sup>®</sup> 是一種胜肽受體放射性核種治療 (Peptide Receptor Radionuclide Therapy, PRRT) 的藥物，成份為 Lu-177 (半衰期：6.65 天) 標記的生長抑制劑類似物，用於治療胃腸胰神經內分泌腫瘤，LUTATHERA<sup>®</sup> 會與腫瘤細胞的表面具有體抑素受體 (somatostatin receptors) 結合，直接將放射同位素送入腫瘤細胞，利用 β 射線造成腫瘤細胞死亡。LUTATHERA<sup>®</sup> 用靜脈輸液的方式給藥，輸注放射性藥物需要 30 分鐘，為了保護腎臟，會在病人另一邊的肢端靜脈額外輸注 4 小時的胺基酸 (amino acid)，故完整的治療程序大約需要 4.5 個小時，會進行四次療程 (至少間隔八週)。因此，台大癌醫經驗分享使用放射性藥物 LUTATHERA<sup>®</sup> 治療之工作流程、病人在住院期間的輻射曝露。

**方法：**病人先注射止吐藥 30 分鐘後，再以輸液的方式注射胺基酸 30 分鐘後，護理師將 LUTATHERA<sup>®</sup> 注入至病人體內，當 LUTATHERA<sup>®</sup> 注射 30 分鐘後，護理師將病人手上的 LUTATHERA<sup>®</sup> 針具和管路移除，改在護理站透過監視系統照護病人，直到胺基酸完全輸液完畢，再次進入病室，移除病人身上胺基酸的管路，病人在隔日離院，隨後於核醫部進行全身掃描。病室內天花板裝設環境偵檢器，並用監控軟體即時得到病人的輻射曝露數據，故可以推算出病人若在一公尺處，開始注射、注射 LUTATHERA<sup>®</sup> 30 分鐘後、直到離院前的輻射曝露。

**結果：**病患輸液 LUTATHERA<sup>®</sup> 藥物的劑量為 200.8 mCi，這段時間只有輕微的噁心和頭暈；從監控軟體可以算出病人一公尺的輻射曝露從一開始為 59.9 μSv/h、注射藥物 30 分鐘後為 45.2 μSv/h、注射藥物 4 小時 (整個療程結束) 後為 28.8 μSv/h、注射藥物 8 小時後為 18.3 μSv/h、隔日上午病人離院為 13.4 μSv/h，在注射後 24 小時的單光子全身造影，看出靜脈留置針處無藥物殘留，LUTATHERA<sup>®</sup> 大部份在腫瘤、肝臟、脾臟、腎臟、泌尿道及腸道累積。

**結論：**此治療方式需要將輸液方式緩慢將 LUTATHERA<sup>®</sup> 和胺基酸注射到病人體內，所以週邊靜脈的留置針狀況是工作同仁要注意的，也可減少藥物的殘留。透過病床上的環境偵測器，得知病人在住院期間的輻射曝露監控數值有無異常，盡可能提醒病人多喝水，加速多餘的輻射劑量排出。

PC-109

## Automatic Lesion Segmentation Application of Artificial Intelligence of FDG PET Imaging of Follicular Lymphoma

Yu-Yi Huang<sup>1,2</sup>, Shih-Han Yang<sup>1</sup>, Jia-Lin Yang<sup>3</sup>, Wen-Yu Hsu<sup>3</sup>, Fou-Ming Liou<sup>3</sup>

<sup>1</sup>Department of Nuclear Medicine, Koo Foundation Sun Yat-Sen Cancer Center

<sup>2</sup>School of Medicine, College of Medicine, National Yung Ming Chiao Tung University

<sup>3</sup>MultiMedia BU R&D Department, ASUSTeK Computer Inc

**Background:** This study intends to use deep learning Convolutional Neural Networks (CNN) model technology to train an application software model that can automatically detect and segmentate follicular lymphoma PET lesions.

**Materials and methods:** The CNN model composes of an input layer, a convolution layer, a pooling layer, a feature map, a fully connected layer, and Softmax function, to form the overall model architecture. From 2002 to 2014, a total of 174 follicular lymphoma patients were treated in our hospital. After screening, 86 image data set can be used for AI training and verification. Lesion segmentation was done using PET VCAR (Volume Computer Assisted Reading) (GE Healthcare, Chicago, IL, USA). Among these 86 data sets, 73 (85%) are used for AI training and 13 (15%) are used for validation. All models are trained and evaluated using five-fold cross-validation on the training set. The whole process combines dice and crossentropy loss to train the network: for running 3D U-Net on all training sets, the program calculates the dice loss for each sample in the batch and averages it. The aim of training model is to reach a Dice Score > 0.8.

**Result:** The training results as follows: Dice (mean) = 0.877 (0.722-0.961); Precision (mean) = 0.898 (0.699-1.0); Recall (mean) = 0.859 (0.68-0.963). The validation results as follows: Dice (mean) = 0.804 (0.593-0.954); Precision (mean) = 0.82 (0.563-0.982) Recall (mean) = 0.801 (0.538-0.931).

**Conclusion:** After training, the results of this preliminary study reached the target of the preset Dice Score > 0.8, which means that it is feasible to use AI to automatically detect lesions in follicular lymphoma PET-CT scan. The next step should consider adding training volume to achieve a Dice Score greater than 0.98, which will facilitate the use of this technology in clinical practice. In addition, the detection results can be used to continue the study of imaging characteristics (radiomics) to deeply analyze whether the imaging characteristics are correlated with the clinical manifestations and prognosis of the disease.

PC-110

## 針對正子造影之標準攝取值 (SUV) 偏高 之根本原因分析報告

賴佳玟 張哲瑋 陳雅鳳 李柏葦 黃兆駿

亞東紀念醫院核子醫學科

**事件調查與發生經過：**2022/03/23 主治醫師反映近期正子造影之 SUV 值偏高，請放射師與原廠工程師進行原因分析，是否有設定錯誤或其他未知問題，建議進一步對正子造影儀做重新校正。

**事件分析與探討根本原因：**核醫正子造影儀之校正設備分密封射源及灌注假體，其中灌注假體對於體積 - 活度 - 計數值有比例轉換的關係，與 SUV 值有關。所以灌注假體有固定的體積並且需要考慮到高比重溶液在長時間靜置導致分布不均 ( 下沉 ) 的可能。所以操作人員需要一定的技術程度。而因工程師於 2022/03/17 對於正子造影儀有進行調校 well counter 數值，有可能在調校過程中輸入錯誤數值，以致影像之 SUV 升高。於 2022/03/28 進行重新調校已恢復正常。

**改善建議及行動方案：**2022/03/28 重新進行調校 well counter，且先將正子控制台及劑量校正器的時間調成一致，再將 1 mCi F-18 打入灌注假體共 5640 c.c. 均勻搖晃後進行掃描，並記錄下藥物灌注前及殘餘的活度與時間。分別進行 2D 及 3D well counter 校正，其 sensitivity 及 activity factor 皆為正常範圍。利用此校正值重組病人影像，其 SUV 值與以往的影像 SUV 相近，誤差值僅 6.57%。而則為調校錯誤的 SUV，可明顯看出其影像相較於其他影像要來得深且 SUV 值偏高。為防止此次事件，建議工程師在進行調校前可先與放射師進行 double check 其藥物活度及時間，以及輸入數值到控制台時也再進行確認。



PC-111

## Diffusely Intense Uptake at Bilateral Lung Fields on Tc-99m MDP Whole Body Bone Scintigraphy – A Case Report

Shu-Mei Lu, Yu-Ling Hsu

*Department of Nuclear Medicine, Ditmanson Medical Foundation Chia-Yi Christian Hospital, Chia-Yi, Taiwan*

**Case:** Here we demonstrate a 63 year-old male who has unusual  $^{99m}\text{Tc}$ -MDP activity pattern throughout both lung field on whole-body bone scan. During his work-up, chest x-ray was also performed. Chest x-ray revealed increased interstitial infiltration over bilateral lung fields and hazy infiltration over right lung field. According to literature, diffuse and symmetric lung uptake pattern can be present on bone scintigraphy in a patient with a history of CKD (chronic kidney disease with renal failure and cardiovascular disease. (fig.1-2)

**Discussion:** There are many causes of increased pulmonary radiotracer uptake, both focal and diffuse, which can be encountered on whole body bone scintigraphy; however, the findings on bone scan alone are often non-specific. Extra-osseous uptake of bone-seeking radiopharmaceuticals has been reported at various sites. Extra-osseous uptake can occur within a tumor, or in muscle, soft tissue, pleura, or lung. Abnormal calcium deposition in soft tissue, followed by chemisorption of Tc-99m MDP, is thought to be a pathogenesis. Diffuse lung uptake on bone scintigraphy has been reported in patients with hyperparathyroidism, hematologic malignancy and solid organ tumor, metabolic abnormality such as renal failure, vasculitis and pulmonary infection. We report a case of patient with metabolic abnormality--renal failure who demonstrated diffuse pulmonary uptake on Tc-99m MDP bone scan.

In patients with terminal renal insufficiency, an increase in serum phosphorus is a predictor of end-stage renal disease with, as a consequence, the development of secondary hyperparathyroidism and metastatic calcifications, especially when the product of serum calcium and phosphorus is elevated. This may be responsible for the diffuse uptake in the lungs of this patient.

PC-112

## 評估 C- 胜鏈胰島素 (C-Peptide) 試劑 在方法學時效性上之改善

古琴鳳 劉怡慶 林秋美 陳素英 曾翠芬 陳怡如 陳宜伶  
蕭莉茹 林家揚 張晉銓

高雄醫學大學附設中和紀念醫院核子醫學部

**前言：**C-peptide 可以作為胰島素分泌的良好指標，C-Peptide 為胰臟製造胰島素 (Insulin) 過程中的副產物，不具生理作用，但在監測胰島素分泌上扮演重要的角色，臨床上常用來評估糖尿病患者自行分泌胰島素的能力，其最大的特點在於只有胰臟本身分泌的胰島素才會斷裂出 C-peptide，注射進入體的胰島素則不會產生 C-peptide，因此能真實反應出胰島素的分泌能力，本研究因應醫師臨床對於報告時效性之需求，希望可加速 C-peptide 報告之時間以增加時效性，故藉由評估試劑原方法學和縮短時間之不同變異性來比較其測試之結果，期望儘快將檢驗數據提供臨床醫師做為治療上之診斷。

**方法：**DIAsource C-Peptide 為一種放射免疫競爭測定法 (RIA)。利用標幟試劑 (125I-C-peptide -Ag\*) 與檢體中 C-peptide-Ag 相互競爭有限數目的 Ab 結合部位，經反應後算出與抗體結合的 125I-C-peptide -Ag\*-Ab，與血液檢體、標準組中的 C-peptide-Ag 量呈反比，以加瑪計數器計算出檢體 C-peptide 的含量。本研究共收集 68 個檢體樣本數，分別進行檢體反應靜置 180 分之原廠商試劑標準流程 (靜置法)，另一組為檢體於振盪器 (SHAKER) 下反應 90 分之縮短時間方法 (振盪法) 來進行檢測，兩者皆在室溫下進行來比較兩者之間差異。

**結果：**本研究統計方法採用 TWO sample T-test 及 Correlation 來比較兩方法上之差異，經 t-test 比較之結果 P 值為 0.91，P 值 > 0.05，再利用兩方法學比較其 Correlation，其 Correlation (相關性) R 值為 0.997。

**結論：**本研究分析進行檢體反應靜置 180 分之原廠商試劑標準流程 (靜置法) 及振盪器 (SHAKER) 下反應 90 分之縮短時間方法 (振盪法) 來進行檢測，不同反應時間和反應條件的測試結果，其結果數據顯示：利用統計學上 TWO sample T-test 比較二者之間的差異度是不明顯 (P 值 > 0.05)，再利用兩者間之 Correlation 相關性比較來佐證，其相關性 R 值更可達到 0.997，故我們認為在兩方法學上是沒有顯著的差異性存在，也可說明本研究之振盪法是可做為急需報告時的選擇，以提供臨床上醫師緊急判斷之依據及需求，對於本實驗室也可提升服務之效率及品質的保證。

PC-113

## 以擬人假體評估 Tc-99m 與 I-123 雙同位素同時攝影於半導體偵檢器中之能量交疊干擾

許琮翔<sup>1,2</sup> 高潘福<sup>1</sup> 姜智傑<sup>2</sup><sup>1</sup> 中山醫學大學附設醫院核子醫學科<sup>2</sup> 中山醫學大學醫學影像暨放射科學系研究所

**目的：**為了解雙同位素 Tc-99m 與 I-123 在同時間攝影時不同能窗下彼此的能量交互干擾情形，本研究使用 Radiology Support Device (RSD) 擬人假體進行掃描，利用半導體偵檢器系統並以 list mode 格式收錄影像資訊，經由後處理重新切割成不對稱能窗找尋不同能窗下能量交疊干擾最少之條件。

**方法：**RSD 假體實驗共分三大組，分別為純 Tc-99m、純 I-123 和同時混合 Tc-99m 與 I-123 雙同位素。其中假體內包含心臟、肝臟以及剩餘的背景分別灌注不同活度濃度溶液，心臟縱隔腔活度比例再分為 1:3 與 1:5 進行評估。Tc-99m 能窗以 140 keV 為中心不對稱能窗下限值分別設定為 8%、9%、10% (3 種)，能窗上限值設定為 3%、4%、5%、6%、7% (5 種)，共 15 種能窗組合。I-123 能窗以 159 keV 為中心不對稱能窗下限值分別開 5%、6%、7%、8%、9% (5 種)。能窗上限值設定 8%、9%、10% (3 種)，共 15 種能窗組合。本實驗使用臨床半導體偵檢器 GE Discovery NM/CT 670 CZT SPECT 進行掃描。數據分析根據所圈選心臟與縱隔腔的 VOI 計算平均活度估計其能量交疊影響，並以交疊干擾 cross-talk ratio： $(\text{雙同位素計數} - \text{單核種計數}) / \text{單核種計數}$  進行分析。

**結果：**實驗結果顯示 Tc-99m 能窗上限值越高則有較多的 cross-talk，反之能窗上限值較低時則能有效降低 cross-talk。實驗結果亦顯示能窗下限值設定的高低對於 cross-talk 無顯著性影響，因此調整能窗上限值並對其進行最佳化可有效控制 cross-talk。在 I-123 能窗中整體 cross-talk 較 Tc-99m 能窗低，在 I-123 能窗下限值達 7%、8%、9% 時 cross-talk 有明顯升高的趨勢，其餘能窗設定範圍之 cross-talk 差異不大，其能窗上限值設定亦無顯著影響。

**結論：**根據實驗結果 Tc-99m 最佳的不對稱能窗之上限值設定為 140 + 3% keV，能窗下限值遭受 cross-talk 影響程度較小。I-123 最佳的不對稱能窗之下限值為 159-6% keV，能窗上限值則對結果影響不顯著。經最佳化後 Tc-99m 交疊干擾最輕微的能窗條件為 140-9% keV~140 + 3% keV 其交疊干擾比率為 19.5%，I-123 為 159-6% keV~159 + 9% keV 其交疊干擾比率為 0.38%。

PC-114

## 甲狀腺癌病人術後接受碘 -131 治療 SDM 輔助評估表之製作一個案報告

邱禹臻 許幼青 廖建國 劉芳馨

佛教慈濟醫療財團法人大林慈濟醫院核子醫學科

**背景：**碘 -131 治療是一種口服藥物，無手術麻醉風險，只需住院治療二至三天，且健保有給付，治療費用低，不會造成家庭經濟負擔。高劑量放射性同位素碘 -131 可消滅癌細胞、減少腫瘤復發並抑制癌細胞成長，100 個治療效果良好的病人中有高達 92 名病人可存活超過 10 年。醫病共享決策 (Shared Decision Making, SDM) 是以病人為中心的臨床醫療執行過程，主要目的是讓醫療人員和病人在進行醫療決策前，彼此交換資訊共同討論，以達成可行之最佳治療選項。本文目的為整理本科碘 -131 治療 SDM 表單製作之過程及成果，提出分享。

**個案報告：**團隊成員由核子醫學科醫師、放射師及護理師所組成，團隊成員於 SDM 主題討論座談會上確定主題，並參加 SDM 工作坊共三次課程，完成醫病共享決策輔助工具研發報告單、決策輔助工具病人及醫療人員試用意見回饋表 ( $\alpha$  test)、成效評估調查病人和家屬及醫療人員問卷 ( $\beta$  test)，教學部確認甲狀腺癌病人術後接受碘 -131 治療 SDM 輔助評估表完整性後依醫學倫理委員意見做修訂。SDM 表單內容包括一、前言：碘 -131 在甲狀腺癌的應用，包括偵測轉移病變、手術後甲狀腺殘餘組織的清除以及轉移病變的治療。甲狀腺癌病患在手術切除甲狀腺組織後，可接受碘 -131 輔助治療清除殘餘組織及治療轉移病灶。二、適用對象：甲狀腺癌病人且已接受甲狀腺全切除、合併遠端轉移或復發者。三、治療簡介：放射性同位素碘 -131 可以破壞未被發現的微小癌細胞病灶，對於無法手術清除的癌組織或遠端轉移、頸部或縱膈腔之淋巴轉移等，高劑量放射性同位素碘 -131 可消滅癌細胞、減少腫瘤復發並抑制癌細胞成長。四、接受或不接受碘 -131 大劑量治療其預後、副作用及風險比較。五、總結與回顧：手術切除腫瘤加上碘 -131 治療，是目前公認甲狀腺癌的最佳治療方式，對於無法手術清除的癌組織或遠端轉移、頸部或縱膈腔之淋巴轉移等，高劑量放射性同位素碘 -131 可幫助消滅癌細胞、減少腫瘤復發並抑制癌細胞成長。碘 -131 治療的副作用一般程度輕微且短暫，大多 1-2 週後即改善，合理範圍的治療劑量，並未增加不孕、遺傳疾病及致癌的機率，造血功能疾病 (白血病) 極為罕見，是一種有效、簡單及安全的治療方法。六、是否接受碘 -131 大劑量治療。

**結論：**手術切除腫瘤加上碘 -131 治療，是目前公認甲狀腺癌的最佳治療方式，對於無法手術清除的癌組織或遠端轉移、頸部或縱膈腔之淋巴轉移等，高劑量放射性同位素碘 -131 可幫助消滅癌細胞、減少腫瘤復發並抑制癌細胞成長。此份 SDM 輔助評估表能夠結合病人自身的偏好跟價值觀，提供病人選擇的依據，由臨床人員和病人共同參與醫療照護，達成醫療決策共識並支持病人做出符合其偏好的醫療決策。

PC-115

## 評估三碘甲狀腺素 (Triiodothyronine, T3) 試劑更換與臨床適用性

林秋美 陳素英 陳宜伶 蕭莉茹 曾翠芬 古琴鳳  
陳怡如 劉怡慶 林家揚 張晉銓

高雄醫學大學附設中和紀念醫院核醫部

**目的：**試劑品牌更換於臨床上是常有的事，如何從各品牌中選擇符合臨床需求與實驗室要求是極為重要的。本實驗室針對試劑品牌更換進行精密度、準確度與相關性評估探討，從中找出符合臨床要求，即精密度、準確度、相關性要高且檢體量少時間要短等要件，以期能儘快提供檢測數據供臨床醫師儘早確立可靠的診斷與用藥。

**材料和方法：**本研究為評估 T3 試劑品牌更換，評估方式將試劑品牌分成 A 試劑（即原試劑）、B 試劑（新試劑）。檢體採用血清共 50 個樣本數，樣本挑選來自 A 試劑已測試過的（25 個值於參考值內，25 個值異於參考值）。用同血清樣本分別進行 B 試劑檢測 1 和 2。檢測 1 和 2 時間相隔 1 週，用於評估試劑精密度、準確度與穩定度。兩個試劑品牌方法學均為放射免疫分析法，原理為競爭型（Competition assay）。

**結果：**試劑 T3 血清濃度（平均值 ± 標準誤差）於 A 試劑、B 試劑檢測 1 和 2，統計檢測結果分別為  $127.42 \pm 19.278$ 、 $156.90 \pm 19.671$  和  $159.04 \pm 19.683$  (ng/dl)。本研究統計 A 試劑 vs. B 試劑檢測 1 其相關係數與截距分別為 0.993； $y = 1.0134x + 27.769$ 、A 試劑 vs. B 試劑檢測 2 其相關係數與截距分別為 0.990； $y = 1.0108x + 30.238$ 、B 試劑檢測 1 和 2 其相關係數與截距分別為 0.989； $y = 0.9994x + 1$ 。另測試 B 試劑重覆檢測 1 和 2 的 inter-run and intra-run 其結果 CV (%) 值均 < 10%。

**結論：**B 試劑第 1 和 2 次的檢測結果與 A 試劑比對，其相關性均 > 0.95 以上；符合本實驗室更換試劑品牌要求。A 試劑、B 試劑檢測 1 和 2 的截距其 y 與 x 之關係更趨近於 1； $R^2$  均 > 0.95 以上，故其試劑品牌更換於臨床上的適用性是可取代的。另針對新試劑開封後不同時間重覆檢測其 inter-run 和 intra-run，其檢測結果 CV (%) 均 < 10% (TEa < 20%；此規範來自 RCPA)，顯示新試劑品牌其精密度、準確度與穩定度均好。故更換成 B 試劑在臨床上是可適用的。也能準確的提供數據供臨床醫師儘早確立可靠的診斷及用藥。

PC-116

## 輻射藥物滲漏之處理與改善措施 – 個案報告

邱禹臻<sup>1</sup> 許幼青<sup>1</sup> 廖建國<sup>1</sup> 莊紫翎<sup>1,2</sup>

<sup>1</sup> 佛教慈濟醫療財團法人大林慈濟醫院核子醫學科

<sup>2</sup> 慈濟學校財團法人慈濟大學醫學系

**背景：**藥物滲漏是指靜脈注射藥物時外漏至皮下組織，使得組織發生浸潤反應，而造成局部肌肉組織的損害，雖然藥物滲漏通常很輕微並且會自然消退，但有些病例會導致嚴重的併發症，包括全層皮膚脫落和肌肉及肌腱壞死，需要進行重建手術甚至截肢，導致住院時間延長、發病率增加和醫療費用增加。在核子醫學科的檢查，大多使用非密封性之低劑量、短半衰期之同位素藥物，這些病患在接受靜脈注射時都可能發生輻射藥物滲漏，所以如何預防輻射藥物滲漏及當發生輻射藥物滲漏時如何處置是非常重要的。

**個案報告：**77歲男性病患，主要診斷為淋巴瘤，病患於2021年9月28日9點20分由急診推床至核子醫學科準備做正子造影檢查，兒子陪同，給予氧氣2 L/min，有留置導尿管，右手肘靜脈注射中，外觀無紅腫，放射師於10點10分靜脈注射<sup>18</sup>F-FDG，之後點滴生理食鹽水注射過程中病人無不適感，11點10分準備上檢查台前發現靜脈注射處腫脹，當下立即停止點滴靜脈輸注，檢查病人衣物、床單及棉被無藥物滲漏情形。此時病患表示靜脈注射處有微腫脹感，又因呼吸喘和背部痠痛所以會一直自己翻身活動，研判可能滲漏原因為病人移動所致，因此擬訂改善措施為-每次靜脈注射後給予每位病患預防藥物滲漏衛教：1.當您感覺注射部位有疼痛、針刺、燒灼感時，應立即按叫人鈴。2.多臥床休息，不宜四處走動。3.靜脈注射處不宜不當的移動。4.打針部位不要用棉被覆蓋住以利觀察。實施改善措施後追蹤至今未再發生輻射藥物滲漏情況。

**討論：**輻射藥物滲漏一般造成的原因包括：1.病患相關因素：兒童及老年患者的小而脆弱的靜脈、長期洗腎者、長期服用類固醇藥物及止痛劑病患的血管大多數有硬化情形、切除淋巴結的病患、病患不當的移動等因素。2.程序相關因素：注射時速度過快導致血管破裂、靜脈留置針有血塊阻塞、注射技巧不佳等因素。避免藥物滲漏的方式可包括：1.執行靜脈注射時應由遠心端到近心端進行注射，優先選擇粗直、彈性好、不易滑動的靜脈注射部位。2.靜脈留置針避免打在關節活動處。3.靜脈留置針處避免大動作活動。4.為了方便觀察，打針部位不要用棉被覆蓋住。5.在給藥前/給藥期間檢查血液回流情況，以確保導管位於靜脈中。6.用生理食鹽水通過靜脈留置針檢查有無任何局部不適或腫脹，然後再注射藥物。

**結論：**當病患感覺注射部位有疼痛、針刺、燒灼感時，應請病人立即告知醫護人員，先評估是否有浸潤的情況，例如：注射部位有無紅、腫、壓、痛情形、針頭周圍有無藥物滲漏、點滴注入速度減慢或停止、反抽無回血、注射時有無阻力等情況，如有以上情形應立即停止靜脈輸液，避免注射部位施壓，也不要沖洗管路，以避免大量滲漏，這樣就能減少病人因輻射藥物滲漏所造成的傷害。

PC-117

## 乳癌前哨淋巴結定位檢查中 發現少見的對側腋下淋巴結

張秀瑛<sup>1</sup> 莊紫翎<sup>1,2</sup>

<sup>1</sup> 佛教慈濟醫療財團法人大林慈濟醫院核子醫學科

<sup>2</sup> 慈濟學校財團法人慈濟大學醫學系

**背景介紹：**在前哨淋巴結定位檢查中，乳房的主要淋巴引流區為同側腋下處，但偶而會往腋外區域引流。最常見的腋外引流處為內側乳腺、鎖骨上、鎖骨下淋巴結以及內乳淋巴結等，往對側乳房腋下處引流是極其少見的。在此我們介紹一位右側乳癌患者在執行前哨淋巴結定位檢查時，意外發現在其對側左側腋下處也有淋巴結活性攝取的病例。

**影像報告：**一名 51 歲右側有一呈現 1.05 公分的乳腺管原位癌女性乳癌患者，在今年 8 月到本科執行術前的前哨淋巴結定位檢查。在患側乳暈處以皮下注射方式注入 Tc-99m Phytate，經 30 分鐘及按摩後進行造影，除常規的前位、前斜位及側位像外另加照 SPECT/CT 以精確定位。檢查結果發現除了乳暈注射處有活性攝取之外，在右側腋下或乳房第一區淋巴結處有一活性攝取，另外在其左側腋下第一區淋巴結處也意外地發現有一活性攝取。

**結論：**前哨淋巴結定位檢查對於乳癌的前哨淋巴結的辨別及定位可以提供非常好的幫助。根據文獻指出在檢查中有 28% 的機率會在患側同側腋下區之外發現淋巴引流，而在對側腋下區發現淋巴引流只有 0.2%，除此之外該文獻也證實了對側腋下淋巴引流有 20.6% 的機率為惡性腫瘤，雖然此次我們所介紹的病例並沒有獲得進一步的切片檢查，但無論如何皆應告知臨床醫師檢查影像中所得。

PC-118

## 核醫造影報告時效之分析及探討

廖建國<sup>1</sup> 許幼青<sup>1</sup> 劉芳馨<sup>1</sup> 莊紫翎<sup>1,2</sup><sup>1</sup> 佛教慈濟醫療財團法人大林慈濟醫院核子醫學科<sup>2</sup> 慈濟學校財團法人慈濟大學醫學系

**背景：**核醫造影檢查後醫師的報告時效，為核醫管理階層例行監控與管理的作業品質之一。本科多年來期望核醫醫師以檢查後 1 日內完成報告為目標，因此每月監控報告時效，並定期分析及檢討。本研究目的即為分析近 3 年報告時效完成率，以作為持續改進之參考。

**方法：**回溯性收集 2020 年 1 月至 2022 年 7 月，例行造影檢查之報告清單資料，分析各年度所有報告之 1 日內及 3 日完成率，並依住院或門診分別統計住院 1 日內、門診 3 日內完成率，再進一步針對作業量較大以及肺臟灌注 / 通氣掃描 (V/Q)、腸胃出血等特殊檢查進行分析，以比較各年度平均值，並進行探討。其中報告完成時間以開單日至報告發出日之時間計算而得，惟 V/Q 及腸胃出血檢查之報告完成時間，以檢查完成日后至報告發出日之時間計算。

**結果：**總計收集 22098 件報告個案，各項目報告數量居前三位者分別為骨骼掃描、心肌灌注掃描、正子造影。整理結果發現，近 3 年所有報告之平均 1 日內及 3 日完成率，分別為 96.1% 及 92.5%，其中近 2 年之 1 日內完成率有明顯進步。進一步分析門診 3 日內及住院 1 日內完成率，可發現近 3 年平均值分別為 95.9% 及 93.5%，其中近 2 年之住院 1 日內完成率也有明顯提升。另外，再針對作業量較大之 3 項檢查以及 V/Q 檢查等 2 項特殊項目進行分析，可得知骨骼掃描、心肌灌注掃描、正子造影等平均 1 日內完成率，分別為 92.7%、100%、99.5%、100%、100%，其中骨骼掃描由於作業量最大其 1 日內完成率相對較低，但仍達 90% 以上，近 3 年亦有持續的進步。

**結論：**分析結果顯示，本科近 3 年所有報告之平均 1 日內完成率為 96.1%，其中近 2 年之 1 日內完成率有明顯進步，顯示我們追求 1 日內完成報告之目標，已有明顯的成效。針對核醫造影之報告時效，管理階層可繼續依管理機制，每年定期分析及檢討，以持續提升服務品質。



PC-119

## 以 HFMEA 改善 RIA 檢驗作業流程之成效分析

廖建國<sup>1</sup> 張素雲<sup>1</sup> 劉芳馨<sup>1</sup> 莊紫翎<sup>1,2</sup>

<sup>1</sup> 佛教慈濟醫療財團法人大林慈濟醫院核子醫學科

<sup>2</sup> 慈濟學校財團法人慈濟大學醫學系

**背景：**醫療照護失效模式與效應分析(HFMEA)為醫療界使用的一種預防性的系統風險分析工具，廣泛應用於改善醫療作業流程。本科實驗室多年前即導入 HFMEA，於每年年初評估前一年核醫檢驗作業流程之失效模式及可能原因。本研究目的即為分析比較近 2 年 HFMEA 之風險評估資料，以了解近 2 年進步與退步的情形，作為持續改進之參考。

**方法：**依 HFMEA 危害分析方法，評估各作業流程之風險，包括主流程與次流程項，進行發生頻率與嚴重度之評估，危害指數以發生頻率與嚴重度之乘積計算，比較 2020 年 (2021 年 1 月評估) 與 2021 年 (2022 年 1 月評估) 之年度風險評估之危害指數，以探討 2021 年之改善成效。

**結果：**近 2 年之風險評估結果，主流程合計 9 項，次流程合計 49 項。比較近 2 年結果，可得知 2021 年各項目之危害指數有降低者計 11 項，包括檢體不良主流程 3 件 (檢體溶血、有檢驗單無檢體、檢驗單醫令錯誤)；檢體簽收主流程 1 件 (檢體資料錯誤)；檢體處理疏失主流程 1 件 (試管標示錯誤)；分析錯誤主流程 1 件 (檢體排列錯誤)；報告疏失主流程 5 件 (報告不應發而發、報告輸入錯誤等)。而 2021 年各項目之危害指數有升高者計 5 項，包括檢體不良主流程 1 件 (重覆開單)、檢體簽收錯誤主流程 1 件 (同仁不慎誤簽)、檢體處理疏失主流程 1 件 (檢體處理時誤用平衡用吸管)、品管異常主流程 1 件 (能力試驗結果不良)、報告疏失主流程 1 件 (因清單順序錯誤而誤發報告)，針對這些項目本實驗室皆已列入 2022 年的優先改善項目。

**結論：**比較近 2 年結果，總計 49 項次流程中危害指數有降低者 (計 11 項) 佔 22.4%，而危害指數有升高者降低 (計 5 項) 佔 10.2%，顯示 2021 年有進步的項目明顯較退步者多，也證明以 HFMEA 改善 RIA 檢驗品質確有成效。管理階層可持續運用 HFMEA 工具，找出作業流程中潛在的失效模式及原因，並加以改善。

PC-120

## 由 RIA 實驗室品質分析 探討管理審查制度之重要性

廖建國<sup>1</sup> 張素雲<sup>1</sup> 劉芳馨<sup>1</sup> 莊紫翎<sup>1,2</sup>

<sup>1</sup> 佛教慈濟醫療財團法人大林慈濟醫院核子醫學科

<sup>2</sup> 慈濟學校財團法人慈濟大學醫學系

**背景：**管理審查制度為認證實驗室重要的品質活動之一，透過一年至少一次的管理審查，實驗室可檢討與審查每年的作業品質。本實驗室於 2016 年通過認證後，依認證規範每年實施管理審查。本研究目的即為分析近六年執行管理審查後之實驗室品質提升情形，以了解其改善成效，並探討管理審查制度之重要性。

**方法：**收集 2017 年 1 月至 2022 年 6 月，RIA 實驗室例行不符合事件紀錄 (包括作業流程中各類異常及品質指標異常事件)，分析各年度不符合事件件數以及其種類，再比較各年度之表現情形，以檢討 RIA 實驗室品質提升狀況，並探討年度管理審查制度於實驗室持續提升品質所扮演的角色。

**結果：**近 6 年總計收集 102 件不符合事件個案，各年度總件數分別為 2017 年 42 件、2018 年 20 件、2019 年 9 件、2020 年 15 件、2021 年 11 件、2022 (1-6 月) 5 件，比較各年度之月平均件數，可發現不符合事件有逐年下降的趨勢，其中 2022 年表現最好，顯示實驗室可達成持續提升品質的目標。再分析各年度不符合事件之種類，可得知報告更改之件數為各年度中發生次數最高的項目 (佔 83.3%)，其他事件則相對較低。進一步比較各項目改善情形，可發現進步最大的為報告更改件數的下降，而報告更改指標異常、檢驗操作錯誤等項也有明顯的改善。

**結論：**由 RIA 實驗室品質分析結果，顯示不符合事件有逐年下降的趨勢。實驗室可透過每年的管理審查，綜整與檢討各類異常事件，並針對年度應加強改善之事項，建立重點審查機制，每月追蹤改善成效，以持續提升作業品質。

PC-121

## RIA 實驗室運用員工建議順利完成試劑更換作業 一個案報告

廖建國<sup>1</sup> 張素雲<sup>1</sup> 薛予婕<sup>1</sup> 莊紫翎<sup>1,2</sup>

<sup>1</sup> 佛教慈濟醫療財團法人大林慈濟醫院核子醫學科

<sup>2</sup> 慈濟學校財團法人慈濟大學醫學系

**背景：**員工建議制度為 TAF 認證實驗室持續提升品質重要的機制之一，本科實驗室每年皆請同仁提案建議，以了解第一線作業同仁對於持續提升品質或服務的想法。本案例即為回顧本實驗室透過員工提案建議，順利完成試劑更換作業之過程，提出分享。

**個案報告：**由於 CIS 廠牌之試劑，廠商已於 2021 年底通知預計於 2022 年 7 月停產，因此本實驗室大部份的試劑將被迫更換。因預期試劑評估及試用所耗費的時間將相當長，為避免替換試劑前之評估及試用等工作未及完成，而導致新試劑的銜接出現問題，員工建議儘早試用並決定 CIS 替換試劑，以提升作業效率及品質。2022 年 2 月本實驗室向採購單位反映後，由採購單位與廠商議訂所提供之試劑，並陸續開始進行試用。試用期間除完成新舊試劑檢驗結果之比對外，尚須進行多項的準備工作，包括驗證生物參考區間、修訂作業標準(12 項)、替換前公告周知、預計全面替換日期、HIS 系統項目內容變更(參考區間等)、能力試驗方法變更、內部品管 CV 值驗證、TAF 申請異動等。經一連串準備工作後，本實驗室於 2022 年 7 月正式全面更換試劑，並於 15 工作日內向 TAF 申請試劑方法之異動，將實驗室新舊試劑比對結果及相關評估審查資料上傳，順利完成試劑更換作業。

**結論：**本實驗室依員工建議提早規劃新試劑評估事宜，先選定預計替換的試劑進行試用與評估，以儘早決定取代之試劑，讓試劑廠商可以提早準備，實驗室也能順利的替換試劑。運用員工建議，可接收到第一線同仁的意見，若方案有益可行，即可規劃執行，以提升作業效率、改善品質或預防可能發生的問題。

PC-122

## 核醫造影室降低未加照影像 而導致之影像品質不良事件—PDCA 經驗分享

廖建國<sup>1</sup> 許幼青<sup>1</sup> 劉芳馨<sup>1</sup> 莊紫翎<sup>1,2</sup>

<sup>1</sup> 佛教慈濟醫療財團法人大林慈濟醫院核子醫學科

<sup>2</sup> 慈濟學校財團法人慈濟大學醫學系

**背景現況：**核醫造影作業中發生影像不良之事件，並不少見。回顧本科近 2 年的發生原因包括未加照影像、病人造影中移動以及放射師影像分析異常等，其中 2021 年發生 2 件因放射師未加照影像而導致之影像品質不良事件，因此已擬訂改善計畫追蹤中。本文目的即為整理 PDCA 改善計畫以及目前的改善成果，提出經驗分享。

**確立問題：**此事件發生原因為放射師執行完檢查後，未仔細核對檢查內容的完整性及正確性，就讓病人下檢查床離開，而發生未加照影像的事件。確立問題後，由管理階層討論，並擬訂改善措施。

**改善計畫：**依據事件發生原因，並經同仁共同檢討後，擬訂改善措施為請同仁落實檢查完立即核對的動作，確認檢查正確後才讓病人離開，並每月監控因未加照影像而導致之影像品質不良件數，定期檢討改善。

**成果追蹤：**依計畫甘特圖每月定期追蹤，直至 2022 年 8 月均無因放射師未加照影像而導致之影像品質不良事件發生。類似不良件數由 2021 年之 2 件，追蹤至今已降至 0 件，初步成效良好。

**結論：**持續提升作業品質，提供優質服務為造影室追求的目標，本科運用 PDCA 手法，降低未加照影像而導致之影像品質不良事件之初步成效良好，雖然改善計畫之效果確認時間為 2022 年 12 月份，但相信透過同仁的共同努力，一定可以將類似之影像品質不良事件再降為 0。

PC-123

## TAF 實驗室主管訓練後之轉訓工作 —經驗分享

廖建國<sup>1</sup> 許幼青<sup>1</sup> 劉芳馨<sup>1</sup> 莊紫翎<sup>1,2</sup>

<sup>1</sup> 佛教慈濟醫療財團法人大林慈濟醫院核子醫學科

<sup>2</sup> 慈濟學校財團法人慈濟大學醫學系

**背景：**全國認證基金會 (TAF) 每年定期舉辦實驗室主管訓練，訓練主題主要為醫學領域實驗室認證業務報告、行政事務報告以及其他認證重要事項宣導等，其內容可包括醫學領域認證現況、國際互相承認概況、認證效益、近期意見回應、近期重要公告事項、認證注意事項等。本科管理階層每年皆參與訓練，並將重要內容進行轉訓。本文目的即為整理本科如何推展轉訓之工作，提出經驗分享。

**轉訓時機：**每年科主任或品質主管參加 TAF 實驗室主管訓練後，於 1 個月內利用科會進行轉訓。轉訓時須全員到齊，若有事無法參加轉訓者，科室將要求該員於會後主動向轉訓主管詢問相關內容，以確保實驗室所有同仁皆能了解轉訓之內容。

**轉訓內容：**主要為認證重要事項宣導，例如 2021 年轉訓內容為遠端評鑑辦理方式說明、電子證書說明、影像醫學認證方案。而 2020 年轉訓內容則為常見處置案例與權利義務規章、對於實驗室管理階層的要求、使用認證標誌與宣稱認證之說明、實驗室不符合事件矯正措施之施行原則等，轉訓主管皆可使用 TAF 訓練所提供之簡報教材進行轉訓，並留存紀錄。

**定期宣導：**經轉訓後之各項重要事項，品質主管可再視同仁了解情形以及其重要性，再適時利用品保會議加強宣導，讓所有同仁再復習一下相關轉訓內容，以加深實驗室同仁的印象，必要時也可以筆試或口試的方式進行測驗，以了解同仁的熟悉程度，並針對同仁較不熟悉的部份進行補強。

**結論：**管理階層每年參加 TAF 實驗室主管訓練，可確保實驗室持續符合認證的最新要求，例如 2020 年已要求認證實驗室應將 TAF 權利義務規章納入品質管理系統，並予以運作及實現。因此，訓練後的轉訓工作就極為重要，可確保參加實驗室主管訓練後，相關重要訊息皆已傳達所有同仁知悉，並落實執行。

PC-124

## 放射性免疫分析轉換試劑之評估與驗證

莊雅晴 郭珮怡 李世昌 邱南津

國立成功大學醫學院附設醫院核子醫學科放射免疫分析

**前言：**臨床上部分疾病患者需要定期血液檢驗以評估疾病的穩定度與治療成效，像是定期追蹤 CEA 作為癌症的預後指標，穩定的檢驗系統對於這些長期追蹤的病患尤其重要，試劑變更是影響檢驗系統穩定性的一大因素，此次本實驗室因面臨試劑停產問題，迫不得已進行試劑更換，因此在轉換試劑前將對新試劑進行嚴謹的評估測試，並將相關評估結果公告臨床單位，以確保檢驗品質並降低更換試劑對於臨床的影響。

### 材料與方法：

1. 受評估項目分別為 TSH、T4、CEA。
2. 檢體收集：上述受評估項目各 40 支病人血清檢體、RANDOX、品管液 BIO-RAD (LOT：40390)
3. 檢驗試劑：
  - (1) TSH 及 CEA 舊有試劑為 CISBIO、新試劑為 BECKMAN COULTER IMMUNOTECH
  - (2) T4 舊有試劑為 MP、新試劑為 BECKMAN COULTER IMMUNOTECH
4. 評估方法：
  - (1) 同日精密度 (Witnin-day Precision)：使用品管液 2 種濃度重覆測定 10 次，計算 mean、SD、CV。
  - (2) 日間精密度 (Between-day Precision)：使用品管液 2 種濃度每日測定 2 次，連續測定 5 天後，計算 mean、SD、CV。
  - (3) 準確度 (Accuracy) 評估：使用已知濃度的能力試驗品管液比對至少 2 隻，允收標準為 SDI < 2.0。
  - (4) 線性 (Linearity) 評估：以高、低濃度檢體經不同比例混合後加以測定，將檢驗結果與「混合比例」的理論結果作圖評估其線性，以統計軟體計算其相關係數，允收標準為  $R^2 > 0.95$ 。
  - (5) 新舊試劑 correlation：取 40 支落在不同數值區間的檢體，分別使用新舊試劑進行測定，將兩種試劑的數值結果以統計軟體計算其相關係數和迴歸方程式，允收標準為  $R^2 > 0.95$ 。

**結果：**以新試劑 BECKMAN COULTER IMMUNOTECH 進行各評估項目檢測，經重複測定其同日精密度與日間精密度符合原廠宣稱數值，以已知濃度知能力試驗評估準確度、以檢體混合比例評估線性，結果皆符合允收標準。新舊試劑 correlation  $R^2 > 0.95$ ，顯示兩者檢驗結果具高度相關性。

**結論：**依據實驗室認證規範，實驗室進行檢驗方法異動前應完成性能評估測試、新舊試劑差異評估、生物參考區間驗證以及人員教育訓練等程序，綜合上述統計分析結果，新試劑 BECKMAN COULTER IMMUNOTECH 通過本實驗室對其再現性、準確度以及新舊試劑相關性之評估測試。實驗室因不可抗拒因素更換試劑，於變更前進行一連串的評估測試、驗證新試劑生物參考區間、制訂標準操作手冊以及人員教育訓練，並公告相關資訊，以確保新試劑之檢驗品質。

PC-125

## 放射免疫分析實驗步驟震盪重要性之探討

駱月娥 邱創新

國防醫學院三軍總醫院核子醫學部

**背景介紹：**競爭性蛋白質結合原理 (competitive protein binding theory) 乃 1960 年由 Dr. Yalow 及 Dr. Berson 兩位博士共同發表，於 1977 年 Dr. Yalow 博士獲頒諾貝爾獎。此原理開創了實驗診斷學的新領域，微量測定也正式開啓了放射免疫分析 (簡稱 RIA) 新的里程碑。後續又發展出另一種新的放射免疫分析法 Immunoradiometric Assay 簡稱 IRMA 法，又稱爲三明治法。本文將探討放射免疫分析實驗步驟震盪之重要性。

**方法：**本次分析探討之實驗項目分別是 CA125 (室溫靜置培育 18-20 小時) 及 CA199 (第一段 37°C 溫箱培育 3 小時、第二段室溫培育 16-24 小時) 腫瘤指標品項，依照仿單所提供之標準操作流程步驟執行標準曲線濃度 (數個濃度)、品管液 (高、中、低濃度)、待測物 (檢樣) 等，將試劑試管標示後 (含 CA125 及 CA199 第一抗體) 加入相同體積檢體量及緩衝液或示蹤劑 (標幟 I-125 第二抗體)，一組未進行震盪、另一組進行震盪 (輕微搖晃試管使內容物呈均勻狀態)，再放置室溫靜置培育，於隔日進行清洗上機計讀結合態試管放射活性 ( $\gamma$ -counter)，接著再套用仿單內程式便得到標準曲線濃度及待測物濃度。

**結果：**CA125 濃度小於 200 U/mL 以下時，實驗步驟有無進行震盪，實驗數據結果差異不大，當濃度大於 200 U/mL 以上時才有明顯差異，未進行震盪步驟標準液及待測物濃度皆有偏低現象 (見圖一、17、18、19、20)。其中 CA125 第 19 號是外部品管比對待測物濃度爲 457 U/mL，未進行震盪步驟組濃度 335 U/mL > 2SD，有進行震盪步驟組濃度 398 U/mL < 2SD。CA199 濃度小於 330 U/mL 以下時，實驗有無進行震盪步驟，實驗數據結果差異亦不大，但，當濃度大於 330 U/mL 以上時，也同樣發生未進行震盪步驟組濃度結果有偏低現象 (見圖二、14、15、16、17、18、19、20、21)。

**結論：**本次探討之腫瘤指標品項 (CA125 及 CA199) 高濃度數據結果發生偏低之現象，乃因 CA125 及 CA199 皆是靜置培育隔日清洗 (內容物未混合均勻造成反應平衡無法達標)，因此，操作者依照仿單確實執行震盪步驟，能讓試管內容物呈均勻狀態後，再進行培育，是 IRMA 實驗反應是否達到反應平衡的重要關鍵步驟，將使實驗確實達到反應平衡而獲得改善，也是產生可靠度及準確性 (accuracy) 加上精密性 (precision) 極高的數據結果的方法，使實驗數據準確性及精準性皆能符合實驗品質管制及實驗品質保證要求，才能確保實驗品質的優良性，並提供臨床醫師作爲病患正確診斷及製定可靠治療方針依據。

PC-126

## 因細胞激素風暴 (CRS) 造成血清含鐵蛋白 (Ferritin) 的虎克 (HOOK) 效應

王安美

台北馬偕紀念醫院核子醫學科

**前言：**人體免疫系統若過度反應會造成人體免疫反應失調，引發俗稱的細胞激素風暴 (Cytokine Release Syndrome, CRS)。與 CRS 有關的細胞激素為 TNF- $\alpha$ 、IL-1 及 IL-6 三大細胞激素，其會使體內的免疫及系統失調造成嚴重發炎反應，並於局部位置，引發發炎因子通過血液循環到全身，過度活躍的免疫反應，會不分敵我的攻擊正常細胞，細胞激素的釋放量太高可能對身體有害甚致為造成死亡。

本次探討的內容以回溯性數據分析個案報告，以兒癌病人因細胞激素風暴造成血中含鐵蛋白 (Ferritin) 發生 Hook 效應之狀況。發生 CRS 狀況下檢測血中 ferritin 濃度很重要，非常具有關鍵性，可作為細胞激素風暴疾病發炎嚴重程度指標，及評估病情是否惡化走向多重器官衰竭。本文即是探討因 CRS 引起 Ferritin 之 HooK effect，實驗室之因應措施。

### 材料方法：

方法：本實驗室使用之 Ferritin 鐵蛋白試劑 (廠牌：Immunotech，100 Tests 包裝)

檢驗原理：雙抗體固相放射免疫分析 (IRMA method)

標準曲線濃度：4.65、18.50、93.00、465.00、1140 (單位：ng/mL)

檢體：兒癌病人的血清檢體

**結果：**依病人抽血時序，可以看出病人 Ferritin 結果值之波動，由經稀釋 20 倍至最後不需經稀釋即可得到結果，因此懷疑是 HooK effect。

**討論：**Hook 效應就是指當待測物濃度過高，高到超過了固相上抗體所能結合的數目。因此反應在結果上就是超過了偵測的線性範圍，因此必須要將檢體先做稀釋，由上述表列序號 5 開始，未經稀釋之結果值卻明顯下降，與抽血時序而言，Ferritin 數據之波動似乎不合，故實驗室將檢體稀釋後，證明是 HooK effect。

由於 RIA 檢驗之方法為批次檢驗方法，故當需要稀釋之檢體需於下一批次稀釋後再驗，如此則可能延後發出報告。而此個案之序號 5 數據讓實驗室以為檢驗過程疏失，為確保不發出錯誤報告，實驗室採取重驗及稀釋，並詢問臨床科主治醫師，確定實驗室所做之結果無誤，之後接收此病人之檢體皆一律稀釋，才避免發出錯誤報告及延遲報告。



PC-127

## RIA 實驗室自行建立生物參考區間 —以 CEA 為例

薛仔婕<sup>1</sup> 張素雲<sup>1</sup> 廖建國<sup>1</sup> 莊紫翎<sup>1,2</sup><sup>1</sup> 佛教慈濟醫療財團法人大林慈濟醫院核子醫學科<sup>2</sup> 慈濟學校財團法人慈濟大學醫學系

**背景：**生物參考區間的查證可依生物參考區間評估指引執行，其中最簡單的方法為收集與分析 20 個健康個體之檢體（男、女各 10 人），其結果若  $\geq 18$  人（90%）落在試劑原廠說明書建議之生物參考區間的範圍內，即可確認該生物參考區間為可接受。若結果未達允收標準（90%），則可將樣本數擴大到 60 人（男、女各 30 人）。如擴大取樣數後仍無法滿足符合該條件，則表示該生物參考區間須重新制定。本研究目的即為整理發表實驗室自行建立生物參考區間之 CEA 檢驗結果。

**方法：**根據生物參考區間評估指引，若擴大取樣到 60 人（男、女各 30 人）後仍無法滿足符合該條件，需收集與分析  $\geq 120$  個檢體（男、女各 60 人），以自行建立符合實驗室自己的生物參考區間。因此，本實驗室著手收集健康人檢體，收集後之檢體使用 Beckman Coulter CEA IRMA Kit 進行分析。刪除與排除極大值與極小值（Outlier）後，計算平均值與標準差，以評估建立新的生物參考區間。

**結果：**總計收集 138 個檢體（男 68 名及女 70 名），CEA 之檢驗結果皆在 10 ng/mL 以內，其中男性與女性無明顯的差別（ $p < 0.05$ ）。依指引中 CLSI C28-A2 建議之極大值與極小值排除規則執行（One-third rule for the ratio D/R：當極大值（極小值）與次極大值（次極小值）之差（D）大於 1/3 的極大值與極小值之差（R），此極大值（極小值）應予以排除），並計算其平均值與標準差（SD）。此次 138 個檢體極大值（9.45）與次極大值（8.09）之差為 1.36，而極大值（9.45）與極小值（0.3）之差為 9.15。D/R = 1.36/9.15 < 1/3，此極大值（9.45）毋須刪除。依此規則計算，極小值（0.3）亦不須排除。所有檢驗結果之平均值為 2.3，2SD 值為 3.25，平均值加 2SD 為 5.55，因此本實驗室的 CEA 生物參考區間訂定為小於 5.55 ng/mL。

**結論：**生物參考區間是臨床判斷健康與否的標準，實驗室必須定期審查生物參考區間是否適用，必要時，實驗室應建立其自己的生物參考區間，以提供臨床醫師作為正確診斷的依據，因此實驗室對於建立生物參考區間工作的意義重大，同時亦可提供給其他實驗室做為參考。

PC-128

## 由 CA19-9 Hook effect 探討 RIA 實驗室之報告審查 一個案報告

張素雲<sup>1</sup> 薛仔婕<sup>1</sup> 廖建國<sup>1</sup> 莊紫翎<sup>1,2</sup>

<sup>1</sup> 佛教慈濟醫療財團法人大林慈濟醫院核子醫學科

<sup>2</sup> 慈濟學校財團法人慈濟大學醫學系

**背景：**IRMA (Immunoradiometric assay) 為 RIA 實驗室廣泛使用之檢驗方法，具有高敏感度、高專一性、測定範圍廣及操作時間短等特性，當待測物質的濃度過高，高到超過了固相上抗體所能夠接合的數目，則可能會發生 Hook effect，造成檢測值偏低，因此在報告審查時就應特別注意，Hook effect 這種情況雖然少見，但是可能影響臨床醫師診斷與治療。

**案例報告：**本院近期有一位胰臟癌之病患，2021 年 8 月 25 日至 2022 年 5 月 18 日之間，固定至本院追蹤 CA19-9 (參考區間： $< 37$  U/mL)，其數值皆落在 59.3~155.06 U/mL 之間變動。此病人於 2022 年 6 月檢驗時，初次報告為 159.01 U/mL，醫檢師懷疑可能有升高之趨勢，於是再進行稀釋及檢測，此批號 CA19-9 最高濃度為 255 U/mL，10X 稀釋後數值  $> 2550$  U/mL，而證實是 Hook effect，再進一步稀釋及檢測正確數值為  $> 255000$  U/mL。

**討論：**1993 年 Cole 等人研究指出，建議可以將待測檢體以 10 個分成一組，再由此檢體中各取小部分等量檢體混合，做成稀釋 10 倍之檢體，一起與原倍檢體進行同一批次之檢測，可以有效偵測 Hook effect，但在臨床實際操作和成本考量上有其困難性。本實驗室例行作業時，利用試劑內最高濃度之 80% 為篩選之標準，幾乎可有效偵測 Hook effect 之病患，但此方法若應用在此病患就無法查覺，若將篩選標準降低為試劑內最高濃度之 60%，便可大幅提升偵測 Hook effect 之效率。

**結論：**針對 CA19-9 及 CA125、AFP 等較容易發生 Hook effect 之項目，原實驗室利用試劑內最高濃度之 80% 為篩選標準，做例行性的複驗，若將篩選標準降低為試劑內最高濃度之 60%，便可大幅提升偵測 Hook effect 之效率。對於檢體量不大的實驗室，這是一個有效的變通方法。

PC-129

## CA125 不同廠牌 RIA 試劑檢驗結果之相關性

黃筱歲<sup>1</sup> 張素雲<sup>1</sup> 薛仔婕<sup>1</sup> 廖建國<sup>1, 1,2</sup> 莊紫翎

<sup>1</sup> 佛教慈濟醫療財團法人大林慈濟醫院核子醫學科

<sup>2</sup> 慈濟學校財團法人慈濟大學醫學系

**背景：**實驗室可能因試劑停產或招標因素而更換不同廠牌之試劑，為符合認證要求，認證實驗室皆會依據 ISO15189 5.6.4 檢驗結果的可比較性之要求，進行新舊試劑的比對。本研究目的即為比對 CA125 不同廠牌 RIA 試劑檢驗結果之相關性，以查證新試劑是否適用。

**方法：**收集病人檢體，分別使用舊廠牌 (CISBIO ELSA-CA125 II) 以及欲更換之新廠牌 (Beckman Coulter/Immunotech IRMA CA125 antigen) 試劑進行檢測，依原廠試劑說明書操作流程進行操作。兩者方法皆為 IRMA 原理，參考值略有不同 (舊試劑： $<35$  U/mL；新試劑： $<31.2$  U/mL)，均使用同一加馬計數器進行計數。獲得兩組檢驗結果後，再使用 Excel 軟體進行線性回歸分析，以得知其相關性及  $r^2$  值等數據，並判定新試劑品質是否可接受 (允收標準為  $r^2 \geq 0.95$ )。

**結果：**總計收集 30 支病人檢體，CA125 檢驗值介於 6.8~245.08 U/mL 間。由於檢驗值大於正常參考值 ( $<35$  U/mL) 之異常檢體取得較為困難，因此收集之異常檢體合計 9 支，其餘 21 支皆為正常檢體。兩組不同廠牌之檢驗結果，經線性回歸分析得知其相關性公式為  $y = 0.8371x - 1.7755$ ， $r^2$  值為 0.9754，符合允收標準，顯示新試劑之品質可接受。

**結論：**比對舊廠牌 (CISBIO ELSA-CA125 II) 試劑與新廠牌 (Beckman Coulter /Immunotech IRMA CA125 antigen) 試劑之相關性，結果顯示兩組試劑檢驗結果呈現高度相關，表示新試劑品質符合要求。RIA 實驗室應建置不同廠牌試劑之比對機制，以符合 ISO15189 的國際標準。

PC-130

## 實習醫事放射師期刊教學與導讀—經驗分享

陳保良<sup>1,2</sup> 許幼青 陳薇璇<sup>1</sup> 莊紫翎<sup>1,3</sup>

<sup>1</sup> 佛教慈濟醫療財團法人大林慈濟醫院核子醫學科

<sup>2</sup> 佛教慈濟醫療財團法人大林慈濟醫院醫學研究部

<sup>3</sup> 慈濟學校財團法人慈濟大學醫學系

**背景：**實習醫事放射師，於各科實習期間均需要期刊報告，但學生於在學期間口頭報告甚少，因此為了使學生了解期刊的選擇方式、期刊呈現架構與簡報製作方式等。因此本篇文章將介紹本科多年來期刊教學與導讀經驗分享，提供給大家參考。

**期刊選擇教學：**我們先以簡報檔方式先講解論文型態（學位論文、研討會論文、期刊論文），論文種類（原著、病例報告、有趣影像、綜論）。再實際利用院內購買的期刊外，或根據學所屬的學校，教導學生如何進入學校圖書館進行期刊查找及選擇。也教導學生如何利用 PubMed 網站進行期刊查找及挑選。

**期刊架構講解：**當學生確定某篇期刊後，我們會依序介紹論文架構，包括，首頁（包刮：期刊名稱、作者、卷期、頁碼），段落（包刮：摘要、簡介、研究目的、材料方法、統計方式、結果、討論、研究限制、結論、參考文獻），依序介紹文章中每段落的撰寫目的與為何要呈現的方式。

**簡報製作教學：**簡報製作我們科是以精簡為原則，要注意字型、字體大小、顏色、背景、對齊或同位素藥物的正確寫法等重要的細節，也可以引導學生從基礎醫學（解剖、生理、病理、藥物）開始講起延伸到文章的內容。

**期刊導讀教學：**當學生製作完簡報後，我們利用預報的方式找出學生在閱讀文章中的問題，並且從中直接修正，也引導學生從問與答中去模擬正式報告時要如何回答問題。

**結論：**雖然這樣的作法學生與老師們會花較多的時間，但我們認為學生未來在挑選期刊或製作簡報會比較熟悉，也會比較快速了解文章的架構與內容呈現的方式。

PC-131

## 導入 EPAs 的教育模式於新進人員教育訓練 一個案報告

許幼青<sup>1</sup> 廖建國<sup>1</sup> 陳薇璇<sup>1</sup> 莊紫翎<sup>1,2</sup>

<sup>1</sup> 佛教慈濟醫療財團法人大林慈濟醫院核子醫學科

<sup>2</sup> 慈濟學校財團法人慈濟大學醫學系

**背景介紹：**可信任專業活動 (Entrustable Professional Activities, EPAs) 是現階段邁向以勝任能力為成果的最佳醫學教育模式，可以讓學員在過程面及結果面中被信任以及放心獨力完成所有醫療行為，同時會根據被監督的等級來決定勝任的表現。EPAs 和傳統單獨只有執行筆試、口試或者是 DOPS…等教學評量方法比較，EPAs 主要是以整體性與統合性的角度去評估學員，所以可以更清楚了解學員的能力到哪裡，教師可以信賴學員的程度，將 EPAs 評核運用在臨床上，可以提升教師和學員彼此之間的信任感，同時也可以提高影像品質和提升病人安全。

**個案報告：**本科目前無學員，故請一位新進同仁模擬進行 EPAs 評核，評核單光子斷層造影檢查 (SPECT) 時，有一名 53 歲風濕性關節炎的患者，右腿局部壓痛，醫師高度懷疑骨髓炎，故安排三相全身骨骼掃描，在執行檢查時，新進同仁發現患者無法平躺，不知道該如何執行檢查，故新進同仁快速找到監督者協助幫忙，完成血流相和血池相檢查，前兩相結束後，教師和新進同仁進行討論後續的骨骼掃描該如何執行，讓新進同仁獨立操作完成其檢查項目，但由於在執行胸部的部分，新進同仁員採用腳高頭低或頭高腳低的方式，發現仍然無法造影到胸部，故仍找監督者協助幫忙，監督者當場指導新進同仁採用側位方式進行前後胸部攝影來完成所有檢查。

**結論：**傳統單獨的評核方式，只能單一片段無法全盤性的瞭解學員實際學習狀況，但 EPAs 可以整體性與統合性的評估學員的詳細情形，除此之外可以根據學員的能力及程度來增加其難度風險或複雜度等。導入 EPAs 於教學中，可以增加學員和教師之間的信任程度，甚至於教師可以非常清楚學員程度來加以訓練，讓學員能成為臨床的優秀人員。

PC-132

## 由全身骨骼掃描輸血事件 探討病人檢查過程中之照護安全一個案報告

王苡安<sup>1</sup> 陳保良<sup>1,2</sup> 廖建國<sup>1</sup> 莊紫翎<sup>1,3</sup>

<sup>1</sup> 佛教慈濟醫療財團法人大林慈濟醫院核子醫學科

<sup>2</sup> 佛教慈濟醫療財團法人大林慈濟醫院醫學研究部

<sup>3</sup> 慈濟學校財團法人慈濟大學醫學系

**背景：**全身骨骼掃描，乃利用放射性同位素鎝 亞甲基二磷酸鹽 (<sup>99m</sup>Tc-MDP) 在人體內骨頭分布之特性，藉由伽瑪閃爍攝影機來擷取影像，評估骨骼病變之相關疾病。全身骨骼掃描可用來癌症患者骨頭轉移及骨科病人疼痛位置評估，對臨床醫師來說有很高的參考價值。癌症患者面臨血紅素低，骨科患者面臨術後有輸血的必要。近期患者到本科進行骨骼掃描檢查時，正在輸血，由於輸血反應嚴重時，極可能影響到生命安全，故本文目的在探討患者在輸血過程中，護理同仁需扮起那些照護安全的角色，故提出分享。

**個案報告：**介紹一位 58 歲女性，高血壓、糖尿病病史。2021 年 11 月右乳癌全乳切除，病理顯示為惡性，分期為 T4bN1M0 (stage IIIB)。目前住院接受第六次化療，疫情關係，無家屬照顧。住院期間患者 Hb 指數為 5.6 g/dL (正常女性 12 g/dL) 加上抱怨雙下背痛，故主治醫師安排了輸血及全身骨頭檢查。患者 13:20 進入本科時，躺床輸血中，顯得虛弱，檢查結束，血品也剛好滴完，護理師立即關掉血品，改滴 0.9% 生理食鹽水，患者無任何不舒服，約 14:10 由輸送人員接回病房。輸血常見反應症狀有輕度、中度、重度，皆可能會發生，因此，輸血患者從一進本科我們就要開始針對輸血患者進行身體評估，若有發熱或發冷，護理人員必須監測體溫，必要時給予烤燈或冰枕。若有蕁麻疹 / 過敏時，向患者說明骨頭掃描時，身體是不能動的，如果覺得身體越來越癢，請用嘴巴說，必要時連絡主治醫師給予過敏藥物使用。若有呼吸困難、低血壓、胸痛，護理人員應立即停止輸血改 0.9% 生理食鹽水滴注，科內血壓計、血氧機、氧氣皆備在患者檢查台旁邊，有需要應立即給予患者用上並連絡核醫主治及在患者檢查單備註科內發生的事情並知會病房主護及主治醫師。骨骼掃描完畢，輸血患者在科內量最後一次生命徵象 (Vital Sign) 正常及身體沒有任何不舒服即可回病房。

**結論：**輸血不良反應並非每個人都會發生，但嚴重時卻會致命，故護理人員一定要隨時注意輸血患者的狀況，以維護病人的照護安全，提升整體醫療品質。

PC-133

## 上下肢淋巴閃爍攝影之皮下注射施打方式 及改善之探討

王苡安<sup>1</sup> 陳保良<sup>1,2</sup> 廖建國<sup>1</sup> 莊紫翎<sup>1,3</sup>

<sup>1</sup> 佛教慈濟醫療財團法人大林慈濟醫院核子醫學科

<sup>2</sup> 佛教慈濟醫療財團法人大林慈濟醫院醫學研究部

<sup>3</sup> 慈濟學校財團法人慈濟大學醫學系

**背景：**淋巴閃爍攝影是使用一種大分子的核醫藥物 <sup>99m</sup>Tc-phytate，這種藥物經皮下注射後會經由淋巴系統進入淋巴結再回到循環，因此可用來做淋巴攝影，就本院而言上肢淋巴水腫通常在乳癌術後常見；下肢淋巴水腫則在婦科癌症或電療患者身上容易發生。本研究目的在探討本科以皮下注射施打後，五分鐘影像呈現是否有打到血管，來做為討論及改善。

**方法：**從 2021 年 9 月至 2022 年 1 月收集淋巴閃爍攝影之個案，施打方式為，一位護理人員負責施打，使用 1 c.c. 空針，施打 4 支，每支 1 mCi，上肢淋巴以皮下注射方式打在左右上肢第二及三指縫；下肢淋巴以皮下注射方式打在左右下肢第二及三趾縫，皆不反抽，皆從患肢打起。皮下施打方式是針頭斜面向上，與皮膚呈 30-40 度，快速刺入皮下。

**結果：**共收集 33 患者，經過核醫主治醫師判讀後，從五分鐘影像得知有 9 位是有打到血管的，比率占 27%，其中有打到血管的影像與未打到血管的影像明顯不同，打到血管的比例似乎比預期還要高，可能的原因有 1. 技術方面問題：下針深度過深、過淺。2. 患者生理或病理問題：太胖或太瘦、躁動、水腫厲害，深度無法辨識。3. 患者心理問題：害怕注射、容易緊張。4. 其他因素問題：年紀太大，無法配合。其中患者躁動或害怕而打到血管判斷為主要的因素。

**結論：**皮下注射對患者來說是真的很痛很不舒服，護理人員施打前給予說明及衛教，能減輕患者的焦慮與不適，患者如果還是焦躁不安，建議由一位護理人員施打，另一位同仁負責安撫或壓制，以利完成此項檢查，降低打到血管比率，提升整體醫療品質。

PC-134

## Comparison of the Effective dose and Convenience of Clinical Work Between the Inflammation Scans of $^{67}\text{Ga}$ -Citrate and $^{18}\text{F}$ -FDG

Chih-Yi Wu<sup>1</sup>, Li-Yu Chen<sup>1</sup>, Ya-Ting Huang<sup>1,2</sup>, Ya-Yao Huang<sup>1,3</sup>

<sup>1</sup>*Primo Biotechnology Co., Ltd, Taipei, Taiwan.*

<sup>2</sup>*Department of Medical Education and Research, Camillian Saint Mary's Hospital*

<sup>3</sup>*Molecular Imaging Center, National Taiwan University, Taipei, Taiwan.*

**Introduction:**  $^{67}\text{Ga}$ -Citrate is routinely used for inflammation scan with scintillation camera in Taiwan. Typically, patients receive 4~6 mCi of  $^{67}\text{Ga}$ -Citrate injection and then the scan will be performed at 48 hours post administration. As needed, the patient has to come back again for an another scan as the comparison images at 72 hours post administration. Thus, the lengthy and patient-unfriendly procedure accompanied by high radiation doses has been the major drawback for the whole inflammation scan procedure of  $^{67}\text{Ga}$ -Citrate. In the other hand,  $^{18}\text{F}$ -FDG has been widely used for inflammation scan with the well diagnostic ability and a friendly 3~4 hour scan protocol.  $^{18}\text{F}$ -FDG inflammation scan not only can acquire the PET/CT or PET/MRI images with good image qualities, also can achieve the patient's low effective dose compared to  $^{67}\text{Ga}$ -Citrate inflammation scan.

**Methods:** We will compare the flexibility and price ratio (drug Price / NHI benefits) between  $^{67}\text{Ga}$ -Citrate and  $^{18}\text{F}$ -FDG in the inflammation scan based on the US SNM guideline and EANM guideline. Also, we will use the EANM dosage card to evaluate the effective dose of 30 kg 5 y/o children and adult performed with  $^{67}\text{Ga}$ -Citrate and  $^{18}\text{F}$ -FDG inflammation scan, respectively.

**Results:** The  $^{18}\text{F}$ -FDG inflammation scan protocol is more convenience and even can achieve better quality images than that of  $^{67}\text{Ga}$ -Citrate inflammation scan. There is similar price ratio of  $^{18}\text{F}$ -FDG inflammation scan (65%) and  $^{67}\text{Ga}$ -Citrate inflammation scan (45~70%). But, the effective doses of  $^{18}\text{F}$ -FDG of child and adult (9.95 mSv and 7.03 mSv, respectively) are significantly lower than  $^{67}\text{Ga}$ -Citrate inflammation scan of child and adult (15.36 mSv and 26.64 mSv, respectively). Moreover, the attenuation and localization procedures of CT during both SPECT/CT and PET/CT imaging will increase 1 mSv of the radiation dose of patients.

**Conclusions:** The  $^{18}\text{F}$ -FDG inflammation scan is much more convenience than  $^{67}\text{Ga}$ -Citrate inflammation scan for patients, let alone the high image quality and the low effective dose. For the nuclear medicine departments with PET scanner(s),  $^{18}\text{F}$ -FDG definitely has the potential to be the first radiodiagnostic option used for clinical inflammation scan as the corresponding good healthcare examination quality and a low personal radiation dose, especially for pediatric patients.



PC-135

## 新冠疫苗注射部位攝取氟 -18 去氧氟化葡萄糖之案例報告

吳麗君 顏玉安 李將瑄 (通訊作者)

奇美醫療財團法人奇美醫院

**簡介：**接種新冠疫苗的常見副作用之一為注射部位疼痛，這些疼痛反應包括紅斑、硬結和壓痛，這些反應通常會在接下來的 4 到 5 天內消退。氟 -18 去氧氟化葡萄糖 (FDG) 在炎症或感染部位，會顯示 18F-FDG 積累增加。

我們報告兩例，在執行全身 PET (含手腳) 時，意外發現手臂上有 FDG 攝取，但是生理檢查並無異狀。回溯該病人 3 個月前，同部位有注射新冠疫苗，其中有一人同側的腋下淋巴結有 FDG 攝取，推測為新冠疫苗後有持續性發炎反應。因為意外發現，與病人本身疾病無關，無法取得病理切片報告，但經追蹤，病人均無異狀，且病人為癌症病人，不會特地回來做 PET，所以無法得知該處是否維持慢性發炎或攝取，但可得知有些人注射新冠疫苗會持續影響注射部位及腋下淋巴結造成 FDG 攝取長達 3 個月以上。

### 病例報告：

#### Case1

一位 58 歲男性鼻咽癌病人，因懷疑復發安排 PET，檢查前 3 個月施打莫德納疫苗第一劑，注射部位為左手臂。在初期全身 PET/CT 影像顯示左上臂有局部 FDG 攝取，其腋下也有淋巴結攝取，與新冠疫苗注射部位相同，病人左上臂外觀並無異樣，推測為施打新冠疫苗後的持續性發炎反應。

#### Case2

一位 35 歲男性淋巴癌病人已化療，因懷疑復發安排 PET 檢查，檢查前 3 個月有施打新冠疫苗，注射部位為左手臂。在初期全身 PET/CT 影像顯示左上臂有局部 FDG 攝取，與新冠疫苗注射部位相同，病人左上臂外觀並無異樣，推測為施打新冠疫苗後的持續性發炎反應。

**結論：**此二病例並非罕見，本院執行全身掃描有包含手腳，才會偶然發現，所以若其它醫院掃軀幹 PET (Torso imaging)，不包括手腳，從顱底掃至大腿中段，這樣就不會看見此現象。所以在全身 PET 上有顯示手臂上或腋下淋巴結有 FDG 攝取，可回溯病人是否有接種新冠疫苗的紀錄並詢問注射部位，可排除偽陽性。故得知有些人在新冠疫苗注射的部位會持續發炎，以及腋下淋巴結有 FDG 攝取，甚至持續 3 個月以上。

PC-136

## 利用第二次局部延遲像排除腸道 有意外發現的局部 FDG 攝取一案例報告

吳麗君 顏玉安 李將瑄 (通訊作者)

奇美醫療財團法人奇美醫院

**簡介：**在接受 PET/CT 的患者中，大約 1.3-3% 的患者在腸道中意外發現 18F-FDG 局部性攝取，胃腸道 FDG 攝取增加的機制尚不清楚，但可能是腸道生理、炎症、良性 (癌前病變) 或惡性，所以意外發現腸道中的局部 FDG 攝取，不應將其視為生理性攝取，有可能為癌前病變或癌症，其比例佔 54-70%，所以在 PET/CT 掃描發現腸道中的局部 FDG 攝取，必須施行大腸鏡。但是我們也注意相對有 30-46% 的病人不需要做大腸鏡，如何才能鑑別真正病灶，降低不必要的侵入性檢查，是需要進一步去研究的。

我們報告一病人，在初期像及延遲像中，在腸道有意外發現的 18F-FDG 局部性攝取，而且 SUVmax 值增加 (6.15 升到 8.38)，並且在 CT 上相對位置有一團軟組織，但在第二次局部延遲像時原先的病灶攝取消散，SUV 值減少 (4.15)，顯示此病灶為偽陽性，屬正常生理腸道，可避免不必要的大腸鏡，故特此提出報告。

**病例報告：**一位 59 歲男性病人，經上消化道鏡及病理證實為食道癌，為癌症分期安排 PET/CT 檢查。初期像顯示在腹部腸道有局部 FDG 攝取，延遲像顯示此處 FDG 攝取增加並且 SUVmax 值增加 (6.15 升到 8.38)，在 CT 上相對位置顯示有一團軟組織，在第 2 次局部延遲像顯示此病灶消散成兩處且 FDG 攝取減少 (SUV max 4.15)，故判讀為偽陽性。

**結論：**當遇到 PET/CT 的腹部腸道有局部 FDG 攝取，在延遲相發現 FDG 攝取增加，可照第二次局部延遲像再次確認，則可排除偽陽性。

PC-137

## COVID-19 確診公布人數與門診開單量之相關性研究 —以南部某醫院核醫科為例

曾宜玲 卓世傑 顏吉龍 張朝鈞 張淑芬 段淑薰 李將瑄

奇美醫療財團法人奇美醫院核子醫學科

**背景介紹：**台灣自 2020 年 1 月 20 日即由疾管署宣布成立「嚴重特殊傳染性肺炎中央流行疫情指揮中心」，以全面防範 COVID-19 此種全球大流行之新興傳染病。並於同年 2 月 27 日，升至最高等級之一級開設。因此隨著疫情起伏，由中央流行疫情指揮中心每日公布的確診人數，也成為台灣民眾極其關注的焦點，並似乎影響了民眾的許多決策行動，包括減少外出用餐等情況。不過，對於攸關病情的醫療檢查，每日公布的確診人數究竟有無影響，卻尚未有足夠之研究進行探討。事實上，若能提早預知是否相關，對於檢查單位之人力調度是有積極幫助的。

**方法：**1. 由「台灣疫情報告」網站（數據來源為衛福部疾管署），下載 2022 年 1 月 1 日至 2022 年 7 月 1 日之全國、台南市及永康區（醫院所在縣市與地區）等三種每日公布確診人數資料。2. 自南部某醫院電腦系統，下載自 2022 年 1 月 3 日至 2022 年 6 月 30 日之門診核醫科檢查每日開單量資料，並分為含週六半日門診與不含週六半日門診之兩類資料。3. 將公布確診日視為 D 日，並分別以 D+1 日，D+2 日及 D+3 日之該日門診開單量資料，與 D 日之三種確診人數資料進行相關性統計，未有門診開單量資料之確診日資料均予以刪除。

**結果：**1. 台灣全國每日公布之確診人數，大約自 4 月初起快速增加，而台南市與永康區也大致開始每日均有確診人數，但全國、台南市及永康區每日公布之確診人數，則差異極大。2. 台灣全國 D+1 日，D+2 日及 D+3 日公布之確診人數與含週六半日門診開單量資料之相關性分別為 -0.242、-0.153、-0.264，不含週六半日門診開單量資料之相關性則為 -0.308、-0.163、-0.334。3. 台南市 D+1 日，D+2 日及 D+3 日公布之確診人數與含週六半日門診開單量資料之相關性分別為 -0.121、-0.003、-0.212，不含週六半日門診開單量資料之相關性則為 -0.173、0.067、-0.219。4. 永康區 D+1 日，D+2 日及 D+3 日公布之確診人數與含週六半日門診開單量資料之相關性分別為 -0.082、0.014、-0.096，不含週六半日門診開單量資料之相關性則為 -0.080、-0.002、-0.055。5. 負相關地區之高低依序為全國、台南市、永康區。6. 負相關日期大小依序為 D+3 日，D+1 日及 D+2 日。

**結論：**本研究發現，每日公布之確診人數與南部某醫院核醫科門診開單量之相關性，大致均為負相關，最明顯的為全國 D+3 日不含週六之 -0.334。所以如再有類似事件發生，各單位或可參考本研究之結果，酌量配置人力。

PC-138

## 甲狀腺攝取計數儀連續或間斷執行 QC 作業 對卡方檢定項目影響之研究

梁育雅 卓世傑 陳興隆 張南雄 林凡珍 顏玉安 李將瑄

奇美醫療財團法人奇美醫院核子醫學科

**背景介紹：**核子醫學部門經常使用甲狀腺攝取計數儀，執行病人甲狀腺攝取率的檢查。為確保甲狀腺攝取計數儀之檢查結果正確，在使用前必需使用標準射源及內部程式進行必要之 QC 作業。再以卡方檢定 (Chi-square Test)，測試甲狀腺攝取計數儀計數值之穩定性。但因甲狀腺攝取計數儀未必每日皆執行 QC 作業，所以連續或間斷執行 QC 作業，對卡方檢定項目是否造成影響，是頗值得探討且較少相關研究的問題。本研究即為針對「甲狀腺攝取計數儀連續或間斷執行 QC 作業對卡方檢定項目影響之研究」。

**方法：**1. 以 Capintec, Inc. 公司生產之 CAPTUS 4000 型，甲狀腺攝取計數儀，及 Eckert & Ziegler 公司生產之 GF-0008 型，Cs-137 射源以及 GF-0009 型，Eu-152 射源 執行連續或間斷之每日 QC 作業。2. 每次連續或間斷 QC 作業合格後，執行 3 次卡方檢定 (計數 10 次，每次 1 分鐘)，並記錄各該 3 次卡方檢定值數據。3. 整理、統計連續或間斷之各該 3 次卡方檢定值數據，以提出結果。

**結果：**1. 連續執行之每日 QC 作業為 136 日，並分為第 1、第 2 與第 3 次等 3 組，共 408 筆卡方檢定資料，間斷執行之每日 QC 作業則為 77 日，也分為第 1、第 2 與第 3 次等 3 組，共 231 筆卡方檢定資料。2. 連續與間斷 QC 作業後之 6 組卡方檢定資料中，其標準差最大為 5.1，最小則為 4.5，中位數最大與最小分別為 9.0、7.1，平均值最大則為 9.8，最小則為 8.9，而 6 組中，眾數最高為 11.3，最低則為 3.2，另最大值中，最高為 31.7，最低為 22.6，至於最小值中，最高為 3.0，最低為 0.6。3. 連續 QC 作業後之 3 組卡方檢定資料中，其第 1 與 2 次之相關係數為 -0.068，第 2 與 3 次之相關係數為 0.038，第 1 與 3 次之相關係數則為 0.025；而間斷 QC 作業後之 3 組資料，其第 1 與 2 次，第 2 與 3 次及第 1 與 3 次之相關係數則分別為 -0.115、-0.060 與 -0.046。

**結論：**本研究發現，甲狀腺攝取計數儀每日品質程序，無論是連續或間斷實施，對之後執行之卡方檢定項目，似乎並無明顯影響，顯示甲狀腺攝取計數儀可能並無需每日均進行品質程序，亦可維持卡方檢定之穩定。

PC-139

## 鐳 223 藥劑注射後輻射劑量率之偵測研究 —以南部某醫院核醫科為例

陳育吟<sup>1</sup> 卓世傑<sup>2</sup> 張南雄<sup>2</sup> 陳興隆<sup>2</sup> 林凡珍<sup>2</sup> 顏玉安<sup>2</sup> 李將瑄<sup>2</sup>

<sup>1</sup> 奇美醫療財團法人奇美醫院泌尿外科

<sup>2</sup> 奇美醫療財團法人奇美醫院核子醫學科

**背景介紹：**鐳 223 (Radium-223) 治療藥劑，目前多使用於去勢抗性攝護腺癌 (castration-resistant prostate cancer, CRPC) 之治療。因為法規及實務上的需要，注射後之廢料存放之輻射防護問題，為核子醫學科必須負責處理之課題。針對注射前調配與注射時之輻射防護問題等相關討論，已有許多的研究與成果，但鐳 223 治療藥劑注射後之輻射劑量率研究，則較為稀少。由於鐳 223 治療藥劑注射後即屬於廢料，需進行儲放。對於儲放而言，鐳 223 仍會產生少量  $\beta$  粒子及  $\gamma$  射線 ( $\alpha$ 、 $\beta$ 、 $\gamma$  發射能量比例：95.3、3.6、1.1) 所引起的輻射劑量，應是更需關注的焦點。

**方法：**1. 收集南部某醫院核醫科，自 2021 年 8 月 19 日至 2021 年 10 月 27 日止，共 15 劑注射後鐳 223 治療藥劑之相關紀錄，每劑 4 筆，共 60 筆資料。2. 以 CRC-PC Smart Chamber 型活度校正儀，測偵注射後之藥劑活度值並記錄。3. 以 Inspector 型蓋格式偵檢器，測偵距離 30 cm 及 100 cm 處之放置於原藥劑屏蔽內的注射後藥劑之輻射劑量率並記錄。4. 以 Inspector 型蓋格式偵檢器，測偵距離 30 cm 處，無屏蔽的注射後藥劑之輻射劑量率並記錄。

**結果：**1. 藥劑活度平均值為 37.36  $\mu\text{Ci}$  最大值為 93.16 最小值為 8.33  $\mu\text{Ci}$ 。2. 距離 30 cm 處無屏蔽藥劑含背景值之輻射劑量率最高與最低分別為 10.08 及 1.75  $\mu\text{Sv/h}$ ，平均為 4.00  $\mu\text{Sv/h}$ 。3. 距離 30 cm 處有屏蔽藥劑含背景值之輻射劑量率最高為 0.55，最低為 0.15  $\mu\text{Sv/h}$ ，平均為 0.27  $\mu\text{Sv/h}$ 。4. 距離 100 cm 處有屏蔽藥劑含背景值之輻射劑量率最高為 0.22，最低為 0.08  $\mu\text{Sv/h}$ ，平均為 0.15  $\mu\text{Sv/h}$ 。5. 藥劑活度值與距離 30 cm 處無屏蔽藥劑之回歸式為  $0.088X + 0.714$ ， $R^2$  為 0.943，與距離 30 cm 處有屏蔽藥劑之回歸式為  $0.005X + 0.090$ ， $R^2$  為 0.863，與距離 100 cm 處有屏蔽藥劑之回歸式為  $0.001X + 0.121$ ， $R^2$  為 0.149，其  $R^2$  值依序遞減，顯示藥劑活度產生之輻射劑量值於無屏蔽及近距離之情形，遠高於有屏蔽及遠距離之值。

**結論：**本研究之回歸式顯示，屏蔽與距離仍是注射後鐳 223 藥劑輻射防護的關鍵，且由於注射後鐳 223 藥劑其 30 cm 處無屏蔽之輻射劑量率，最高與平均值仍有 10.08 及 4.00  $\mu\text{Sv/h}$ ，所以作業時仍應注意盡量勿將藥劑移出屏蔽，以減少輻射劑量。

PC-140

## RIA 廢水變更儲存作業方式之分享 —以高雄榮民總醫院的經驗為例

張春梅

高雄榮民總醫院核子醫學科

**背景介紹：**同位素治療病房前置作業，新增放射免疫分析實驗作業場所 RIA- 實驗室 (3) 非密封作業場所，原大樓地面下的 RIA 廢水槽永久停止使用。

**方法：**第一階段進行非密封作業場所輻射安全評估乙次，包括核醫科 RIA 廢水變更作業流程及舊 RIA 廢水槽除污計畫。第二階段進行非密封放射性物質場所輻射安全測試，實際測量及報告、工程 案會議、現場勘查及圖面討論會議。第三階段進行物理性破壞原有廢水排放管路，包括核 3 個廢水槽進(出)水閥、核廢料室、製藥室、熱核室及 RIA 實驗室水槽，並配合原子能委員會線上審查。

**結果：**建置同位素病房，動工前 9-12 個月，先進行 RIA 廢水變更儲存作業方式，以因應廢水槽改建，廢水桶使用、儲藏、分析及排放，皆符合游離輻射防護法管制標準。

**結論：**RIA 廢水槽停用，儲存方式改為廢水桶，除了醫事人力工作負荷增加外，管理放射性廢水之困難度，也提升不少。建置智能化廢水槽管理系統，必有助於推展核醫治療及檢查業務。

PC-141

## 中部某區域教學醫院更換鈷 -57 平板射源經驗分享

張添信 陳慶元

佛教慈濟醫療財團法人台中慈濟醫院核子醫學科

**背景介紹：**伽瑪單光子造影設備，必須每日測試影像均勻度 (Uniformity) 為臨床檢查前的例行作業，絕大部分的核子醫學科都會使用鈷 -57 (Co-57 sheet sources) 密封式平板射源來測試造影設備當日均勻度情況，以進一步了解機器設備可否進行臨床檢查，鈷 -57 與核醫常用藥物鎝 ( $^{99m}\text{Tc}$ ) 能峰接近 122 keV 和 140 keV，其半衰期為 270 天，劑量選擇約在 10 ~ 15 毫居禮 (mCi) 所以常被選用來校正儀器設備的核種，本篇主要找出新出廠的鈷 -57 平板射源，校正均勻度失敗的原因及如何解決與探討。

**案例報告：**本院於今年進行儀器汰舊換新 (GE NMCT 860)，廠商提供一塊新的鈷 -57 平板型密封射源 15 毫居禮，並經過輻防擦拭測驗通過標準，設備工程師使用平板射源測試每日影像均勻度，均無法達到儀器設備規定容許度  $\leq 5\%$ ，無論是使用造影區域 (UFOV) 或中心點造影區域 (CFOV) 皆無法達到機器要求數值，但改用鎝的點射源進行測試則設備表現正常範圍數值 1~2% 區間，表示機器設備均勻度尤佳，每日均勻度校正測試時，在收集一張影像為 4000k Counts (計數率) 即會停止收集光子數，新機種的 SPECT/CT 有提供專用平板射源放置架，在放置平板射源有固定放置位置，測試多次新平板射源放置發現有一面固定方向是可以通過均勻度在  $\leq 5\%$  範圍內，其他面或轉方向則無法通過均勻度容許值，經測試多次，最後找出平板射源最佳放置方向並貼上記號與放置架定位，其後皆正常通過均勻度容許值。

**結論：**剛出廠新的鈷 -57 平板型密封射源因射源內含有鈷 -56 (半衰期 77 天) 與鈷 -58 (半衰期 71 天)，且其能峰皆屬於中高能與鈷 -57 的 122 keV 相差甚遠又使用準直儀為低能量專用，也就因為鈷的其他同位素雜質過多，導致影像均勻度容許值一直無法通過，在初始測試時當無法通過均勻度，可以多測試轉面或上下前後面測試，會有一面的雜質可能較少或平均則可以通過均勻度測試，並施作記號以利後續每日量測使用，等待約莫 2 個月後鈷 -56 與鈷 -58 衰敗過程時，剩整塊平板型密封射源也會趨近穩定成鈷 -57。

PC-142

## The Imaging Pattern of Pre-capillary Pulmonary Hypertension in Tc99m MAA Perfusion Scintigraphy by SPECTCT Technique

Yu-Wen Chen<sup>1,4</sup>, Chun-Yuan Chu<sup>2,4</sup>, Tsung-Hsien Lin<sup>2,4</sup> Zen-Kong Dai<sup>3,4</sup>

<sup>1</sup>*Department of Nuclear Medicine*

<sup>2</sup>*Division of Cardiology*

<sup>3</sup>*Department of Internal Medicine, Division of Cardiology*

<sup>4</sup>*Department of Pediatric, Kaohsiung Medical University Hospital, School of Medicine  
Kaohsiung Medical University, Kaohsiung, Taiwan*

**Purpose:** Newly definition of pulmonary hypertension (the 7<sup>th</sup> ESC) is the mean pulmonary artery pressure is over 20 mmHg, PCWP less (or over) 15 mmHg and PVR over 2 wood unit. There are five category of pulmonary hypertension as primary pulmonary hypertension, left heart related pulmonary hypertension (the most common), lung disease related pulmonary hypertension, chronic thromboembolic pulmonary hypertension (CTEPH) and the others. Among them, primary (group 1) and chronic thromboembolic type (group 4) are belong pre-capillary entity. Tc99m MAA lung perfusion scintigraphy is the choice method to identify pre-capillary pulmonary flow distribution in the diagnosis of CTEPH algorithm. In this study, we discriminate imaging pattern of precapillary perfusion hypertension.

**Patients and Methods:** In here, four female patients (age 14-80 years old), two primary type and two CTEPH, had Tc99m MAA scintigraphy with SPECTCT technique (two with Tc99m DTPA aerosol ventilation imaging).

**Results:** Typically inhomogeneous perfusion, moth-eaten pattern is shown in the patients with primary pulmonary hypertension. Wedge perfusion defects (by PIOPED definition), associated with heterogeneous cluster of perfusion in the rest lung is shown in the patients with CTEPH.

**Conclusion:** Tc99m MAA (a molecular sieve principle) is still a physiological imaging choice to provide high sensitivity to evaluate the pulmonary perfusion distribution, under pulmonary hypertension with or without thrombotic occlusion, even challenge of newly dual energy CT technique.



PC-143

## 探討數位式 PET/CT 對於頭頸癌病患 進行快速掃描的可能性

陳詩媽<sup>1,2</sup> 詹勝傑<sup>1,3</sup> 施宜伶<sup>5</sup> 李家瑋<sup>5</sup> 劉淑馨<sup>1,4</sup>

<sup>1</sup> 佛教慈濟醫療財團法人花蓮慈濟醫院核子醫學科

<sup>2</sup> 花蓮縣醫事放射師公會

<sup>3</sup> 慈濟大學醫學院

<sup>4</sup> 慈濟科技大學醫學影像暨放射科學系

<sup>5</sup> 奇異亞洲醫療設備股份有限公司

**背景：**<sup>18</sup>F-FDG 正子造影檢查是透過 PET/CT 成像系統，偵測葡萄糖在人體內的細胞代謝情形，常用於惡性腫瘤診斷、分期、治療與預後追蹤以及偵測體內發炎。隨著時代的進步，新型數位式 PET/CT 使用 SiPM 探測器取代傳統的光電倍增管，重組技術也不斷進步，使得影像品質大幅提升。過去使用類比式 PET/CT 遇到躁動的病患時，往往無法提供正確影像給臨床醫師做出診斷，雖然數位式 PET/CT 有更好的技術可以縮短造影時間，但如何使這些病患接受快速掃描又能確保影像品質，現今仍沒有確切的證據證明。

**目的：**本實驗為回溯性研究，利用影像後重組，測試數位式 PET/CT 不同掃描時間及影像重組方式，對影像品質和活度參數的影響。

**材料與方法：**15 位頭頸癌病患皆於 GE Discovery MI 上以 List-mode 掃描。以 Q. clear  $\beta$  值 550，時間為 150 秒為參考組，再根據不同掃描時間 (60 秒、90 秒及 120 秒) 和不同 Q. clear 的  $\beta$  值 (550、600、650 及 700) 進行影像重組。本篇研究利用 AW Server 3.2 軟體中 PET VCAR 圈選 SUV 大於 2.5 的 VOI，分析其  $SUV_{mean}$  及 SNR。

**結果：**實驗結果發現，除了在造影時間 120 秒且搭配的  $\beta$  值大於 650 外，降低造影時間不論使用何種  $\beta$  值都會顯著地降低影像的 SNR 值 ( $p < 0.05$ )。 $SUV_{mean}$  值於不同  $\beta$  值及掃描時間無顯著性差異 ( $p > 0.05$ )。

**結論：**本次實驗發現利用數位式 PET/CT 進行快速掃描是可行的，但掃描時間仍不應低於 120 秒且須將 Q.clear 的  $\beta$  值設定在 650 以上，如此便能在不影響影像品質及量化下縮短照相時間。

PC-144

## 鉈 -201 和鎝 -99m MIBI 心肌灌注掃描的選擇： 以病人角度為觀點

黃慧娥 洪佑昇

奇美醫療財團法人柳營奇美醫院核子醫學科

**目的：**心肌灌注掃描在大多數醫院由檢查醫師決定以鉈 -201 或鎝 -99m MIBI 做為追蹤劑。我們希望知道如果病人可以做醫療檢查前的共同決策，對於鉈 -201 和鎝 -99m MIBI 兩者檢查方式會有什麼考量，和傾向以何種追蹤劑最為檢查藥物。

**方法：**我們提供兩種不同檢查各自的特點的資訊給病人，在自己可以選擇檢查藥物的前提下，病人提出自己偏好以鉈 -201 或鎝 -99m MIBI 做為檢查藥物。提供的資訊包括有：檢查流程、施打劑量、等待時間、造影時間、影像品質、藥物半衰期、輻射曝露、對周遭接觸者的影響等。統計 2022 年 5、6 月在本院核醫科接受心肌灌注掃描檢查的部份病人，共 128 位，平均年齡 66.2 歲。其中男性 76 位，平均年齡 64.5 歲，介於 36 至 92 歲；女性 52 位，平均年齡 70 歲，介於 42 至 88 歲。

**結果：**選擇鉈 -201 為檢查方式的有 108 位 (84.4%)，選擇鎝 -99m MIBI 有 6 位 (4.7%)，無意見或兩者皆可接受的有 14 位 (10.9%)。

**結論：**在自己可以選擇檢查藥物的前提下，偏好以鉈 -201 做為檢查方式的病人，遠遠多於選擇以鎝 -99m MIBI 做為檢查方式的病人，而最大的考量因素是檢查總花費時間。

PC-145

## 使用電子 E 化工作車施打核醫藥物， 防止藥物錯誤及病患錯誤

楊士頤 莊穎昌 歐銘凱 李世昌

國立成功大學醫學院附設醫院影像醫學部核子醫學科

**背景介紹：**核子醫學檢查使用放射性核種同位素施打至人體，再由伽瑪攝影機 ( $\gamma$ -camera) 採集 r-ray 和電腦處理成像，所以藥物的施打正確性對核醫檢查來說，是必要的重點。護理師在於不同核醫檢查施打同位素時，往往操之過急，病患同時多人要執行施打藥物，而粗心拿錯了藥物做了施打，導致病患檢查失敗重新排定受檢。

如何簡化流程以及降低施打藥物錯誤；電子 E 化的輔助是一個重要的好工具，E 化作業，系統提示，防止打藥錯誤、病患錯誤。

### 方法：

1. 收集 2018 年至 2019 年的異常事件紀錄 - 病患無如期完成檢查。原因分析：藥物施打錯誤、病患錯誤，針對此兩個主因，做矯正措施，減少錯誤率。
2. 確認藥物正確：設立醫令碼對應之核醫藥物，開立核醫檢查申請單時，紙本檢查單上會有藥物名稱可讓護理師先做確認。
3. 確認病患身分正確給藥：施打前，除了做病患身分辨識 (檢視健保卡 / 自述出生年月日) 外，使用醫院電腦 HIS 門診系統執行 barcode 條碼給藥，刷病患檢查單及藥品 barcode，作為兩方電子身分及藥物核對，當條碼比對不正確則電腦系統以紅色底色提示請勿給藥。
4. 每月品質管理會議分析核醫藥損原因及異常事件通報，是否有因施打藥物錯誤或病患錯誤事件發生作為數據統計監控。

**結果：**於 2020 年完成 E 化設定啓用，結果發現，2018 年藥物錯誤有 2 件，2019 年藥物時間錯誤有 1 件，2020 年藥誤錯誤及病患錯誤的異常事件 0 件。有效的把關減少錯誤，排除藥損的機率，確保病患受檢安全，未被施打錯誤的藥物，完成受檢服務。

**結論：**藉由建立 E 化系統及功能完備的工作車，不僅能提升病患就醫檢查完成率，降低給藥錯誤造成的病患安全，整體呈現 E 化系統提供臨床護理師實質上運用之價值。

PC-146

## 血液中甲狀腺球蛋白 (Thyroglobulin) 自體抗體干擾試驗和試劑更換之評估

曾翠芬 劉怡慶 林秋美 許玉春 楊雅晴 林家揚 張晉銓

高雄醫學大學附設中和紀念醫院核醫部

**背景介紹：**由甲狀腺濾泡上皮細胞分泌之甲狀腺球蛋白 (Thyroglobulin) 其為分子量 660,000 Da 的醣蛋白，為 T4、T3 的前驅蛋白。Thyroglobulin 全由甲狀腺細胞獨自完成因此構成了甲狀腺的特異標記，可做為甲狀腺癌的病人術後追蹤有無復發或轉移。

**方法：**(一) 自體抗體干擾試驗，取 40 支檢體依照試劑說明書之步驟，血清和回收溶液 2 倍稀釋，然後原 40 支檢體和 2 倍稀釋的 40 支檢體分別使用套裝試劑測試 Thyroglobulin 濃度，報告依照其公式做計算。(二) 試劑更換評估，取已使用原廠牌 (CIS) 分析過有報告之檢體 37 支，再利用新廠牌 (Beckman) 試劑重新測驗，分析原理為固相的免疫放射三明治測定法 (IRMA)，使用 2470 Automatic Gamma counter (Wizard<sup>2</sup>)，統計軟體 Microsoft Office Excel 2007，參考值 < 50 ng/mL。

**結果：**(一) 自體抗體干擾試驗的 40 支檢體有 3 支結果小於 80%，依原廠說明書訂定之標準得知本次檢測結果有 7.5% 可能受抗 -Tg 自體抗體干擾。(二) 試劑更換評估新、舊廠牌同測的 37 支血液檢體 Thyroglobulin 的濃度結果其  $R^2 = 0.976$  (P-value 0.225)，新廠牌 (Beckman) 測得的 inter-run、intra-run 之 CV% 分別為 6.54、1.61 (N = 20)，Inkit control 報告是 27.06 & 25.26 ng/mL。

**結論：**(一) 套裝試劑已謹慎的選擇試驗中的單株抗體大幅降低抗 -Tg 自體抗體干擾，但本次的實驗結果有 7.5% (N = 40) 受其影響可能造成報告不正確，受干擾的原報告分別是 < 0.3、1.64 和 23.52 ng/mL，臨床醫學實驗室如果將每支檢體都加做干擾試驗實際上是有困難的，所以這個部分應再深思熟慮解決可能存在的問題。(二) 依據本實驗室訂定新試劑的允收標準本次的測試結果二廠牌套裝試劑其報告的相關性  $R^2$  已大於 95% (P-value > 0.05)，且 inter-run、intra-run 之 CV% 也小於原廠測試的 6.6% 和 4.8%，Inkit control 允收為  $23.2 \pm 7.4$  ng/mL，就以上統計結果將 Thyroglobulin 體外放射免疫法試劑更換成同分析原理的新廠牌是可行的。

PC-147

## TSH 在不同轉速下結果之比較

盧永承

嘉義基督教醫院核子醫學科

**背景介紹：**因 2017 年 5 月，歐盟官方期刊 (Official Journal of the European Union) 正式發佈了歐盟體外診斷醫療器材法規 (IVDR)，預計今年 5 月施行以取代體外診斷醫療器材指令 (IVDD)，製造商需更新技術文件和流程以滿足新法規更嚴格的要求，導致原有試劑製造商供應中斷。在尋找其他替代方案時發現 IZOTOP 廠牌的 TurboTSH 放射免疫分析，其震盪培育只需 30 分鐘，大大縮減反應時間，而原廠說明書建議培育應以轉速 200~600 rpm 下進行。因此本篇目的是為了解 TSH 在極短培育時間中在不同轉速下其結果是否有差異。

**方法：**目前實驗室有二台震盪器設備，可使用轉速範圍為 0~400 rpm，因此我們收集了 60 支包含低中高濃度之病人檢體，以原廠標準操作步驟進行分析，並分別以 200、300、400 rpm 震盪培育 30 分鐘，收集其結果，並以統計方法 paired t-test 來互相檢定三者間的 TSH 結果是否具有差異性。

**結果：**TSH 結果在轉速 200 rpm 下分別與 300 rpm 及 400 rpm 之 paired t-test 檢定，p 值分別為 < 0.0001 及 0.0042 均小於 0.05，表示轉速 200 rpm 不管是與 300 rpm 或是與 400 rpm 的 TSH 結果都是具有差異性，儘管它們的相關係數是 0.9996 與 0.9983。而 300 rpm 及 400 rpm 之間的 paired t-test 檢定，p 值為 0.65，則代表 TSH 在這二種轉速下的結果是沒有差異性的。

**結論：**實驗室在評比試劑最終的結果若是選擇了 IZOTOP 的 TurboTSH，在標準操作步驟下，實驗室可依震盪器是否滿載的狀況下自由選擇 300 或 400 rpm 來進行培育，這樣不僅有利於各項目的進行而且也能改善 TAT (Turn around time)。

PC-148

## Establishment of Normal Pulmonary Quantitative Uptake Ratio in Ga-67 SPECT/CT Scintigraphy

Yuh-Feng Wang<sup>1</sup>, Tzyy-Ling Chuang<sup>2,3</sup>, Yu-Ching Hsu<sup>2</sup>, Nan-Jing Peng<sup>1,4</sup>

<sup>1</sup>Department of Nuclear Medicine, Taipei Veterans General Hospital, Taipei, Taiwan

<sup>2</sup>Department of Nuclear Medicine, Dalin Tzu Chi Hospital, Buddhist Tzu Chi Medical Foundation, Chiayi, Taiwan

<sup>3</sup>School of Medicine, Tzu Chi University, Hualien, Taiwan

<sup>4</sup>School of Medicine, National Yang Ming Chiao Tung University, Taipei, Taiwan

**Introduction:** Gallium-67 (Ga-67) lung scans are commonly used to assess the disease activity of alveolitis and interstitial lung disease. In interstitial lung disease, the lung uptake of Ga-67 is thought to reflect the inflammatory activity of effector cells in the lung. The accumulation of Ga-67 in the lungs is closely related to the intensity of the inflammatory process of the pathological classification of lung biopsy sections.

**Methods:** The uptake index for Ga-67 lung scan was reported as a quantitative explanation describing the distribution and intensity of tracer absorption. However, different studies use different reference points for evaluating background activity as the default standard, and the size and drawing method of the region of interest (ROI) are also different. Obviously, differences between readers and institutions must be reduced, so there is a need for standardization of interpretation. The current nuclear medicine technology has developed from a planar image to a three-dimensional SPECT, combined with CT, to become a hybrid SPECT/CT. We have developed a technology that avoids the interference of the active uptake of the covered tissues, reduces the subjectivity of the analysis, and generates the Ga-67 uptake index in the lung tissue.

**Results:** This is a preliminary result of our study. 3D uptake of Ga-67 to the lung fields and correspondence soft tissue of upper arms were collected. We hope to establish the normal range of normal subjects' index norm. In the following studies, increased lung Ga-67 intake is defined as an uptake value higher than the average Ga-67 intake of healthy subjects plus 2 standard deviations. With collect representative diseased subjects, we can further compare the cases of normal and patient groups to determine the diagnostic benefit of norms.

**Conclusions:** There are many semi-quantitative and quantitative methods in the literatures. Quantitative methods provide the inflammatory activity index of the disease process related to lung lavage and histopathological scoring when the tissue is inflamed. It can also be used for treatment and follow-up to evaluate the severity of the disease and the treatment.

PC-149

## 三維影像視覺化 分析在正子斷層掃描技術腫瘤標記之探討

俞長青<sup>1</sup> 丁健益<sup>2,3</sup> 李佩穎<sup>2</sup> 曹毓安<sup>4</sup>

<sup>1</sup> 高雄榮民總醫院核子醫學科

<sup>2</sup> 中山醫學大學醫學影像暨放射科學系

<sup>3</sup> 中山醫學大學附設醫院

<sup>4</sup> 醫研雲集股份有限公司

**背景介紹：**因為臨床正子斷層掃描影像並無法針對感興趣的位置進行特定標誌組織結構立體化。本研究主要將正子斷層掃描影像建置三維影像視覺化進行分析，並建立快速重組程序來顯示病患腫瘤立體化之相對位置。利用調整影像參數，針對腫瘤進行標誌分析，使影像可以顯示不同結構色彩之立體化影像。使醫療人員在判讀或是病灶標的可以更加明確，也可使病患更好理解病灶與影像的關係與位置。

**方法：**本研究主要使用 Miil (醫學影像繪圖軟體)、DICOM 格式之正子斷層掃描影像、處理器 (Intel Core-i7)、顯示卡 (NVIDIA GTX 1070)。首先將正子斷層掃描影像匯入 Miil，調整窗階與窗寬，使用 3D 影像或半自動渲染將腫瘤標誌物以不同顏色區分，調整透視度與色彩，最後匯出標示成 3D 立體影像進行分析。

**結果：**結果顯示正子斷層掃描影像可藉由三維影像視覺化分析進行腫瘤標誌分析。此分析 3D 影像重組影像時間與臨床系統相比減少 3 倍以上。另外在影像分析內容可利用不同顏色腫瘤標記功能可呈現腫瘤及周邊組織之結構。組織量測結果也與臨床所分析之尺寸誤差在 5% 以內。

**結論：**三維影像視覺化分析可提供醫療人員診斷、標示以及定位病灶功能，並且藉由半自動渲染功能可以顯著減少重組的時間、提高腫瘤標誌之準確度，讓醫療人員及病人能理解各器官的相關位置及疾病的變化。

PC-150

## 使用 OSCE 評估核醫科醫事人員 及放射實習學生對於放射性物質潑濺之處置能力

龔瑞英<sup>1,3</sup> 張志維<sup>1</sup> 陳耀文<sup>1</sup> 黃莆蓉<sup>1</sup> 陳玉雪<sup>2</sup>  
蔡昭璋<sup>1</sup> 謝祖怡<sup>2\*</sup> 蔡世傳<sup>1,3\*</sup>

<sup>1</sup> 臺中榮民總醫院核子醫學科

<sup>2</sup> 臺中榮民總醫院教學部

<sup>3</sup> 中臺科技大學醫學影像暨放射科學系

\* 指導作者

**背景介紹：**醫療游離輻射工作場域中，僅有使用非密封放射性射源單位有放射性物質潑濺汙染之困擾，發生放射性物質潑濺時應快速進行輻射偵測並除去污染，可限縮放射性物質擴散程度並防止污染的傳播。單位每年舉辦意外處置演練以提升輻防人員處置熟練度，但除輻防人員外，應廣為教育同仁使其皆有輻射汙染處置之基本概念，又放射系所學生為醫療院所輻射防護人員產出之大宗，輻射度量及除汙應為其放射專業養成教育之一環；本研究使用 OSCE 評估單位內醫事人員及放射實習學生對於放射性物質潑濺之處置能力。

**方法：**設計教學型『放射性藥品潑濺意外處理』OSCE 教案，將處理流程項目逐一列表，以 Delphi's Method 確立評分表信度及專家效度。本次 OSCE 測驗一共 18 人參與，包括 10 位核醫科人員 (6 位放射師及 4 位護理師) 及 8 位放射實習學生，教案及評核項目經專家確定後以 Angoff 方法確保測試通過成績達及格目標，並採用常態分配高低分組之前後 27% 進行考題難易度及鑑別度之分析。

**結果：**接受測驗考生層級及職類有部分差異，Angoff 採用放射師測驗 18 分為全員及格分數 (滿分為 38 分，百分位為 47.36 分)，並以考官評核分數進行計算加總為總分，高分組平均分數為 65.32 分 (前 27%)，低分組平均分數為 2.92 分 (後 27%)，兩者差距 62.40，測驗試題難易度為難，鑑別度極佳。評核平均分數如下：全體考生為 30.72 分 (及格分數 47.36 分)，不具輻防執照放射師為 51.82 分，具輻防執照放射師為 75.66 分，護理師為 46.26 分，放射實習學生為 8.62 分。整體及格人數僅 7 人 (38.8%)，其中 4 位為放射師，3 位為護理師，放射實習生無人及格。

**結論：**藉由本測驗得知單位尚有 3 成人員對輻射處置不熟悉，學生則無任何相關處置觀念及經驗，往後將透過實體及線上授課教學，並搭配 VR 虛擬實境為延伸教材使用，以使核醫科同仁皆有相關處理能力，以保障自身及職場安全。



PC-151

## Gallbladder Visualization in Tc-99m Labeled RBC Bleeding Scan and SPECT/CT: A Case Report

Yu-Chien Shiau, Po-Wei Li, Ya-Huang Chen, Chia-Wen Lai, Che-Wei Chang,  
Chao-Chun Huang, Yen-Wen Wu, Shan-Ying Wang

*Division of Nuclear Medicine, Far Eastern Memorial Hospital, New Taipei, Taiwan*

**Introduction:** Tc-99m labeled RBC bleeding scan is usually utilized for detection and localization of GI bleeding. Gallbladder is usually not visualized during the imaging. We report a case of GI bleeding with gallbladder visualization noted in Tc-99m labeled RBC bleeding scan and SPECT/CT images.

**Case report:** The 66 year-old male with DM, hypertension, Parkinsonism, multiple hepatic hemangioma, and history of GI bleeding 7 years ago, suffered from sudden weakness and dizziness. The patient had stool with dark greenish color without blood tingled or tarry-like. Because of persisted symptoms above, he was brought to ER and admitted. Lab data showed normocytic anemia (Hb: 6.7), acute kidney injury (Cre 1.36 mg/dL), and hyponatremia. A blood transfusion was given. CXR showed no significant finding and EKG showed LVH. PES showed reflux esophagitis, gastritis, and duodenal ulcer scar. CFS revealed incomplete colonoscopy but no obvious tumor was noted. Tc-99m labeled RBC bleeding scan and SPECT/CT were arranged, and the result showed visualization of gallbladder during 2nd to 24th hours, and visualization of terminal ileum and colon in the 6th and 24th hours, suspecting GI bleeding probably from around terminal ileum. SPECT/CT confirmed the location of tracer uptake in gallbladder. Since his condition was getting stable after transfusion without overt GI bleeding, he was discharged with OPD follow-up.

**Conclusions:** In Tc-99m labeled RBC bleeding scan, gallbladder is usually not visualized, although there were several case reports showing that gallbladder could be rarely visualized in RBC bleeding scan. Most of those cases had anemia, chronic renal failure, and received blood transfusion. And the visualization was not due to bleeding in the gallbladder. Thus it is recommended that when interpreting the images of RBC bleeding scan in patients with anemia and chronic renal failure, care should be taken of the gallbladder visualization to avoid false positive impression.

PC-152

## Gallium Uptake in Brown Adipose Tissue in Adult with Hypomyopathic Dermatomyositis

Yi-Ching Lin<sup>1,2</sup>, Shih-Chuan Tsai<sup>1</sup>

<sup>1</sup>Department of Nuclear Medicine, Taichung Veterans General Hospital, Taichung, Taiwan

<sup>2</sup>Department of Public Health, China Medical University, Taichung, Taiwan

**Introduction:** Hypomyopathic dermatomyositis (HDM) is a rare autoimmune syndrome characterized by specific cutaneous lesions and subclinical elevations of muscle enzymes without muscle weakness. Polyarthrititis, rapid progressive interstitial lung disease, and increase risk of cancer may clinically present.

**Case report:** A 22-year-old female had painless erythematous patches over the right temporal area for months. The erythematous patches extended to the upper and lower eyelids of the right eye with swelling gradually. Under the tentative diagnosis of pre-septal cellulitis, antibiotic with Zinforo® was administered. But she was not responsive to the medication and felt general malaise. Laboratory examination showed elevating CK level while autoimmune profile showed AC-4 Nuclear fine speckled ANA positive and strongly positive anti-NXP2 Ab. Both sensory and motor conduction study, needle EMG of four limbs were normal. Dermatomyositis was suspected. Gallium scan (Fig. A) was performed for detecting possible inflammatory or infectious foci and cancer screening, which showed mildly increased intensity at the right periorbital area (short arrows, Fig. B). Increased gallium uptake at the supra- & infra- clavicular regions was incidentally noted on SPECT/CT images, where brown adipose tissue located (arrow heads, Fig. C). BAT uptake of Ga-67 have been described in neonate and child but not adult. Hypomyopathic dermatomyositis was therefore diagnosed. She currently underwent immunosuppressive therapy with hydroxychloroquine and methylprednisolone under well condition.

**Conclusion:** Accidentally finding of increased gallium uptake in the brown adipose tissue of neck is demonstrated in SPECT/CT images, which mimics malignance on planar images but easily to identifying in SPECT/CT images.

PC-153

## 五歲以下幼兒之胃排空功能評估 — 案例報告

蔡富任 胡璿 蘇詩琪

高雄榮民總醫院核子醫學科

**背景介紹：**成人之胃排空功能檢查在臨床上應用得十分廣泛，然而對於幼童病患，因其案例較少且多半不易配合，因此幼童胃腸道排空檢查之經驗相對缺乏。Kwatra 等 (2020) 發表 2273 例兒童胃排空造影，提出了以喝下示蹤劑後一小時及三小時時胃部殘留的比率來評估胃排空功能，並提出年齡分層之標準範圍。本案例即是參考上述做法嘗試用於臨床實務。

**病例報告：**一位 5 歲女童因橫膈裂孔疝氣於 3 個月前進行修補手術，術後出現持續之腹脹、嘔吐、消化不良情形，懷疑手術影響其胃部功能故安排此檢查。我們以 1 豪居禮之 Tc-99m Phytate 溶於 200 ml 牛奶中並讓患童喝下，喝完後隨即平躺並收集前後平面影像、1 小時之前後動態影像、以及一小時後之前後平面影像，再以胃部與去除胃部之腹部區域繪製 ROI 並以其比值計算胃排空分率。

**討論：**依照 Kwatra 等 (2020) 發表之參考值，5 歲兒童之於 1 小時及 3 小時之胃排空比率為 42% 及 86%。而本案例於 1 小時之胃排空比率僅為 36，超出文獻裡提供之正常範圍。臨床上成人常用線性回歸或指數回歸來推估胃排空達一半的時間 (T1/2) 來診斷是否胃排空有延遲的現象。然而考慮到兒童容易有無法配合的情形，此個案所採用之以兩次靜態影像計算排空比率的方法，較不會因為收集動態影像過程中患童的移動造成影像品質不良，也可以減少鎮靜地使用以及儀器占用的時間。

PC-154

## Disseminated Tuberculous Infection Mimic Distant Metastases in a Case of Oral Cancer on F-18 PET/CT

Tsu-Hsiang Chang, Hung-Pin Chan, Chang-Chung Lin

*Department of Nuclear Medicine, Kaohsiung Veterans General Hospital, Kaohsiung, Taiwan*

**Introduction:** Disseminated tuberculous infection is a clinical challenge of diagnosis in clinical practice. Patients may present no obvious symptoms or complaint during hospitalization. X-ray or CT scan sometimes used in routine but may have some limitation. In previous articles, F-18 FDF PET/CT may play an important role for diagnosis in occult infection with whole body imaging. Today, we presented a case of squamous cell carcinoma of left lower lip s/p surgery and adjuvant radiotherapy, with painless nodule over his right axilla and suspected distant metastasis. F-18 FDG PET/CT scan showed disseminated FDG avidity and suspected distant metastasis. The pathology specimens of lesions showed necrotizing granulomatous inflammation. He underwent anti-TB treatment.

**Methods:** The F-18 Fluorodeoxyglucose (FDG) PET scan from head to feet was performed 1 hour after intravenous injection of 10 mCi FDG on a GE Discovery 710 PET/CT system.

**Results:** The PET/CT scan showed disseminated FDG uptake in the peritoneum and increased uptake in right axilla. Surgery for tumor excision of abdomen was done, and the pathology specimens showed necrotizing granulomatous inflammation. With positive acid-fast bacillus (AFB) staining and TB-PCR, he was treated for extrapulmonary tuberculosis with isoniazid, rifampin, ethambutol, and pyrazinamide.

**Conclusions:** According to this case:

1. PET/CT scan correctly guided biopsy to the exact location of active lesion.
2. PET/CT may be a suitable modality with whole body imaging for Disseminated Tuberculous infection diagnosis.

PC-155

## Challenges in the Diagnosis of Urinothorax in a Middle-aged Man

Jiun-Chang Wu<sup>1</sup>, Yi-Lin Hsieh<sup>1,2</sup>, Ku-Hung Lin<sup>3</sup>,  
Chi-Feng Pan<sup>4</sup>, Wen-Chien Huang<sup>1,2</sup>

<sup>1</sup>Department of Surgery, MacKay Memorial Hospital, Taipei, Taiwan

<sup>2</sup>Division of Thoracic Surgery

<sup>3</sup>Department of Nuclear Medicine

<sup>4</sup>Division of Nephrology, Department of Internal Medicine

**Introduction:** Urinothorax, defined as accumulation of urine in the pleural space, is a rare form of pleural effusion (PE). Due to its sparseness, leading to the physician's lack of experience, the diagnosis of urinothorax is challenging. The objective of this clinical case report is to highlight the unusual disease to avoid incorrect diagnosis.

**Case report:** This is a 56-year-old man presenting to the hospital with shortness of breath for 3 days. He complained decreased urine output in recent one month. Deteriorated renal function was found when we checked laboratory study, and hemodialysis was initiated. Chest radiography revealed massive right PE. We performed thoracentesis, and much floating particle appearing in PE. Creatinine level was 9.6 mg/dL in serum and 9.9 mg/dL in PE. We arranged technetium-99m diethylenetriamine pentaacetate (Tc-99m DTPA) split renal function scan, reporting estimated glomerular filtration rate (eGFR) was 13.0 ml/min in right, and 11.6 ml/min in left kidney. Gradual accumulation of radioactivity in right hemithorax was noted during the examination; therefore the diagnosis of urinothorax was made. Renal echo discovered bilateral hydronephrosis. Bilateral ureterovesical junction (UVJ) obstruction was unveiled when double J catheter was inserted bilaterally. Right urinothorax was relieved thereafter.

The most common etiology of urinothorax is obstructive uropathy resulted from ureteral stricture or nephrolithiasis. Pleural and serum creatinine ratio should be greater than 1. If laboratory study is not supportive to establish diagnosis, Tc-99m DTPA renal scan can be arranged, revealing migration of radioactivity from kidney to pleural cavity. The mechanism of urine transit is not well established. Some experts agree with that it spreads directly through anatomical defects of the diaphragm, while others believe it migrates into the pleural space through diaphragmatic lymphatics. Management of urinothorax depends on correction of obstructive uropathy.

**Conclusions:** Diagnosing urinothorax is difficult owing to its rareness, leading to lack of awareness of the timing when thoracentesis should be implemented urgently. Combination of obstructive uropathy and sudden emerging massive PE raises concern of urinothorax. In analysis of PE, pleural and serum creatinine ratio would be greater than 1, and Tc-99m DTPA renal scan proves the spreading from genitourinary tract to pleural cavity.

PC-156

## Clinical Analysis of 24 Chronic Idiopathic Constipation Cases by Gallium-67 Colon Transit Study: an Observational Research from a Tertiary Care Hospital in Taiwan

Jiun-Chang Wu<sup>1</sup>, Cheng-Ta Lai<sup>1,2</sup>, Ku-Hung Lin<sup>3</sup>

<sup>1</sup>Department of Surgery, MacKay Memorial Hospital, Taipei, Taiwan

<sup>2</sup>Division of Colorectal Surgery

<sup>3</sup>Department of Nuclear Medicine

**Introduction:** Constipation is the most common digestive complaint worldwide. The definition of chronic constipation in this study should meet the diagnostic criteria of Rome IV for functional constipation for at least three months. The cause of chronic idiopathic constipation (CIC) remains unknown, in other words, it's not caused by underlying illness or adverse effect of medication. Gallium-67 (Ga-67), if given orally, is not absorbed from the bowel and more than 98% is excreted in the feces. With its relatively long half-life (78 hours), Ga-67 is suitable for colon transit study. The aim of this study is to analyze CIC cases by Ga-67 colon transit study in MacKay Memorial Hospital.

**Methods:** From September 2020 to January 2022, the Ga-67 colon transit study was attempted in 24 patients, comprising of two men and 22 women. The mean age among these patients was 41.5 years old. All patients had negative findings in colonoscopy.

For colon transit study, patients ingested 300 ml water containing 1.0 millicurie Ga-67. Image acquisition was proceeded in 6, 24, 48, 72 hours after radioactive substance given. The signal was obtained by a qualified gamma camera in anterior and posterior views. All study results were reported by certified nuclear physicians.

**Results:** In 24 patients, 11 were reported normal transit while the other 13 were reported delayed transit. Mean estimated emptying half-time in normal and delayed studies was 18.6 and 52.1 hours, respectively. In patients with normal transit, it mostly showed good passage of tracer through colon, with minimal residual radioactivity at 48 hours image, and the estimated emptying half-time would be less than 28.8 hours. On the contrary, in patients with delayed colon transit, it likely showed slow passage of tracer through colon, with marked tracer stasis in left hemicolon at 72 hours image. One patient received colon transit study and followed by subtotal colectomy. Three patients underwent the study as post-operative surveillance. The other 20 patients underwent this examination as a reference to plan future colectomy.

**Conclusions:** CIC affects more than one tenth population worldwide but diagnosis of CIC is difficult. With nature of long half-life and not absorbed from gastrointestinal tract, Ga-67 is suitable for colon transit study, which provide objective and reliable evidence to help establish diagnosis of CIC, and may offer clinical information for pre-operative survey and post-operative follow up in patients receiving colectomy.

PC-157

## 以 GE Xeleris 4 工作站內建的 Aladdin 功能 自訂唾液腺功能造影 Workflow

郭建瑋 蘇詩琪

高雄榮民總醫院核子醫學科

**背景介紹：**各廠牌工作站設有多種內建造影檢查 workflow，其中有各式參數設定，可配合常見臨床檢查步驟及各種變化，然而不一定能滿足使用者無窮無盡的需求。使用者可利用原廠提供的程式工具組來撰寫 workflow，自定義原本預設 workflow 未提供的計算方式，使其更加貼近檢查需求，甚至排版輸出畫面，利於判讀兼具美觀。

**方法：**我們針對一篇唾液腺造影論文「Scoring analysis of salivary gland scintigraphy in patients with Sjögren's syndrome」(Ann Nucl Med. 2003 Dec;17(8):627-31)，依照其闡述的步驟計算唾液腺分泌分率 (excretion rate)。背景 ROI 畫在腦部，時間 - 活性曲線須對背景做校正。曲線經校正後，分泌分率 = (最大活性 - 刺激後最小活性) / 最大活性。另外我們也參考其他論文計算攝取分率 (uptake ratio) = 最大活性 ROI 平均值 / 同時間背景活性 ROI 平均值。

**結果：**實際病患應用中，若病人於造影過程中沒有移動，只要妥當畫好 ROI，即可讓程式自動跑出時間 - 活性曲線，並依設定之排版、套色、字體大小、座標位置將各種計算結果標示在畫面上。

**結論：**自行撰寫之 workflow 最大好處就是提供預設 workflow 所沒有配置的功能。以此論文為例，因為 ROI 大小不同，我們需要 A 曲線對 B 曲線做校正，而不是單純四則運算相減。另外，Aladdin 也讓我們在輸出二次截圖的排版與套色有一定程度上的自由。然而在開發過程期間，不斷測試與驗證每個步驟的正確性為必不可少之過程，也會需要處理各種意料之外的 bug。

PC-158

## Bizarre Image of Diffused Soft Tissue Radio Uptake of Osteosarcoma

Hsin-Ning Wang, Chien-Hsin Ting

*Department of Nuclear Medicine, Taipei Veteran General Hospital, Taipei, Taiwan*

**Introduction:** Osteosarcoma is one type of osteogenesis cancer. The epidemiology of osteosarcoma with two peaks, one during teenagers, the other was in older adulthood. Difference from other kind of tumors which have increased uptake in whole body bone scan indicated of bone cortex reaction, increased uptake in bone scan of osteosarcoma also represents tumor itself. As a result, whole body bone scan becomes one of the most frequent used examinations for evaluating skip metastasis in osteosarcoma.

**Case Report:** This 67 year-old female was diagnosed with osteosarcoma over left thigh in 2014, pT2bN0M0, with the wide excision of tumor on 2014/10/22. Unfortunately, lung metastasis was identified later and disease progression years by years. The first whole body bone scan was done in our hospital at 2020 and the image revealed extra-osseous uptake over lung metastasis. At the follow up scan on 2021, new lesion over greater trochanter of right femur was noted. At the time of the latest image on 2022 during admission, the image revealed severe progression radio uptake not only in bone, but also with multiple soft tissue uptake over bilateral chest, abdomen and pelvis. One month later after the latest image, the patient died.

**Discussions:** Whole body bone scan serves as an evaluation tool for skip bony metastasis in osteosarcoma. Due to the property of tumor itself, the image shows increased radiotracer uptake over tumor. However, although there was frequently seen that skip bony metastasis in osteosarcoma in whole body bone scan, diffused uptake over almost whole body and especially in the soft tissue in abdomen and pelvic was not so common. In this case, image severity was compatible with disease progression and the patient died later on. Therefore, whole body bone scan also serves as an inexpensive indicator for change of underlying disease and provided information of disease status for clinical use.



PC-159

## The Reactive Lymphadenopathy Pattern in FDG PET/CT after COVID-19 Vaccination

Hsin-Ning Wang, Nan-Jing Peng

*Department of Nuclear Medicine, Taipei Veteran General Hospital, Taipei, Taiwan*

**Introduction:** Vaccination before PET scan might lead misdiagnosis due to reactive lymph nodes. In this study, we would like to analyze the relationship between COVID-19 vaccination and FDG-F-18-PET images.

**Methods:** We collected patients who received COVID-19 vaccination and also had FDG-F-18-PET images study within 30 days in 2021. The locations of those lymphadenopathy were divided into two groups: axillary lymph nodes, and supraclavicular lymph nodes. The types of vaccine were also divided into two groups: mRNA (Moderna, BNT), and the others (AZ, Medigen). Differences were considered to be significant at  $p < 0.05$ .

**Results:** There were 179 patients received vaccine before 30 days of the PET scan. 43 of them (24.0%) had ipsilateral axillary lymph nodes uptake, and 7 (3.9%) with ipsilateral supraclavicular lymph nodes uptake (chi-square  $p$  value  $< 0.0001$ ). In those having uptake of the ipsilateral upper limb lymph nodes, mRNA group were 37 within 114 patients and the other types of vaccine were 17 within 65 patients. The  $p$  value of Chi-squared test for types of vaccine was 0.17.

**Conclusions:** In our analysis, most frequent area of vaccine reactive lymph nodes located at ipsilateral axillary of injection side. Furthermore, the small  $p$  value indicates the significance of the dominant uptake over ipsilateral axillary area. The physiological explanation for this difference might be axillary lymph node is nearer from the injection site than the supraclavicular lymph nodes. Therefore, the interpretation of PET scan should be caution when patients received vaccine injection, especially the ipsilateral axillary region, no matter types of vaccine. We suggested that for those with cancer history and need to have PET scan for evaluation should have their COVID-19 vaccine injection at the contralateral side of tumor.

PC-160

## 核醫淚囊閃爍攝影檢查 (Dacryoscintigraphy) 案例分享

黃信慈 陳慶元

佛教慈濟醫療財團法人台中慈濟醫院核子醫學科

**簡介：**史蒂芬強森症候群 (Stevens-Johnson Syndrome, SJS) 是發生在身體皮膚與黏膜組織上的發炎過敏反應。大約有 50-88% 史蒂芬強森症候群患者會出現急性眼部症狀，發病症狀可能是輕微的像是眼瞼或結膜水腫；中度的則是結膜發炎，角膜上皮缺損或潰瘍；重度的則為眼瞼球粘連，角膜上皮缺損，若沒有得到適當診治，可導致嚴重後遺症，影響視力減退甚至失明等；在後遺症的影響中則是乾眼症最為嚴重。

**案例報告：**該案例為 20 歲男性因雙眼視力模糊，乾澀刺痛，伴隨紅腫畏光有分泌物，以及鼻竇沾黏和全身黏膜受損將近十年以上；無抽菸，有藥物過敏、喘、呼吸困難合併慢性阻塞性肺疾病症狀需要 24 小時呼吸器的依賴狀態下，經耳鼻喉科醫師評估先安排鼻竇電腦斷層，報告結果為鼻竇發炎。由於臨床懷疑史蒂芬強森症候群出現眼部急性症狀引發鼻淚管阻塞，因此至本科安排核醫淚囊閃爍攝影檢查。

**結果：**放射性同位素 Free Tc-99m 0.4 mCi / 0.5 c.c 以滴管吸入管內，讓患者平躺在檢查床上，枕頭墊高 30 度，再將藥物滴入兩側眼角，並用紗布吸取多餘的藥物，後立即進行眼部連續掃描。動態成像掃描在 5 分鐘時進行，靜態成像掃描分別在 5、10、15 至 30 分鐘後結束。影像結果顯示沒有任何放射性藥物進入雙眼淚管，高度懷疑兩側鼻淚管阻塞的可能性很大。隨後外科醫師進行內視鏡手術治療，重建淚液通道後，患者不適症狀逐漸改善，目前門診持續追蹤中。

**結論：**史蒂芬強森症候群是一項罕見的嚴重疾病，更會對患者眼睛健康造成長遠影響。因此，患者應在病發初期儘早接受診治，降低嚴重後遺症的風險。臨床治療照護原則包括停用誘發藥物、補充體液、減低痛楚及預防傷口感染，除了藥水藥膏輔助外，用溼熱毛巾做眼睛熱敷加按摩可以減少鼻淚管阻塞。核醫淚囊閃爍攝影檢查可有效提供淚管阻塞之評估，有助於臨床後續的治療。

PC-161

## SUVmax May Help to Differentiate Thymoma from Lymphoma in Anterior Mediastinum on FDG PET/CT Scan

Li-Jen Huang, Jui-Hung Weng

*Department of Nuclear Medicine, Chung-Shan Medical University Hospital, Taichung, Taiwan*

**Introduction:** A 24-year-10-month-old male with no underlying disorders or genetic disease experienced sudden chest pain recently. Suspicious anterior mediastinal mass was initially noted. The patient was then admitted for further workup, including PET/CT scan. This case study aims to differentiate anterior mediastinal masses' F18-FDG PET/CT uptake patterns.

**Methods:** A GE Discovery MI.PET/CT scanner was used to perform FDG-PET/CT scans 60 minutes after administering 7.6 mCi of [F-18] FDG intravenously. Low-dose CT scanning is performed without contrast. Vertex to above knees is covered by the scan area. If necessary, delayed scanning is acquired 3 hours following injection. Attenuation correction is applied iteratively during image reconstruction.

**Results:** An atypical peripheral hypermetabolic mass was found on FDG-PET/CT that measured about 12 cm at its widest point and had an SUVmax of 6.7. It involved the left heart's border and anterior mediastinum, as well as bilateral pleural effusions (left > right) and minimal pericardial effusion. For the mass in the anterior mediastinum, a non-Hodgkin lymphoma was first considered the most likely diagnosis.

**Conclusions:** Thymoma and lymphoma median maximal standardized uptake value differed dramatically: 4.35 versus 18.00. A maximum standardized uptake value less than 12.85 was associated with thymoma with a sensitivity of 100%, and a positive predictive value of 88.89%. A maximum standardized uptake value less than 7.50 demonstrated a positive predictive value of 100% for thymoma. Thus, in practical use, tumors with a maximum standardized uptake value less than 7.50 are more likely thymoma. Tumors with a maximum standardized uptake value greater than 7.50 should be biopsied to rule out lymphoma. Lymphomas tend to have a maximum standardized uptake value greater than 12.85. Moreover, if we combine PET SUV levels with additional parameters of MRI imaging, namely, the combinations of the TIC pattern (washout pattern or persistent/plateau pattern), SUVmax ( $\geq 11.6$ ,  $< 11.6$ ), and maximal diameter ( $\geq 6.8$  cm,  $< 6.8$  cm), high diagnostic accuracy of differentiating thymic epithelial tumor and malignant lymphoma/malignant germ cell tumor can be achieved.

## 大會組織

**主辦單位：**中華民國核醫學學會

**協辦單位：**國立台灣大學醫學院附設醫院

行政院原子能委員會核能研究所

經濟部技術處

**指導委員**（依姓氏筆畫順序，尊稱省略）

王安美、王昱豐、李將瑄、杜高瑩、林立凡、周大凱、邱南津、邱創新  
吳東信、吳彥雯、陳宜伶、陳輝墉、翁瑞鴻、許幼青、曹勤和、黃文盛  
黃英峰、黃奕琿、黃淑華、黃雅瑤、彭南靖、程紹智、詹勝傑、張智勇  
楊邦宏、廖炎智、廖建國、鄭媚方、蔡世傳、樊裕明、顏若芳、謝德鈞

**法律顧問** 蔡雅琴

**論文評選組**（依姓氏筆畫順序，尊稱省略）

召集人 王昱豐

執行秘書 陳保良

壁報臨床組 王安美、何恭之、林立凡、胡蓮欣、張晉銓、張朝鈞、許幼青  
陳宜伶、陳惠萍、曾能泉、黃奕琿、黃淑華、楊士頤、樊裕明  
蔡世傳、蔡雅琴

壁報基礎組 李振弘、張文議、張志賢、陳昱宏、陳傳霖、程紹智、楊邦宏  
樊修秀

口頭臨床組 汪姍瑩、林宜澗、林明賢、邱宇莉、莊紫翎、路景竹

口頭基礎組 田育彰、吳東信

**秘書處**（依姓氏筆畫順序，尊稱省略）

秘書長 路景竹

執行秘書 柯冠吟、莊佩儒、陳建榮

秘書 楊月桂、吳璫廷



贊助廠商

士宣生技股份有限公司

元新儀器股份有限公司

台灣拜耳股份有限公司

台灣飛利浦有限公司

台灣諾華股份有限公司

西門子醫療設備股份有限公司

貝克西弗股份有限公司

奇異亞洲醫療設備股份有限公司

昶洋貿易股份有限公司

恩典科研股份有限公司

泰歷藥品儀器股份有限公司

常捷生醫科技股份有限公司

富特茂股份有限公司

量子輻射科技有限公司

臺灣新吉美碩股份有限公司

衛采製藥股份有限公司

龍霆科技企業有限公司

依筆畫排序

